Supramolecular Chemistry of Poly(ester imide)s

A thesis submitted in part fulfilment of the degree of Doctor of Philosophy

Department of Chemistry

Marcus Knappert

2019

Abstract

For some copolymeric foldamers (synthetic polymers that adopt specific folded conformations) it was found that the copolymers sequence could be analysed by ^{1}H NMR spectroscopy. For the analysis, a singlet resonance of the copolymer split into several resonances ("splitting pattern") when a polycyclic aromatic intercalator (e. g. pyrene) was added, often into an apparent triplet. Each of the resonances was produced by (at least one) sequence in the copolymer backbone. The ratio of the resonances indicated thus the ratio of the sequences present in the copolymer. This effect allows thus to analyse copolymers with long repeat units, each consisting of an intercalator binding and an intercalator non-binding unit. In the present thesis, different homo-(polyesters imide)s and co-(polyesters imide)s were synthesized. These were mixed in solution with intercalators (pyrene, perylene or anthracene) in different concentrations and ^{1}H NMR spectra of the solutions were measured. From the resulting ^{1}H NMR spectra, conclusions about conformation of the copolymer and their sequencing could be drawn.

During the optimization of the diacyl chloride-based synthesis of the various homo-(polyesters imide)s and co-(polyesters imide)s it was found that a low reaction temperature is a decisive factor in achieving a high molecular weight (Chapter 2). Thereby, an average inherent viscosity η_{inh} of 0.70 dL g^{-1} could be achieved for the poly(ester imide)s of this study, whereas structurally related polyester imides from the literature had an average inherent viscosity of η_{inh} of 0.50 dL g^{-1}.

Using said synthesis, a homologous series of naphthalene diimide-based homo- and co-poly(ester imide)s with different spacer lengths was produced (Chapter 3). A subsequent titration of the homologous series of poly(ester imide)s with said intercalators revealed a dependency of the complexation strength on the spacer length with a sharp resonance in complexation strength for the polymers comprising a spacer of 2 methylene groups.

In titrations of various co-poly(ester imide)s the copolymers sequenceability was found to be positively related to the difference in binding strength between the intercalator binding unit and the intercalator non-binding unit (Chapter 4). The sequenceability could thus be controlled by the choice of the binding or non-binding repeats units, as well as by choosing a spacer of appropriate length. The sequenceability was thereby significantly improved compared to previous examples. In some of the splitting patterns, the splitting patterns of the polymers could be assigned to the sequences in the polymer backbone using a mathematical model.

Even though sequenceability is in the current system based on a binding and a non-binding unit, it could be shown that sequenceability can be achieved by using only binding naphthalene diimide-based binding units (Chapter 5). This was achieved by modifying the binding strength of the naphthalene diimide units using by spacers of appropriate length, so that a sequenceable copolymer of strongly binding naphthalene diimide-units and weakly binding naphthalene diimide-units could be produced. This concept could also be successfully transferred to poly(ether imide)s.

The sequencing was used to follow the formation of new sequences during the transesterification of two homopolymers. It was found that the splitting pattern intensity ratios observed by ^{1}H NMR were during the transesterification process as expected in view of the intercalation sequencing theory. Thus, an application for sequencing could be demonstrated and the intercalation sequencing theory could be confirmed.

Summarizing, the intercalation sequencing theory was extended, various sequenceable copolymers were found and an application for intercalation sequencing was presented.

Declaration of original authorship

I confirm that this is my own work and the use of all material from other sources has been properly and fully acknowledged.

Marcus Knappert

Acknowledgements

I would like to thank my supervisor Professor Howard Colquhoun for his kind guidance throughout my PhD and for treating us students with such respect as if we would be colleagues. It was a pleasure to work with him, he devoted a tremendous amount of time and I left every meeting with restored confidence. I would also like to thank my co-supervisor Dr Fred Davis in particular for his synthesis-related contributions to the project, his ideas have indeed inspired me. Special appreciation also goes to Tianqi 'Jessie' Jin, who collaborated with me on her master thesis; the collaboration was very scientifically fruitful and I could develop personally.

I would also like to thank Professor Wayne Hayes, his group and my colleagues in the Colquhoun group for practical help and advice in numerous situations, as well as for making Reading University an enjoyable place, in particular Ben Baker, Priya Singh, Oli Balmford, Adam ODonnell, Sara Salimi, Alex Gavriel and Pengcheng Zhu. I would like to thank those in the department who have lent their time and expertise to this study; Jessica Godleman kindly contributed to my NMR analysis, Radek Kowalczyk acquired unusual NMR spectra, Nick Spencer obtained mass spectroscopic data, Kate Lim kindly assisted me to improve my English, Corinne McEwan introduced me to Lab104, Flavien Leroux shared his practical experience with me, Lewis Hart and Tahkur Singh Babra gave me advice on the arrangement of my results. This PhD project was fully funded by European Union (Marie Skłodowska-Curie Network EURO-SEQUENCES, grant number 642083). I would like to express my gratitude.

Finally, I am grateful for the continual support given by my family and my wife Sandra, without whom the completion of this thesis would not have been possible. I would also like to thank Jesus Christ, who presumably created me and made this work possible.

Table of Contents

List of abbreviations

$Đ$	dispersity
x	number of methylene groups
χ	degree of randomness
$\Delta\delta$	chemical shift
η_{inh}	inherent viscosity
^{13}C NMR	carbon-13 nuclear magnetic resonance
^{1}H NMR	proton nuclear magnetic resonance
ADMET	Acyclic diene metathesis
B_0	field strength of a magnetic field
BPDA	3,3′,4,4′-biphenyltetracarboxylic dianhydride
BPDI	3,3′,4,4′-biphenyltetracarboxylic diimide
$CaCO_3$	calcite
CDP	cyclodepolymerization
$CHCl_3$	chloroform
$CDCl_3$	chloroform, deuterated
DMSO	dimethyl sulfoxide
DMSO-d_6	dimethyl sulfoxide, deuterated
COSY	correlation spectroscopy
CT	charge-transfer
DADD	1,12-diaminododecane
DAN	1,5-dialkoxynaphthalene
DBTO	dibutyltin oxide
DMAc	*N,N*-dimethylacetamide
DMF	*N,N*-dimethylformamide
DNA	deoxyribonucleic acid
DP_n	number average degree of polymerization
DSC	differential scanning calorimetry

ED-ROP	entropically driven ring-opening polymerization
EDEA	(ethylenedioxy)bis(ethylamine)
Et_3N	triethylamine
GPC	gel permeation chromatography
HFDA	4,4′-(hexafluoroisopropylidene)diphthalic dianhydride
HFDI	4,4'-(hexafluoroisopropylidene)diphthalic diimide
HFIP	1,1,1,3,3,3-hexafluoro-2-propanol
HOMO	highest occupied molecular orbital
ITC	isothermal titration calorimetry
JRES	*J*-resolved
K_a	association constant
K_C	equilibrium constant
LUMO	lowest unoccupied molecular orbital
M_n	number average molar mass
NDI	1,4,5,8-naphthalene tetracarboxylic diimide
NMP	*N*-methylpyrrolidone
NMR	nuclear magnetic resonance
PC	polycarbonate
PEI	poly(ester imide)
PEN	poly(ethylene 2,6-naphthalate)
PET	poly(ethylene terephthalate)
PMDI	pyromellitic diimide
pyrene-d_{10}	perdeuterated pyrene
SAXS	small-angle X-ray scattering
TFA	2,2,2-trifluoroacetic acid
TFE	2,2,2-trifluoroethanol
TFMB	2,2'-bis(trifluoromethyl)benzidine

T_g	glass transition temperature
T_m	melting point
TPE	thermoplastic elastomers
UV/vis	ultraviolet–visible
WAXS	wide-angle X-ray scattering

1 Introduction and theory

1.1. Polyesters

1.1.1. Definition of polyesters and reactions

Polyesters are defined as polymers which contain an ester linking group in every repeat unit (Figure 1).[1]

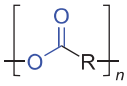

Figure 1: General structural formula of a polyester.

Polyesters can be obtained by a wide range of reactions of which the most important are the reaction of acids and alcohols, alcoholysis and or acidolysis of low-molecular weight esters or the alcoholysis of acyl chlorides (Scheme 1).

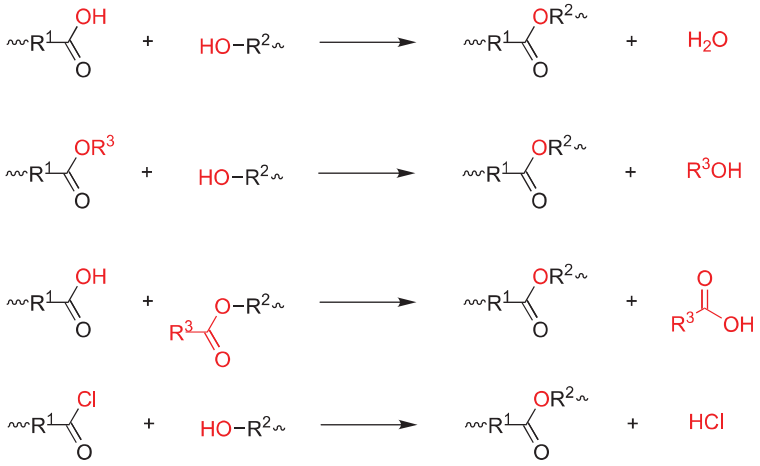

Scheme 1: Some of the most common methods for polyester synthesis.

Polyester are also accessible by chain-growth polymerization via ring-opening polymerization of lactones (Scheme 2) and lactides, this synthesis is also applied on the industrial scale.[2,3]

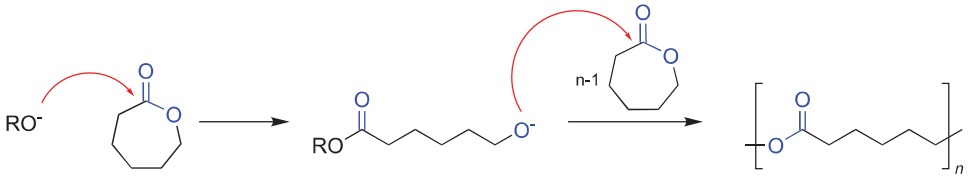

Scheme 2: Synthesis of a polyester via ring-opening polymerization of a lactone (ε-caprolactone).

Numerous other reactions have been reported for the synthesis of selected polyesters, but are limited to laboratory-scale syntheses using specific conditions, for example using dicarboxylic acid salts and dialkyl halides or reactions between bisketenes and diols.[4]

1.1.2. Classification of polyester according to structure

Polyesters are one of the economically most important classes of polymers, driven especially by PET, which is counted among the commodity plastics; in 2000 around 30 million tons were produced worldwide.[4] The variety of structures and properties in the polyester family is very large, depending on the nature of the R group (Figure 1).[1]

The family of polyesters comprises:

- Linear aliphatic high molecular weight polyesters (M_n >10,000) are low-melting (m. p. 40 – 80 °C) semicrystalline polymers and exhibit relatively poor mechanical properties. Their inherent degradability, resulting from their hydrolytic instability, makes them suitable for applications where a possible environmental impact is a concern, e.g. packaging, disposable items or agricultural mulch films[5] or in biomedical and pharmaceutical applications.[6]
- Aliphatic linear low-molar-mass (M_n < 10,000) hydroxy-terminated polyesters are used as macromonomers for the production of polyurethanes.
- hyperbranched polyesters are used as as rheology modifiers in thermoplastics or as crosslinkers in coatings[7] due to their particularly low viscosity, good solubility and high functionality[8]
- Aliphatic–aromatic polyesters, including poly(ethylene terephthalate) and poly(butylene terephthalate), are high-melting semicrystalline materials (m. p. 160–280 °C) that and have found use as engineering thermoplastics, fibers and films.
- Wholly aromatic linear copolyesters present superior mechanical properties and heat resistance and are used in a number of high-performance applications.
- Unsaturated polyesters are produced from multifunctional alcohols and unsaturated dibasic acids and are cross-linked thereafter; they are used as matrices in composite materials. Alkyd resins are made from polyfunctional alcohols and fatty acids and are

used widely in the coating and composite industries as they can be cross-linked in the presence of oxygen. Also rubber-like polyesters exist, called thermoplastic polyester elastomers (ester TPEs).

1.2. Thermodynamics of polycondensation reactions

Polyesterifications are grouped by some authors[4,9] into two main categories: a) equilibrium polyesterifications (mainly alcohol-acid reaction, alcohol–ester and acid–ester interchange reactions, carried out in bulk at high temperatures), and b) non-equilibrium polyesterifications, using highly reactive monomers (for example acid chlorides or activated carboxylic acids, mostly carried out at lower temperatures in solution).

The acid-alcohol based polyesterification (Scheme 1, top) is one example of an equilibrium reaction. The ratio between the polymer-forming ester group (-C(O)O-) and the condensation product water (H_2O) against the acid-based (-C(O)OH) and alcohol-based (-OH) monomers is described by the equilibrium constant K_C (equation 1):

$$K_C = \frac{[...-C(O)O-...][H_2O]}{[-C(O)OH][-OH]} \qquad 1$$

The equilibrium constant of the acid-alcohol based polyesterification is typically $K_C \leq 10$, what is not high enough to obtain high-molecular weight polymers ($DP_n \geq 100$), as the number average degree of polymerization (DP_n) can be calculated from the equilibrium constant K_C as follows (equation 2):[10]

$$DP_n = K_C^{0.5} + 1 \qquad 2$$

In equilibrium reactions, it is therefore necessary to remove the condensation product continuously and efficiently from the reaction medium in order to drive the equilibrium towards polymer.[10] The condensation product is therefore removed at reduced pressure and high temperatures (150–320 °C, depending on the monomers) to prevent the back reaction.[6] With the progress of the reaction, the concentration of active chain ends is decreasing and the viscosity of the melt or solution increasing. For an increase of the reaction rate, the reaction is carried out at high end group concentration (preferably in the bulk), promoted by the elevated temperatures.

Equilibrium constants of magnitude $K_C \geq 10^4$ are achieved when using reactive reactants (acid chlorides or acid anhydrides) or activating agents like 1,1′-carbonyldiimidazole. Using these reactants, molecular weights required for technical applications can be achieved even without active removal of the condensation product.

The mentioned classification of the synthesis reactions into equilibrium and non-equilibrium reactions described here is used in the following sections.

1.2.1. Equilibrium-based polyesterification

Direct bulk polyesterification at high temperatures (150 – 290°C) is well-suited and used on the industrial scale for the production of aliphatic polyesters, unsaturated polyesters and aromatic–aliphatic polyesters (Scheme 3):

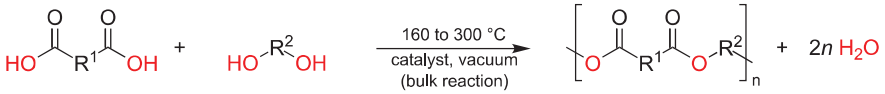

Scheme 3: Synthesis of a polyester via direct esterification.

Monomers containing phenolic or tertiary hydroxyl groups exhibit a low reactivity with carboxylic acids and cannot be polymerized via direct acid alcohol-based polyesterification.[4] In the case of PET production, however, the direct process has several advantages, in particular a higher reaction rate, a higher attainable molecular weight, the release of water instead of methanol and lower storage costs of the acid when compared to the ester due to the lower weight.[1]

The term transesterification is typically used to describe hydroxy–ester, carboxy–ester, and ester–ester exchange reactions. The hydroxy–ester exchange reaction possesses the highest rate of reaction and is used for the production of numerous aromatic–aliphatic and wholly aromatic polyesters.[4] The transesterification based synthesis is particularly useful for when high melting and poorly soluble dicarboxylic acids are used. In addition, alcohols as condensation product are more volatile and thereby easier to remove than water.[11]

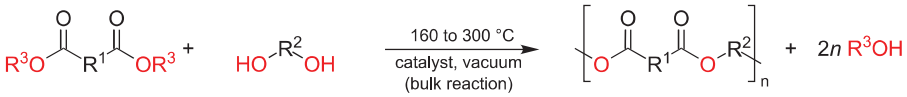

Scheme 4: Synthesis of a polyester via alcoholysis of a low-molecular-weight ester.

The high-temperature melt synthesis between bisphenol diacetates and aromatic dicarboxylic acids (Scheme 4) or in reverse between between bisphenols and aromatic dicarboxylic acid diphenyl esters (carried out at 220 to 320 °C upon the release of acetic acid) is, besides the acyl chloride based synthesis, the preferred route to wholly aromatic polyesters.[4]

1.2.2. Non-equilibrium-based polyesterification

The reaction between diacyl chlorides and alcohols or phenolic compounds has been widely applied to polyester synthesis and has been subject of numerous reviews and book chapters.[4,9,10,12] The reaction is carried out at lower temperatures than the equilibrium methods; possible types are the high-temperature solution condensation, amine catalysed and interfacial reactions. In addition, the use of activating agents is counted as non-equilibrium method. The equilibrium constants for the acyl chloride-based condensation yielding yielding arylates and polyarylates are very high indeed and are reported to be 4.3×10^3 and 4.7×10^3, respectively. This reaction is thus often referred to as a 'non-equilibrium' polyesterification.

Even though the acyl chloride based synthesis is also subject of reports in the patent literature, it is unlikely that the reaction is utilized on the production scale.[13] The method is limited by the acid dichlorides' high cost, its sensitivity to hydrolysis and the occurrence of side reactions.[14]

The high temperature reaction (100 to > 300 °C) of an diacyl chloride with an dialcohol yields the polyester and hydrogen chloride (Scheme 5). Under these relatively high temperatures the reaction proceeds rapidly without a catalyst.[12]

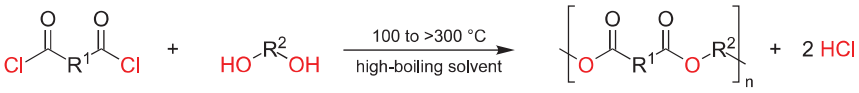

Scheme 5: Synthesis of a polyester via alcoholysis of an diacyl chloride without a catalyst.

The conversion of the reaction can be followed by titration of the evolved hydrogen chloride. A wide variety of solvents has been described including chlorinated benzenes (e.g. dichlorobenzene), chlorinated naphthalenes or diphenyls, as well as non-chlorinated aromatics like terphenyls, benzophenones or dibenzylbenzenes. The reaction was also applied successfully to the preparation of highly crystalline and poorly soluble polymers which require high temperatures to be kept in solution (at least until a sufficiently high molecular weight was achieved).[15]

In an interfacial acyl chloride-based reaction, the alcohol (generally in fact a phenol) is dissolved in the form of an alkoxide in an aqueous NaOH solution, the acyl chloride in an organic solvent immiscible with water such as dichloromethane, chlorobenzene or *n*-hexane, the reaction occurs at the interface under high-speed agitation near room temperature (Scheme 6).[12]

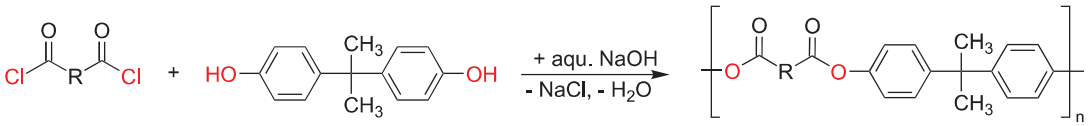

Scheme 6: Interfacial acyl chloride-based synthesis of a polyester.

The procedure is used for the production of polyarylates (polyesters based on bisphenols), polyamides, polycarbonates, poly(thiocarbonate)s, and others.[16]

Since the the molecular weight of the product obtained by a high-temperature synthesis can be seriously limited by side reactions, this problem is circumvented by the mild temperatures of interfacial polycondensation. The procedure is applied to the commercial production of bisphenol-A-based polyarylates like Unitika's U-Polymer.[4] Water could be in some cases replaced by an immiscible organic solvent (e. g. in the the adiponitrile/carbon tetrachloride system).[12] The procedure is of little use in the production of polyesters based on aliphatic diols which have higher pK_a values than phenols and therefore do not form alcoholate ions in aqueous solutions.[4]

The base catalysed reaction of an acyl chloride with an alcohol may also be carried out in one phase using tertiary amines (e. g. triethylamine, Et_3N) or pyridine (Scheme 7) as acid acceptors:

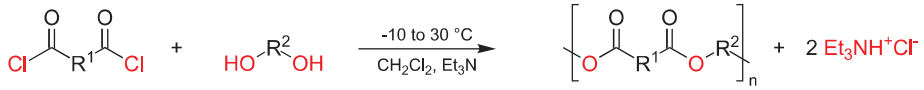

Scheme 7: Amine-catalysed acyl chloride-based synthesis of a polyester.

While acyl chloride-based polyesterifications proceed only very slowly at room temperature without a catalyst, the amine accelerates the reaction in several possible ways, although the mechanism is not fully understood.[12] However, it is known that tertiary amines can cause side-reactions such as the formation of ketenes and ketene dimers.[17]

Instead of acyl chlorides, so-called activating agents can be used, such as 1,1'-carbonyldiimidazole, dicyclohexylcarbodiimide, or trifluoroacetic anhydride. The polycondensation proceeds via the *in situ* conversion of the carboxylic acid into a more reactive intermediate while the activating agents are consumed. The reaction proceeds, for example, via an intermediate *N*-acylimidazole which reacts with catalytically acting sodium alkoxide (Scheme 8):[4]

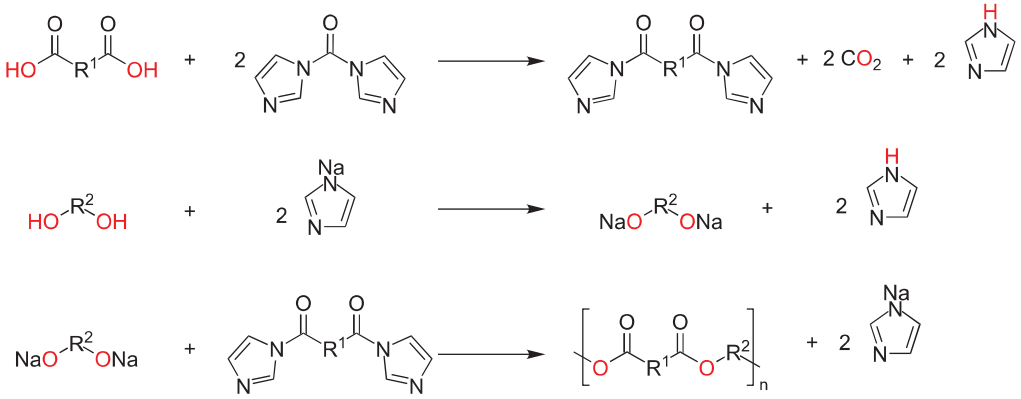

Scheme 8: Synthesis of a polyester using 1,1′-carbonyldiimidazole carbodiimide.

The use of activating agents for the production of high-melting aromatic polyesters and polyamides under mild conditions has been subject of intensive academic research since the 1980s, but the reactions have not gained commercial acceptance as similar results can be achieved with cheaper reactants.[4]

1.2.3. Aliphatic *vs.* aromatic polymers

Thermally stable polymers, which have a high proportion of aromatic structures, are also called high-performance plastics; this application-oriented classification compares such polymers with engineering plastics and commodity plastics. The continuous service temperature of high-performance plastics is generally stated as being higher than 150 °C,[18] whereas engineering plastics (such as polyamide or polycarbonate) are often defined as thermoplastics that retain their properties above 100 °C.[19] Commodity plastics (such as polyethylene or polypropylene) have in this respect even greater limitations, but they are manufactured in great amounts at low cost.

Poly(ester imides) contain an aromatic imide group in the repeat unit, the imide-based polymers have a high proportion of aromatic structures in the main chain and belong to the class of thermally stable polymers. Such polymers contain structures that impart high melting temperatures, resistance to oxidative degradation and stability to radiation and chemical reagents. Among the thermally stable polymers with commercial relevance are polyimides, polysulf-

ones, polyetherketones, and polybenzimidazoles. Of these, polyimides are most widely applied.[20] The polymers' structures result also in poor processing characteristics, in particular a high melting point and low solubility. The named properties are in particular based on a high percentage of aromatic carbons in the polymer backbone which produces a certain stiffness.[21] Approaches for an improvement of processability include the incorporation of flexible spacers into the backbone, the attachment of stable pendent groups or the incorporation of non-symmetrical structures.[20] Flexible spacers include, for example, ether or hexafluoroisopropylidene, carbonyl or aliphatic groups like isopropylidene; these groups allow bond rotation between aromatic rings. Less symmetrical structures, for example based on *meta*- or *ortho*-linked monomers introduce structural disorder and thereby decrease the crystallinity.[4]

The generally poor processability of aromatic polymers (for example, a high melting point and a low solubility) also limits the available options for synthesis and may require strong electron-donating co-solvents like HFIP or TFA for analysis (e. g. ^{1}H NMR spectroscopy) which themselves can introduce further practical limitations.

1.3. Acyl chlorides

The acyl chloride-based esterification is a common method for the synthesis of esters and for the synthesis of polyesters (polyesterification). Acyl chlorides (R-CO-Cl) are highly reactive compounds derived from carboxylic acids (R-CO-OH) in which the hydroxyl group was replaced by a chlorine atom.

1.3.1. Preparation of acyl chlorides

Acyl chlorides are most commonly synthesized[22] from a carboxylic acid and an inorganic acyl chloride such as thionyl chloride (Scheme 9):[23]

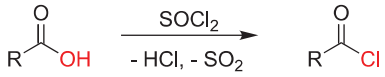

Scheme 9: Production of acyl chlorides with thionyl chloride.

Thionyl chloride[24] is a well-suited reagent as all the by-products (HCl, SO_2) are gases and residual thionyl chloride can be easily removed as a result of its low boiling point (76 °C). Also phosphorus trichloride (PCl_3),[25] phosphorus pentachloride (PCl_5)[26] or oxalyl chloride[27] ($[COCl]_2$) can be used. Relative to thionyl chloride, oxalyl chloride is more expensive

but also a milder reagent and therefore more selective. Acyl bromides and iodides are synthesized accordingly but are less common.[28] In addition, the Appel reaction can be used, having the advantage that no hydrogen chloride is released.[29]

1.3.2. Reactivity of acyl chlorides

Carboxylic acid halides are among the most reactive and versatile compounds in organic chemistry, and the full range of possible reactions has been reviewed.[30] Acyl chlorides have a greater reactivity than other carboxylic acid derivatives like acid anhydrides, esters or amides (Figure 2):[31]

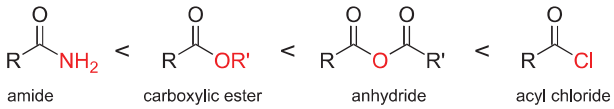

Figure 2: Relative reactivity of carboxylic acid derivatives.

Acid chlorides can therefore be used to synthesize all compounds listed as being of lower reactivity. The high reactivity of the acid chloride is based on the chloride ion being a weak base and an excellent leaving group so that even weak nucleophiles attack the carbonyl group. When compared to its parent compound (the carboxylic acid) the higher reactivity can be explained by the hydroxyl group being a much worse leaving group.

1.3.3. Reactions of acyl chlorides

Acid chlorides react with a large number of nucleophilic compounds like carboxylic acids (to anhydrides), alcohols or phenols (to esters), amines (to amides) or metal organic compounds such as Grignard reagents.[30] The alcoholysis of acyl halides (the alkoxy-dehalogenation) is believed to proceed via an S_N2 mechanism (Scheme 10).[32] However, the mechanism can also be tetrahedral or S_N1 in highly polar solvents[33] (while the S_N2 reaction involves a concerted reaction, the tetrahedral addition-elimination pathway involves a discernible intermediate)[34].

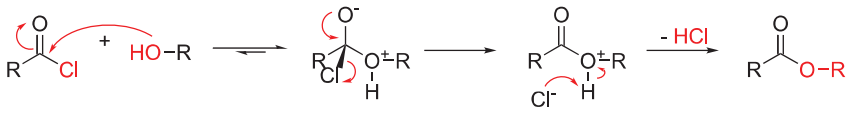

Scheme 10: Mechanism of ester formation via the alcoholysis of an acyl chloride.

During the nucleophilic substitution, the equilibrium can be shifted towards the product by capturing the hydrogen chloride with a base such as dilute sodium hydroxide solution or a basic solvent like pyridine or *N,N*-dimethylformamide. The used of dilute sodium hydroxide

solution results in formation of two phases (aqueous/organic): this type of reaction is called Schotten-Baumann reaction. Both pyridine as solvent and the two-phase reaction are used in the synthesis of polyesters and polyamides (e. g. for the so-called *nylon rope trick*[35]). Amines like pyridine furthermore catalyse the reaction of the acyl chlorides via an nucleophilic catalysis mechanism (Scheme 11). The amine attacks the carbonyl bond and presumably[36] forms first a transient tetrahedral intermediate and afterwards, by the displacement of the leaving group, a quaternary acylammonium salt. This quaternary acylammonium salt is more susceptible to attack by alcohols or other nucleophiles.

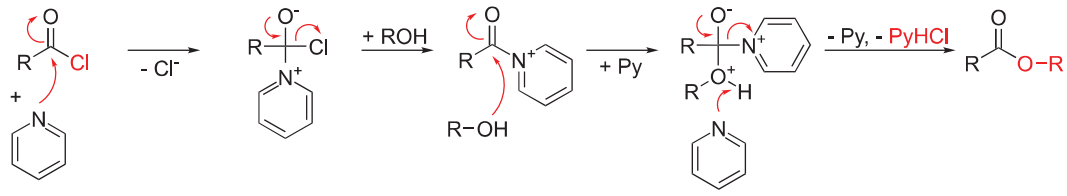

Scheme 11: Amine-catalysed ester formation using pyridine.

Besides nucleophilic substitution, acid chlorides can also participate in electrophilic aromatic substitution, the most common being the Friedel-Crafts acylation, in which the acyl group replaces a hydrogen atom in an aromatic system, catalysed by a Lewis acid like iron trichloride.[37]

1.4. Monomer sequences of polymers

The term sequence refers to a defined order of distinct elements. If different elements are present, for example the monomers A and B in a copolymer, they can be arranged in various ways. This has consequences on the materials properties and can be used for information storage as demonstrated by DNA. In the following, the analysis of sequences is described and the impact of a polymer's sequence on its properties.

1.4.1. Detection of sequences

The methods for sequence analysis of synthetic polymers differ from the sequence analysis of biopolymers (e. g. DNA or proteins). Synthetic polymers are produced by chain-growth or step-growth polymerization and show thereby polydispersity, whereas biopolymers are synthesized by complex template-based mechanisms and are sequence-defined and monodisperse. Synthetic polymers are a mixture of macromolecules of different length and sequence and are analysed via statistical measures (e. g. the degree of polymerization, comonomer composition or dyad and triad fractions).[38] Nuclear magnetic resonance (NMR)

spectroscopy is known as the most widely applied and "one of the most powerful techniques" for the sequence analysis of synthetic copolymers.[38,39] NMR spectroscopy allows determination of the relative abundance of comonomer sequences at the level of dyads and in cases of small repeat units even triads or more. It also allows the detection and quantification of chain defects and chain end groups, cyclic oligomers and by-products.[39] However, limitations of NMR spectroscopy are that it cannot, so far, provide information about the sequence distribution along the chain, like gradients, clusters or a long-range order.[38]

Monitoring the relative abundance of comonomer sequences is a common technique and is used, for example, to observe the progress of transesterification reactions between PET and PEN in their blends.

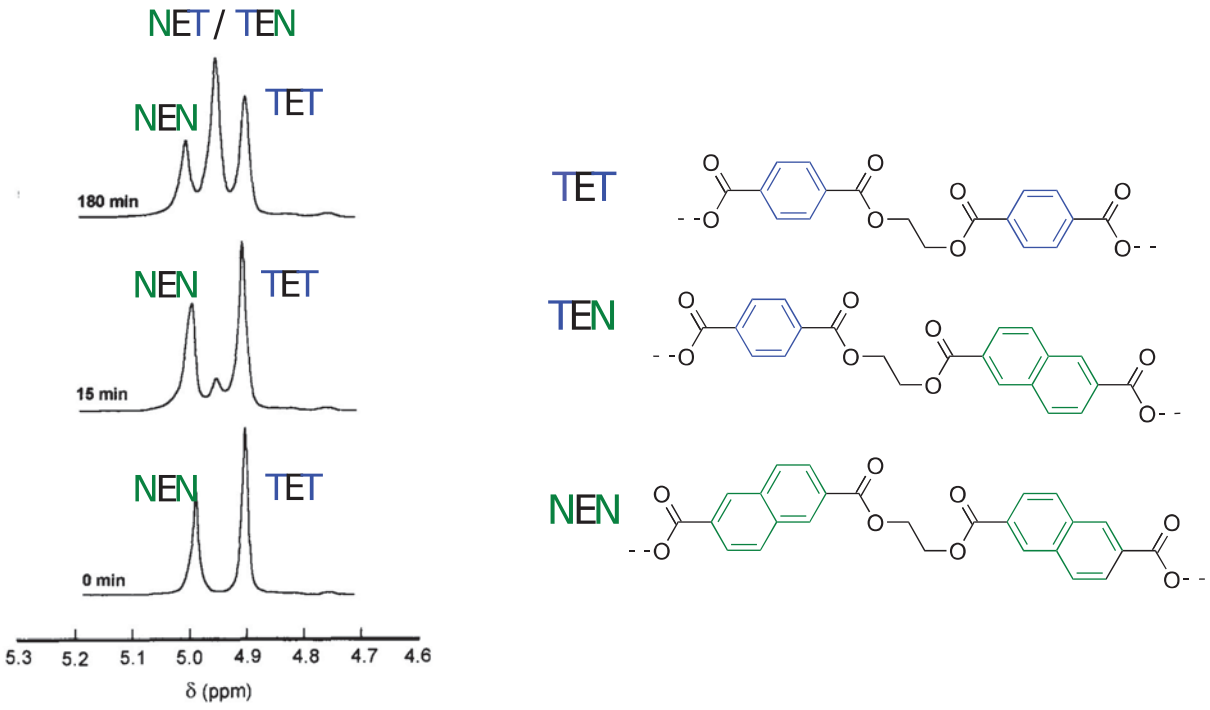

Figure 3: Left: ^{1}H NMR spectra of a PET/PEN 1:1 blend, used with permission.[40] With the progress of the reaction, the TET and NEN resonances are decreasing in intensity and the NET/TEN resonance emerges. Right: Structural formulae of polymer segments with assigned resonances.

During such a transesterification reaction, three resonances representing four diads can be distinguished via ^{1}H NMR spectroscopy by different chemical shifts of the oxyethylene units: The diads -terephthalate-oxyethylene-terephthalate- (TET) and -naphthalate-oxyethylene-naphthalate- (NEN), which are also present in the homopolymers poly(ethylene naphthalate) und poly(ethylene terephthalate), as well as the (indistinguishable) diads -terephthalate-oxyethylene-naphthalate- (TEN) and -naphthalate-oxyethylene-terephthalate- (NET), which

are exclusively present in the copolymer. In the spectrum of a 1:1 physical PET/PEN mixture, only the resonances corresponding to the diads TET and NEN are present at 4.90 and 5.00 ppm, respectively. Once a transesterification reaction occurs, a new resonance at 4.95 ppm emerges that increases in intensity with the reaction time, corresponding to the TEN / NET sequences (Figure 3).[39]

The example of poly(ethylene naphthalate) and poly(ethylene terephthalate) is relatively simple, as only the aromatic part of the polymers differ (naphthalate *vs.* terephthalate). In a blend of poly(ethylene naphthalate) and polytrimethylene terephthalate, already six resonances can be distinguished, since both, oxyethylene and oxypropylene, form three resonances.[41] The sequence patterns can become even more complex, when triads can be distinguished spectroscopically.[39] The extractable information is limited by the difference in chemical shift and the resonance width. In addition to ^{1}H NMR spectroscopy, also ^{13}C NMR spectroscopy is a common method for the sequencing shown above, which is characterized in particular by a very narrow resonance width.

Deconvolution and assignment of these triad-based resonances allows a quantitative determination of the degree of randomness and the average block length via integration of the distinguishable resonances. In a 1:1 mixture of two linear two-component 1:1 polycondensates $(A_1B_1)_n$ and $(A_2B_2)_n$ (with molecular weight high enough to neglected chain-ends), equations 3 and 4 are valid:

$$[A_i] = [B_i] \qquad (i = 1,2) \tag{3}$$

$$[A_1B_2] = [A_2B_1] \tag{4}$$

Equation 3 states that the molar ratio of all four repeat units is identical and equation 4 states that both types of copolymer are of identical concentration. In this case, the degree of randomness χ is calculated as given by equation 5:

$$\chi = \frac{[A_iB_j]}{[A_1][A_2]} \qquad (i,j = 1,2) \tag{5}$$

In the beginning of a transreaction process (e. g. transesterification or transamidation), the degree of randomness $\chi \approx 0$ as the system comprises a physical mixture of homopolymers or block copolymers. During the transreaction process χ increases up to $\chi = 1$ for a fully random copolymer. If $\chi > 1$ it indicates a tendency of the monomers to form alternating structure, up to $\chi = 2$ for a completely alternating copolymer.[42] The degree of randomness χ gives thereby statistical information about the polymer sequence. The calculation can be modified for three-component[43] and four-component[44] polycondensates.

NMR spectroscopy is used in industrially relevant systems to study the sequence distribution of copolymers or the occurrence of transesterification in polyester blends. A change in sequence distribution can effect the crystallinity, and transesterification can affect the compatibility of two otherwise incompatible polyesters, as described in the next Chapter. Depending on their degree of randomness, copolyesters can show different thermal transitions and behaviours.[45]

1.4.2. Impact on material properties

The sequence analysis of polymers is potentially useful, as the sequence has influence on the material properties. While it has long been known that the sequence of proteins is the basis for their properties, numerous examples of synthetic copolymeric materials are now known, in which the sequence of the comonomers has an impact on the macroscopic properties.[46]

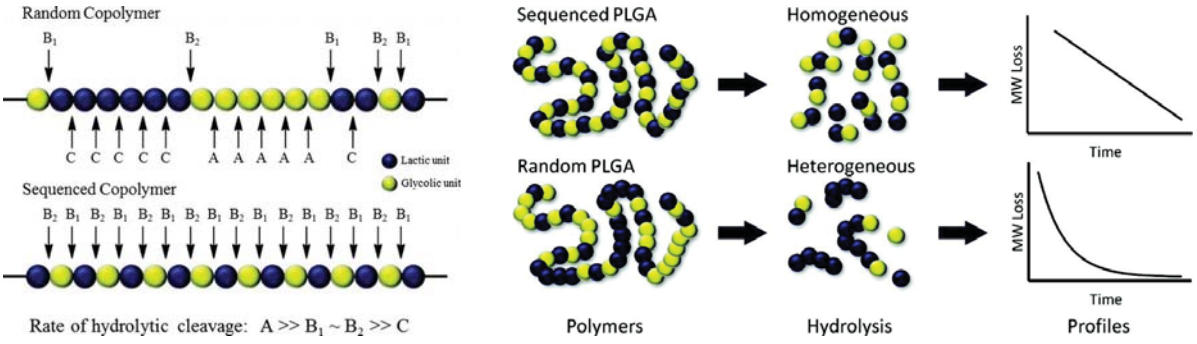

Figure 4: Left: Comparison between a random lactide-co-glycolide copolymer and an alternating lactide-co-glycolide copolymer. The random copolymer has in alternating sections the bonds B_1 and B_2 with intermediate hydrolysis rate and in blocky sections bond with the fast or slow hydrolysis rates A and C. The alternating copolymer has only bonds B_1 and B_2 with the intermediate hydrolysis rate B_1 and B_2. Right: Due to the blocky sections, the hydrolysis rate of the random copolymer is very fast initially but very slow at the end, whereas the alternating copolymer shows a steady rate. Used with Permission.[47]

It was found that the degradation kinetics of microparticles of the biodegradable aliphatic co-polyester poly(lactide-co-glycolide) are affected by its comonomer sequence (Figure 4). For alternating copolymers, nearly linear degradation profiles were found, whereas an exponential and overall higher degradation rate was found for random copolymers. The hydrolysis rate dependence on the sequence is ascribed first to the different reactivity of the comonomer bonds. The random copolymer has a high number of bonds of monomers of the same type, the same bonds which would be present in a homopolymer (bonds C and A). Such bonds have apparently a different hydrolysis rate than bonds between monomers of different type (bond B_1 and B_2), given in the alternating copolymers. A second reason for the different degradation kinetics is that a random copolymer contains at least small blocks of the same monomer. Such blocks are known to form microdomains which accelerate hydrolysis of the units within.[47,48]

Another study investigated sequence-specific peptoids (non-natural protein-like polymers) which exert a high degree of control over calcite ($CaCO_3$) mineralization, even in nanomolar concentration. The polymer's sequence could be used to tune the peptoid-crystal interactions and so control the growth rate and morphology.[49]

Acyclic diene metathesis (ADMET) can be used to prepare polyethylenes with precisely spaced alkyl branches from α,ω-dienes (Figure 5). The regular primary structure translates into a more uniform and narrower lamellar thickness in comparison to regiorandom polyethylene analogues. As a consequence, the precision polymers possess higher crystallinity and thereby sharper melting transitions and greater heats of fusion.[50,51]

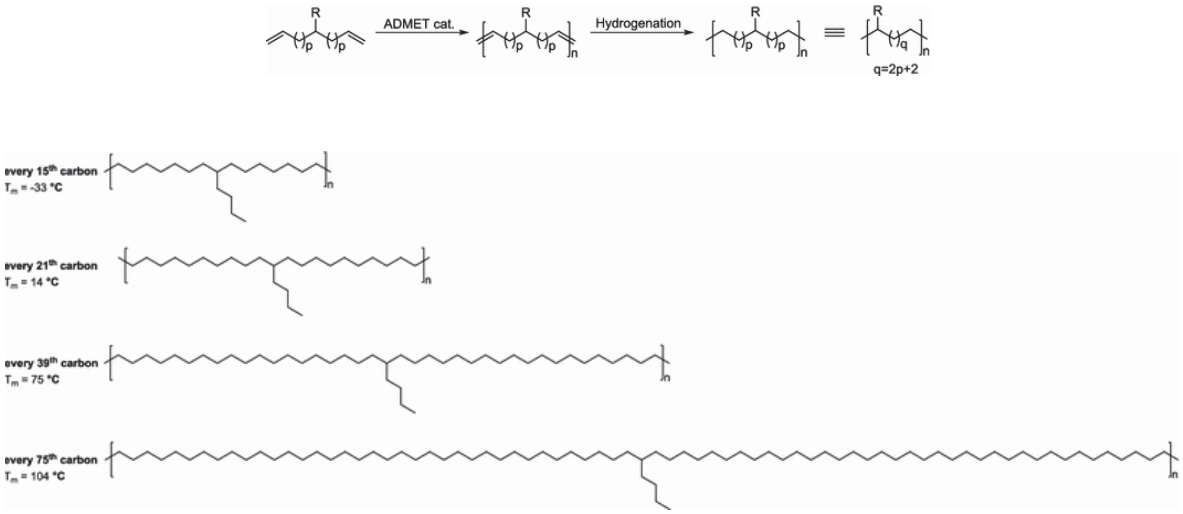

Figure 5: Left: Synthesis of polyethylene with sequence controlled branching via ADMET. Right: Three different polyethylenes with sequence controlled branching and the conversion with imidazole to an ionomer, used with permission.[50]

ADMET polymerization can also be used to produce precision ionomers via the quaternization of a bromide functionalized polymer with 1-methylimidazole.[52] The regioregular polyolefin-based precision ionomers exhibit higher melting points than regiorandom analogues, presumably caused by a different morphology due to their regioregularity.[53]

For technical applications, not only fully sequence-controlled polymers are of interest (as given for example in artificial sequence-defined polymers[54] or proteins[55]), but even if only a certain degree of statistical control exists.[56] For example, a random copolymer has a different sequence than a block copolymer and both differ in their macroscopic properties.[57]

Such statistical control allows the morphology of some materials to be controlled by changing the sequence. One example is the transesterification between homopolymers in a blend. The interchange reaction converts the mixture of homopolymers into a mixture of block copolymers. Further processing of the block copolymers randomises the copolymers sequence to shorter blocks until a fully random microstructure is obtained. The extent of transesterification and therefore the material's properties can be controlled by the reaction time. Increasing reaction time leads to more homogeneous interfaces and also affects the polymer's rheological and crystallization behaviour.[7] Also the macrostructure can be controlled to some degree: For example, phase separation between two incompatible polymers can lead to the formation of microspheres. One example is a phase-separated architecture in which PET microspheres are embedded in polycarbonate. By adoption of adequate temperature and reaction time, the PET microspheres are coated and stabilized by a copolymer formed *in situ* at the interface between the homopolymers (Figure 6).[58]

Other examples of the influence of sequence on macroscopic properties due to the degree of transesterification are the variable structure of CO_2-foamed polymers,[60] the control and maximising of tensile strength,[61] and the formation of a compatibiliser between matrix and particles to enhance stress transfer in the sample under mechanical load.[62] All these examples illustrate why it is useful to know the sequence of technically used polymer, or at least the degree of randomness/blockiness.

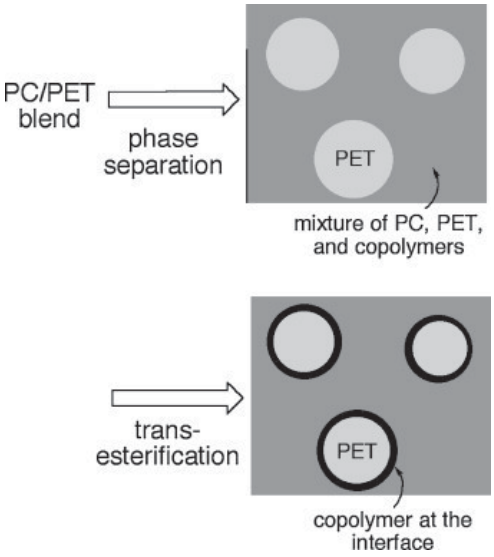

Figure 6: Phase separation occurring at the beginning of the reactive blending followed by interfacial transesterification allows to control the morphology, in this case the formation of microspheres. Used with permission.[59]

Interestingly, not only can a mixture of different homopolymers be randomized, but also the reverse process could be carried out in some cases (Figure 7). Fakirov *et al.* found that a kind of cycle could be carried out, as random copolymer could thus be turned back into a block copolymer (two homopolymers → block copolymer → random copolymer → block copolymer).[63,64] In case of some polymer blends it was found that sequential reordering is driven by the crystallization occurring at high temperatures (280 °C). Similar results were reported by other researchers.[65] The presence of a transesterification catalyst did speed up the reordering. In case of another polymer blend it was found that the crystallinity was only introduced when the melt was slowly cooled to room temperature; in this case the sequential reordering was miscibility-induced.[66] The immiscibility of the monomer repeat units near room temperature did therefore induce a reordering of the chain sequence. The interchange reaction requires usually very high temperatures, but recently, catalyst have been developed which allow the exchange reaction to proceed at lower temperatures.[67,68]

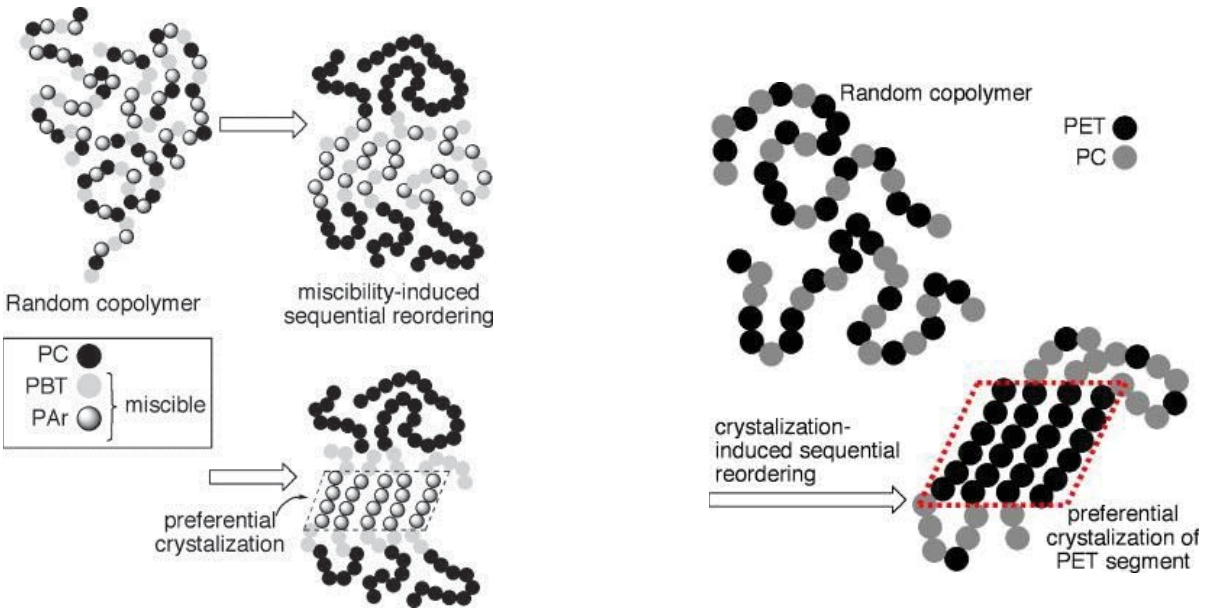

Figure 7: Sequential reordering: Left: Miscibility-induced sequential reordering.[59] Right: Crystallization-induced sequential reordering.[59] Used with permission.

1.5. Transesterification

Transesterification is a commonly used reaction. It is, for example, utilized in the production of biodiesel[69] or for the production of low molecular weight compounds[70]. Transesterification can also be used for the production of polyesters via a chain-growth or step-growth mechanism. It is applied in the modification of finalized polymers at side chains [e. g. in the production of poly(vinyl acetate phthalate) from poly(vinyl acetate)] as well as for modification of the main chain. The following section discusses exclusively the transesterification of finalized polymers in the main chain.

Transesterification reactions between polymers are described in the melt, in solution and in solid materials. Transesterification reactions in the melt are used for the production and modification of co-poly(ester)s from homo-poly(ester)s (during the "blending"), in solution for the production of macrocycles and in the solid in so-called vitrimers.[98]

1.5.1. The use of transesterification in polymer science

1.5.1.1. Transesterification in blends

The physical mixing of molten polymers is called blending. Blending is a successful and inexpensive technique that is used on an industrial scale[59] because it provides polymers which can combine the desirable properties of their parent polymers. A drawback is that most pairs of

homopolymers are thermodynamically immiscible with each other,[6] and so simple blending affords only materials with poor mechanical properties. Transesterification is a way to improve the interfacial properties of polymer blends by the (partial) formation of copolymers[39] without the need for compatibilizers. The exchange reactions between the blended polymers allows compatibility and miscibility of otherwise immisible polymers and cause, furthermore, drastic changes in physical and chemical properties.[3] Blending with transesterification ("reactive blending") can produce new materials with tailored properties and also allows the preparation of block copolymers,[71] which would otherwise be inaccessible via polycondensation.

Kotliar[72] and Wang[73] have reviewed transesterification and transamidation in polymer blends, respectively. The possible ester exchange reactions involve alcoholysis, acidolysis, and transesterification. In amides the amino-nitrogen takes the corresponding part of the oxygen and acidolysis, aminolysis, and transamidation are possible. These reaction types are also found in polymer blends.[3] Interchange reactions are one way to control the polymer sequence: the reaction proceeds from ordered to disordered structures while increasing the degree of randomness.[74] A physical blend of homopolymers reacts first to block copolymers, and continuing reactions reduce the size of homopolymeric segments and form finally fully random microstructures called statistical copolymers (Figure 8).[59] By the degree of transesterification the occurrence of particular sequences can be controlled, which can also lead to particular morphologies, e. g. microspheres (Chapter 1.4.2).

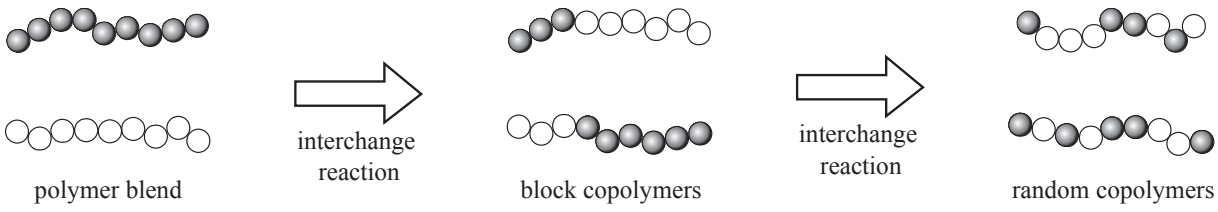

Figure 8: In a blend, two polymers are initially only physically mixed (left). Through interchange reactions, individual segments of the polymer chains are exchanged, creating block copolymers (middle). By further exchange, copolymers with a fully random sequence are finally formed (right).[59] Used with permission.

In academic investigations, mostly the rate of reaction was studied.[72] The progress of the transesterification can be followed as the ratio of the integrals of product and reactant resonances in the ^{1}H or ^{13}C NMR spectra.[75,76] The integrals represent the ratio of the sequences in homo- and copolymers; this is described in detail in Chapter 1.4.1. Since the progress of transesterification is thereby measurable, the reaction can be continued until the desired material properties have been achieved. Alternatively, DSC thermograms can be measured; since

the proportion of random sequences increases with increasing transesterification, the proportion of crystalline regions decreases and the melting peak disappears. The investigation may thus be performed by NMR spectroscopy and additionally by DSC.[61,77–81] Such investigations were carried out for a variety of polymer systems,[82,83] for example PET with PBT[84] or PEN[75], polyamides[64,85] or PC[80,86].

Three possible mechanisms of transesterification in polymer blends have been described in the literature:[72,74,87] alcoholysis, acidolysis, and ester–ester interchange (Figure 9). In low molecular weight esters the alcoholysis reaction rate $k_{\text{alcoholysis}}$ is dominating:[88]

$$k_{\text{alcoholysis}} >> k_{\text{acidolysis}} \approx k_{\text{interchange}}$$

It has been also found for some polymer interchange reactions that almost exclusively hydroxyl end groups are active.[89] However, the rate constants depends on a variety of parameters, including molecular structure and reaction conditions.[87] As the three mechanisms can in practice only rarely be distinguished, all three of the above mechanisms are often collectively referred to as transesterification.[88]

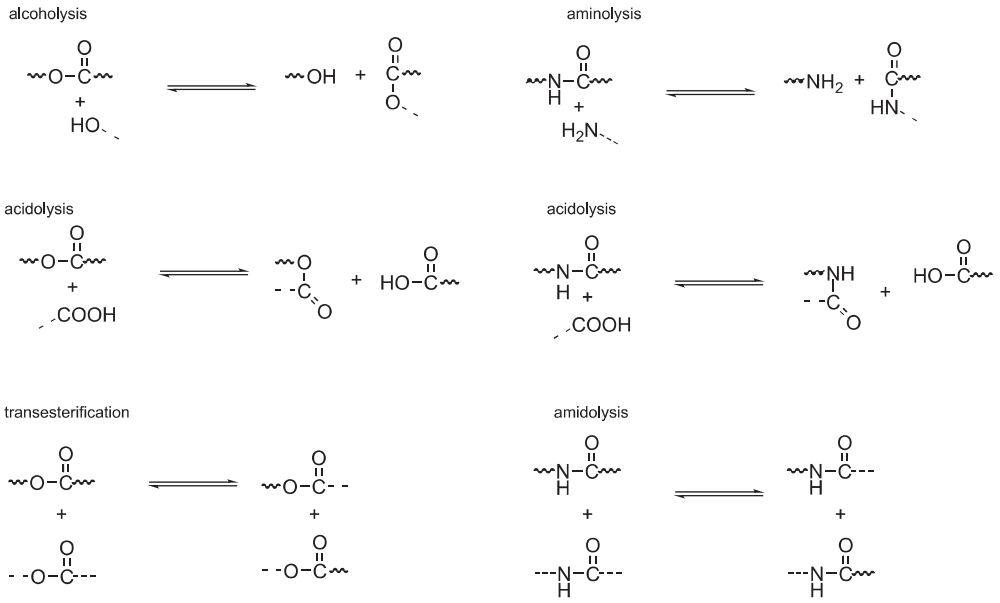

Figure 9: Left: The three mechanisms of transesterification, being alcoholysis, acidolysis and transesterification. Right: The three mechanisms of transamidation, being acidolysis, aminolysis and amidolysis.[59] Used with permission.

Transesterification is driven in the case of lactones during the ring-opening polymerization by the enthalpic gain of the relief of ring strain.[90] In contrast, transesterification between polymers in a blend does not involve any significant structural change (which could be accompanied by an enthalpic change). The interchange reaction is therefore entropically driven by the proceeding randomization of the polymer sequence.[59]

1.5.1.2. Transesterification in solution

Transesterification, previously described in bulk is also possible in solution, and is used for the production of block copolymers, e.g. in 1,2-dichlorobenzene as solvent.[71,91] When transesterification is carried out in very low polymer concentrations (e. g. 2 wt%), macrocycle formation (or "cyclodepolymerisation") dominates over polymer exchange reactions. Macrocyclic monomers can be used for the recycling of condensation polymers and can be converted back to high-molar-weight polymers via entropy-driven ring-opening polymerization.[92,93] This avoids energetically unfavourable depolymerisation during recycling.[94]

Such reactions exploit the well-known[95,96] ring−chain equilibria (Figure 10). In the presence of a catalyst and under suitable conditions, a equilibrium between condensation polymers and a corresponding family of homologous macrocyclic oligomers exists.[92]

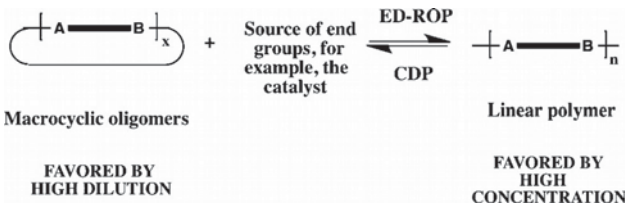

Figure 10: Equilibrium between macrocyclic oligomers and linear polymers. The reaction towards the polymer is called *entropically driven ring-opening polymerization* (ED-ROP), the back reaction *cyclodepolymerization* (CDP).[92] Used with permission.

Cyclodepolymerization is one possibility for the production of macrocycles among others. For the conversion of a polymer into macrocycles, the polymer is heated at high dilution (maximum ~2 wt%) for several hours, generally in the presence of a catalyst. Upon cooling, residual polymer often precipitates and the macrocycles can subsequently be isolated from solution. Yields are typically high (>85%) and the method can be used on a large scale (at least tens of grams, possibly even kilograms).[92]

Entropy-driven ring-opening polymerization for the conversion of the macrocycles to polymer is based on a shuffling of the linkages between the repeat units. Macrocycles are usually virtually strainless, so the enthalpy of polymerization is close to zero. At high concentrations, the polymer-macrocycle-equilibrium lies heavily on the side of the polymers; under neat conditions the mixture may contain >98% polymer and <2% macrocycles.[92]

1.5.1.3. Transesterification in bulk

Ester exchange reactions are also found in bulk polymers at elevated temperatures. One of the applications is in dynamic covalent polymer networks.[15] While conventional thermosets (crosslinked polymers) are fixed in shape once polymerized, thermosets based on dynamic covalent bonds can be reshaped. Various examples have been reviewed, based on sulfur related chemistry, Diels-Alder chemistry, transcarbamoylation, transesterification and others.[97] One well-known class of polymers, the so-called vitrimers, was introduced in 2011 by Leibler *et al*.[98] The initial vitrimers were based on an epoxy resin containing ester groups, which could be reprocessed with an injection machine in a quasi-molten state or deformed to complex shapes after heating. The moldability was based on carboxylic acids and β-hydroxy-esters, which would react at elevated temperatures in the presence of zinc acetate as catalyst in a transesterification reaction (Figure 11). This allows the network to behave dynamically and release stress by reshaping. It also allows healability of the thermoset.[99]

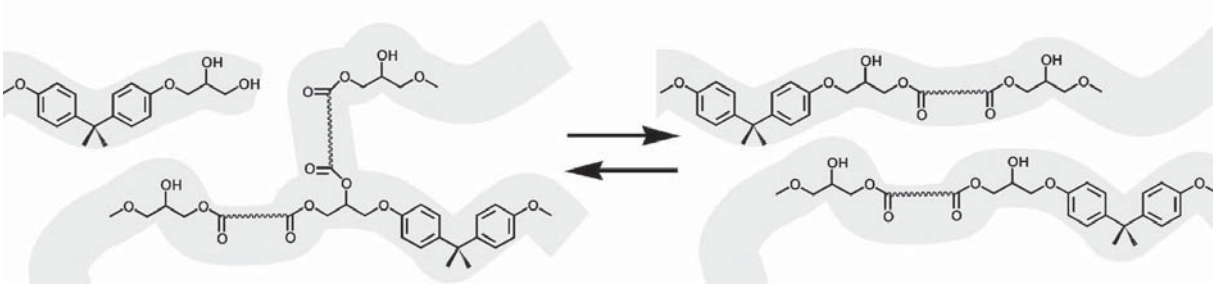

Figure 11: The concept of the vitrimers, which is based on crosslinked polymers with the ability for transesterification. The overall number of chains remains constant during the scope of the reaction.[98] Used with permission.

Another application of transesterification in bulk is in solid-state polymerization, which is used for the production of high molecular weight step-growth polymers, such as polyamides and polyesters. Solid state polymerization is performed at a temperature higher than the glass transition temperature (T_g) but lower than the melting point (T_m);[100] this gives the end groups in the amorphous areas a sufficient mobility to react while the condensation products are removed by a passing an inert gas stream.[101] When compared to the conventional melt synthesis,

solid state polymerization has some advantages, including the greater heat stability of the polymers in the solid compared to the melt,[102] a high degree of crystallinity which builds up during the increase in molecular weight[103] and the low environmental pollution because of the absence of solvents and a reduced temperature[104].

1.6. Non-covalent interactions

1.6.1. Supramolecular chemistry

Supramolecular chemistry comprised initially just the non-covalent interactions between a 'host' and a 'guest' molecule leading to the formation of a host-guest complex with a higher degree of order and possible functions like recognition, catalysis or transport. Modern supramolecular chemistry encompasses furthermore molecular devices and machines, molecular recognition, interfaces with complex matter (using self-assembly for the construction of multi-nanometre scale devices) and nanochemistry (e. g. nanoparticles). Jean-Marie Lehn, one of the prominent contributors in supramolecular chemistry and Nobel Prize in 1987, defined it as the "chemistry of molecular assemblies and of the intermolecular bond".[105] Other definitions include "the chemistry of the non-covalent bond" and "non-molecular chemistry".[106] In the following, various non-covalent interactions that form the basis of supramolecular chemistry are reviewed and discussed.

1.6.2. Non-covalent Interactions

A non-covalent bond is an electromagnetic, attractive interaction between molecules in which no electrons are shared between the binding partners (which differs thus from a covalent bond).[107] During the formation of a covalent bond, two atomic orbitals overlap and share electrons in newly formed (hybrid) orbitals, as described by the valence bond theory. In contrast, non-covalent interactions do not involve the formal sharing of electrons. Non-covalent interactions can be classified as electrostatic interactions (including ionic, hydrogen[108] and halogen bonding[109]), π-interactions, ligand-field interactions,[110] hydrophobic effects[111] or van der Waals forces. Non-covalent interactions are relatively weak; while covalent bonds range from 450 to 950 $kJ \cdot mol^{-1}$, non-covalent interactions are only in a range from 5 to 120 $kJ \cdot mol^{-1}$ (Table 1).[112]

Table 1: Overview of covalent and non-covalent interactions with examples.[112]

	Interaction type	Bond energy (kJ·mol^{-1})	Examples
	Covalent bond	< 450 (single) < 650 (double) < 950 (triple)	organic molecules
Electrostatic interactions	Ion–ion	200–300	NaCl
	Ion–dipole	50–200	crown ether complexes[113]
	Dipole–dipole	5–50	acetone
	Hydrogen bonding	4–120	DNA base pairing[114]
	π-π-stacking	< 50	benzene/hexafluorobenzene[115]
	Dispersion forces	< 5	liquid noble gases[113]
	Hydrophobic	solvent-related	Cyclodextrin inclusion compounds[116]

Even though a single non-covalent interaction is much weaker than a single covalent bond, the combination of numerous non-covalent bonds allows a considerable global binding energy. This forms the basis for functions such as self-organising molecules (like the DNA double-helix), enzyme catalysis, ion binding or molecular recognition and transport processes.[105]

1.6.2.1. Electrostatic Interactions

Electrostatic interactions include ion-ion, ion-dipolar and dipole-dipole interactions. Electrostatic interactions are not based (like e. g. covalent bonds) on the sharing of electrons but on the coulombic attraction between opposite charges or dipoles. Electrostatic interactions do not show any geometric orientation because the electrostatic field around a charge is uniform in all directions, and they are called therefore non-directional. Depending on the degree of polarization, electrostatic interactions are divided into ion-ion interactions (also called ionic bonds), ion-dipole interactions and dipole-dipole interactions. Based on Coulomb's law, the strength of the listed interactions decreases linearly with the decreasing polarization and with the inverse square of the distance.

Ion-ion interactions lie in the range 200-350 kJ·mol^{-1} and are thus the strongest non-covalent interactions. They are common in many inorganic compounds (e. g. sodium chloride, Figure 12a) but also in organic compounds as salts of carboxylic acids or amino acids. The high bonding energy is expressed in the high melting point of sodium chloride at 801 °C[117]. Even though ion-ion interactions are non-directional, ionic compounds form regular structures (crystals), driven by the energetic gain of efficient packing, called lattice energy. Ion-dipole interactions occur between (formally charged) ions and polar molecules, e. g. a sodium cation in water. The interaction ranges in strength from *ca.* 50 – 200 kJ·mol^{-1}. Dipole-dipole interactions typically exhibit bond strengths of only 5 – 50 kJ·mol^{-1} due to the weak polarization involved. These weak forces are expressed in, for example, the melting point of the carbonyl compound acetone (Figure 12b), which is at -95 °C[118] considerably lower than that of sodium chloride.

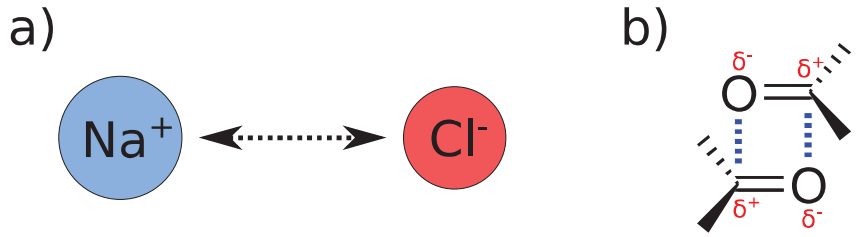

Figure 12: Left: Ion-ion interactions in sodium chloride. Right: Dipole-dipole interactions in acetone.

1.6.2.2. van der Waals forces

van der Waals forces are weak attractive interactions between uncharged atoms or molecules, and are thus a special case of electrostatic interaction.[107] However, while electrostatic interactions are active between permanent dipoles or charges, van der Waals forces are describing the interaction when at least one temporary dipole is involved. The average bond energy is on the order of 5 kJ·mol^{-1}.[119]

van der Waals forces can be divided into the Keesom force (betweeen permanent–permanent dipoles), Debye (permanent–induced dipoles) force, and London dispersion force (fluctuating induced-dipole induced-dipole interaction). The Keesom force originates from the attraction between two re-orientable permanent dipoles. The strength of the Keesom interaction diminishes with the inverse sixth power of the distance, while the interaction energy of two spatially fixed dipoles depends on the inverse third power of the distance. The Debye force is observed when one molecule with a permanent dipole approaches another molecule without dipole. The given dipole deforms the other molecule's electron cloud, inducing a second, re-

verse dipole and causes mutual attraction. The London force occurs between two molecules without any (initial) dipole. It is induced by random fluctuations of electron density in an electron cloud, causing a temporary dipole. This dipole acts like the permanent dipole given in the Debye forces and leads to mutual attraction. The strength of the forces is therefore determined by the polarisability of the molecule.[107,112] The change in binding strength as a function of the distance depends on the type of interaction (Table 2).

Table 2: Comparison of the binding strength dependence on the distance for some interactions.[107]

	Monopole	Dipole	Induced-dipole
Monopole	1/r	$1/r^2$	$1/r^4$
Dipole		$1/r^3$	$1/r^6$
Induced-dipole			$1/r^6$

1.6.2.3. π-interactions

π-Interactions are attractive forces between the π-electrons of an aromatic system and a dipole or charge. Depending on the dipole or charge, they can be categorized into π-π interactions[115], cation-π interactions,[120] anion-π interactions,[121] and polar-π interactions[122].

π-π-Interactions (between simple aromatics, like the benzene·hexafluorobenzene complex) are a special case of van der Waals forces, involving π-conjugated surfaces.[123] The exact nature of π–π interactions is still under debate.[115,123–125] They are used in various supramolecular systems for folding and assembly utilising alternating, face-centred electron-rich and electron-deficient aromatic units as building blocks.[115] In 1990, Hunter and Sanders proposed a model for π-π-interactions.[124] A distinction is made between simple aromatics (such as benzene or naphthalene) and stacking pairs in which one aromatic system is polarized by strongly electron-withdrawing groups: the latter is also called aromatic donor–acceptor interaction. For the two systems, completely different interactions apply and different geometries are formed.

Benzene serves as a model compound for the spatial orientation of simple, underivatized aromatics. The electrostatic attraction and repulsion based on the spatial orientation is summarized in Figure 13. The stacking behaviour of benzene is based on its quadrupole moment. At the two faces it is electron-rich, at the edges electron-poor. The quadrupole moment allows two possible attractive interactions of two benzene rings: In the case of the edge-to-face orientation, the rings are perpendicular one another other, giving a T-shaped geometry. In the off-

set stacked arrangement, the benzene rings are parallel (stacked) but offset relative to one another. In the off-set stacked arrangement the σ-framework of one benzene ring attracts the ring below it while the repulsion of π-electrons is minimised. A geometry that comes to mind by using the term π-π interactions is the stacked orientation, but in benzene itself this orientation is a non-favorable, since the same charges point to each other.[125]

Substituted or polycyclic aromatics adopt upon aromatic donor-acceptor interactions different geometries. While the electron density distribution of electron rich aromatics resembles benzene's electron density distribution, the electron withdrawing groups of electron-poor aromatics create in a central area of relative electron deficiency and thereby reverse the overall quadrupole moment (Figure 14). This contrary polarization of the two aromatic systems leads to a preference for face-to-face pairing.[127]

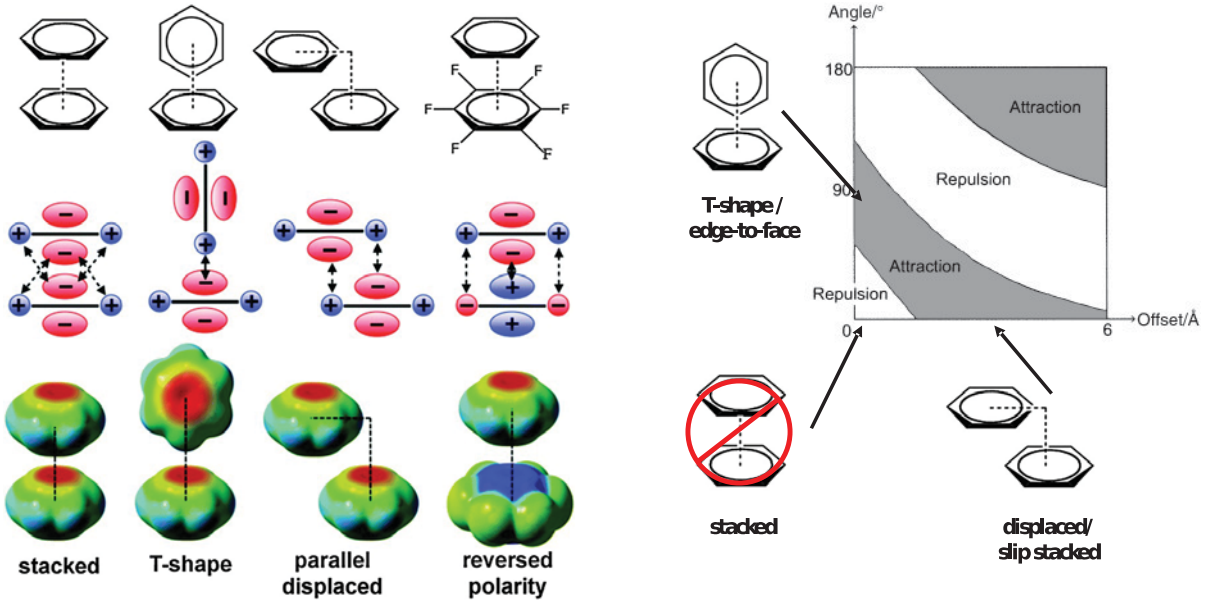

Figure 13: A) Stacked, t-shape, and displaced stacking geometry of benzene and the location of the polarization (blue are positive and red negative charges),[107,125] used with permission. B) Stacking geometries of benzene and intramolecular forces. T-shaped and displaced geometry causes an attractive force, the stacked geometry a repulsive force,[126] used with permission.

The aromatic donor–acceptor interactions have been exploited successfully by a number of research groups to create, with electron-rich and electron-deficient aromatic stacking, a variety of supramolecular architectures and assemblies.[128–132] π-Stacking also plays a role in the folding of proteins and DNA and can be exploited in synthetic systems such as supramolecular polymers.[133]

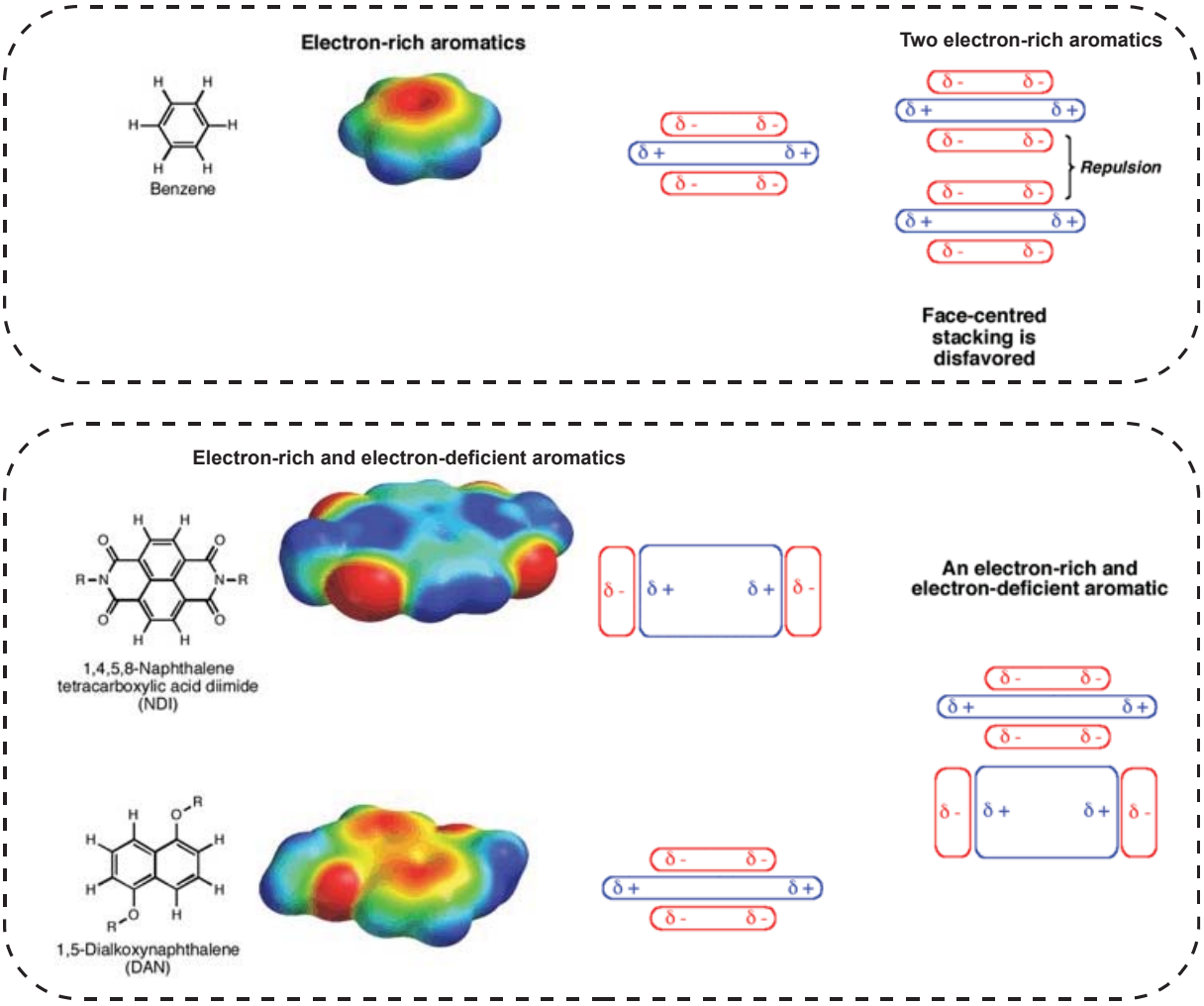

Figure 14: DFT calculation of the electrostatic potential surfaces for representative aromatic units. A) Benzene possesses electron-rich faces, so face-centered stacking of benzene rings is disfavoured. B) The electron-rich aromatics (such as 1,5-dialkoxynaphthalene) combined with electron-deficient aromatics (such as 1,4,5,8-naphthalenetetracarboxylic diimide, which possess a opposed quadrupole moment) favours in this case face-centred stacking. Adapted and used with permission.[115]

The face-centred stacked arrangement can be accompanied by π orbital mixing between the orbitals of the adjacent molecules. Donor-acceptor interaction occurs when one molecule has a empty orbital of low energy (acceptor) and the other molecule a filled orbital of high energy (donor). When these molecules align in appropriate orientation and distance, a charge transfer can occur from the donor to the acceptor, which stabilizes the now formed complex.[107] Often a

so-called charge transfer absorbance band can be observed due to light absorption by exciting an electron from the donor's HOMO π orbital to the acceptor's LUMO π orbital. This is not observed in the individual molecules, because the HOMO–LUMO energy gap of the formed complex is smaller than the HOMO–LUMO energy gaps of the individual molecules.[115]

As already investigated by Hunter and coworkers,[125] other interactions besides the aromatic donor-acceptor interaction also play a role in the assembly of electron-rich and electron-poor aromatics. These include solvophobic interactions and electronic interactions of the ligands. When solvent–solvent interactions are stronger than solvent–aromatic interactions, the solvent tends to a minimization of its surface and drives the aromatic molecules towards each other. The effect is particularly important in polar solvents which exhibit strong attractive interactions between the solvent molecules. It was found that solvent effects play a key energetic role, in particular in hydrogen-bonding solvents such as water.[134] Also direct electrostatic substituent-substituent interactions can play a considerable role in stacked geometries.[135,136]

1.6.3. Solvophobic interactions

Solvophobic interactions can be observed when non-polar molecules are brought into a polar solvent. The non-polar molecules show an apparent repulsion of the polar solvent; this is the reason that "oil" is insoluble in water.[137] However, the phenomenon is attributed to the attractive forces in the polar solvent, so that polar molecules tend to minimize any surface with non-polar molecules. At the interface between non-polar molecules and polar solvent a disruption of the dynamic weak interactions is caused (e. g. hydrogen bonds in water) as the non-polar molecules are unable to form attractive interactions. The polar interactions force the solvent to reorient around the non-polar molecules, and this leads to a structured "cage" (or clathrate). The polar solvent molecules in the clathrate have restricted mobility and thereby significantly reduced translational and rotational entropy. The non-polar molecules are thereby forced together to minimise the disruptive effect.[138]

1.6.4. Hydrogen bonding

Hydrogen bonding is an attractive force occurring between a hydrogen atom bound to an electronegative atom (such as nitrogen, oxygen, or fluorine) and an adjacent atom bearing a lone pair of electrons (Figure 15).[139] It is a special case of the commonly present dipole-dipole interactions[140]; however, hydrogen bonding is given its own category because it is, at up to 120 kJ/mol, uniquely strong (Table 1). Hydrogen is the only atom that uses the inner shell (1S) electron(s) in the covalent bond to an electronegative atom, and hydrogen nucleus is

thereby particularly exposed in the opposite direction. The hydrogen atom can thereby approach the adjacent lone pair of electrons more closely than other positively polarized atoms (distance limited by the Pauli exclusion effects). Since electrostatic attractions depend on the distance, hydrogen bonding is noticeably stronger than the average dipole-dipole interaction.[141,142]

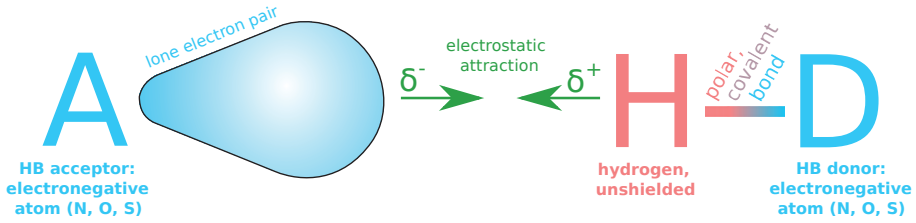

Figure 15: Hydrogen bonding, which is based on a electrostatic attraction between the basic electron lone pair of an electronegative atom and an deshielded proton attached to an electronegative atom. Based on a figure of Prof. Loren Dean Williams, Georgia Tech.

1.7. Foldamers

In natural copolymers, the characteristic properties do not only result from the sequence of monomers (the so-called primary structure), but from the folding caused by accumulation of weak inter- or intramolecular interactions (including hydrogen-bonding and hydrophobic interaction) to give ordered structures. These structures of higher order are the basis for biological functionality such as catalytic activity. In proteins, the most common types of secondary structures are the α-helix and the β-pleated sheet.

The term foldamers is used to describe synthetic polymers (or oligomers) that adopt specific, folded conformations in solution.[143,144] These macromolecules have attracted attention due to the possible emulation of natural systems and the design of functional artificial materials.[143] To achieve an ordered assembly, the entropic costs have to be compensated by an enthalpy gain from intra- or inter-chain noncovalent interactions;[145] these can be hydrogen bonding, CT interactions or other supramolecular forces listed in the section above. In the following, all examples focus on foldamers or conformationally restricted macromolecules: various examples have been reviewed.[145,146]

Iverson and co-workers reported the folding of a series of donor-acceptor containing oligomers based on alternating 1,5-dialkoxynaphthalene (DAN) and 1,4,5,8-naphthalene diimide (NDI) connected by flexible amino acid linkers (Figure 16).[147] The folded structure by intra-chain stacking was indicated by a red-shift of the CT bands of higher oligomers in UV/vis spectroscopy what suggests more than two groups being stacked simultaneously. As such a

red-shift is highly dependent on the distance and the orientation, it support the idea of the aromatic rings being electronically coupled via a stacked arrangement in a parallel configuration. ^{1}H NMR spectra gave further evidence for the proposed structure: besides a complexation shift of the diimide protons, COSY NMR spectroscopy indicated a restriction of rotational motion of the backbone from the presence of diastereotopic signals for the methylene groups and NOE measurements showed enhanced signals for the protons of adjacent aromatic rings.

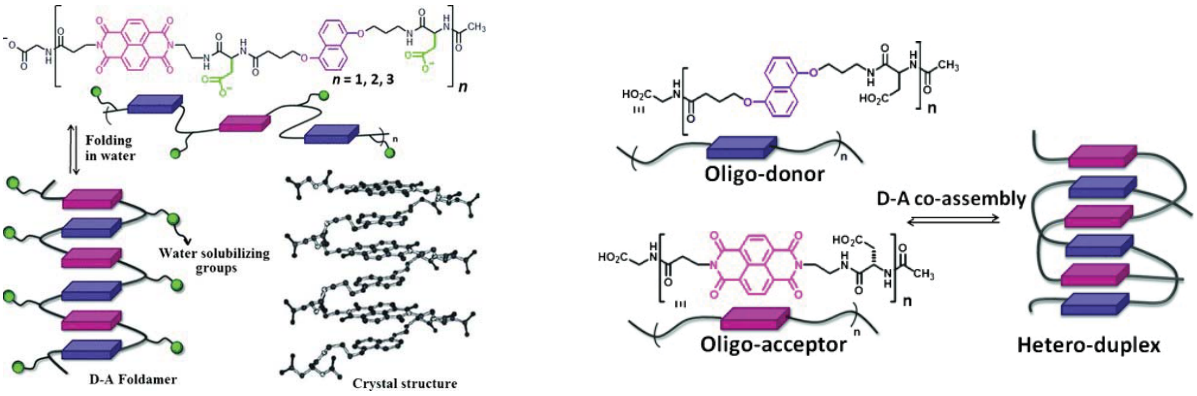

Figure 16: Left: NDI / DAN-based oligomers are folding in aqueous solution into a homoduplex. Right: The DAN-based and NDI-based homo-oligomer co-assemble in solution to a heteroduplex.[147,148] Used with permission.[145]

Iverson and co-workers also reported the folding of structurally similar NDI or 1,5-dialkoxynaphthalene-based homo-oligomers to hetero duplex stacks.[148] A Job plot using NMR spectroscopy data provided evidence for a 1:1 complexation mode. The complex strength was followed as a function of the oligomers length via ^{1}H NMR spectroscopy and isothermal titration calorimetric (ITC). It was found that every extension of the chain led to an increase in binding strength, with oligomers from $x = 1$ to $x = 4$ showing binding strengths from 1.3×10^{2} to 3.5×10^{5} M^{-1}, respectively. This remarkable effect of the chain length was attributed to the effect of multiple binding sites.

Ramakrishnan and co-workers presented a folding system based on high-molecular-weight polymers synthesized via polyimidization (M_n = 17,000). The alternating copolymer consists of pyromellitic diimide and 1,5-dialkoxynaphthalene linked by hexa(oxyethylene) as a flexible chain with cation coordinating ability. The foldamer has a certain similarity with the previously presented system (Figure 17), but is based on high-molecular-weight polymers instead of oligomers.[149]

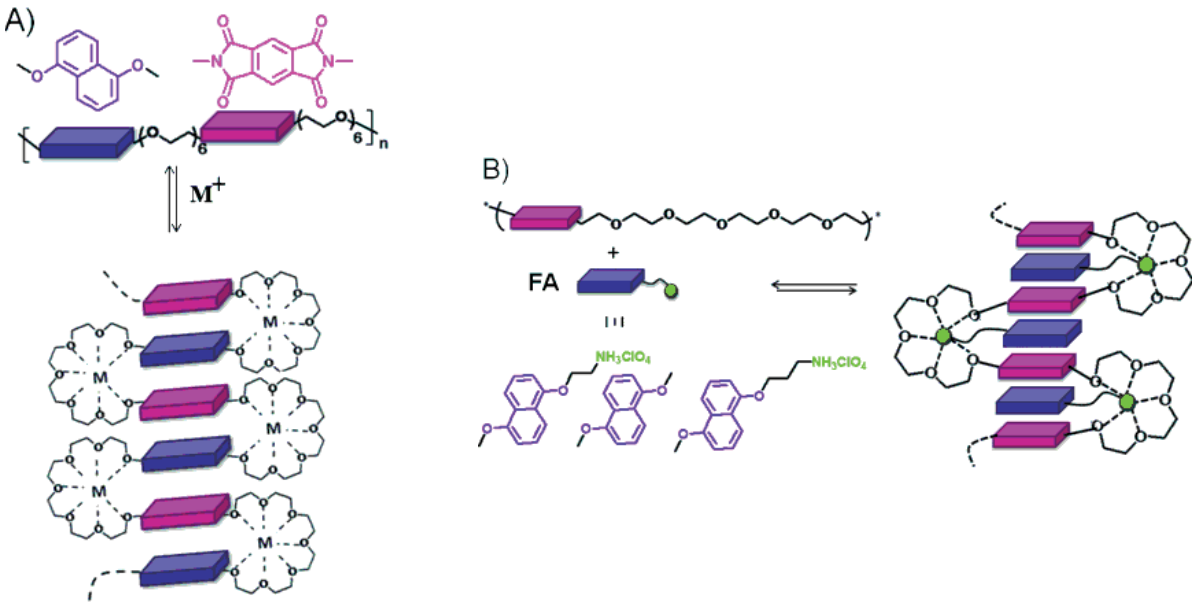

Figure 17: A) The PMDI / 1,5-dialkoxynaphthalene-based polyimide froms in solution a homoduplex. B) The PMDI-based homo-poly(imide) forms in the presence of the small molecule intercalator DAN-derivative a heteroduplex. Used with permission[145].

Evidence for the stacking conformation was provided by UV/vis and ^{1}H NMR spectroscopy. UV/vis spectroscopy revealed the occurrence of a charge-transfer band (at 450 nm) which was not present in the UV/vis spectra of individual donors or acceptor model homopolymers. Also the aromatic resonances showed a complexation shift in ^{1}H NMR spectroscopy in comparison to the individual model homopolymers. A signification additional complexation shift in NMR and increase of the complexation band in UV/vis spectra was found in the presence of alkali metal ions, which can form complexes with the hexaethylene oxide spacer. All the combined evidence supported the model shown in Figure 17. The group found also a size-dependence of the complexation ability of the hexaethylene oxide spacer. Potassium showed the strongest effect with an additional complexation shift of up to 0.5 ppm, while sodium and lithium produced complexation shifts of 0.3 and 0.1 ppm, respectively. Conversely, a systematic study of the spacer length from tetra(oxyethylene) to hexa(oxyethylene) was carried out, the polymer with the shortest tetra(oxyethylene) spacer showed the strongest complexation behaviour.[150]

Ramakrishnan's group synthesized, as in the previous examples, foldamers in which donor and acceptor were located in two separate molecules.[151,152] This was carried out in the shape of a electron-accepting PMDI /hexa(ethylene oxide)-based homopolymer and electron-donating DAN derivative as the small molecule, bearing an ammonium functionality. ^{1}H NMR and UV/vis spectroscopy revealed again a folded conformation. The ammonium functionality provides

ionic interactions with the ethylene oxide-spacer, and DAN a donor-acceptor interaction with PMDI. Interestingly, the folding could be suppressed by extraction of the alkali metal cation from the solution via the addition of 18-crown-6. A separate addition of equimolar amounts of DAN or an ammonium salt (so to say separated functionalities) led to minor complex formation only. In an alternative approach, both internal donors and binding sites for cation-induced folding were comprised in one macromolecule, thus a two-step folding of the macromolecules was achieved.[153]

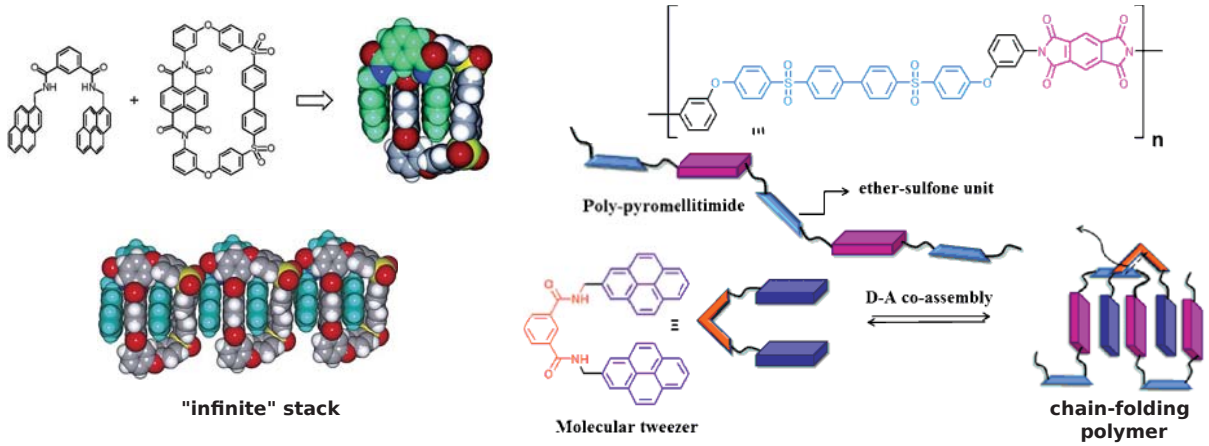

Figure 18: Left: Heterocomplex from polymer and small molecule (so-called tweezer).[154] Right: The polymer analogous to the macrocycle adopted in the presence of the tweezer a stacked conformation in solution.[155] The "infinite" stack of alternating donor and acceptor units (left) inspired the authors to create an analogous chain-folding polymer (right). Used with permission.[145]

Colquhoun and co-workers reported foldamers which were derived from a bisamide-functionalized pyrene-based tweezer complexing a pyromellitic diimide/4,4'-biphenylenedisulfone-based macrocycle (Figure 18, left).[154] The described complex as well as related complexes showed a high binding affinity (K_a = 9 200 ± 200 M^{-1}) as the complex was supported by simultaneous hydrogen bonding and CT interactions. In the crystal, the group found a "infinite" sequence of alternating donor and acceptor units (Figure 18, right) and extended the strategy later later to a macromolecular system, conceptually by opening the macrocycles and joining them into a polymer. The analogous polymer in solution did indeed fold into an "infinite macrocycle stack" around the described tweezer,[155] as indicated by ^{1}H NMR spectroscopy and supported by X-ray crystal structures of model oligomer-complexes[156]. This so-called chain-folding effect could be used for ^{1}H NMR spectroscopic analysis of copolyimide-sequences comprising up to 27 aromatic rings and is the basis for the work described in the present thesis.

1.8. References

1 H. Köpnick, M. Schmidt, W. Brügging, J. Rüter and W. Kaminsky, in *Ullmann's Encyclopedia of Industrial Chemistry*, Wiley-VCH Verlag GmbH & Co. KGaA, Weinheim, Germany, 2000.

2 C. Jerome and P. Lecomte, *Adv. Drug Deliv. Rev.*, 2008, **60**, 1056–76.

3 O. Dechy-Cabaret, B. Martin-Vaca and D. Bourissou, *Chem. Rev.*, 2004, **104**, 6147–6176.

4 M. E. Rogers and T. E. Long, *Synthetic Methods in Step-Growth Polymers*, John Wiley & Sons, Inc., Hoboken, NJ, USA, 2003.

5 X. Kong, H. Qi and J. M. Curtis, *J. Appl. Polym. Sci.*, 2014, **131**, 40579–40586.

6 H. Park, J. Seo, H.-Y. Lee, H.-W. Kim, I. B. Wall, M.-S. Gong and J. C. Knowles, *Acta Biomater.*, 2012, **8**, 2911–2918.

7 T. Gurunathan, S. Mohanty and S. K. Nayak, *Polym. Plast. Technol. Eng.*, 2016, **55**, 92–117.

8 B. Testud, D. Pintori, E. Grau, D. Taton and H. Cramail, *Green Chem.*, 2017, **19**, 259–269.

9 S. V. Vinogradova, *Polym. Sci. U.S.S.R.*, 1977, **19**, 769–808.

10 A. Duda and S. Penczek, in *Biopolymers Online*, eds. Y. Doi and A. Steinbüchel, Wiley-VCH Verlag GmbH & Co. KGaA, Weinheim, Germany, 2005, pp. 371–383.

11 A. Ravve, *Principles of Polymer Chemistry*, Springer New York, New York, NY, 2012.

12 F. Pilati, in *Comprehensive Polymer Science and Supplements*, Elsevier, 1989, pp. 275–315.

13 K.-W. Lienert, in *Progress in Polyimide Chemistry II*, ed. H. R. Kricheldorf, Springer Berlin Heidelberg, Berlin, Heidelberg, 1999, vol. 141, pp. 45–82.

14 M. Sokolsky-Papkov, R. Langer and A. J. Domb, *Polym. Adv. Technol.*, 2011, **22**, 502–511.

15 B. D. Dean, M. Matzner and J. M. Tibbitt, in *Comprehensive Polymer Science and Supplements*, Elsevier, New York, 1989, pp. 317–329.

16 V. V. Korshak and V. A. Vasnev, in *Comprehensive Polymer Science and Supplements*, Elsevier, New York, 1989, pp. 167–196.

17 H. R. Kricheldorf, O. Nuyken and G. Swift, *Handbook of Polymer Synthesis*, CRC Press, Florida, 2004.

18 D. Parker, J. Bussink, H. T. van de Grampel, G. W. Wheatley, E.-U. Dorf, E. Ostlinning, K. Reinking and F. Schubert, in *Ullmann's Encyclopedia of Industrial Chemistry*, Wiley-VCH Verlag GmbH & Co. KGaA, Weinheim, Germany, 2011.

19 H.-G. Elias and R. Mülhaupt, in *Ullmann's Encyclopedia of Industrial Chemistry*, Wiley-VCH Verlag GmbH & Co. KGaA, Weinheim, Germany, 2015, pp. 1–70.

20 P. E. Cassidy, T. M. Aminabhavi and V. S. Reddy, in *Kirk-Othmer Encyclopedia of Chemical Technology*, John Wiley & Sons, Inc., Hoboken, NJ, USA, 2000.

21 T. Whelan, *Polymer Technology Dictionary*, Springer Netherlands, Dordrecht, 1994.

22 M. F. Ansell, in *Acyl Halides (1972)*, John Wiley & Sons, Ltd., Chichester, UK, pp. 35–68.

23 M. B. Smith and J. March, *March's Advanced Organic Chemistry: Reactions, Mechanisms, and Structure, 7th Edition*, Wiley-Blackwell, Hoboken, 7th edn., 2007.

24 J. S. Pizey, *Synthetic Reagents, Vol. 1*, Halsted Press, New York, 1974.

25 C. F. H. Allen and W. E. Barker, *Org. Synth.*, 1932, **12**, 16.

26 R. Adams and R. L. Jenkins, *Org. Synth.*, 1923, **3**, 75.

27 R. Salmon and I. V. Efremov, in *Encyclopedia of Reagents for Organic Synthesis*, John Wiley & Sons, Ltd, Chichester, UK, 2008, pp. 329–329.

28 E. Keinan and M. Sahai, *J. Org. Chem.*, 1990, **55**, 3922–3926.

29 M. J. Taschner, in *Encyclopedia of Reagents for Organic Synthesis*, John Wiley & Sons, Ltd, Chichester, UK, 2001, vol. 1, pp. 12–15.

30 N. O. V. Sonntag, *Chem. Rev.*, 1953, **52**, 237–416.

31 J. Buddrus, *Grundlagen der Organischen Chemie*, Gruyter, New York, 2011.

32 T. W. Bentley, G. Llewellyn and J. A. McAlister, *J. Org. Chem.*, 1996, **61**, 7927–7932.

33 C. H. Bamford and C. F. H. Tipper, *Comprehensive Chemical Kinetics: Ester Formation and Hydrolysis and Related Reactions*, Elsevier, Amsterdam, 1972.

34 J. M. Fox, O. Dmitrenko, L. Liao and R. D. Bach, *J. Org. Chem.*, 2004, **69**, 7317–7328.

35 P. W. Morgan and S. L. Kwolek, *J. Chem. Educ.*, 1959, **36**, 182–184.

36 P. Hubbard and W. J. Brittain, *J. Org. Chem.*, 1998, **63**, 677–683.

37 M. Rueping and B. J. Nachtsheim, *Beilstein J. Org. Chem.*, 2010, **6**, 1–24.

38 H. Mutlu and J.-F. Lutz, *Angew. Chem. Int. Ed.*, 2014, **53**, 13010–13019.

39 A. M. de Ilarduya and S. Muñoz-Guerra, *Macromol. Chem. Phys.*, 2014, **215**, 2138–2160.

40 S. C. Lee, K. H. Yoon, I. H. Park, H. C. Kim and T. W. Son, *Polymer*, 1997, **38**, 4831–4835.

41 D.-H. Huang, E. M. Woo and L.-T. Lee, *Colloid Polym. Sci.*, 2006, **284**, 843–852.

42 K. L. L. Eersels, A. M. Aerdts and G. Groeninckx, in *Transreactions in Condensation Polymers*, Wiley-VCH Verlag GmbH, Weinheim, Germany, pp. 267–317.

43 R. Yamadera and M. Murano, *J. Polym. Sci. Part A-1 Polym. Chem.*, 1967, **5**, 2259–2268.

44 J. Devaux, P. Godard, J. P. Mercier, R. Touillaux and J. M. Dereppe, *J. Polym. Sci. Polym. Phys. Ed.*, 1982, **20**, 1881–1894.

45 W.-D. Li, J.-B. Zeng, X.-J. Lou, J.-J. Zhang and Y.-Z. Wang, *Polym. Chem.*, 2012, **3**, 1344.

46 J.-F. Lutz, M. Ouchi, D. R. Liu and M. Sawamoto, *Science*, 2013, **341**, 1238149–1238149.

47 J. Li, R. M. Stayshich and T. Y. Meyer, *J. Am. Chem. Soc.*, 2011, **133**, 6910–6913.

48 J. Li, S. N. Rothstein, S. R. Little, H. M. Edenborn and T. Y. Meyer, *J. Am. Chem. Soc.*, 2012, **134**, 16352–16359.

49 C. L. Chen, J. Qi, R. N. Zuckermann and J. J. Deyoreo, *J. Am. Chem. Soc.*, 2011, **133**, 5214–5217.

50 N. F. Sauty, L. C. da Silva, M. D. Schulz, C. S. Few and K. B. Wagener, *Appl. Petrochemical Res.*, 2014, **4**, 225–233.

51 P. Atallah, K. B. Wagener and M. D. Schulz, *Macromolecules*, 2013, **46**, 4735–4741.

52 B. S. Aitken, C. F. Buitrago, J. D. Heffley, M. Lee, H. W. Gibson, K. I. Winey and K. B. Wagener, *Macromolecules*, 2012, **45**, 681–687.

53 Z.-L. Li, L. Li, X.-X. Deng, A. Lv, C.-H. Wang, F.-S. Du and Z.-C. Li, *J. Polym. Sci. Part A Polym. Chem.*, 2013, **51**, 2900–2909.

54 J.-F. Lutz, J.-M. Lehn, E. W. Meijer and K. Matyjaszewski, *Nat. Rev. Mater.*, 2016, **1**, 16024.

55 G. Petsko and D. Ringe, *Protein Structure and Function*, Oxford University Press, London, 2008.

56 N. Badi, D. Chan-Seng and J.-F. Lutz, *Macromol. Chem. Phys.*, 2013, **214**, 135–142.

57 K. Matyjaszewski and K. A. Davis, *Statistical, Gradient, Block and Graft Copolymers by Controlled/Living Radical Polymerizations*, Springer Berlin Heidelberg, Berlin, Heidelberg, 2002, vol. 159.

58 H. Yoon, Y. Feng, Y. Qiu and C. C. Han, *J. Polym. Sci. Part B Polym. Phys.*, 1994, **32**, 1485–1492.

59 T. Maeda, H. Otsuka and A. Takahara, *Prog. Polym. Sci.*, 2009, **34**, 581–604.

60 P. Gong and M. Ohshima, *Polym. Eng. Sci.*, 2015, **55**, 375–385.

61 C. Wu, C. D. Han, Y. Suzuki and M. Mizuno, *Macromolecules*, 2006, **39**, 3865–3877.

62 Y. Guo, J. He, X. Zhang, S. Sun and H. Zhang, *J. Macromol. Sci. Part B*, 2015, **54**, 823–835.

63 S. Fakirov, M. Sarkissova and Z. Denchev, *Macromol. Chem. Phys.*, 1996, **197**, 2837–2867.

64 Z. Denchev, M. Sarkissova, S. Fakirov and F. Yilmaz, *Macromol. Chem. Phys.*, 1996, **197**, 2869–2887.

65 L.-J. Li, R.-T. Duan, J.-B. Zhang, X.-L. Wang, L. Chen and Y.-Z. Wang, *Ind. Eng. Chem. Res.*, 2013, **52**, 5326–5333.

66 Z. Fakirov, S; Sarkissova, M.; Denchev, *Macromol. Chem. Phys.*, 1996, **197**, 2889–2907.

67 M. G. Stanton and M. R. Gagne, *J. Am. Chem. Soc.*, 1997, **119**, 5075–5076.

68 J. M. Hoerter, K. M. Otte, S. H. Gellman, Q. Cui and S. S. Stahl, *J. Am. Chem. Soc.*, 2008, **130**, 647–654.

69 A. B. Ferreira, A. Lemos Cardoso and M. J. da Silva, *ISRN Renew. Energy*, 2012, **2012**, 1–13.

70 J. Otera, *Chem. Rev.*, 1993, **93**, 1449–1470.

71 T. Debuissy, E. Pollet and L. Avérous, *Eur. Polym. J.*, 2017, **90**, 92–104.

72 A. M. Kotliar, *J. Polym. Sci. Macromol. Rev.*, 1981, **16**, 367–395.

73 R. S. Porter and L.-H. Wang, *Polymer*, 1992, **33**, 2019–2030.

74 A. D. Litmanovich, N. A. Platé and Y. V. Kudryavtsev, *Prog. Polym. Sci.*, 2002, **27**, 915–970.

75 R. M. Medina, D. Likhatchev, L. Alexandrova, A. Sánchez-Solís and O. Manero, *Polymer*, 2004, **45**, 8517–8522.

76 Y. H. Zhao, G. H. Xu, H. T. Jia and J. Sheng, *J. Macromol. Sci. Part A*, 2003, **40**, 461–473.

77 D. E. Martinez-Tong, M. Soccio, A. Sanz, T. A. Ezquerra, N. Lotti, A. Munari and A. Nogales, *Soft Matter*, 2012, **8**, 6723.

78 Z. Denchev, H. R. Kricheldorf and S. Fakirov, *Macromol. Chem. Phys.*, 2001, **202**, 574–586.

79 G. Y. Zhang, J. W. Ma, B. X. Cui, X. L. Luo and D. Z. Ma, *Macromol. Chem. Phys.*, 2001, **202**, 604–613.

80 K. H. Wei and K. F. Su, *J. Appl. Polym. Sci.*, 1996, **59**, 787–796.

81 S. Collins, A. M. Kenwright, C. Pawson, S. K. Peace, R. W. Richards, W. A. MacDonald and P. Mills, *Macromolecules*, 2000, **33**, 2974–2980.

82 V. M. Nadkarni and A. K. Rath, in *Handbook of Thermoplastic Polyesters*, Wiley-VCH Verlag GmbH & Co. KGaA, Weinheim, FRG, 2005, pp. 835–869.

83 V. M. Nadkarni and A. K. Rath, in *Handbook of Thermoplastic Polyesters*, Wiley-VCH Verlag GmbH & Co. KGaA, Weinheim, FRG, 2005, pp. 869–893.

84 B. Jacques, J. Devaux, R. Legras and E. Nield, *J. Polym. Sci. Part A Polym. Chem.*, 1996, **34**, 1189–1194.

85 S. Matsumura, A. R. Hlil, C. Lepiller, J. Gaudet, D. Guay, Z. Shi, S. Holdcroft and A. S. Hay, *Am. Chem. Soc. Polym. Prepr. Div. Polym. Chem.*, 2008, **49**, 511–512.

86 E. B. Gowd and C. Ramesh, *Polymer*, 2005, **46**, 7443–7449.

87 H. R. Kricheldorf and Z. Denchev, in *Transreactions in Condensation Polymers*, Wiley-VCH Verlag GmbH, Weinheim, Germany, pp. 1–78.

88 C. M. McCullagh and J. Blackwell, in *Comprehensive Polymer Science and Supplements*, Elsevier, New York, 1989, pp. 389–410.

89 T. Tanguy, J. P. Bonnet, Y. V. Kudryavtsev, M. Tessier and A. Fradet, *Macromolecules*, 2010, **43**, 9318–9327.

90 A. Duda, A. Kowalski, S. Penczek, H. Uyama and S. Kobayashi, *Macromolecules*, 2002, **35**, 4266–4270.

91 H. Erduranli, B. Hazer and M. Borcakli, *Macromol. Symp.*, 2008, **269**, 161–169.

92 P. Hodge, *Chem. Rev.*, 2014, **114**, 2278–2312.

93 S. Salhi, M. Tessier, R. El and A. Fradet, *Polymer*, 2014, **55**, 73–82.

94 D. Tillier, H. Lefebvre, M. Tessier, J. C. Blais and A. Fradet, *Macromol. Chem. Phys.*, 2004, **205**, 581–592.

95 J. J. L. Bryant and J. A. Semlyen, *Polymer*, 1997, **38**, 4531–4537.

96 J. A. Semlyen, Ed., *Cyclic Polymers*, Springer Netherlands, Dordrecht, 1986.

97 W. Zou, J. Dong, Y. Luo, Q. Zhao and T. Xie, *Adv. Mater.*, 2017, **29**, 1606100.

98 D. Montarnal, M. Capelot, F. Tournilhac and L. Leibler, *Science*, 2011, **334**, 965–968.

99 M. Capelot, D. Montarnal, F. Tournilhac and L. Leibler, *J. Am. Chem. Soc.*, 2012, **134**, 7664–7667.

100 T. M. Chang, *Polym. Eng. Sci.*, 1970, **10**, 364–368.

101 S. N. Vouyiouka, E. K. Karakatsani and C. D. Papaspyrides, *Prog. Polym. Sci.*, 2005, **30**, 10–37.

102 S. D. Bruck, *Ind. Eng. Chem. Prod. Res. Dev.*, 1963, **2**, 119–121.

103 R. Srinivasan, P. Desai, A. S. Abhiraman and R. S. Knorr, *J. Appl. Polym. Sci.*, 1994, **53**, 1731–1743.

104 L. Li, N.-X. Huang, Z.-H. Liu, Z.-L. Tang and W.-S. Yung, *Polym. Adv. Technol.*, 2000, **11**, 242–249.

105 J.-M. Lehn, *Angew. Chem. Int. Ed.*, 1990, **29**, 1304–1319.

106 J. W. Steed and J. L. Atwood, *Supramolecular Chemistry*, John Wiley & Sons, Ltd, Chichester, UK, 2009.

107 E. V. Anslyn and D. A. Dougherty, *Modern physical organic chemistry*, University Science Books, Sausalito, Calif., 2006.

108 P. A. Kollman and L. C. Allen, *Chem. Rev.*, 1972, **72**, 283–303.

109 G. Cavallo, P. Metrangolo, R. Milani, T. Pilati, A. Priimagi, G. Resnati and G. Terraneo, *Chem. Rev.*, 2016, **116**, 2478–2601.

110 J. Zhao, D. Yang, X.-J. Yang and B. Wu, *Coord. Chem. Rev.*, 2019, **378**, 415–444.

111 N. T. Southall, K. A. Dill and A. D. J. Haymet, *J. Phys. Chem. B*, 2002, **106**, 521–533.

112 J. W. Steed, D. R. Turner and K. Wallace, *Core Concepts in Supramolecular Chemistry and Nanochemistry*, Wiley-Blackwell, Chichester, UK, 2007.

113 G. W. Gokel and H. D. Durst, *Synthesis*, 1976, **1976**, 168–184.

114 J. Šponer, J. Leszczynski and P. Hobza, *J. Biomol. Struct. Dyn.*, 1996, **14**, 117–135.

115 C. R. Martinez and B. L. Iverson, *Chem. Sci.*, 2012, **3**, 2191–2201.

116 G. Crini, *Chem. Rev.*, 2014, **114**, 10940–10975.

117 V. P. Sachanyuk, G. P. Gorgut, V. V. Atuchin, I. D. Olekseyuk and O. V. Parasyuk, *J. Alloys Compd.*, 2008, **452**, 348–358.

118 P. B. Fleming and R. E. McCarley, *Inorg. Chem.*, 1970, **9**, 1347–1354.

119 H.-J. Schneider, in *Encyclopedia of Supramolecular Chemistry*, eds. J. W. Steed, J. L. Atwood and M. Dekker, New York, 2004, pp. 1550–1556.

120 J. C. Ma and D. A. Dougherty, *Chem. Rev.*, 1997, **97**, 1303–1324.

121 B. L. Schottel, H. T. Chifotides and K. R. Dunbar, *Chem. Soc. Rev.*, 2008, **37**, 68–83.

122 C. J. Pace and J. Gao, *Acc. Chem. Res.*, 2013, **46**, 907–915.

123 S. Grimme, *Angew. Chem. Int. Ed.*, 2008, **47**, 3430–3434.

124 C. A. Hunter and J. K. M. Sanders, *J. Am. Chem. Soc.*, 1990, **112**, 5525–5534.

125 C. A. Hunter, K. R. Lawson, J. Perkins and C. J. Urch, *J. Chem. Soc. Perkin Trans. 2*, 2001, 651–669.

126 R. P. Matthews, T. Welton and P. A. Hunt, *Phys. Chem. Chem. Phys.*, 2014, **16**, 3238–3253.

127 J. H. Williams, J. K. Cockcroft and A. N. Fitch, *Angew. Chem. Int. Ed.*, 1992, **31**, 1655–1657.

128 J.-M. Lehn, *ChemInform*, 2010, **41**, 155–172.

129 C. G. Claessens and J. F. Stoddart, *J. Phys. Org. Chem.*, 1997, **10**, 254–272.

130 J. J. Reczek, K. R. Villazor, V. Lynch, T. M. Swager and B. L. Iverson, *J. Am. Chem. Soc.*, 2006, **128**, 7995–8002.

131 J. J. Reczek and B. L. Iverson, *Macromolecules*, 2006, **39**, 5601–5603.

132 V. Percec, M. Glodde, T. K. Bera, Y. Miura, I. Shiyanovskaya, K. D. Singer, V. S. K. Balagurusamy, P. A. Heiney, I. Schnell, A. Rapp, H.-W. Spiess, S. D. Hudson and H. Duan, *Nature*, 2002, **419**, 384–387.

133 E. Krieg, M. M. C. Bastings, P. Besenius and B. Rybtchinski, *Chem. Rev.*, 2016, **116**, 2414–2477.

134 E. A. Meyer, R. K. Castellano and F. Diederich, *Angew. Chem. Int. Ed.*, 2003, **42**, 1210–1250.

135 S. E. Wheeler, *J. Am. Chem. Soc.*, 2011, **133**, 10262–10274.

136 S. E. Wheeler and K. N. Houk, *J. Am. Chem. Soc.*, 2008, **130**, 10854–10855.

137 T. P. Silverstein, *J. Chem. Educ.*, 1998, **75**, 116–118.

138 A. Marmur, *J. Am. Chem. Soc.*, 2000, **122**, 2120–2121.

139 E. Arunan, G. R. Desiraju, R. A. Klein, J. Sadlej, S. Scheiner, I. Alkorta, D. C. Clary, R. H. Crabtree, J. J. Dannenberg, P. Hobza, H. G. Kjaergaard, A. C. Legon, B. Mennucci and D. J. Nesbitt, *Pure Appl. Chem.*, 2011, **83**, 1637–1641.

140 A. D. McNaught and A. Wilkinson, *IUPAC Compendium of Chemical Terminology*, IUPAC, Research Triagle Park, NC, 2014, vol. 1077, p. 2014.

141 T. Steiner, *Angew. Chem. Int. Ed.*, 2002, **41**, 48–76.

142 P. A. Kollman and L. C. Allen, *Chem. Rev.*, 1972, **72**, 283–303.

143 D. J. Hill, M. J. Mio, R. B. Prince, T. S. Hughes and J. S. Moore, *Chem. Rev.*, 2001, **101**, 3893–4012.

144 D.-W. Zhang, X. Zhao, J.-L. Hou and Z.-T. Li, *Chem. Rev.*, 2012, **112**, 5271–5316.

145 A. Das and S. Ghosh, *Angew. Chem. Int. Ed.*, 2014, **53**, 2038–2054.

146 A. Nagai and K. Takagi, *Conjugated Objects Developments, Synthesis, and Applications*, Taylor & Francis, New York, 1st edn., 2017.

147 R. Scott Lokey and B. L. Iverson, *Nature*, 1995, **375**, 303–305.

148 G. J. Gabriel and B. L. Iverson, *J. Am. Chem. Soc.*, 2002, **124**, 15174–15175.

149 S. Ghosh and S. Ramakrishnan, *Angew. Chem. Int. Ed.*, 2004, **43**, 3264–3268.

150 S. Ghosh and S. Ramakrishnan, *Macromolecules*, 2005, **38**, 676–686.

151 S. G. Ramkumar and S. Ramakrishnan, *J. Chem. Sci.*, 2008, **120**, 187–194.

152 S. Ghosh and S. Ramakrishnan, *Angew. Chem. Int. Ed.*, 2005, **44**, 5441–5447.

153 S. G. Ramkumar and S. Ramakrishnan, *Macromolecules*, 2010, **43**, 2307–2312.

154 H. M. Colquhoun, Z. Zhu and D. J. Williams, *Org. Lett.*, 2003, **5**, 4353–4356.

155 H. M. Colquhoun and Z. Zhu, *Angew. Chem. Int. Ed.*, 2004, **43**, 5040–5045.

156 H. M. Colquhoun, Z. Zhu, C. J. Cardin and Y. Gan, *Chem. Commun.*, **23**, 2004, 2650.

2 Synthesis and Characterization of semi-aromatic poly(ester imide)s

2.1. Abstract

The synthesis of high-molecular weight polymers is of general technical interest as numerous properties depend on the molecular weight, such as tensile strength, impact strength and melt viscosity. Materials with superior mechanical properties can be obtained by the production of polymers with high molecular weights.[1] The synthesis of high-molecular polymers via step-growth polymerization can be challenging. Although optimizations of the molecular weight of poly(ester imide)s were carried out,[2] the average inherent viscosity η_{inh} of the polymers reported in the literature via the acyl chloride route in high-boiling solvents was only 0.50 dL g^{-1}.

In the current study, homo- and random co-poly(ester imide)s were synthesized successfully from bis(hydroxyethyl)diimides and aliphatic linear bifunctional acyl chlorides in the high boiling solvents 1,2-dichlorobenzene or 1-chloronaphthalene. It was found that the use of milder conditions than previously described (e. g. 30 minutes at 120 °C instead of 24 h at 208 °C) did lead to poly(ester imide)s of considerably higher molecular weight with an average inherent viscosity η_{inh} of 0.70 dL g^{-1} and molecular weights (M_n) between 20 k and 30 k g·mol^{-1} (GPC).

2.2. Introduction

The aim of the current chapter was to synthesize high-molecular weight model poly(ester imide)s which carry information that could potentially be extracted by intercalation-sequencing.[3]

Such polymers necessarily had to contain imide groups to form the charge-transfer complexes required for intercalation-sequencing; in the current study the polymers should furthermore contain ester groups in the main chain to be used for transesterification experiments, as described in Chapter 6. Since poly(esterimide)s are accessible from a wide variety of reactions, a method had to be chosen that would give effective and consistent results. The work described in the Chapters 3 to 6 required polymers with a DP_n of at least 20 (M_n thus about 7 k), as endgroup signals have in this case in ^{1}H NMR spectra an intensity of only 5% of the signal of the repeat unit. Endgroup signals in NMR spectra are problematic as they often interfere with the aromatic imide resonances and thereby complicate the intercalation-sequencing.

2.3. Theory

2.3.1. Polyesterification *versus* polyimidization

Poly(ester imide)s are polymers containing the carboxylic ester functionality and the imide functionality. In principle, the polymerization would be imaginable via the formation of either of the two groups. However, the most common imidization reaction involves an anhydride and an amine. Carboxylic acid esters are not stable under the conditions used for imidization but react with amines under ester aminolysis (Scheme 1):[4]

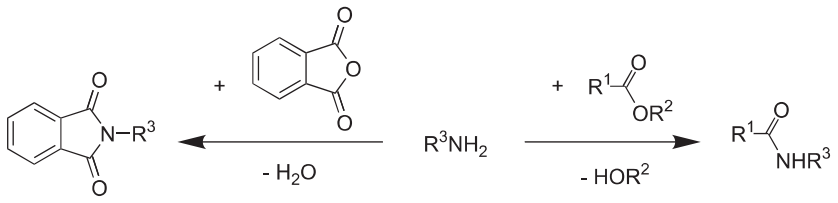

Scheme 1: Amines can react both, via imidization with an anhydride (left) and via aminolysis with an ester (right).

Aminolysis would occur as a side reaction during a imidization reaction of ester-containing monomers and cleave the growing polymer chain. Therefore, poly(ester imide)s have to be prepared via ester formation from monomers comprising imide units. Aromatic imides are known for their high stability[5]; in particular under acidic[6] conditions, monomers containing imide groups are not affected by the conditions applied during the ester formation.

2.3.2. Melting point and solubility

Poly(ester imides) can be prepared via all reactions used for the synthesis of polyesters. A general distinction, however, has to be made between aliphatic polyesters (e. g. poly[butylene succinate][7]) and mainly aromatic polyesters, like Xydar, also called poly(arylates).[8] While aliphatic polyesters are prepared from relatively flexible, low-melting monomers, the more rigid, aromatic polyesters and equally poly(ester imides) possess higher melting points and a lower solubility which require often processing via different methods. For example, succinic acid has a melting point of 190 °C[9] and poly(butylene succinate) a melting point of 106 °C[10] (Figure 1): the melt polymerization is therefore typically carried out at 120 °C.[10,11] Xydar is prepared from 1,4-benzenedicarboxylic acid, [1,1'-biphenyl]-4,4'-diol and 4-hydroxybenzoic acid; [1,1'-biphenyl]-4,4'-diol has a melting point of 283 °C[12] and the polymer a melting point of 421 °C. To avoid degradation, a prepolymer is prepared in the melt at 320 °C which is granulated and postcondensed (in the solid phase) at 365 °C.[11]

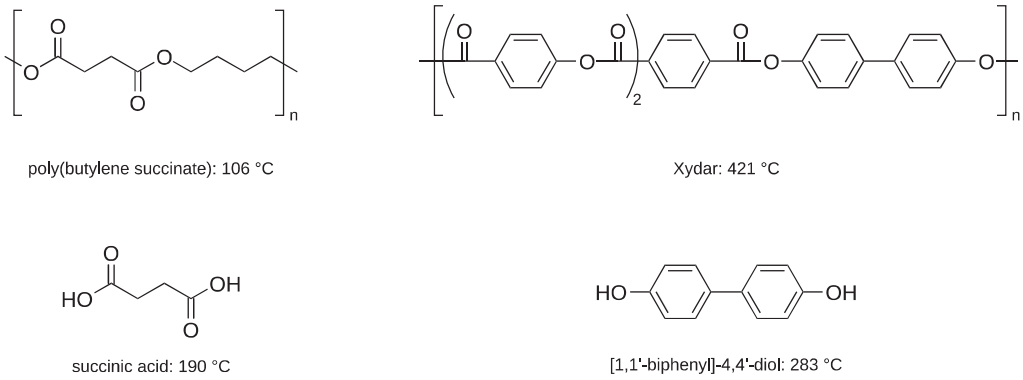

Figure 1: Comparison of the melting point of a typical aliphatic (a) and a typical aromatic polyester (b) and its monomers. It can be seen that both, the aromatic polymer and its monomer have a significantly higher melting point as a result of the rigidity of the aromatic sub-units.

In the present thesis, the polymers are semi-aromatic. In case of the well-examined semi-aromatic PET it was found that degradation of pure PET begins at about 300 °C followed by the release of small molecules at about 400 °C.[13] The polymers studied the present thesis contain both poorly fusible aromatic units (as in Xydar) and readily degradable aliphatic units (as in the semi-aromatic PET). So it is obvious that neither the methods of aliphatic nor mainly aromatic polymers can be transferred directly to the present system: some of the possible methods are listed in Chapter 1. After considering and attempting different methods, a solvent-based polyesterification between diacyl chlorides and bis(hydroxyethyl)diimides was chosen.

2.4. Synthesis

The synthetic approach to monomers and polymers used in the present thesis is shown in Scheme 2, exemplified for homo-poly(ester imide)s based on the pyromellitic diimide (PMDI) residue (polymers **3** to **10**). The other homo-poly(ester imide)s and 1:1 co-poly(ester imide)s (**13** to **46**, Figure 6) and their monomers were synthesized accordingly.

The bis(hydroxyethyl)diimides used as monomers (e.g. compound **1**) were obtained by the reaction of an aromatic dianhydride with 2-aminoethanol in DMF/toluene while removing the co-produced water by Dean-Stark distillation,[14] followed by purification via recrystallization. The poly(ester imide)s were synthesized from the bis(hydroxyethyl)diimide and an aliphatic linear bifunctional acyl chloride in a high boiling solvent (1,2-dichlorobenzene or 1-chloronaphthalene). By using acyl chlorides of various lengths, homologous series of polymers were accessible which differed only in the number of methylene groups *x* in the aliphatic diacid residue, which ranged between 1 and 8.

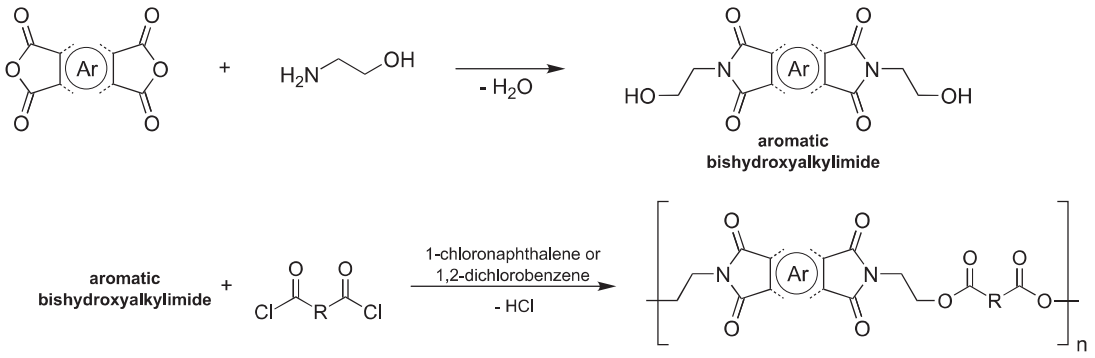

Scheme 2: General synthesis of the poly(ester imide)s of the current work: An aromatic anhydride was reacted with 2-aminoethanol to an aromatic bishydroxyalkylimide. The obtained bishydroxyalkylimide was polymerized with an bisacylchloride to a poly(ester imide)s.

2.4.1. Monomer synthesis

2.4.1.1. Bishydroxyalkylimides

The hydroxyalkylimide monomers which were used or synthesized for this study are shown in Figure 2. The hydroxyalkylimides **1**, **2** and **4** were synthesized successfully via imidization, while **3** was received from an industrial producer. The compounds were already known in the literature.[15,16] A similar synthesis was chosen, derived from the procedure reported previously.[14]

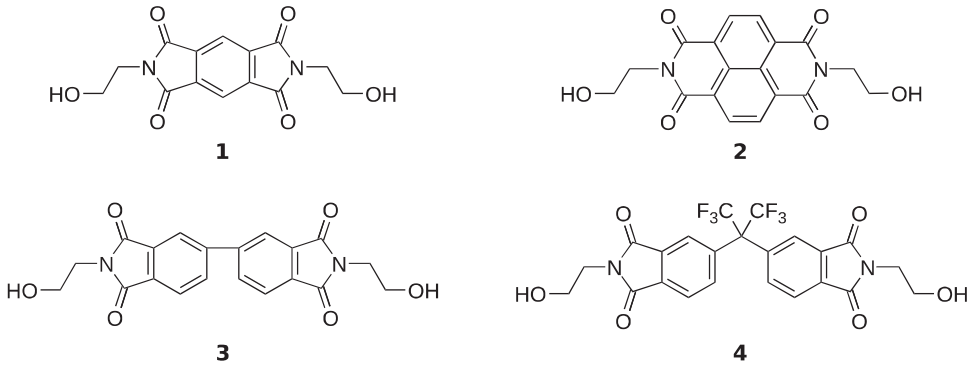

Figure 2: Structural formulas of the monomers used in the current study. *N,N′*-bis(2-hydroxyethyl)pyromellitic diimide (**1**), *N,N′*-bis-(2-hydroxyethyl)-4,4'-biphthalimide (**2**) *N,N′*-bis-(2-hydroxyethyl)-naphthalene diimide (**3**), *N,N′*-bis(2-hydroxyethyl)-hexafluoroisopropylidene-diphthalimide (**4**).

The hydroxyimide monomers were synthesized via the imidization of a commercially available aromatic dianhydride with aminoethanol (Scheme 3). The imidization proceeds first via the formation of an amic acid which is rapidly formed even at ambient temperature reacting a dianhydride with a diamine in a high-boiling, polar, aprotic (e. g. DMAc, NMP or DMF) or polar protic (phenolic) solvent.[5] The reaction occurs by a nucleophilic attack of the amino group on the carbonyl carbon of the anhydride group, followed by an opening of the anhyd-

ride ring forming the amic acid.[17] The ring closure and formation of the imide can proceed via 2 different pathways:[18] In pathway one the amine of the amic acid can attack the carbonyl carbon to close the ring and, after a proton rearrangement, water is eliminated. In pathway two the amic acids releases a proton and abstracts then the proton of the amine. The negatively charged amine closes the ring as in path one and water is released after abstraction of a proton.

The imidization proceeds faster in the presence of such polar amide-based solvents due to solvation which allows the amic acid group to orient itself in a favourable conformation required for cyclization[19] and due to the basicity of the amide solvent that allows it to accept protons.[20] In addition, the monomers have a good solubility in the polar DMF because of the polar imide group.

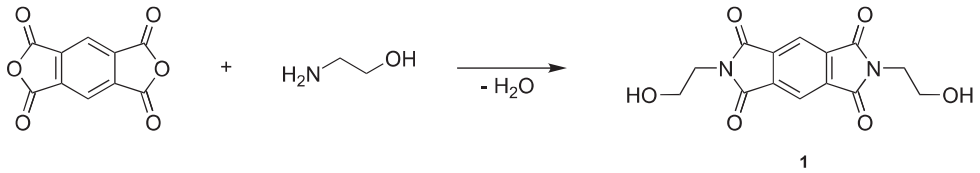

Scheme 3: Exemplified monomer synthesis via imidization.

In the literature, the by-product water formed during the imidization was left in the reaction mixture; the crude product was subsequently purified by precipitation.[21–25] In the current study, the by-product water was removed as an azeotrope in a Dean-Stark apparatus to drive the equilibrium towards the product. This might be the cause for the improved yields (93% in case of NDI, as opposed to 80 to 90% in the literature). The PMDI, HFDI and BPDI-based monomers (**1**, **3** and **4**) were soluble in amine-based solvents such as *N,N*-dimethylformamide and gave transparent solutions during the synthesis and the recrystallization. The NDI-based monomer (**2**), however, gave a strongly dark coloured solution, so a source of intense light had to be used to observe the point of full dissolution during the recrystallization. After recrystallization, the ^{1}H NMR spectra of the compounds did not show any signs of impurities (Figure 3).

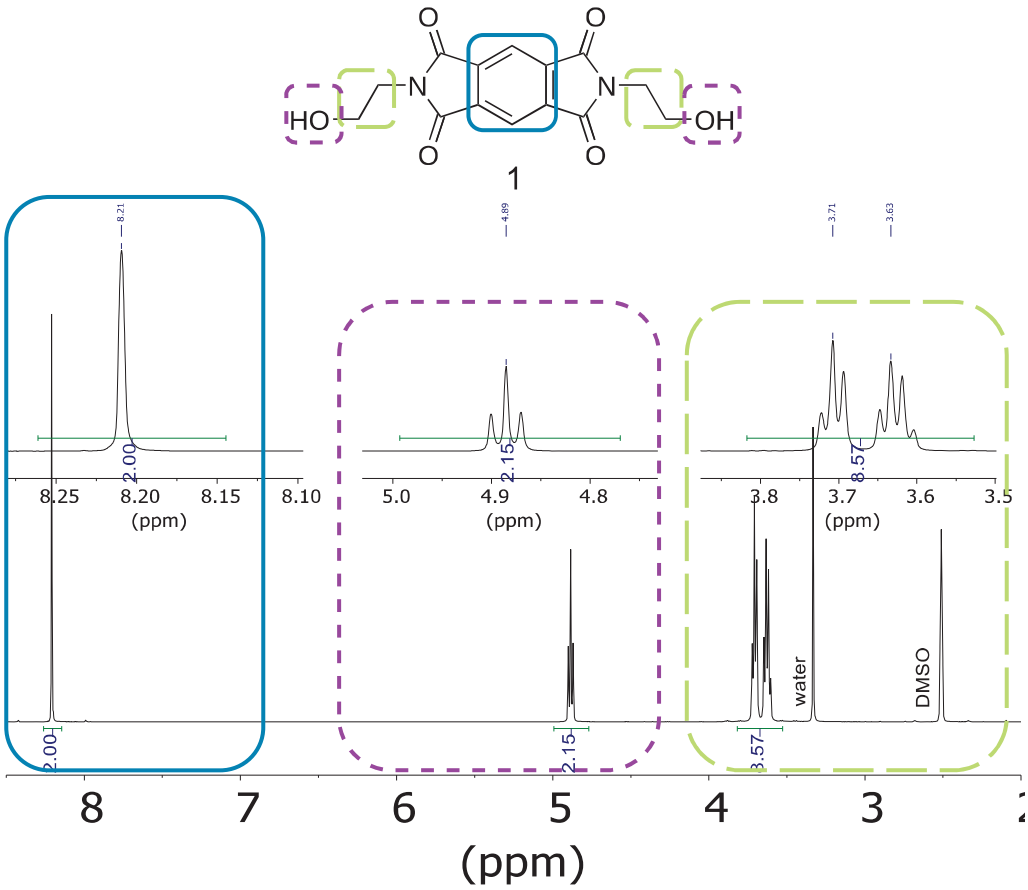

Figure 3: ^{1}H NMR spectrum of the PMDI-based bishydroxyalkylimide **1**.

A DSC analysis of the monomers was carried out up to 300 °C. Above this temperature TGA showed a loss of weight (sublimation or decomposition). An exemplary DSC thermogram is presented in Figure 4. In case of the HFDI and BPDI-based monomers (**3** and **4**), only a single, sharp transition at high temperature was observed which was interpreted as a melting point. However, the PMDI-based and NDI-based monomers (**1** and **2**) show additional thermal transitions, most probably liquid crystalline transitions (at 154 °C in case of the PMDI-based monomer) in addition to the melting point (at 282 °C). The NDI-based monomer did not show a melting point up to the temperature where weight loss was observed in TGA (300 °C).

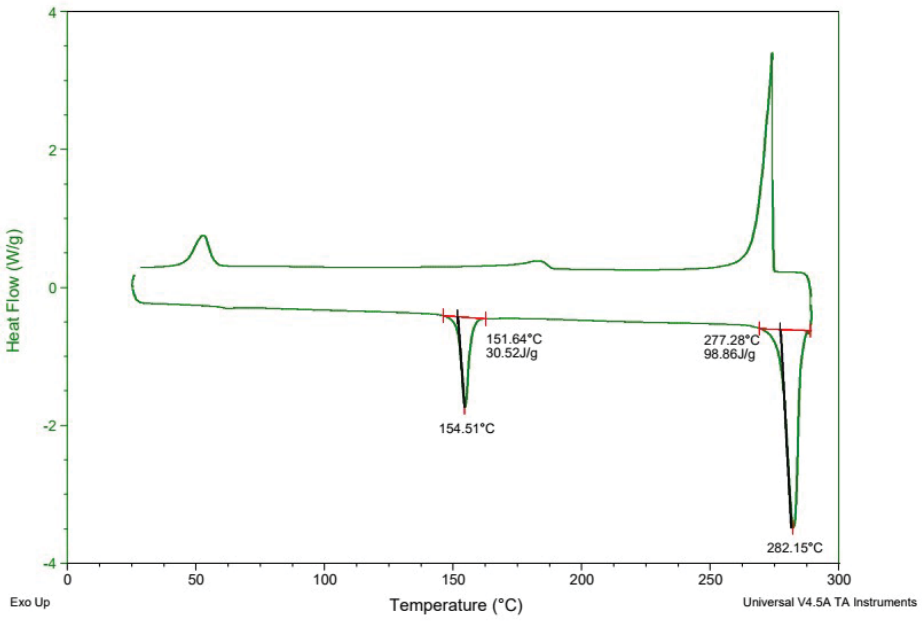

Figure 4: Thermogram of PMDI-based monomer (**1**).

2.4.1.2. Acyl chlorides

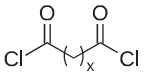

5 to **12**
for *x* = 1 to 8

Figure 5: Acyl chlorides

Aliphatic carboxylic acid chlorides are among the most versatile and reactive class of organic compounds. They are long-used and well-understood for various synthetic purposes.[26] In the present thesis, aliphatic linear bifunctional carboxylic acyl chlorides containing 1 to 8 methylene groups (**5** to **12**) were used (Figure 5), i.e. propanedioyl dichloride (malonyl chloride) to decanedioyl dichloride (sebacoyl chloride). All of these are known in the literature and commercially available. Most acyl chlorides were obtained from a commercial supplier and distilled at reduced pressure for further purification. Due to its high cost, heptanedioyl dichloride was synthesized by reaction of the diacid with thionyl chloride and again subsequently purified via distillation similar to a known procedure[27] (Scheme 4):

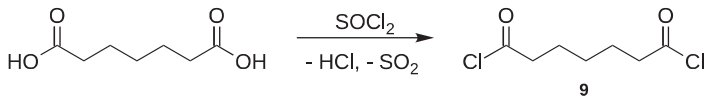

Scheme 4: Synthesis of heptanedioyl dichloride (**9**) from heptanedioic acid with thionyl chloride.

The colourless oil obtained after distillation showed only the expected signals in the ^{1}H NMR spectra without unexpected resonances indicating the presence of impurities.

2.4.2. Polymer Synthesis

The synthesis of the polymers investigated in the present thesis is based on the polyesterification of the previously produced bis(hydroxyethyl)diimide with an acyl chloride in a high-boiling solvent (1-chloronaphthalene or 1,2-dichlorobenzene) at high temperature (120 to 220 °C) under dry nitrogen (Scheme 5). The polymers were purified and residual chloro-arene solvent removed by re-precipitation of the polymer dissolved in $CHCl_3$/HFIP (6:1, *v:v*) in an excess of methanol.

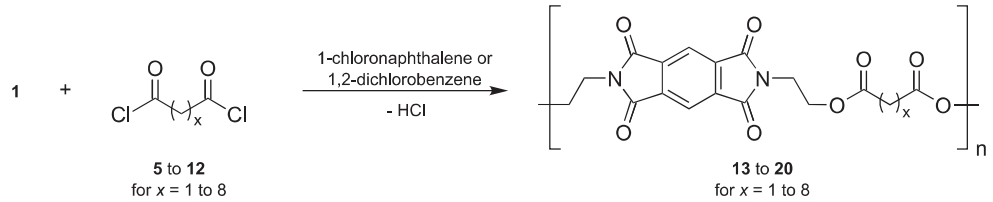

Scheme 5: Exemplified polymer synthesis via acyl chloride based polyesterification. Polymers **13** to **20** differ only in *x*, the number of methylene groups in the aliphatic diacid residue, which ranges between 1 and 8.

The permutation of the bis(hydroxyethyl)diimide and of acyl chlorides with a different number of methylene groups gave access to a large number of poly(ester imide)s (Figure 6). Since only the monomer's non-reactive core was varied while the functional groups remained identical, one method could be used for the synthesis of all of the polymers and only one class of reaction had to be optimized.

The structures of these homopolymers were validated using ^{1}H NMR, ^{13}C NMR and IR spectroscopy and the materials were characterized by solution viscometry. Exemplified for the PMDI-based polymer **17** in Figure 7, it can be seen that the polymers are distinguished by clean, well-resolved ^{1}H NMR spectra due to their high symmetry, the absence of stereocenters and a small number of distinguishable resonances in the aromatic region. This simplicity is particularly important when the aromatic imide resonance is shifting and splitting during in-

tercalation-sequencing (see later Chapters). It is furthermore useful to have "free space" in the ^{1}H NMR spectrum during the intercalator sequencing, as the sequencing involves substantial complexation shifts of the aromatic imide resonances.

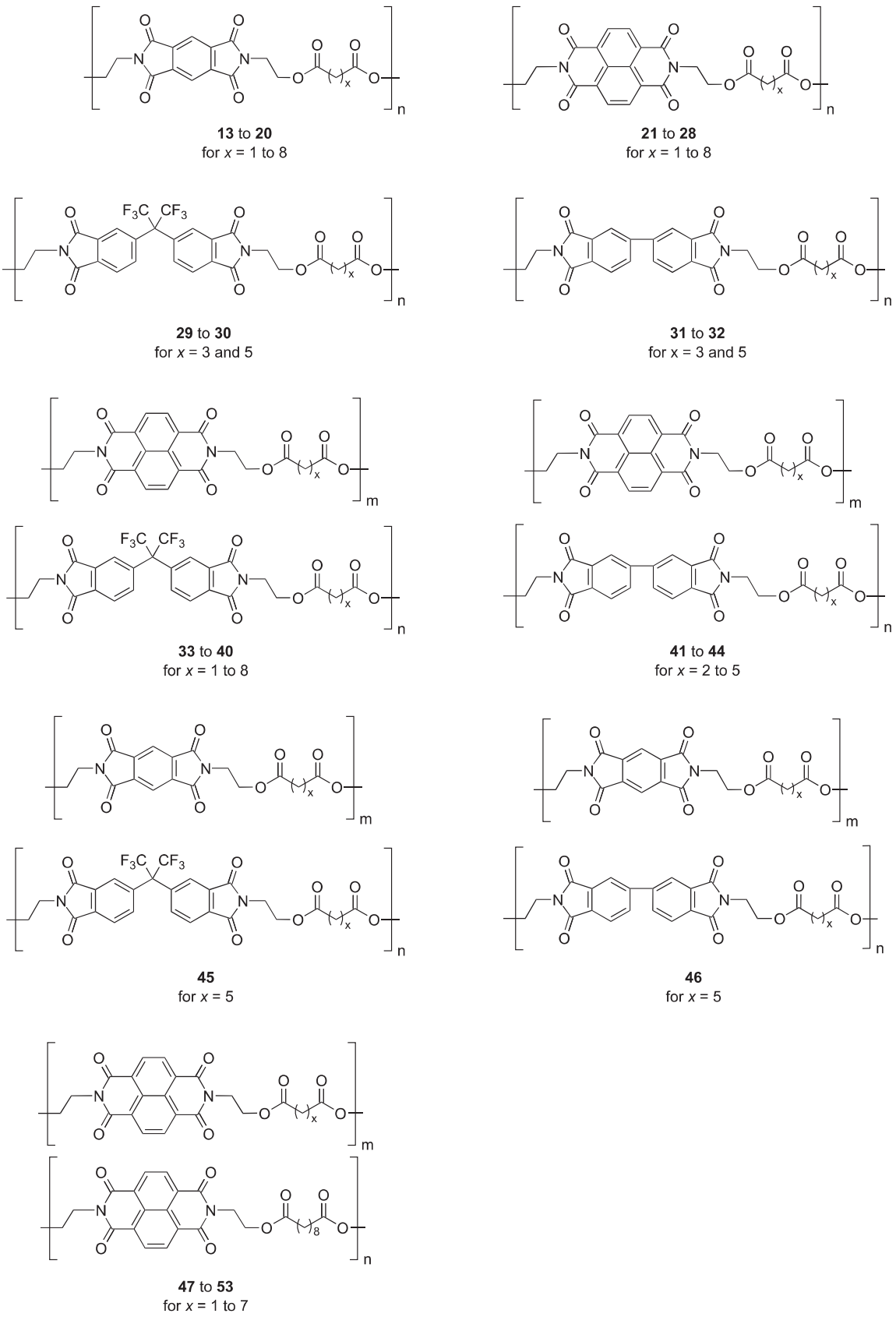

Figure 6: The PMDI, NDI, HFDI and PBDI-based homo- and co-poly(ester imide)s **13** to **46** synthesised in the present thesis using combinations of monomers **1** to **4** and **5** to **12**. By using bisacylchlorides **5** to **12**, several homologous series of polymers were obtained differing in the number of methylene groups *x*, and in the structure of the diimide core.

With exception of the HFDI-based homopolymers **29** and **30**, all poly(ester imide)s were insoluble in THF, DMF, or chlorinated solvents, so that their molecular weights could not be investigated by GPC analysis. The HFDI-based homopolymers **29** and **30** had a molecular weights (M_n) of 30,200 (dispersity $Đ = 2.07$) and 20,400 ($Đ = 1.92$), respectively by GPC (Figure 8). However, many of the polymers were soluble in mixtures of chlorinated solvents such as chloroform or dichloromethane with proton-donor solvents such as trifluoroethanol or hexafluoropropan-2-ol, in which their inherent viscosities and NMR spectra could be measured.

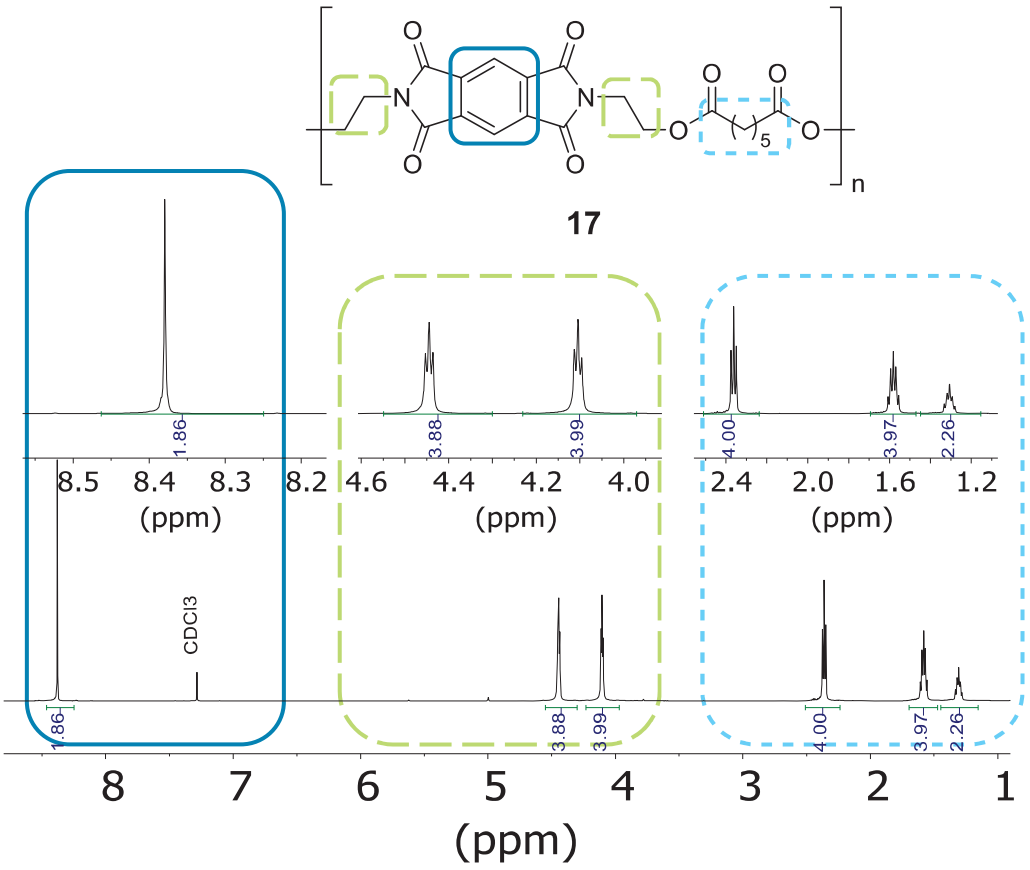

Figure 7: ^{1}H NMR spectrum of the PMDI-based homo-poly(ester imide) **17** with expansion (above).

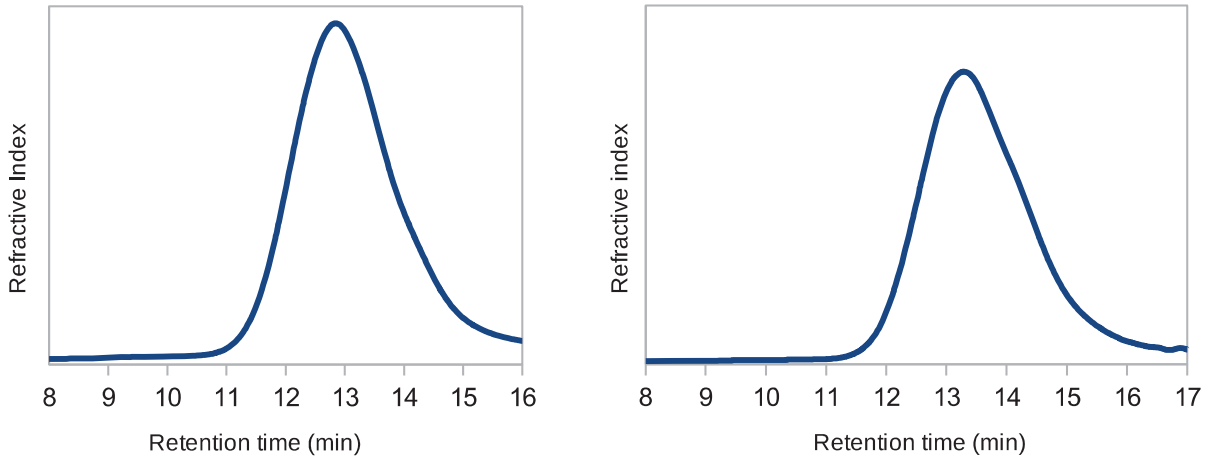

Figure 8: GPC curves for the HFDI-based polymers **29** (left) and **30** (right), THF used as eluent.

The average inherent viscosity of all polymers synthesised in the present thesis (Table 1) is *ca*. 0.70. In contrast, the average viscosity in nine publications of structurally related poly(ester imide)s via acyl chloride based polymerisations in high boiling solvents is 0.50.[2,16,28–34] In the literature, the polymerisations were almost always carried out at higher temperatures; the optimization described in Section 2.5 was thus evidently successful.

Table 1: Inherent viscosities (η_{inh} in dL g^{-1}) of the polymers synthesized in the present thesis of copolymer and homopolymer ("homo").

x =	NDI homo	PMDI homo	NDI/ HFDI	NDI/ BPDI	BPDI homo	HFDI homo	PMDI/ BPDI	PMDI/ HFDI
1	0.17	0.48	0.81					
2	0.56	0.36	0.20	0.98				
3	1.54	0.60	0.26	1.31	1.08	0.83		
4	0.75	0.55	1.09	0.84				
5	0.58	0.59	0.61	0.19	0.51	0.56	0.36	0.27
6	0.19	0.62	1.26					
7	1.20	0.37	1.20					
8	0.93	0.59	1.37					

Their thermal characteristics of the polymers were investigated by DSC (Table 2). As usual, two heating/cooling cycles were performed but only the second cycle was considered. None of the NDI-based homo- or co-polymers but all of the PMDI-based homopolymers showed a melting point; two exemplary thermograms are presented in Figure 9.

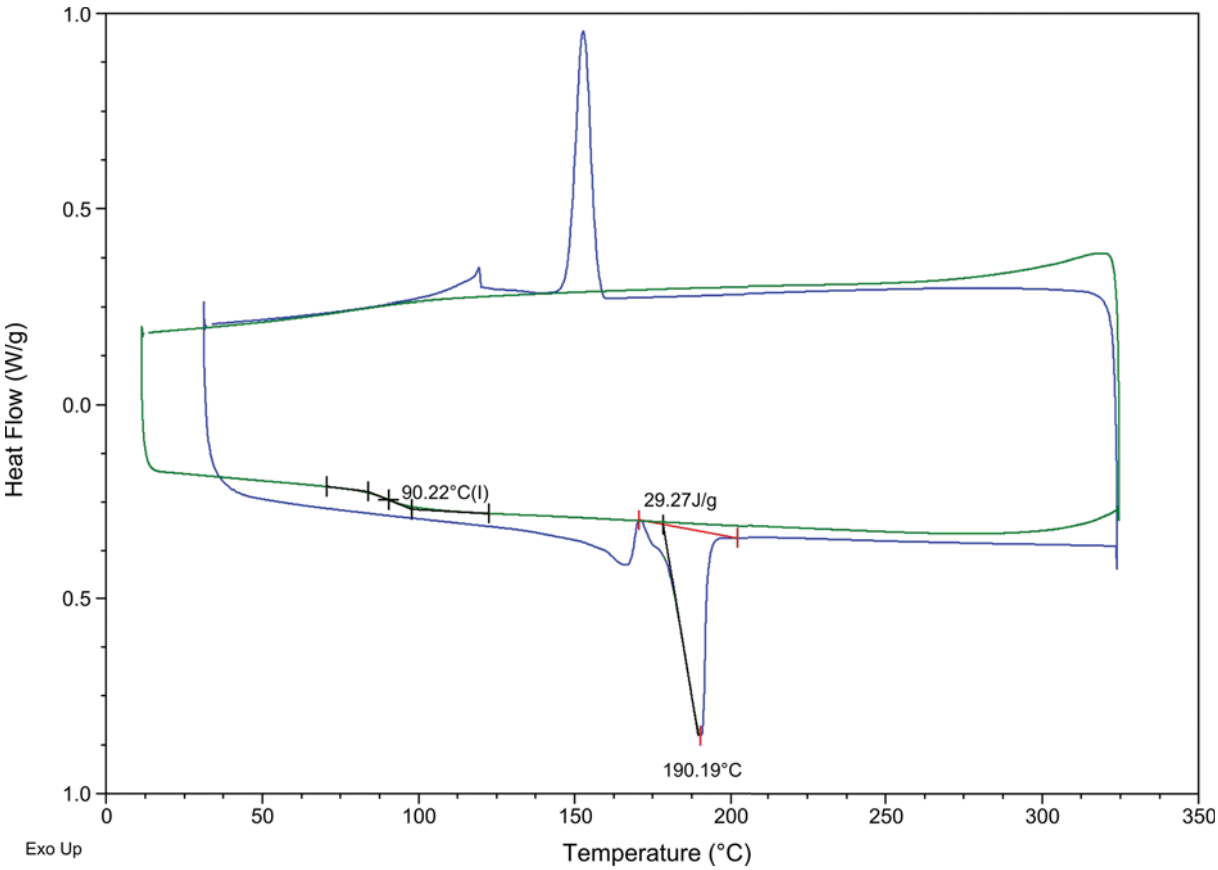

Figure 9: Exemplary thermograms of the NDI-based homopolymer x = 5 (**25**, green) which shows a T_g at 90 °C but no melting point and the PMDI-based homopolymer x = 5 (**17**, blue) which show a melting point at 190 °C preceded by a crystallization. For both polymers, the 2nd heating and cooling cycle is presented.

The glass transition mid-points of the NDI-based polymers show a clear dependency on the spacer length x (Figure 10). The NDI-based polymers show for short spacers markedly higher glass transition points, this tendency is particularly pronounced for the NDI-based homopolymers (**21** to **28**). The glass transition points of polymers with long aliphatic spacers approach the glass transition points of aliphatic polyesters as the aliphatic part dominates the overall structure.

The NDI-based all-aliphatic copolymers have lower glass transition points than the other NDI-based copolymers. The BPDI-based homopolymers (**31** and **32**) have nearly identical glass transition points to the HFDI-based homopolymers (**29** and **30**), and both are comparable to the NDI-based polymers. The NDI / BPDI-based and the NDI / HFDI-based copolymers show again very similar glass transition points.

No glass transition points could be identified for the PMDI-based homopolymers. Their melting points exhibit a pronounced odd-even effect[41] but show no further dependency on the spacer length.

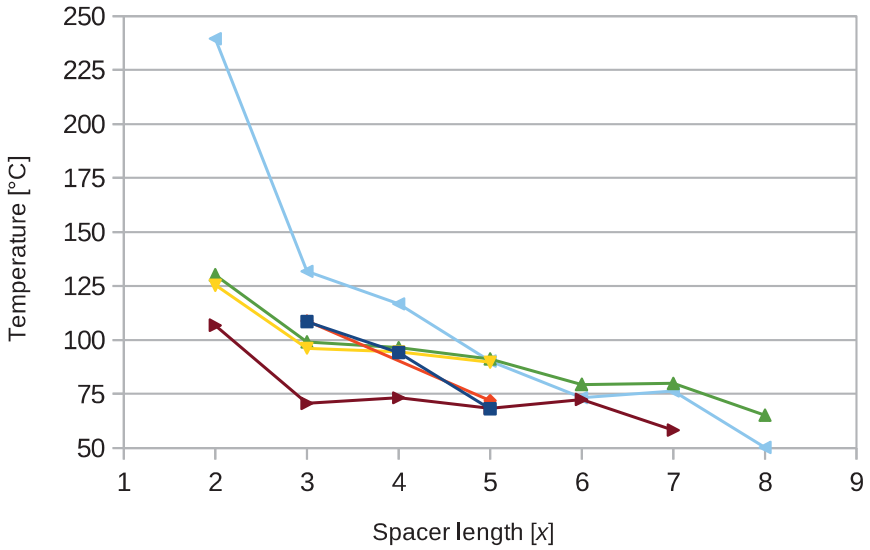

Figure 10: Glass transition temperatures T_g of the investigated polymers. ◀ = NDI-based homopolymers (**21** to **28**). ▲ = NDI / HFDI-based copolymers (**33** to **40**). ▼ = NDI / BPDI-based copolymers (**41** to **44**). ▶ = all-aliphatic NDI-based copolymers (**47** to **53**). ◆ = HFDI-based copolymers (**29** to **30**). ■ = BPDI-based homopolymers (**31** to **32**).

2.5. Optimization of the molecular weight

Initially, the acyl chloride based polyesterification without a hydrogen chloride acceptor was investigated under the conditions described for such reactions in the literature.[2,16,28–34] That is, refluxing the monomers in a high boiling solvent for between 3 to 20 h or until the HCl formation ceased (either in 1,2-dichlorobenzene[2,31,34], 1,2,3-trichlorobenzene[30,32,33] or diphenyl ether[6,29] which have a boiling point of 180 °C[35], 208 °C[36] or 258 °C[37], respectively). Following the conditions from the literature, the synthesis was initially carried out at high temperatures (170 °C, specifically) and long reaction times (24 hours). These conditions did not yield polymers with the required molecular weight (inherent solution viscosities of maximum η_{inh} = 0.2 dL·g^{-1}), as end groups were clearly visible in ^{1}H NMR and the imide resonance did thereby not appear as a sharp singlet but was flanked and overlayed by various smaller resonances. During the supramolecular titrations required for the intercalation-sequencing, the end group resonances had a different complexation shift from the main diimide resonance and were overlapping the main splitting pattern; this complicated the intercalation-sequencing. Therefore, the polymerization conditions had to be optimized to achieve polymers of higher molecular weight sufficient for supramolecular titrations.

Table 2: DSC data of the investigated homopolymers (homopol.) and copolymers (copol.)

	x		T_g	T_m	J/g (T_m)
PMDI homopol.	1	**13**	-	194	37
	2	**14**	-	233	43
	3	**15**	-	223	29
	4	**16**	77	253	33
	5	**17**	-	190	29
	6	**18**	-	217	26
	7	**19**	-	203	27
	8	**20**	-	207	27
NDI homopol.	2	**22**	240	-	-
	3	**23**	132	-	-
	4	**24**	117	-	-
	5	**25**	90	-	-
	6	**26**	73	-	-
	7	**27**	76	-	-
	8	**28**	50	-	-
HFDI homopol.	3	**29**	109	-	-
	5	**30**	72	-	-
BPDI homopol.	3	**31**	109	-	-
	5	**32**	68	-	-
NDI / HFDI copol.	2	**34**	130	-	-
	3	**35**	99	-	-
	4	**36**	96	-	-
	5	**37**	91	-	-
	6	**38**	79	-	-
	7	**39**	80	-	-
	8	**40**	65	-	-
NDI/ BPDI copol.	2	**41**	125	-	-
	3	**42**	96	-	-
	4	**43**	95	-	-
	5	**44**	90	-	-
PMDI / BPDI copol.	5	**46**	79	-	-
NDI all-aliphatic copol.	2	**48**	107	-	-
	3	**49**	71	-	-
	4	**50**	73	-	-
	5	**51**	68	-	-
	6	**52**	72	222	11
	7	**53**	58	-	-

The above conditions were chosen by previous workers because the concentration of the reactive end groups decrease with an increasing degree of polymerization. Even though low molecular weight acyl chlorides and alcohols react already at room temperature or below,[38] such harsh conditions were chosen to achieve a sufficient conversion as the concentration of reactive end groups decreases during the progress of the reaction. However, in the present thesis it was visually observed that the polymerization reaction began already during rapid heating at about 100 °C as it was evidenced by the dissolution of the monomer, the formation of a viscous, transparent solution and the formation of a gas (presumably HCl, as indicated by its acidic reaction with damp pH-paper). After about 30 minutes the HCl formation ceased. It was also observed in the literature for one case that the reaction was completed within 40 minutes.[16] It was therefore an obvious idea to choose less rigorous reactions conditions (lower temperatures and shorter reaction time). It is generally known that milder conditions are preferable when possible,[39] as they lead to fewer side reactions and thereby promote the formation of polymers of higher molecular weight.

The polymerization reaction was systematically optimized, varying the parameters time and temperature, using the NDI-based homopolymer $x = 5$ (**25**) as the model system (Figure 11). Polymers of high inherent viscosity could only be obtained for short reaction times and low reaction temperatures. It was quickly evident that increased temperature or time led to a significantly reduced inherent viscosity.

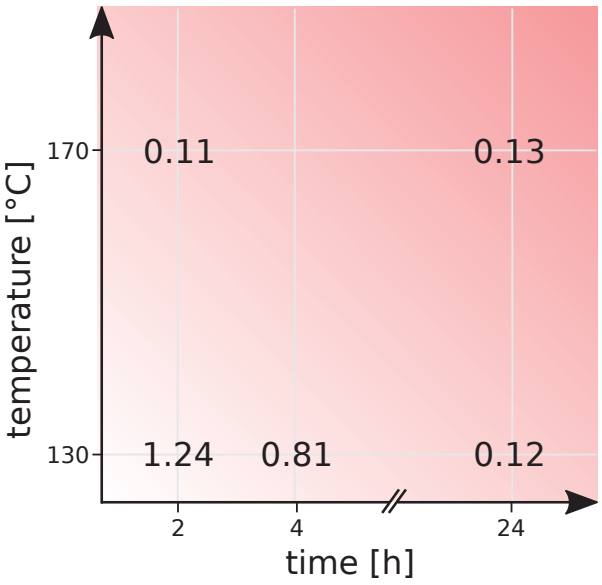

Figure 11: The diagram shows the polymerization time plotted against the polymerization temperature and the resulting inherent viscosity. It is evident that an increase in polymerization time or polymerization temperature decreases the inherent viscosity. Each viscosity value is the average of three polymerizations.

The optimized reaction conditions (e. g. 2 h at 130 °C) gave access to polymers with an average inherent viscosity of η_{inh} = 0.70 (Table 1). These polymers showed thereby considerably higher inherent viscosities than the polymers reported in the literature (η_{inh} = 0.50).[2,16,28–34] These optimized conditions were used successfully unless higher temperatures were required to keep the polymers in solution during synthesis.

Wang and Lin had previously worked on the optimisation of the diacyl chloride based poly(ester imide) synthesis and reviewed various experiments.[2] They came the the conclusion that the concentration would be the most promising parameter for optimization while a temperature of 200 °C for 20 h was regarded as ideal the optimum. The group achieved a maximum inherent viscosity of η_{inh} = 0.60 dL g^{-1} at a reaction concentration of 0.6 mmol/mL. At higher concentrations, cross-linking was observed while at lower concentrations the inherent viscosity was reduced, probably due to the formation of macrocycles.[40] The polymerizations in the current study were carried out at a constant concentration of 2.5 mmol/mL. The concentration was chosen to reduce the formation of macrocycles, and the formation of cross-linked material was only observed at temperatures above 170 °C.

2.6. Conclusions

This chapter describes the synthesis of high-molecular poly(ester imide)s and the particular significance of choosing mild polymerization conditions.

The synthesis was based on the polyesterification of NDI-based, PMDI-based, BPDI-based and HFDI-based bis(hydroxyethyl)diimides and aliphatic linear bifunctional diacyl chlorides in the high boiling solvents 1,2-dichlorobenzene or 1-chloronaphthalene to give the corresponding homo- and co-poly(ester imide)s. A large number of analogous polymers was produced (41 overall) by permutation of the bis(hydroxyethyl)diimides and the chain-length *x* of the aliphatic acycl chlorides. The ^{1}H NMR spectra of the polymers were simple due to the polymers' high symmetry and did not show any signs of impurities. The average inherent viscosity η_{inh} of 0.70 dL g^{-1} was notably higher than the average inherent viscosity viscosity η_{inh} of the polymers reported in the literature of η_{inh} = 0.50 dL g^{-1}. Molecular weights (M_n) could be determined via GPC only for the HFDI-based homopolymers **29** and **30**, and were *ca.* 20k and 30k g·mol^{-1}, respectively.

The use of mild conditions for the synthesis (i.e. 30 minutes at 120 °C instead of 24 h at 208 °C) yielded polymers with an average inherent viscosity η_{inh} of 0.70 dL g^{-1}; this is considerably higher than the average inherent viscosity of η_{inh} of 0.50 dL g^{-1} reported in the literature. An increase of either temperature from 130 to 170 °C or of the reaction time from 2 to 4 h reduced the inherent viscosity significantly (from 1.24 dL g^{-1} to 0.11 or 0.81 dL g^{-1}, respectively). Even though the solubility of polymers is better at elevated temperatures and the current polymers contain a extended and thereby hardly soluble aromatic system, the synthesis could be carried out under comparatively mild conditions of only 120 °C. Since high temperatures of 200 °C and above are used widely for the synthesis of aromatic polymers, the increase in molecular weight by the use of mild conditions described here might be applicable for the improvements of various other high-performance polymers.

2.7. References

1 M. Chanda, *Plastics Technology Handbook*, CRC Press, New York, 2017.

2 C. S. Wang and C. H. Lin, *Polymer*, 1999, **40**, 4387–4398.

3 J. S. Shaw, R. Vaiyapuri, M. P. Parker, C. A. Murray, K. J. C. Lim, C. Pan, M. Knappert, C. J. Cardin, B. W. Greenland, R. Grau-Crespo and H. M. Colquhoun, *Chem. Sci.*, 2018, **9**, 4052–4061.

4 W. A. Jacobs and M. Heidelberger, *Org. Synth.*, 1927, **7**, 16.

5 R. G. Bryant, in *Kirk-Othmer Encyclopedia of Chemical Technology*, John Wiley & Sons, Inc., Hoboken, NJ, USA, 2006.

6 J. Clayden, N. Greeves and S. Warren, *Organic Chemistry*, Oxford University Press, New York, 2012.

7 J. Xu and B.-H. Guo, *Biotechnol. J.*, 2010, **5**, 1149–1163.

8 S. V Vinogradova, V. A. Vasnev and P. M. Valetskii, *Russ. Chem. Rev.*, 1994, **63**, 833–851.

9 V. Chikhalia, R. T. Forbes, R. A. Storey and M. Ticehurst, *Eur. J. Pharm. Sci.*, 2006, **27**, 19–26.

10 X. Kong, H. Qi and J. M. Curtis, *J. Appl. Polym. Sci.*, 2014, **131**, 40579–40586.

11 H. Köpnick, M. Schmidt, W. Brügging, J. Rüter and W. Kaminsky, in *Ullmann's Encyclopedia of Industrial Chemistry*, Wiley-VCH Verlag GmbH & Co. KGaA, Weinheim, Germany, 2000.

12 F. Du, Q. Zhou, D. Liu, T. Fang, Y. Shi, Y. Du and G. Chen, *Synlett*, 2018, **29**, 779–784.

13 F. Samperi, C. Puglisi, R. Alicata and G. Montaudo, *Polym. Degrad. Stab.*, 2004, **83**, 3–10.

14 S. W. Sankey, D. Turner, H. Colquhoun, S. Jones, Copolyesterimides derived from *N,N'*-bis-(hydroxyalkyl)-3,3',4,4'-diphenylsulfonetetracarboxylic diimide and films made therefrom, US Patent 9422399, 2016.

15 T. Hirata, M. Sato and K. Mukaida, *Macromol. Chem.*, 1993, **194**, 2861–2874.

16 M. Bruma, I. Sava, F. Mercer, I. Negulescu, W. Daly, J. Fitch and P. Cassidy, *High Perform. Polym.*, 1995, **7**, 411–420.

17 A. N. Pravednikov, I. Y. Kardash, N. P. Glukhoyedov and A. Y. Ardashnikov, *Polym. Sci. U.S.S.R.*, 1973, **15**, 399–410.

18 J. A. Kreuz, A. L. Endrey, F. P. Gay and C. E. Sroog, *J. Polym. Sci. Part A-1 Polym. Chem.*, 1966, **4**, 2607–2616.

19 L. A. Laius, M. I. Bessonov, Y. V. Kallistova, N. A. Adrova and F. S. Florinskii, *Polym. Sci. U.S.S.R.*, 1967, **9**, 2470–2478.

20 M. Ghosh and K. L. Mittal, *Polyimides: Fundamentals and Applications*, CRC Press, New York, 1996.

21 C. Kulkarni and S. J. George, *Chem. Eur. J.*, 2014, **20**, 4537–4541.

22 R. F. Semeniuc, R. R. Baum, J. J. Veach, K. A. Wheeler and P. J. Pellechia, *Inorganica Chim. Acta*, 2013, **400**, 228–238.

23 C. P. Harvey and J. D. Tovar, *J. Polym. Sci. Part A Polym. Chem.*, 2011, **49**, 4861–4874.

24 M. S. Refat, I. Grabchev, J. M. Chovelon and G. Ivanova, *Spectrochim. Acta - Part A Mol. Biomol. Spectrosc.*, 2006, **64**, 435–441.

25 P. Ponce, L. Fomina, F. Perez and S. Fomine, *J. Mol. Struct. Theochem*, 2001, **541**, 131–139.

26 N. O. V. Sonntag, *Chem. Rev.*, 1953, **52**, 237–416.

27 L. C. Xiaojiang. C. Y. Wu, D. Gai, Novel transcription factor modulators, US 0256775, 2014.

28 Y. Chen, R. Wombacher, J. H. Wendorff, J. Visjager, P. Smith and A. Greiner, *Biomacromolecules*, 2003, **4**, 974–980.

29 M. Bruma, B. Schulz, T. Kopnick and J. Robison, *High Perform. Polym.*, 2000, **12**, 429–443.

30 R. Pardey, S. S. Wu, J. Chen, F. W. Harris, S. Z. D. Cheng, A. Keller, J. Aducci, J. V. Facinelli and R. W. Lenz, *Macromolecules*, 1994, **27**, 5794–5802.

31 S. Fomine, M. Marin, L. Fomina, R. Salcedo, E. Sansores, J. M. Mendez, C. F. Jimenez and T. Ogawa, *Polym. J.*, 1996, **28**, 641–646.

32 J. Adducci, J. V. Facinelli and R. W. Lenz, *J. Polym. Sci. Part A Polym. Chem.*, 1994, **32**, 2931–2936.

33 R. Pardey, A. Zhang, P. A. Gabori, F. W. Harris, S. Z. D. Cheng, J. Adduci, J. V Facinelli and R. W. Lenz, *Macromolecules*, 1992, **25**, 5060–5068.

34 H. R. Kricheldorf, N. Probst, M. Gurau and M. Berghahn, *Macromolecules*, 1995, **28**, 6565–6570.

35 V. Roháč, V. Růžička, K. Růžička and K. Aim, *J. Chem. Eng. Data*, 1998, **43**, 770–775.

36 C.-G. Jaw, I.-M. Chen, J.-H. Yen and Y.-S. Wang, *Chemosphere*, 1999, **39**, 2607–2620.

37 C. H. Byers and D. F. Williams, *J. Chem. Eng. Data*, 1987, **32**, 344–348.

38 W. A. Johnson, *Invitation to Organic Chemistry*, Jones & Bartlett Learning, Burlington (US), 1999.

39 A. Rudin and P. Choi, in *The Elements of Polymer Science & Engineering*, Elsevier, San Diego, 2013.

40 H. R. Kricheldorf, S. Böhme and G. Schwarz, *Macromolecules*, 2001, **34**, 8879–8885.

41 F. Tao and S. L. Bernasek, *Chem. Rev.*, 2007, **107**, 1408–1453.

3 Polymers that show structural preferences in π-stacking

3.1. Abstract

One of the basic requirements for intercalation sequencing is a non-covalent binding unit. In supramolecular chemistry generally, it is necessary that multiple binding sites are located within a single host molecule due to the weakness of the non-covalent bonds. This is also the case in the current systems, where the chain-folding of the polymer backbone forms a stack of alternating donor-acceptor-complexes with the intercalator. The combination of multiple binding sites allows thereby an optimization of the association strength.[1]

Based on computer simulations, this chapter describes the synthesis, characterization and optimization of a novel naphthalene diimide-based structural unit with particularly high binding strength for electron-rich aromatic molecules.

Three homologous series of homo- and copoly(ester imide)s based on 1,4,5,8-naphthalene diimide or pyromellitic diimide were synthesized successfully. The copolymers consist of a imide-based pyrene-binding unit, aliphatic spacers and a non-pyrene-binding unit. The homopolymers comprise an imide-based pyrene-binding unit and spacers only. The complexation strength between the polymer's pyrene-binding diimide core and three different aromatic hydrocarbons was investigated as a function of spacer length $(CH_2)_x$. All homologous series of NDI-based homo- and copoly(ester imide)s consistently showed a peak in complexation strength with a spacer-length of two methylene groups in the diester residue -$OOC(CH_2)_xCOO$-: even one methylene group more or less decreases the complexation strength by around 60% from the peak value.

The strongly complexing structural unit could facilitate the intercalation sequencing of copoly(ester imide)s or be used for the design of supramolecularly crosslinked materials.

3.2. Introduction

The association constant of a donor-acceptor-complex depends on several parameters, including the donating and the accepting ability of donor and acceptor, respectively, a geometric congruence between the donors HOMO and the acceptors LUMO, potential steric hindrance of substituents and the solvent polarity.[2] When multiple binding sites are located within a single host molecule to enhance the binding, the association constant also depends on a possible three-dimensional complementarity between host and guest. In the current systems, mul-

tiple potentially complementary binding sites are available for a single aromatic donor as the polymer backbone forms a stack of alternating donor-acceptor-complexes.[3] The association strength can be improved substantially by size-matching hosts and guests.[1]

The exclusive binding of molecular hosts and size-matching guests only is a well-known principle in supramolecular chemistry.[4] This finds its correspondence in the lock-and-key model for substrate-enzyme-binding in biology.[5] While countless possible options exist for the creation of complementarity binding sites, numerous synthetic examples in the literature utilize a specific spacer length for the optimization of the binding behaviour:

Ramakrishnan and coworkers presented a folding copolymer system with alternating donor (pyromellitic diimide, PDI) and acceptor units (dialkoxynaphthalene, DAN) connected by polyethylenglycol linkers (Figure 1a).[6] The polyethylenglycol linkers $-(CH_2-CH_2-O-)_x$ were used in a range from $x = 4$, 5 or 6; the shortest spacer $x = 4$ exhibited the greatest propensity to form a folded chain. Rath and coworkers presented an example of a porphyrin-based macrocyle connected by alkane spacers from $x = 4$ to $x = 8$ which showed catalytic activity.[7] The spacer length affected the number and arrangements of the guests and their reactivity (Figure 1b).

Other examples include the variation of the alkane spacer length in a pyrene-based macrocyle acting as a rotaxane around single wall carbon nanotubes (Figure 1c) or in the binding of fullerenes:[8] Martín and coworkers achieved a particularly high binding constant for C_{60} fullerene by variation of the alkane spacer length in a tetraathiafulvalene-based semi-aromatic guest (Figure 1d).[9] Yamago and coworkers demonstrated size-selective binding of [10]cycloparaphenylenes (10 para-linked macrocyclic benzene rings) with C_{60} fullerenes while longer or shorter cycloparaphenylenes proved to be inactive (Figure 1e).[10]

It is furthermore well-known that the selectivity in binding between crown ethers and specific metal ions depends on the size of the macrocycle and thereby on the match in size with the ion involved (Figure 1f).[11]

It is known that naphthalene diimides and pyromellitic diimides form donor-acceptor complexes[12] with aromatic molecules such as anthracene,[2] pyrene[13] and perylene.[14,15] Such diimides can either be components of small molecules,[16] or of polymers.[17,18]

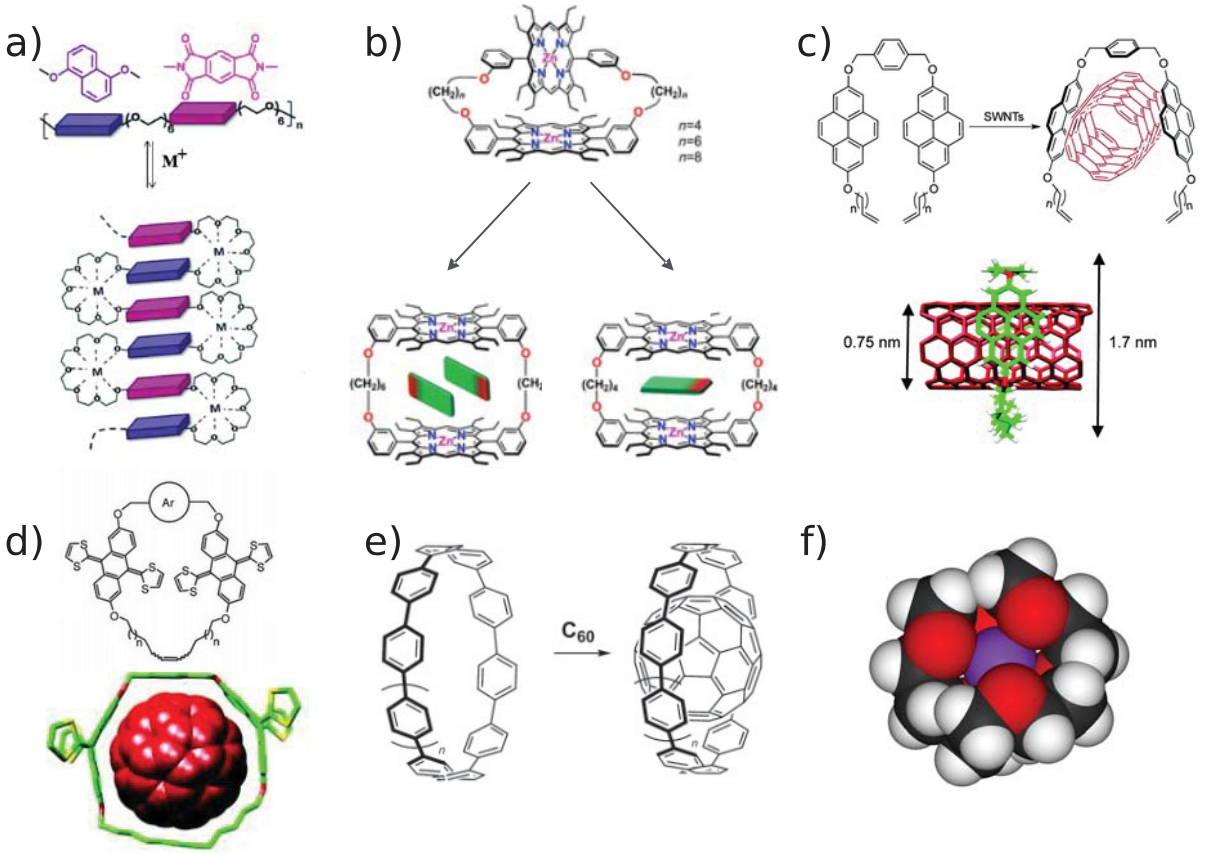

Figure 1: Overview of different host-guest systems, in which the spacer length plays a role for the binding behaviour. **a** is a foldamer, which has a similarity to the current system. In systems **a** - **d** and **f** an aliphatic spacer was varied for binding optimization, in system **e** an aromatic spacer (all figures used with permission).[6–11]

Thus, it has been shown that complexes between π-donors such as pyrene and designed co-polymers containing diimide units may have, in solution and in the solid state, not a random-coil but a specific chain-folded conformation stabilized via complementary π-π-stacking interactions between electron-poor diimide residues and electron-rich aromatics such as pyrene (Figure 2). This conformation was demonstrated by single crystal X-ray crystallographic analysis of model complexes, computational simulation, and by ^{1}H NMR spectroscopy. As a result of the folded conformation of the polymer chain in the complex, the total complexation shift of a diimide proton is generated not only by the ring-current of a pyrene molecule bound directly at the "observed" diimide residue but also, to a progressively decreasing extent, by pyrene molecules complexed at neighbouring imide units, and at their neighbours in turn, and so on outwards in both directions from the observed diimide residue.

For a binary copolymer in which one co-monomer unit can form complexes with pyrene (the "binding" unit generally based on either 1,4,5,8-naphthalene diimide or pyromellitic diimide) but the other co-monomer is unable to do so, there will be chain-sequences containing binding

imide units with other binding diimide units as neighbours and sequences containing diimide units with neighbouring residues which cannot bind pyrene. As a result of the folded chain conformation, binding of pyrene at neighbouring diimide residues also contributes to the total ring-current-induced complexation shift. Thus, diimide residues with neighbouring diimides show a higher total complexation shift than those having non-binding units as neighbours. Also the neighbours of neighbours and so on can, in principle, generate ring-current shielding effects, so that a wide range of total complexation shifts are produced depending on the chain sequence around the "observed" diimide. Ring-current shielding has previously been shown to be effective over a range of up to 12 Å.[19] The total ring-current shielding of the central diimide residue produced by complexing pyrene molecules is thus different for different sequences so that, in the presence of pyrene, copolymer sequences containing up to nine comonomer residues have been distinguished by ^{1}H NMR spectroscopy.[20] The chain-folding effect thus allows, under certain conditions, a detailed analysis of the fine-structure of the copolymer. This analysis can be compared to the traditional analysis of a polymer's tacticity (Figure 3). However, the chain-fold-based analysis has the advantage that much longer sequences may be identified: in a previous example 7 repeat units containing 112 (= 7·16) atoms, including heteroatoms.[20]

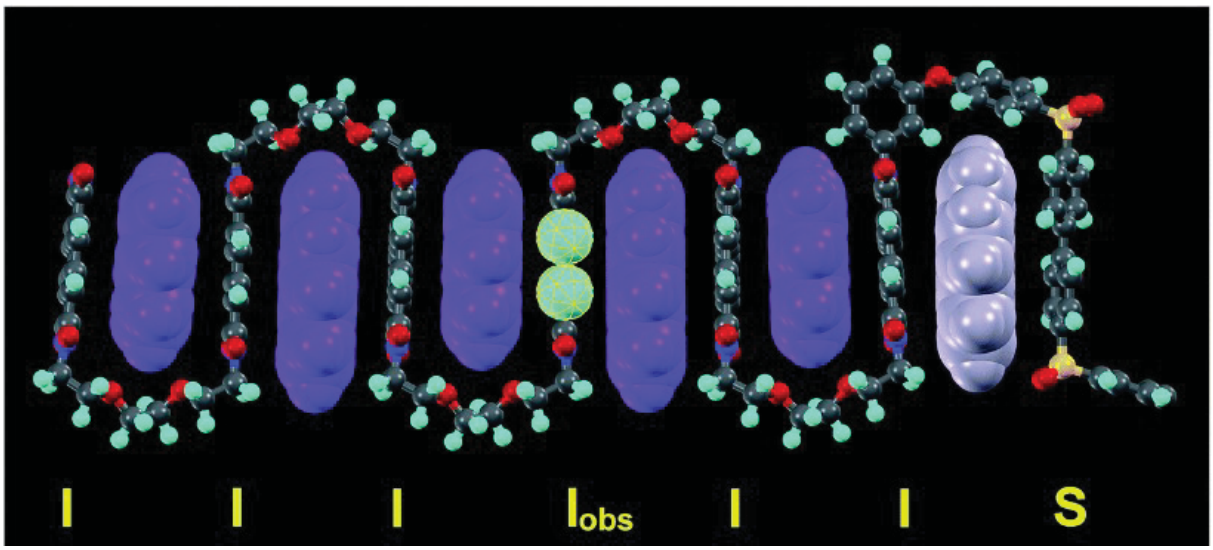

Figure 2: Computational simulation of the chain-folded confirmation of a polymer chain in solution or in bulk in which attractive interactions occur between pyrene and the imide groups in the polymer, keeping the polymer chain in a non-random conformation (used with permission).[20]

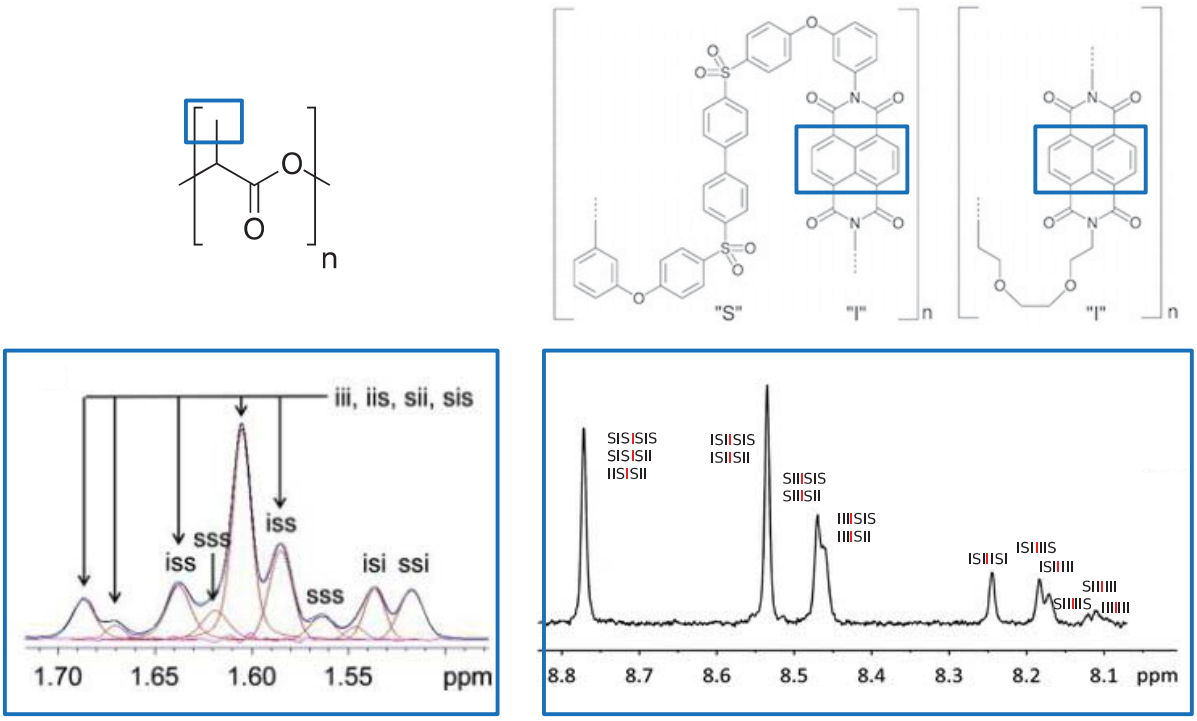

Figure 3: Left: Traditional analysis of tacticity by ^{1}H NMR spectroscopy, revealing syndiotactic (s) and isotactic (i) triplets, used with permission.[21] The analysis allows to distinguish different triplet sequences containing the same chemical group (CH_3-), depending on its stereochemical environment in the chain. Right: Intercalator sequencing,[20] the same chemical group (-CH=) can be distinguished, depending on the monomer sulfone (S) and imide (I) -based sequences sequence in which it is located, (used with permission).

In the present thesis, an investigation of supramolecular sequence-detection in poly(ester imide)s is described, a class of polymers well-known in the literature.[22] They are generally synthesized via polycondensation of diacid chlorides with diols (either in pyridine[23,24] or a high boiling solvent,[25] the latter approach being chosen in this study) or by melt-transesterification of diesters with diols at temperatures >200 °C under vacuum.[26,27] Naphthalene diimide-based polymers related to the homopolymers synthesized in this study are reported to be accessible by melt transesterification,[28] but this approach did not give access to polymers with aliphatic diacid residues [-OOC(CH_2)$_x$COO-] shorter than $x = 6$, due to the high melting points of the monomers.

In the present thesis, the successful synthesis of three homologous series of homo- and co-poly(ester imide)s based on the 1,4,5,8-naphthalene diimide is described: a sharp maximum in complexation strength with pyrene, anthracene and perylene is found for a certain, specific, length of an aliphatic spacer ($x = 2$).

3.3. Results and Discussion

3.3.1. Investigated polymers

The general synthesis of the homo- and co-poly(ester imide)s used in this study (Figure 4) was based on the polyesterification of bis(hydroxyethyl)diimides with diacyl chlorides in a high-boiling solvent (1-chloronaphthalene or 1,2-dichlorobenzene), as described in Chapter 2. The polymers were generally insoluble in THF, DMF, or chlorinated solvents. However, many of the polymers were soluble in mixtures of chlorinated solvents such as chloroform or dichloromethane with proton-donor solvents such as trifluoroethanol or hexafluoropropan-2-ol, in which their inherent viscosities and NMR spectra could be measured.

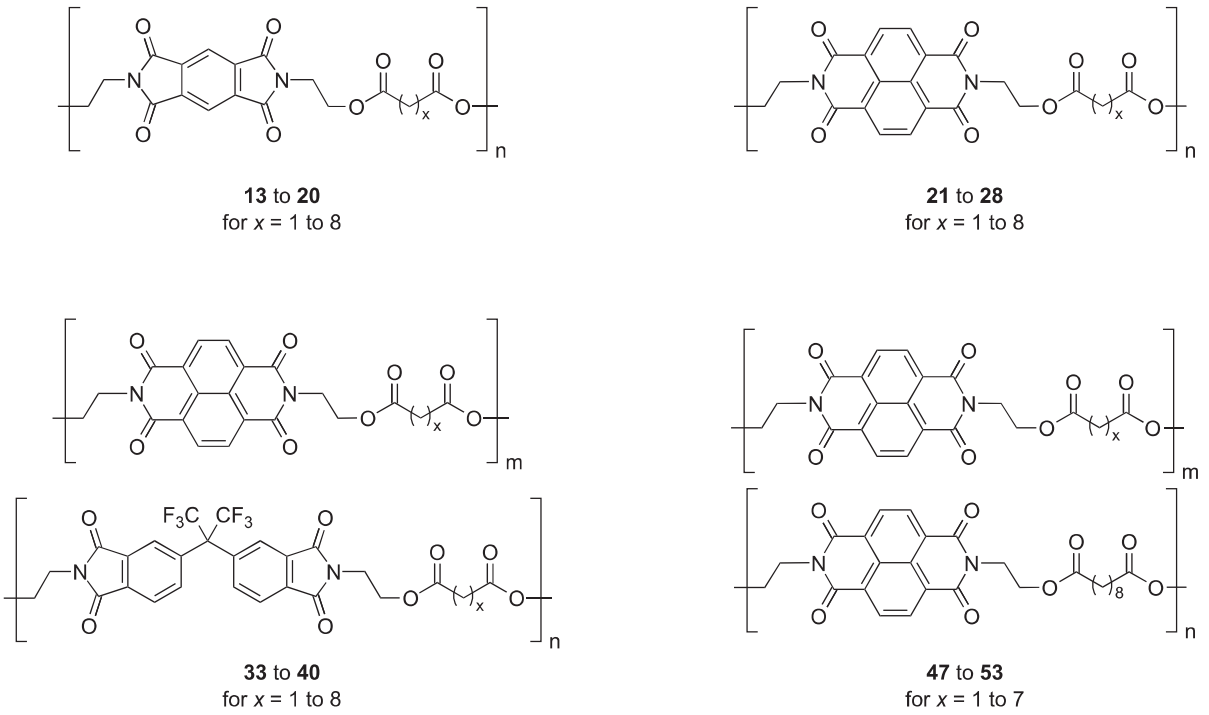

Figure 4: Above left: PMDI-based homopolymers (**13** to **20**) Above right: naphthalene diimide-based homopolymers (**21** to **28**). Below left: NDI / HFDI-based copolymers (**33** to **40**). Below right: all-aliphatic NDI-based copolymers (**47** to **53**). In each case, a range of polymers was obtained by varying the number of methylene groups *x*.

3.3.2. Investigations of supramolecular binding strength

All the PMDI-based and NDI-based polymers described in this study show complex formation with aromatic hydrocarbons such as pyrene, perylene and anthracene, as apparent from upfield shifts of the aromatic diimide proton resonances in their ^{1}H NMR spectra and the formation of charge-transfer colours in the polymer/aromatic hydrocarbon solutions. The aromatic hydrocarbons were used in the perdeuterated form to avoid overlap of resonances with

those of the polymer. These supramolecular polymer complexes show fast exchange on the NMR timescale, as separate resonances corresponding to bound and unbound diimide residues are not observed.

The complexation shift of the poly(ester imide)s with aromatic hydrocarbons was found to be dependent on the number of methylene groups x in the spacer between the diimide residues. For example, homopolymer $x = 2$ (**22**) shows a large complexation shift (0.51) with pyrene while the corresponding naphthalene-based homo-poly(ester imide) $x = 5$ (**25**) shows a much smaller complexation shift (0.15 ppm) in a solution of identical concentration (Figure 5).

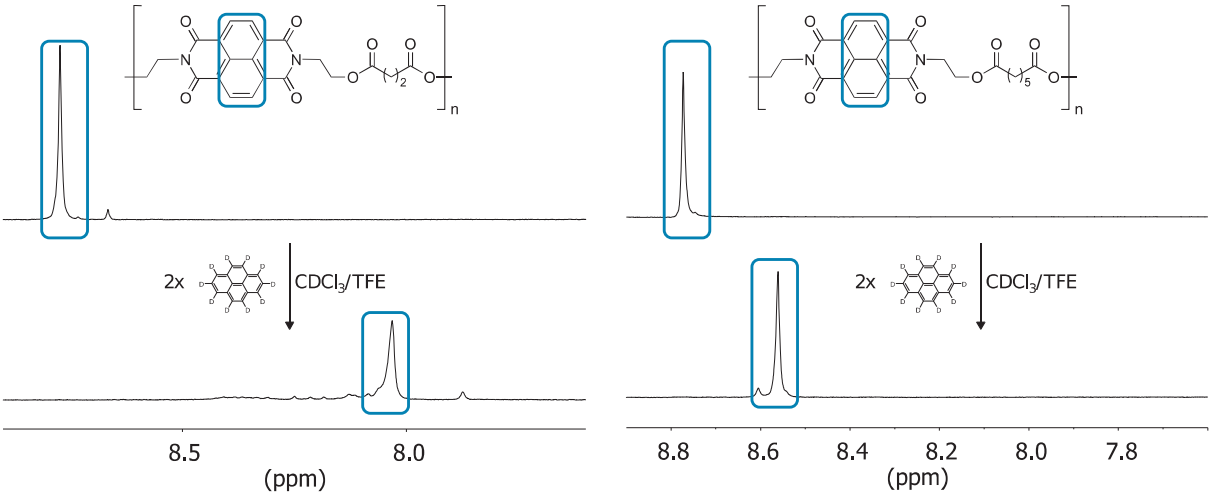

Figure 5: Variation of NDI complexation shift with diacid spacer length: Left: based homopolymer with spacer length $x = 2$ (**22**), showing a large complexation shift in the presence of two equivalents of pyrene-d_{10} per diimide residue (0.51 ppm). Right: homopolymer with spacer length $x = 5$ (**25**), showing only a small complexation shift (0.15 ppm).

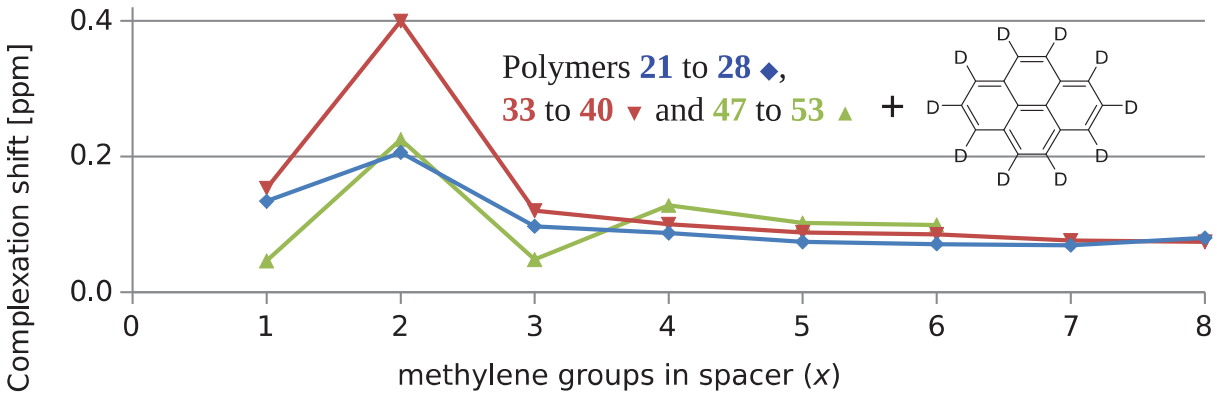

Figure 6: Comparison of complexation shifts (Δδ, ppm) of the aromatic imide protons in poly(ester imide)-pyrene complexes as a function of the spacer length from $x = 1$ to $x = 8$; using solutions comprising 3 mM intercalator and 4 mM polymers (see Chapter 8.11.1). The three graphs show the complexation shift of the aromatic imide protons in the NDI-based homopolymers (◆, **21** to **28**), in the NDI / HFDI-based copolymers (▼, **33** to **40**) and the all-aliphatic copolymers (▲, **47** to **53**).

For a systematic investigation of this effect, three homologous series of homo- and copoly(ester imide)s based on 1,4,5,8-naphthalene diimide were synthesized, each homologous series differing in the number of methylene groups *x* in the aliphatic spacer between the NDI units. The ^{1}H NMR complexation shifts were compared by preparing a 4 mM solution of each polymer containing 3 mM of an aromatic hydrocarbon. The complexation shift was calculated by subtracting the chemical shift of the aromatic diimide resonance in the presence of the aromatic hydrocarbon from the chemical shift of the same aromatic diimide resonance in the absence of any aromatic hydrocarbon. The complexation shift was used as a proportional measure of the complexation strength of the polymer-aromatic hydrocarbons-complexes. The complexation shifts of the three homologous polymer series with pyrene can be found in Figure 6. It can be seen that the complexation shift of all three polymers is weak for long spacers ($x = 8$ to 6) but increases slowly as the chain-length becomes shorter. Towards the optimum of $x = 2$ the binding strength increases very markedly before dropping sharply again for the shortest spacer with $x = 1$. The drop in complexation strength between the peak values of the three polymers and the adjacent values is about 65%. It is therefore clear that the NDI-based polymer with a spacer length of $x = 2$ (**22**) shows an energetic maximum for the complexation of pyrene.

The complexation shift shown in the Figure 6 could in case of the homopolymers be measured simply by comparing the position of the aromatic imide resonance. For the copolymers, the investigation is complicated by the fact that the presence of pyrene causes, in ^{1}H NMR in addition to a complexation shift, a splitting of the imide resonance (for example into 9 resonances, Figure 7). These copolymers are of particular interest because they are suited for intercalation sequencing. HFDI is known as a non-binding unit in the literature and thereby creates binding/non-binding co-polymers **33** to **40**. The all-aliphatic NDI-based copolymers exploits the observation that NDI connected by long spacers binds aromatic hydrocarbons only weakly and thereby generates strongly binding/mostly non-binding polymers; the polymers and the underlying concepts are the subject of Chapter 5.

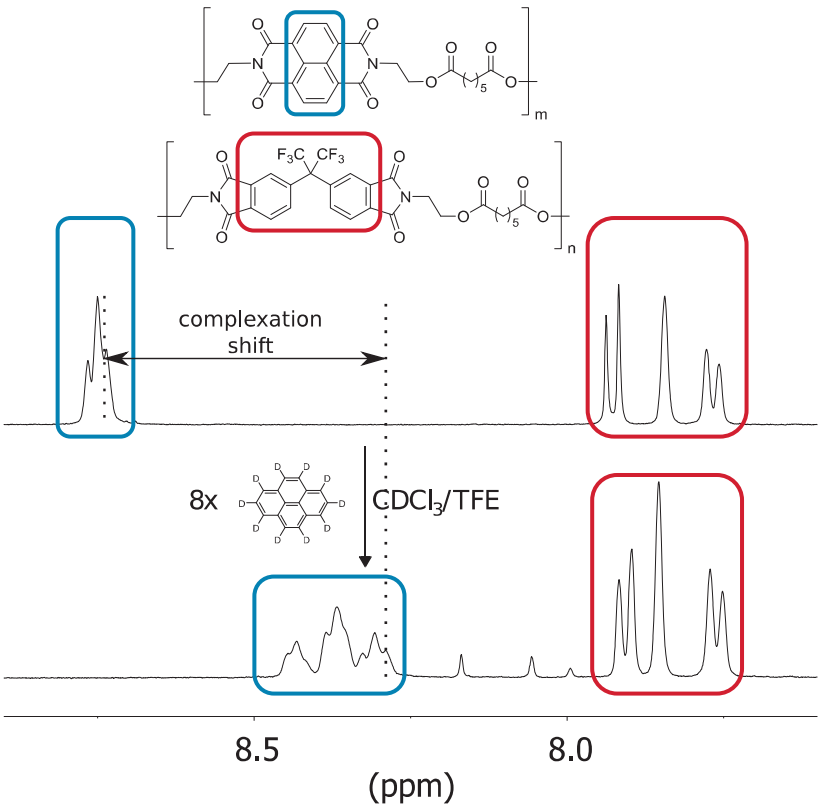

Figure 7: The aromatic imide resonance (blue box) of the NDI / HFDI-based co-poly(ester imide) x = 5 **37** shows in the presence of pyrene, besides a complexation shift, also a distinct splitting. For the calculation of the complexation shift, the resonance with the highest complexation shift was used, as this resonance contains the highest number of NDI-units. Between 8.1 and 7.9 ppm the spectrum shows the resonances of the residual protons of pyrene-d_{10} (only 98% deuteration).

This splitting of the aromatic imide resonance is caused by the presence of different sequences in the polymer backbone containing a different amount and ordering of NDI units. The co-operative effect of the pyrene binding leads to different chemical shifts for these sequences and makes them therefore distinguishable in ^{1}H NMR. As a measure of the binding strength of a copolymer, only the resonance with the strongest chemical shift was considered, as this resonance consists of the sequence with the highest amount of NDI units (NDI-NDI-NDI, etc.).[20] These sequences are identical to a correspondingly long sequences of an NDI homopolymer. It would be thus expected that complexes of these sequences show the same complexation shift as the corresponding NDI homopolymers, in both the NDI / HFDI copolymers (**33** to **40**) as well as in the all-aliphatic NDI-based copolymers (**47** to **53**). Indeed, the copolymers with long spacers (x = 4 to 8) show complexation shifts very similar to those of the homopolymers. The NDI / HFDI-based copolymers show for the strongly binding copolymer with a spacer length of x = 2 shows an even higher complexation shift. The aliphatic non-binding polymers show some divergence for the polymers with the spacer of x = 1 and 3, as these show a re-

duced complexation shift. Overall, however, the copolymers complexation shift shows a good conformity with the homopolymers one as the polymer with the spacer length of $x = 2$ is in each case by far the strongest binding polymer.

3.3.3. Computational studies of binding strength

The following computer simulations and evaluations were performed by Dr Ricardo Grau-Crespo and Scott Midgeley.

To find a possible explanation for the dependency of the binding strength on the number of methylene groups in the backbone, computational studies of chain-folding and pyrene-binding NDI / HFDI-based polyester-imides were performed. These computational studies were based on a form of Density Functional Theory with correction for dispersion forces. A chain-folding conformation was assumed, as numerous indications are given for such conformation (see Chapters 4 and 5). As can be seen in the following, a polymer chain with a length of more than two NDI residues was simulated, as a single chain fold showed very little difference in binding energy as a function of spacer length and proved thereby to be an inadequate model for binding. In the computational studies, longer segments of polymer chains were investigated (in total 7 folds containing 8 NDI residues) and their energies of binding to pyrene were studied to achieve a more realistic approach.

A unit of the energy-optimized polymer chains can be seen in Figure 8. In case of the NDI / HFDI-based $x = 5$ copolymer (**25**), which binds in comparison the weakest, the NDI residues are the least aligned towards the pyrene molecule and show the smallest overlap. The degree of binding strength is in the literature accounted for by the high congruence of the pyrene's HOMO and the NDI's LUMO and the efficient overlapping of the molecules based on a parallel, co-facial alignment.[15] In space-filling view (not shown), it becomes visually evident that in case of the HFDI-based $x = 2$ copolymer (**22**), pyrene fits more tightly in the polymers chain-fold than the other two copolymers (**21** and **25**).

The calculated energies can be seen in Table 1. The results are exactly in accord with the NMR-derived results, i.e. polymer **22** binds more strongly than polymer **21**, and polymer **25** is an even weaker binder than polymer **22** (binding energies shown as negative values).

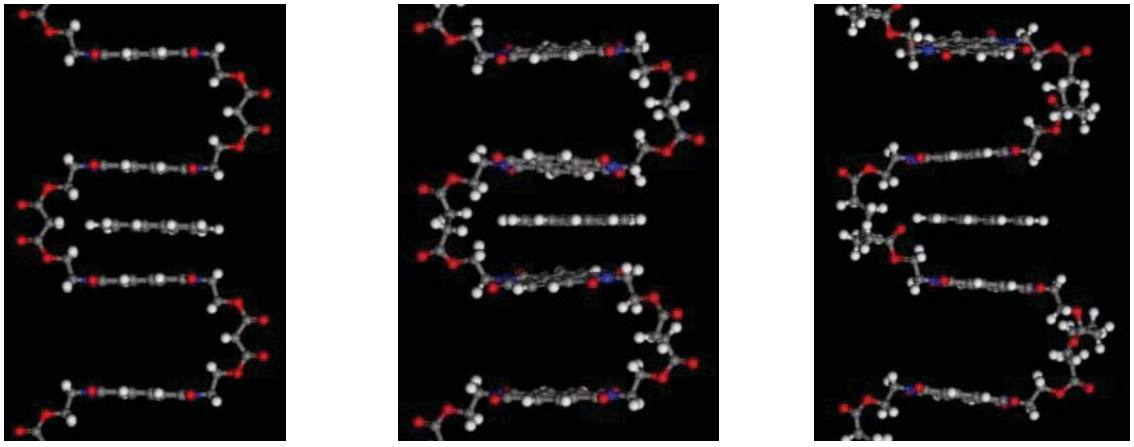

NDI-based x = 1 pol. (**21**) + pyrene | NDI-based x = 2 pol. (**22**) + pyrene | NDI-based x = 5 pol. (**25**) + pyrene

Figure 8: Units of the energy-optimized polymer chains of the NDI / HFDI-based x = 1 copolymer (**21**, left), of the NDI / HFDI-based x = 2 copolymer (**22**, middle) and of the NDI / HFDI-based x = 5 copolymer (**25**, right).

Table 1: Calculated binding energies.

polymer	binding energy (eV)
NDI / HFDI-based x = 1 copolymer (**21**)	-1.49
NDI / HFDI-based x = 2 copolymer (**22**)	-1.74
NDI / HFDI-based x = 5 copolymer (**25**)	-0.84

3.3.4. Other aromatic hydrocarbons

The complexation shift of complexes of the three homologous series of polymers was also investigated as a function of the spacer length x with other aromatic hydrocarbons, namely perylene and anthracene (both used in perdeuterated form). All samples were prepared with the concentration used above (solutions containing 4 mM polymer in terms of NDI residues and 3 mM aromatic hydrocarbon). It is apparent from a comparison of Figure 6, Figure 9 and Figure 10 that perylene causes at equal concentrations a higher complexation shift than pyrene, whereas anthracene causes a much lower complexation shift: this tendency is known from the literature.[14,29] The relative binding behaviour of perylene with the NDI homopolymers or the NDI / HFDI-based copolymers resembles pyrene's binding behaviour (Figure 9): The polymers with a spacer length of x = 2 (**22** and **34**) shows a particularly high complexation shift which decreases for longer or shorter spacers. The drop in complexation strength

from the peak value to the adjacent values is around 70% and 45% in the case of perylene and anthracene, respectively. Just as for the titration with pyrene, the NDI / HFDI-based copolymers show complexation shifts almost identical to those of the homopolymers for all spacer lengths but $x = 2$ (**34**); the latter shows again a greater complexation shift. The all-aliphatic NDI-based copolymers with a spacer length of $x = 2$ (**48**) shows with perylene interestingly not a weaker but a stronger complexation shift which is near identical to the corresponding NDI / HFDI-based copolymer $x = 2$ (**34**).

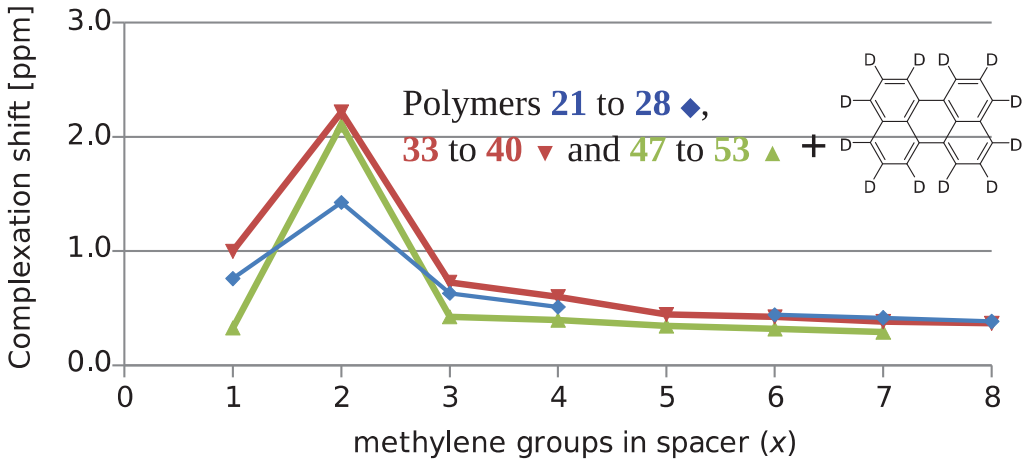

Figure 9: Comparison of complexation shifts (Δδ, ppm) of the aromatic imide protons in poly(ester imide)-perylene complexes as a function of the spacer length from $x = 1$ to $x = 8$; using solutions comprising 3 mM intercalator and 4 mM polymers (see Chapter 8.11.1). The three graphs show the complexation shift of the aromatic imide protons in the NDI-based homopolymers (◆, **21** to **28**), in the NDI / HFDI-based copolymers (▼, **33** to **40**) and the all-aliphatic copolymers (▲, **47** to **53**).

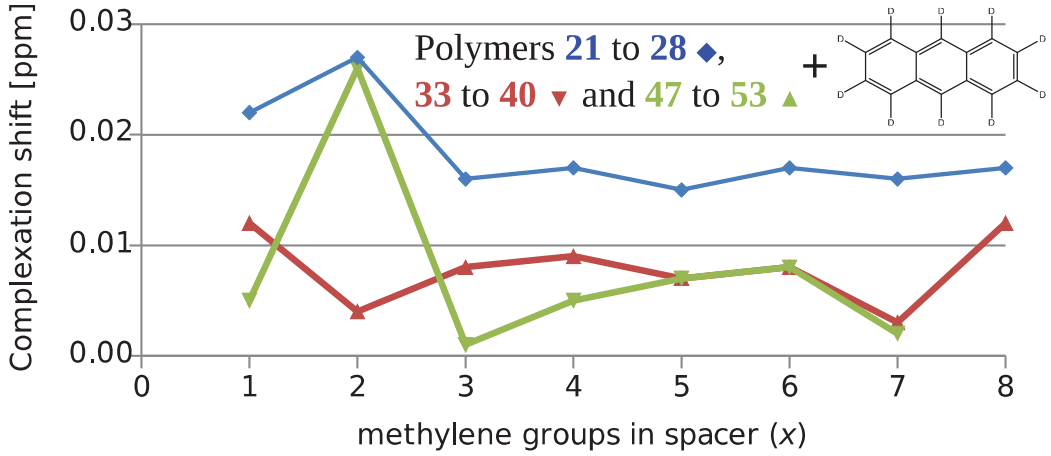

Figure 10: Comparison of complexation shifts (Δδ, ppm) of the aromatic imide protons in poly(ester imide)-anthracene complexes as a function of the spacer length from $x = 1$ to $x = 8$; using solutions comprising 3 mM intercalator and 4 mM polymers (see Chapter 8.11.1). The three graphs show the complexation shift of the aromatic imide protons in the NDI-based homopolymers (◆, **21** to **28**), in the NDI / HFDI-based copolymers (▲, **33** to **40**) and the all-aliphatic copolymers (▼, **47** to **53**).

Anthracene shows overall such a low complexation shift that the values are presumably more noisy and less reliable (Figure 10). However, it is clear that both, the NDI homopolymer (**22**) and the all-aliphatic NDI-based copolymer (**48**) with a spacer length of $x = 2$ show the strongest complexation shift. The NDI / HFDI-based copolymer (**33** to **50**) do not show any recognisable trend. Overall, a high degree of similarity in binding strength is found between the series of homopolymers (**21** to **28**) and the copolymers (**33** to **53**), and a high similarity of trends in binding strength between the three aromatic hydrocarbons. In summary, it was found that the binding structural unit of the NDI homopolymer with a spacer length of $x = 2$ causes with the different aromatic hydrocarbons the highest complexation shift, while the complexation shift falls of quickly for longer or shorter spacers. This trend has been found when the $x = 2$ spacer is present in different copolymers, as well as in different complexes with different aromatic hydrocarbons. The binding strength of the NDI unit is therefore mostly independent of the presence of non-binding units towards pyrene (like HFDI).

3.3.5. PMDI-based homopolymers

The same investigation was carried out with the homologous series of homo-poly(ester imide)s based on pyromellitic diimide (**13** to **20**) with pyrene (Figure 11) and perylene (not shown). Interestingly, the binding strength was found to be mainly independent of the spacer length x. The overall binding strength for the pyromellitic diimide-based polymers was found to be lower than the binding strength of the naphthalene-based polymers for all investigated aromatic hydrocarbons. This stands in agreement with the literature.[30]

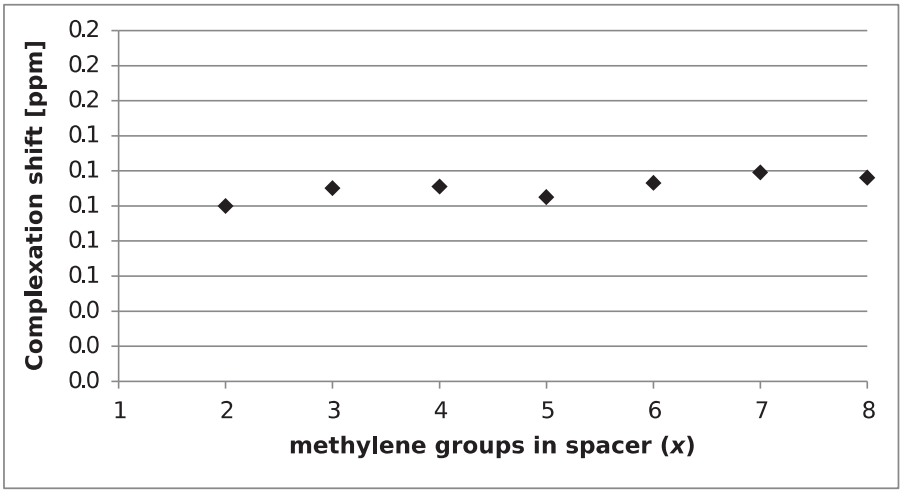

Figure 11: Comparison of complexation shifts (Δδ, ppm) of the aromatic imide protons in the PMDI-based poly(ester imide)-pyrene complexes as a function of the spacer length from $x = 1$ to $x = 8$. The graph show the complexation shift of the aromatic imide protons in the PMDI-based homopolymers (◆, **13** to **20**).

3.3.6. Quantification: Binding studies

After this semi-quantitative investigation, the binding strength of six representative polymer-aromatic hydrocarbon complexes was estimated by ^{1}H NMR titration for quantitative comparability. Solutions of a constant concentration of aromatic hydrocarbon (anthracene and perylene near saturation) and a variable concentration of polymer were prepared. The complexation shift of the diimide protons as a function of aromatic hydrocarbon concentration was followed by ^{1}H NMR spectroscopy, and from these values the association constant was calculated via an online tool.[31,32] It can be seen from comparison of Table 2 with Figure 6, Figure 9 and Figure 10 that the measured association constants correspond well with the trends observed for complexation shifts alone. Previous investigations found accordingly for a macrocyclic NDI-based system[29] the same relative complexation strength perylene > pyrene > anthracene and for NDI-based chain-folding dimers[14] similar absolute values of NDI oligomer·perylene K_a = 270 M^{-1} and NDI oligomer·pyrene K_a = 50 M^{-1}, respectively.

Table 2: Calculated binding constants of polymer- aromatic hydrocarbon complexes.

		Associate Constants (K_a/M^{-1}), guest		
	Spacer length	**anthracene**	**pyrene**	**perylene**
NDI-based polymer, host	x = 2 (**3**)	27 ± 5	171 ± 4	267 ± 9
	x = 5 (**6**)	11 ± 2	56 ± 2	96 ± 13

3.4. Conclusions

A new strongly binding NDI-based structural unit was designed and synthesized successfully as a part an extended series of an extended series of homo- and co-poly(ester imide)s. The structural unit showed a sharp maximum in binding strength for a spacer length of x = 2.

The homologous series' of homo- and co-poly(ester imide)s were synthesized from the bis(hydroxyethyl)diimide (naphthalene diimide or pyromellitic diimide) and aliphatic linear bifunctional acyl chlorides. By using diacyl chlorides of various length, homologous series' of polymers were accessible which differ only in x, the number of methylene groups in the aliphatic diacid residue, which ranges between 1 and 8.

The binding strength was investigated qualitatively and quantitatively. For the qualitative comparison, identical concentrations of polymer with an identical concentration of an aromatic hydrocarbon were added to a solution and the complexation shift in the ^{1}H NMR spec-

trum was compared. A particularly high binding strength was found for a spacer lenght of x = 2. The binding strength of the aromatic hydrocarbons was found to be anthracene > pyrene > perylene: all three hydrocarbons showed the same peak in binding strength at x = 2. In the quantitative comparison, the association constant was determined for selected complexes. The previous qualitative examination was confirmed and quantified: a K_a of 270 M^{-1} was found for the complex with the maximum binding strength (NDI-based homopolymer x = 2 [**22**] with perylene).

The structural binding unit of the homologous series of NDI-based homopolymers is identical with the corresponding unit in the homologous series of the NDI-based copolymers. The copolymers contain in addition to the binding structural unit non-binding or weakly-binding units towards aromatic hydrocarbons. While it would therefore be expected that the homologous series of NDI-based homopolymers and NDI-based copolymers would show the same trend in binding behaviour, this was precisely observed.

Thus a new binding structural unit was synthesized and characterized. Compared to previous binding structural units, this structural unit is characterized by a particularly high binding constant, improved solubility in polymer form and the presence of ester groups. The ester groups allow further exchange reactions, which are explored in Chapter 6.

3.5. References

1 J. Atwood, G. W. Gokel and L. Barbour, *Comprehensive Supramolecular Chemistry II*, Elsevier, 2nd edn., Amsterdam, 2017.

2 A. Das and S. Ghosh, *Angew. Chem. Int. Ed.*, 2014, **53**, 2038–2054.

3 Z. Zhu, C. J. Cardin, Y. Gan and H. M. Colquhoun, *Nat. Chem.*, 2010, **2**, 653–660.

4 K. Ariga and T. Kunitake, *Supramolecular Chemistry — Fundamentals and Applications*, Springer-Verlag, Berlin/Heidelberg, 2006.

5 F. A. Bettelheim, W. H. Brown, M. K. Campbell, S. O. Farrell and O. J. Torres, *Introduction to General, Organic and Biochemistry*, Brooks/Cole, Belmont (California), 2012.

6 S. Ghosh and S. Ramakrishnan, *Macromolecules*, 2005, **38**, 676–686.

7 P. Mondal, S. Sarkar and S. P. Rath, *Chem. Eur. J.*, 2017, **23**, 7093–7103.

8 A. López-Moreno and E. M. Pérez, *Chem. Commun.*, 2015, **51**, 5421–5424.

9 D. Canevet, M. Gallego, H. Isla, A. De Juan, E. M. Pérez and N. Martín, *J. Am. Chem. Soc.*, 2011, **133**, 3184–3190.

10 T. Iwamoto, Y. Watanabe, T. Sadahiro, T. Haino and S. Yamago, *Angew. Chem. Int. Ed.*, 2011, **50**, 8342–8344.

11 Y. Inokuchi, O. V Boyarkin, R. Kusaka, T. Haino, T. Ebata and T. R. Rizzo, *J. Phys. Chem. A*, 2012, **116**, 4057–4068.

12 J. H. Williams, J. K. Cockcroft and A. N. Fitch, *Angew. Chem. Int. Ed.*, 1992, **31**, 1655–1657.

13 H. M. Colquhoun, Z. Zhu and D. J. Williams, *Org. Lett.*, 2003, **5**, 4353–4356.

14 L. R. Hart, N. A. Nguyen, J. L. Harries, M. E. Mackay, H. M. Colquhoun and W. Hayes, *Polymer*, 2015, **69**, 293–300.

15 M. Yeh and H. Lin, *Phys. Chem. Chem. Phys.*, 2014, **16**, 24216–24222.

16 S. V. Bhosale, C. H. Jani and S. J. Langford, *ChemInform*, 2008, **39**, 331–342.

17 S. Ghosh and S. Ramakrishnan, *Angew. Chem. Int. Ed.*, 2005, **44**, 5441–5447.

18 B. W. Greenland, M. B. Bird, S. Burattini, R. Cramer, R. K. O'Reilly, J. P. Patterson, W. Hayes, C. J. Cardin and H. M. Colquhoun, *Chem. Commun.*, 2013, **49**, 454–456.

19 H. M. Colquhoun, Z. Zhu, C. J. Cardin, Y. Gan and M. G. B. Drew, *J. Am. Chem. Soc.*, 2007, **129**, 16163–16174.

20 J. S. Shaw, R. Vaiyapuri, M. P. Parker, C. A. Murray, K. J. C. Lim, C. Pan, M. Knappert, C. J. Cardin, B. W. Greenland, R. Grau-Crespo and H. M. Colquhoun, *Chem. Sci.*, 2018, **9**, 4052–4061.

21 K. Suganuma, H. Matsuda, H. N. Cheng, M. Iwai, R. Nonokawa and T. Asakura, *Polym. Test.*, 2014, **38**, 35–39.

22 H. R. Kricheldorf, in *Progress in Polyimide Chemistry II*, Springer Berlin Heidelberg, Berlin, Heidelberg, 1999, vol. 141, pp. 83–188.

23 J. A. Cade and W. Gerrad, *Nature*, 1946, **158**, 877–877.

24 S. E. Mallakpour and E. Kowsari, *Polym. Adv. Technol.*, 2006, **17**, 174–179.

25 H. R. Kricheldorf, N. Probst, M. Gurau and M. Berghahn, *Macromolecules*, 1995, **28**, 6565–6570.

26 X. Kong, H. Qi and J. M. Curtis, *J. Appl. Polym. Sci.*, 2014, **131**, 40579.

27 Yong He, Pujing Zuo, Zinong Ye, Masatoshi Aoyama, Xin Zeng, Xiangqun Fan, Xiaji Dai, Jing Lu, Solid-phase polymerization method for preparing high-molecular-weight aliphatic polyester, US 20140100350 A1, 2014.

28 H. R. Kricheldorf and P. Jahnke, *Eur. Polym. J.*, 1990, **26**, 1009–1015.

29 H. M. Colquhoun, Z. Zhu, D. J. Williams, M. G. B. Drew, C. J. Cardin, Y. Gan, A. G. Crawford and T. B. Marder, *Chem. Eur. J.*, 2010, **16**, 907–918.

30 L. Chen, Y. Zhang, L. Wang and Y. Liu, *J. Org. Chem.*, 2013, **78**, 5357–5363.

31 P. Thordarson, *Chem. Soc. Rev.*, 2011, **40**, 1305–1323.

32 http://www.supramolecular.org, accessed 1 June 2019.

4 Supramolecular identification of copolymer sequence via NMR spectroscopy

4.1. Abstract

The monomer-sequence of a copolymer is a fundamental parameter that influences mechanical and other properties and is industrially utilized. Intercalation sequencing is a technique that can be used to analyse the sequence of imide group-containing polymers, but so far, no systematics about the deliberate design of sequenceable polymers are known. In the present thesis a framework was found which allows such a systematic approach.

Novel, sequenceable poly(ester imide)s were synthesized by the reaction of hydroxy-bearing imide-based monomers with diacyl chlorides; the electron-poor imide is able to form donor-acceptor complexes with electron-rich aromatics and thereby provides a basis for intercalation sequencing.

Four imide-based monomers with different binding strengths were first evaluated in homopolymers and later incorporated in otherwise identical copolymers. The sequenceability and the sequence-related splitting pattern of the imide resonance could thereby be followed as a function of the complexation strength. It was found that most sequence information can be extracted when the difference in binding strength between the binding unit and the non-binding unit is maximised. A further variation of the binding strength could be achieved by using different aliphatic spacers, and this resulted in further changes in the sequenceability of the copolymers. The different resonances of the splitting patterns of the aromatic imide resonance were assigned by mathematical/atomistic models to the different sequences found in the random copolymers. Finally, the titration concentration was optimized and preliminary results suggest that titrations can also be carried out via ^{13}C NMR spectroscopic analysis.

Previously, only few sequenceable polymers were known in the literature, but in this study it was possible to produce numerous other examples. The maximising in binding strength difference between binding and non-binding units may serve as a general method for the creation of sequenceable polymers.

4.2. Theory

4.2.1. Copolymers and present goal

Intercalation sequencing is a technique used to determine the sequence of co-poly(imide)s via ^{1}H NMR spectroscopy. So far, it is not applicable to all possible co-poly(imide)s, but is has been described for five different polymers only.[1–5] For intercalation sequencing, it is desirable to obtain ^{1}H NMR spectra with a maximum number of distinguishable sequences which are expressed as resonances in ^{1}H NMR spectra with a resolution high enough to be distinguishable. A splitting into a large number of resonances is desired, as a corresponding amount of information can be extracted from the ^{1}H NMR spectrum. All examples in the literature show a splitting into three resonances,[1–4] with the exception of one work which shows a splitting into 10 resonances[5] (Figure 1).

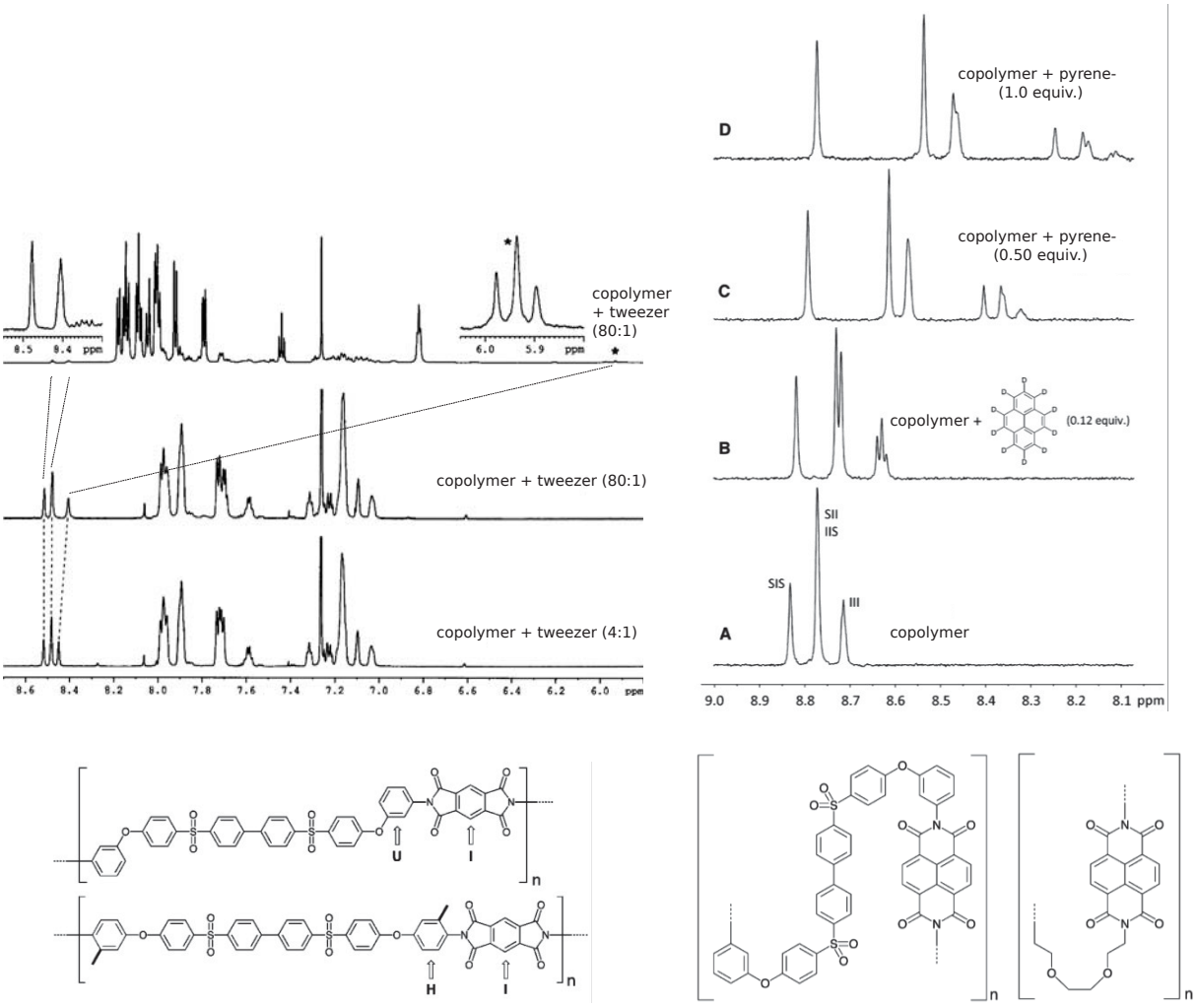

Figure 1: Two examples of successful intercalation sequencing of polyimides. In the left example,[4] one resonance splits into three resonances, in the right example[5] nine resonances emerge from two initial resonances, used with permission.

Since only a few examples of successful intercalation sequencing have been described so far and those examples showed a low information density only, further potentially information storing polymers (synthesized as described in Chapter 2) are investigated in this chapter. Four different monomers (NDI, PMDI, BPDI and HFDI-based) were evaluated in terms of information extractability by incorporating them into various binary co-poly(ester imide)s and titrating these with electron-rich aromatic intercalators. The monomers were systematically permutated to gain insights into the best possible information extractability.

4.2.2. Mathematical model of complexation strength

Intercalation sequencing provides information[6] about the sequence (order of co-monomers) of binary copolymers. The technique allows therefore to distinguish between two different elements (monomer residues) and their relationship in a linear order; a copolymer chain can thereby be represented as a string of numbers (for a binary copolymer e. g. “1” and “0”). This is a common approach for the representation of digital information and is also related to the traditional approach for the representation of a protein’s primary sequence as a string of letters.[7]

The distinguishability between monomer units within a polymer chain in intercalation sequencing is based on a difference in complexation shift in ^{1}H NMR spectroscopy. The different complexation shift is in turn based on different binding constants. In supramolecular chemistry, binding strength is a fundamental parameter.[8] The binding strength indicates to which extent host and guest interact with each other. Unlike in computer science, however, there are not only two possible values for the binding strength (1 and 0, symbolized in the following by ■ and □, respectively), but there is a wide range of possible binding constants. Binding units with a reduced binding constant are thus symbolized by 0.7 (or graphically, in greyscale, by ■) and mainly non-binding units by 0.3 (■). For graphical symbols it is evident that sequences with a large difference in binding constant, based on 1 and 0 (■/□), are due to a higher contrast easier to read than sequences with a smaller difference in binding constant, 0.7 and 0.3 or ■/■ (Figure 2, exemplary sequences based on the ASCII code). The contrast would translate in NMR spectroscopy to the resonance resolution.

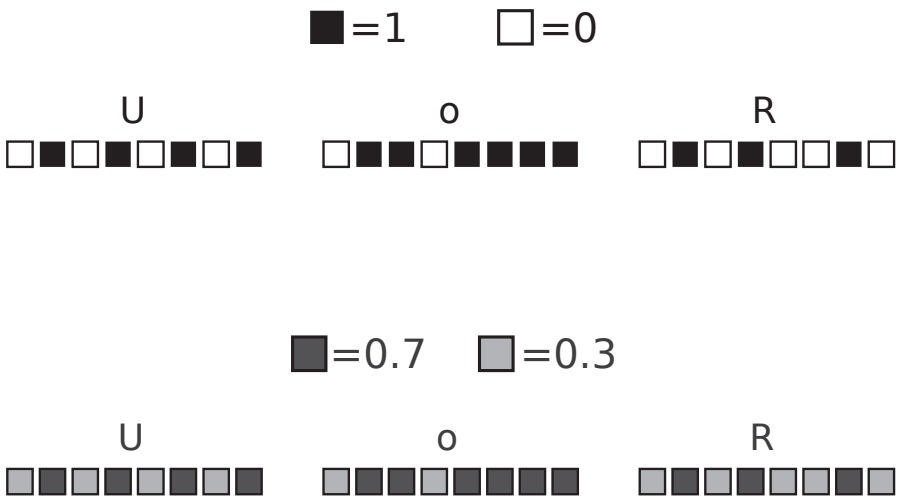

Figure 2: The sequence UoR (University of Reading) in ASCII code, top: made from a strongly binding monomer made from a strongly binding unit (1 or graphically ■) and non-binding unit (0 or □); bottom: made from a weakly binding unit (0.7 or ■) and a mainly non-binding unit (0.3 or ■). The top row with a larger difference in binding constant has a higher contrast and thereby a higher readability.

Structural elements that differ more in their binding constant should also be more easily distinguishable in NMR spectroscopy. Therefore, the hypothesis was adopted that the resolution of the splitting pattern and thereby the number of distinguishable resonances will depend on the difference in complexation strength between the two different co-monomers. This hypothesis was tested here by permutation of different monomers in the polymer backbone. The symbolism in strongly and weakly binding units (■ and ■) and mostly and completely non-binding units (■ and □) helps to assess polymers in terms of sequenceability at first glance and helps to understand the concept.

4.3. Investigating building blocks: Binding and non-binding homopolymers

The present chapter examines different diimide-based monomers as building blocks for potentially sequenceable polymers. The behaviour of the building blocks was first examined by incorporation in homopolymers (Figure 3), because the binding sections of the random copolymers are identical to sections of corresponding length in homopolymers. Therefore, an identical behaviour of the binding structural unit was expected when comprised in homopolymers and copolymers: This was indeed experimentally confirmed in Chapter 3. Two binding diimide-based structural units NDI and PMDI and two non-binding units HFDI and BPDI were selected because they are based on commercially available dianhydrides.

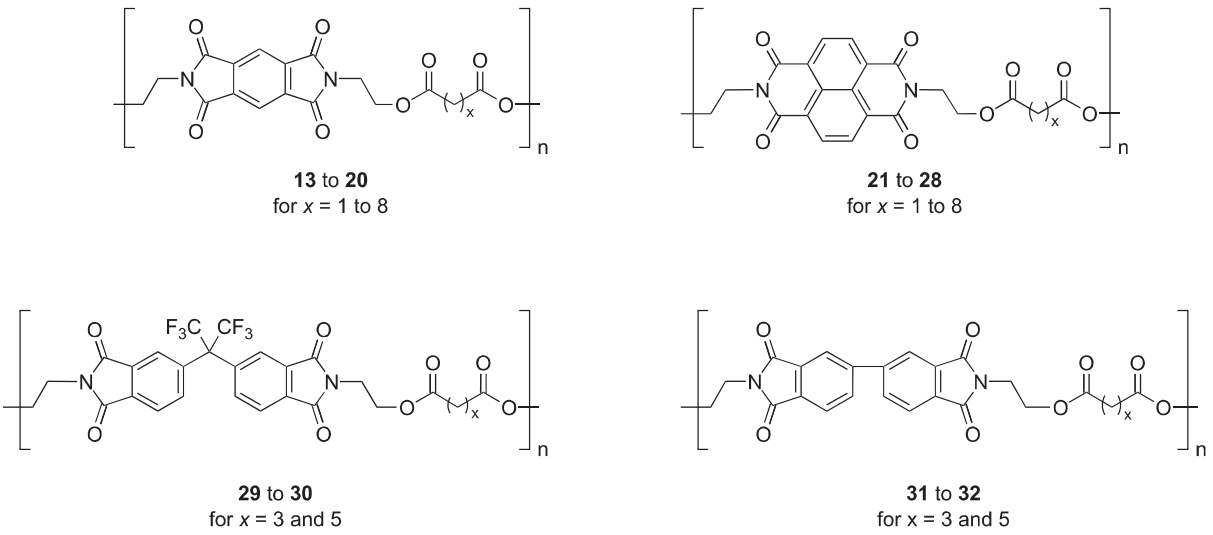

Figure 3: PMDI-based (**13** to **20**), NDI-based (**21**to **28**), HFDI-based (**29** and **30**) and BPDI-based homopolymers (**31** and **32**) used used in this work as representatives to indicate the binding strength.

The binding and non-binding polymers were also prepared with a range of spacer lengths: An extensive study of the polymers of all spacer lengths was carried out in Chapter 3. Here, the four imide-based homopolymers are compared with the spacer length $x = 5$ as a representative set of polymers with a focus on sequenceability.

4.3.1. Binding units: Naphthalene and pyromellitic diimides

The aromatic sub-units of naphthalene diimide (NDI) and pyromellitic diimide (PMDI) (Figure 4) are electron deficient and so form donor-acceptor complexes[9] with aromatic donors such as anthracene,[10] pyrene[11] or perylene.[12,13] Such diimides can either be components of small molecules,[14] or of polymers.[15,16] Complex formation in polymers is exploited for the synthesis of foldamers[10,15,17] and the basis for sequence recognition in copolyimides.[18]

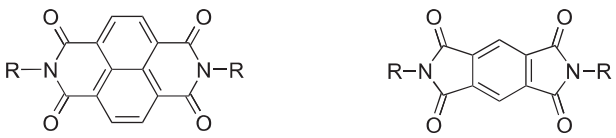

Figure 4: Naphthalene diimide (left) and pyromellitic diimide (right).

Various other donors and acceptors are commonly used in addition to those mentioned (Figure 5). They belong all to the class of π-donors and π-acceptors (lone-pair donors like phosphine are not included) and many are based on aromatic systems.

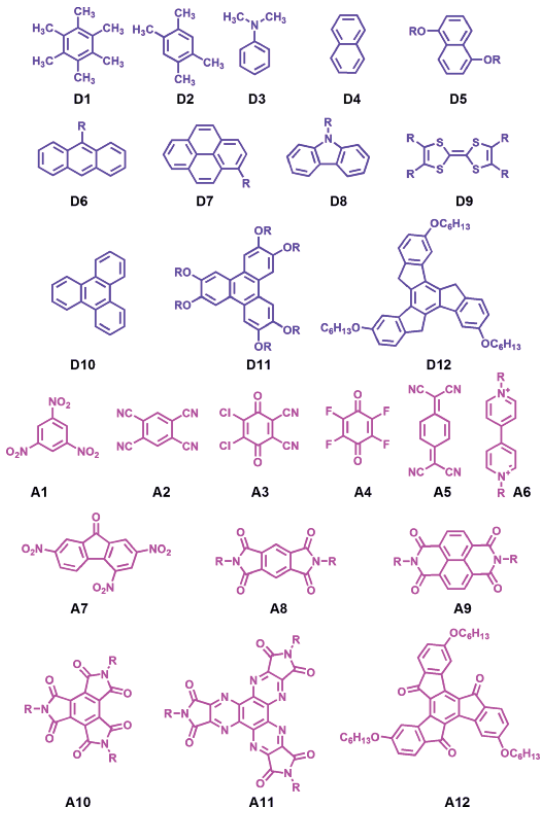

Figure 5: Examplary π-donors (D1 to D12) and π-acceptors (A1 to A12) used for the creation of supramolecular structures, used with permission.[10]

A previous systematic study[19] investigated the co-assembly of a series of three donors (carbazole, phenothiazine and pyrene) and three acceptors (pyromellitic diimide, naphthalene diimide, and perylene diimide) grafted on a polymer backbone. Out of the nine combinations, pyrene–NDI (D7–A9) was identified as combination with the greatest degree of π-stacking.

This behaviour was not mainly attributed to the π-electron density, as carbazole and phenothiazine show lower oxidation potentials than pyrene (they are better donors) while PMDI and NDI have nearly identical electron affinity. The higher binding strength was instead accounted for by the high congruence of the pyrene's HOMO and the NDI's LUMO and the efficient overlapping of the molecules based on a parallel, co-facial alignment (Figure 6). A later theoretical analysis supported these results.[13] It was found that the association constant of NDI in chloroform is three times greater than that of PMDI (in complexation with a dihydroxynaphthalene derivative).[10]

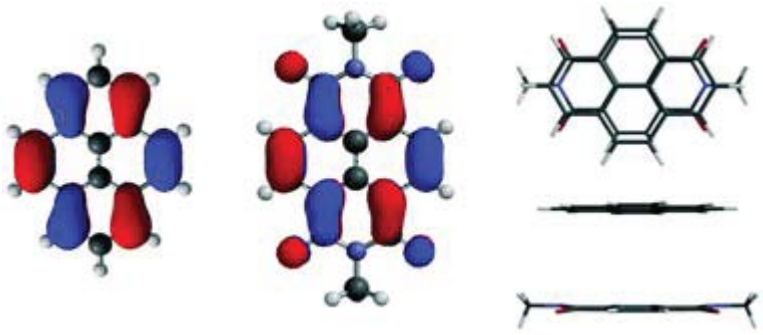

Figure 6: The HOMO of pyrene (left) is highly congruent with the LUMO of NDI (middle); this leads to a efficient co-facial overlapping, used with permission.[19]

The binding behaviours of the NDI and the PMDI units in the current system were determined by investigating homopolymers **25** and **17**. For the synthesis, first the corresponding anhydrides were converted with 2-aminoethanol to the bis-hydroxyethyl diimide monomers (Chapter 2); this is a common strategy in the literature.[14] Subsequently, these were reacted with diacyl chlorides via polyesterification to afford homo-poly(ester imide)s.

As expected, the NDI-based homopolymer (**25**) shows, with K_a = 55 M^{-1}, a significantly higher binding constant than the PMDI-based homopolymer with K_a = 10 M^{-1} (**17**, see Chapter 3). This can readily be seen in Figure 7; the NDI-based homopolymer shows in presence of a 8 mM pyrene solution a complexation shift of 0.16 ppm, the PMDI-based homopolymer only a complexation shift of 0.11 ppm. The strongly binding NDI unit is therefore symbolized in the following by (■), the weakly binding PMDI unit by (■).

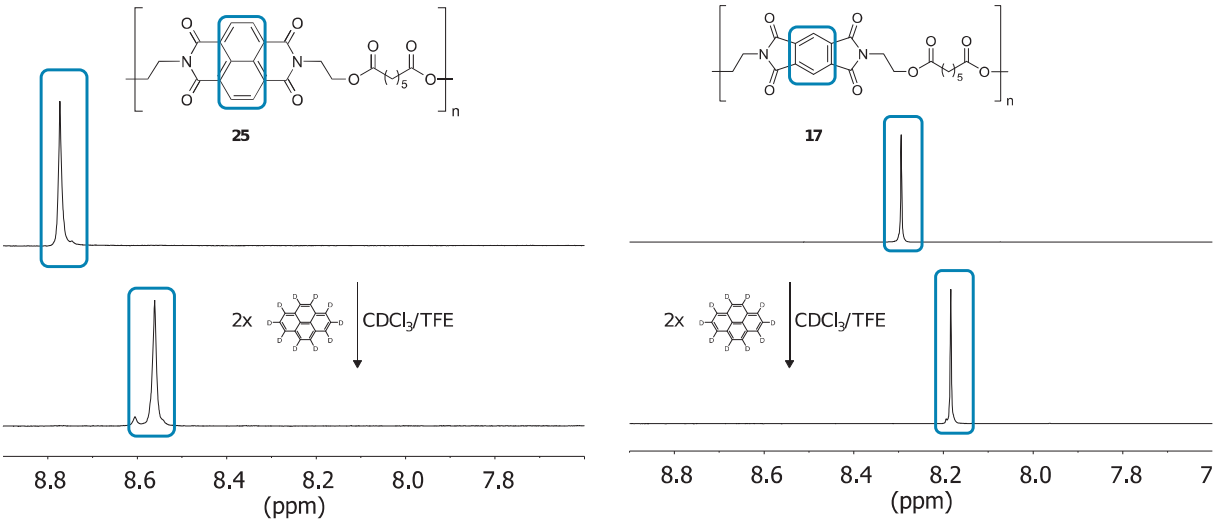

Figure 7: ^{1}H NMR spectrum of the NDI-based homopolymer x = 5 (**25**) and the PMDI-based polymer x = 5 (**17**) in the absence (top) and in the presence of 8 mM pyrene-d_{10} (2x excess, bottom).

It was furthermore found that not only the diimide core effects the binding strength, but in the case of NDI-based polymers also the length of the aliphatic spacer connecting the diimide cores (as described in Chapter 3). Therefore, in some cases also the spacer length *x* was permutated besides the diimide core.

4.3.2. Non-binding units: HFDI and BPDI-based homopolymers

Since information extractable polymers consist of binding and non-binding units, also co-monomers which do not bind pyrene or other aromatic hydrocarbons had to be chosen. In the previous work on information extractable polymers,[1–5] imide-containing repeat units were used for both the binding and non-binding repeat units; this concept is continued in the current chapter, using HFDI and BPDI as potentially non-binding units (Figure 8). While aromatic imides readily form charge-transfer interactions as electron-deficient species, it was necessary to chose imides which do not participate in such interactions. In the selection of such imides it was possible to rely on extensive previous research as shown below.

Figure 8: HFDI (left) and BPDI (right).

Polyimides are the most extensively utilized heat-resistant polymers in industry.[20] Polyimides tend to show internal (intra- and inter-chain) charge-transfer complexation which leads to a yellow to brown coloration. The charge-transfer complexation also contributes to the polymers high thermomechanical properties.[21] This inherent colour and thus the charge-transfer complexation itself can be problematic when optically transparent polyimide films are required, as in end-user or in optical applications. It was demonstrated that the colour intensity of polyimides is related to the monomer structure,[22] and charge-transfer complexation can thus be mitigated by choosing appropriate structures.

Mitigating structures can be flexible and bulky linkage groups which are traditionally introduced between the aromatic rings of the monomer.[23,24] They enhance not only the transparency, but also the solubility and processability of the polymer by disrupting of intramolecular conjugation or by making the chain packing less efficient (to prevent intermolecular CT formation).[21] A close relationship between the degree of packing and the intermolecular charge-

transfer complexation exists. For example, a significant increase in charge-transfer complex formation was observed with closer chain packing as demonstrated from combined fluorescence and SAXS measurements.[25] Consequently, common strategies for the prevention of charge-transfer complexation in polyimides include the use of fluorinated monomers (mostly limited to polymers derived from HFDI or 2,2'-bis(trifluoromethyl)benzidine, TFMB)[26] or the use of aliphatic (usually cycloaliphatic)[27] monomers. In principle, both strategies have been applied in this study: HFDI-based polymers were used in this chapter, and monomers with mostly aliphatic structure in Chapter 5.

Another guide in the search for non-binding monomers is the intensity of internal charge-transfer complexation of different monomers, which has been systematically compared.[22] The strength of charge-transfer complexation was measured by the depth of the polyimide's colour as detected by UV/vis absorption of polymers formed from various monomers.

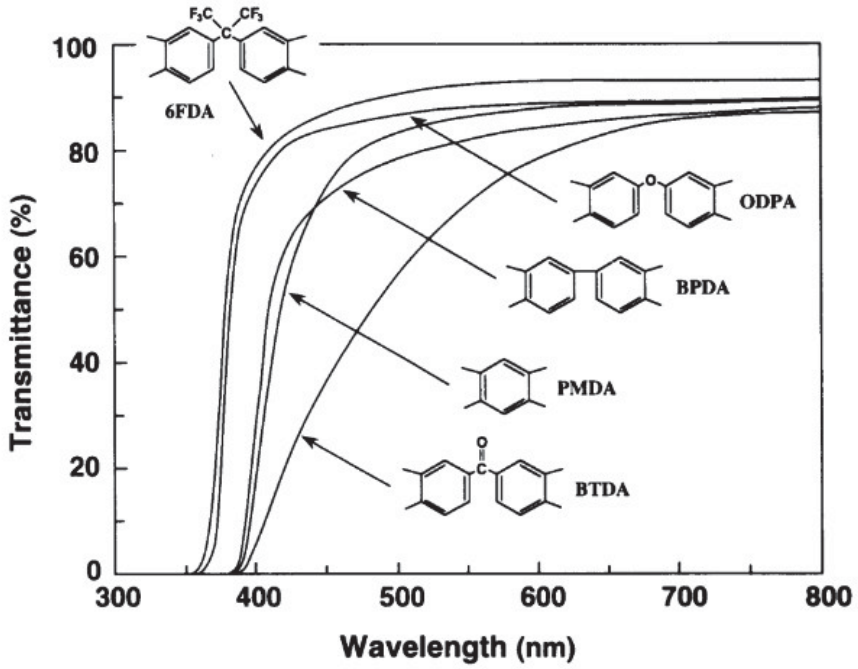

Figure 9: UV/vis absorption spectra of five polyimide films from the anhydrides shown and the diamine 2,2′-bis(trifluoromethyl)benzidine (TFBD). The HFDI-based polymer (top) produces the lowest coloration of all polyimides, the BPDI-based polymer shows an intermediate coloration.[22]

Previous work indicated HFDI and BPDA to be promising candidates for information extractable polymers. HFDI was previously applied successfully in an information extractable polymers (extracting sequence information at just the triplet level),[1] BPDI showed in the work of a previous PhD student[28] particularly low binding and was therefore a promising candidate.

This was supported by the findings presented in Figure 9, which show that a HFDI-based polymer owned a very low coloration (due to charge-transfer complexation) and a BPDI-based polymer an intermediate coloration.[22] Therefore, HFDI and BPDA-based monomers were used as a basis for information extractable polymers in this work. The properties and synthesis of the corresponding dianhydrides have been presented in a review.[29]

4.3.2.1. HFDI-based homopolymers

The incorporation of trifluoromethyl groups in polyimides has been investigated to obtain polyimides of improved processability, a low dielectric constant, increased hydrophobicity and high optical transparency. An improved processability is achieved because the incorporation of trifluoromethyl groups increases the solubility in organic solvents and lowers the T_g.[26,30,31] Polyimides based on 4,4'-hexafluoroisopropylidene-diphthalic anhydride (HFDA) have found wide-spread use in applications as electronics,[32] optical applications,[33] and the aerospace industry.[34]

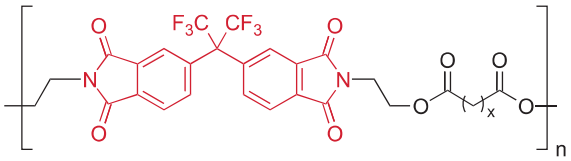

Figure 10: The HFDI-based homopolymer: the HFDI-unit is marked red. HFDI-based homopolymers were synthesized with a spacer-length of $x = 3$ (**29**) and $x = 5$ (**30**).

Even though the HFDI unit is relatively rigid, it causes a distortion of the backbone symmetry (Figure 11) and thereby prevents a parallel alignment of the polymer chains,[21] owed to the steric hindrance between the bulky trifluoromethyl groups.[26] A simulation of an HFDI-containing tetramer showed a bent and twisted conformation at the hexafluoroisopropylidene linkage $–C(CF_3)_2–$.[36] Incorporation of hexafluoroisopropylidene groups furthermore restricts intra-segmental and inter-segmental mobility.[23]

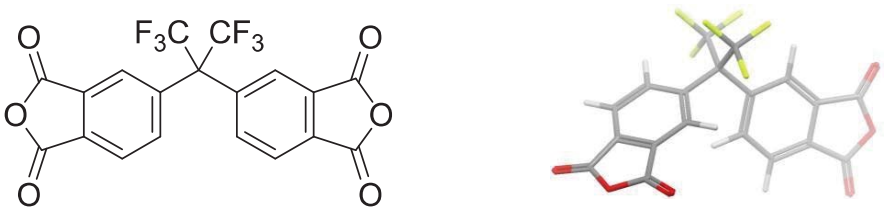

Figure 11: Structure of 4,4′-(hexafluoroisopropylidene)diphthalic anhydride (HFDI, left) and a molecular model (right).[35]

The listed restrictions hinder effective chain packing and the disrupted packing leads to amorphous character and increases the free volume in the bulk polymer. This enhances the permeability for gas molecules; therefore, HFDI is also incorporated in polymers used in membranes for gas separation.[31]

Since the trifluoromethyl groups are electron-withdrawing, they increase the electron affinity of the molecule and should thereby enhance CT interactions. The opposite is actually the case: HFDI shows due to the hindrance of the trifluoromethyl groups very little charge-transfer interaction.[22] Therefore, the aromatic donor-acceptor interactions present in other imides are effectively inhibited, as shown in Figure 9. Also the low polarizability of fluorine and fluorinated groups weakens the intermolecular interactions.[22] This makes HFDI a promising candidate for a non-binding building block in information extractable polymers.

To incorporate 4,4′-(hexafluoroisopropylidene)diphthalic anhydride (HFDA) in a poly(ester imide) via the reaction with an diacyl chloride, it must be reacted to a bishydroxyl imide-containing monomer. This was achieved by forming the bisdiimide from the anhydride with 2-aminoethanol (Scheme 1), as described in Chapter 2:

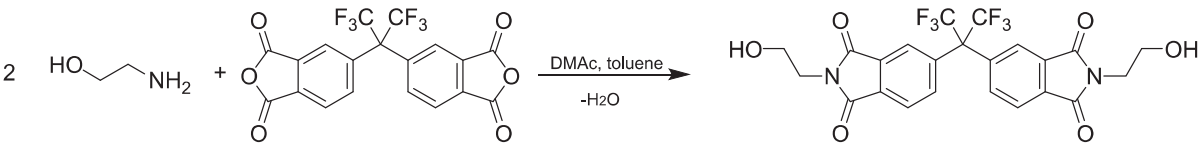

Scheme 1: Reaction of 4,4′-(hexafluoroisopropylidene)diphthalic anhydride with 2-aminoethanol to give bis(hydroxyethyl)hexafluoroisopropylidene biphthalimide

The bis(hydroxyethyl)hexafluoroisopropylidene biphthalimide obtained in the reaction was used in a second step as a monomer for the polymerization with a diacyl chloride (pentanedioyl dichloride or heptanedioyl dichloride) to give the HFDI-containing homopolymers **29** and **30** and was used in later stages of this work as a co-monomer.

An investigation of possible complex formation with pyrene as example was carried out following the complexation shift via ^{1}H NMR spectroscopy. The ^{1}H NMR spectrum in the presence of a 25 times molar excess of pyrene-d_{10} per diimide residue showed a maximum complexation shift of only 0.02 ppm (Figure 12). As expected, the data show therefore only very weak complex formation.

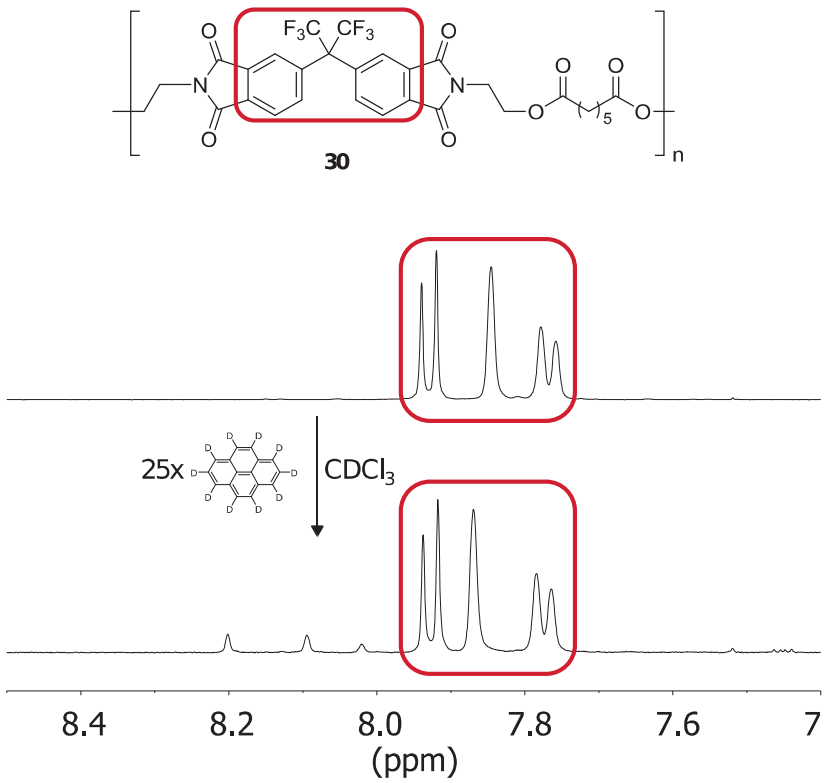

Figure 12: ^{1}H NMR spectrum of the HFDI-based homopolymer **30** in the absence (top) and presence (bottom) of a 25 fold excess of pyrene-d_{10}. The aromatic protons show only a very small complexation shift of 0.02 ppm.

When compared to the complexation shift of the imide resonance of the NDI homopolymer (■), the complexation shift of the HFDI-based homopolymer is negligible. HFDI should therefore be suitable as a non-binding moiety in pyrene-binding/non-binding copolymers and is in the following symbolized (□). In addition, the HFDI-based homopolymer showed excellent solubility in various organic solvents (THF, dichloromethane, etc.) and is thus expected to act in a copolymer as a solubilizing unit. This is not surprising, as HFDI is known to give polyimides an improved solubility in organic solvents.[37]

4.3.2.2. BPDI-based homopolymers

3,3',4,4'-Biphenyltetracarboxylic dianhydride (BPDA, Figure 13) is a common monomer for the synthesis of polyimides via imidization with diamines.[38] It is used on an industrial scale for the synthesis of Upilex R (from BPDA and 4,4'-oxydianiline) and Upilex S (from BPDA and *p*-phenylenediamine).[39] Upilex S is of great commercial significance due to its low cost (for a polyimide) and high performance.[40]

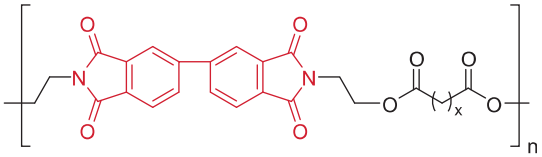

Figure 13: The BPDI-based homopolymer: the BPDI-unit is marked red. The aliphatic spacer was used with a length of $x = 3$ (**31**) and $x = 5$ (**32**).

The biphenyl unit of BPDA and its carboxylic residues are electronically conjugated through the biphenyl linkage.[41] The conformation of BPDA (Figure 14) can therefore be planar and does not contain a twist, as is found in HFDI. When incorporated in polyimides, the offset geometry of the BPDA moiety results in a kinked and rigid structure. Such polymers are only able to rotate around the C-C bond of the biphenyl group which enhances the rigidity[23] and gives it together with a strong molecular association between the chains a high molecular orientation.[42]

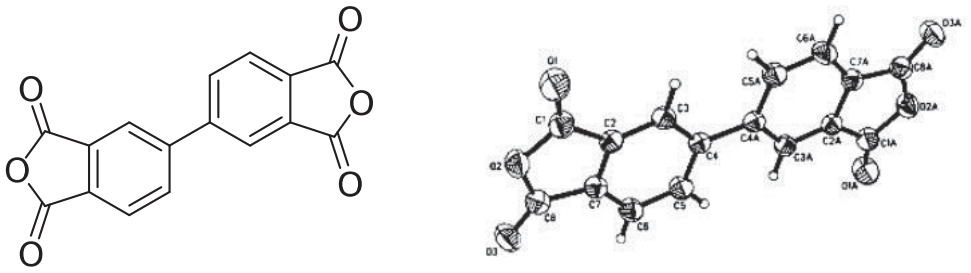

Figure 14: Structural formula of 3,3',4,4'-biphenyltetracarboxylic dianhydride (left) and its X-ray structure (right), used with permission.[29]

One study compared a BPDA/*p*-phenylendiamine-based homopolymer with the PMDA/*p*-phenylendiamine-based homopolymer.[43] WAXS results suggested for both polymers high degrees of crystal orientation. A molecular simulation suggested that the BPDA/*p*-phenylendiamine-based polyimide chains has a loosely folded orientation whereas the PMDA/*p*-phenylendiamine-based polyimide has a rigid and straight orientation. BPDA affects also polymer processability: due to its rigidity, BPDA-based polymers exhibit also a low solubility in organic solvents.[34]

BPDA has no bulky groups and is, in contrast to HFDA, an essentially linear and potentially coplanar structure: a stronger CT activity is thus expected. Figure 9 shows that BPDA, when incorporated into polymers, actually produces a medium-intensity charge transfer band. A colourless polyimide film based on BPDA can only be obtained when it is combined with aliphatic monomers.[26]

For the incorporation into a polymer, BPDA must be reacted with 2-aminoethanol via imidization to give a bis-hydroxyethyl imide-containing monomer (Scheme 2), as described for HFDI:

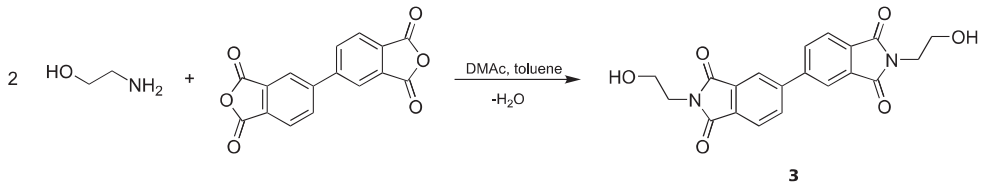

Scheme 2: Reaction of 3,3',4,4'-biphenyltetracarboxylic dianhydride (BPDA) with 2-aminoethanol to give *N,N'*-bis-(2-hydroxyethyl)biphthalimide

N,N'-Bis-(2-hydroxyethyl)biphthalimide was used as a monomer with a diacyl chloride for polymerization to the poly(ester imide)s **31** and **32**. In order to investigate the suitability of BPDI as non-binding unit, a ^{1}H NMR spectrum of the BPDI-based homopolymer **32** was measured in the presence and the absence of a 25 fold excess of pyrene-d_{10} and a complexation shift of 0.15 ppm was found (Figure 15). In contrast to the HFDI-based homopolymer (□), the BPDI-based homopolymer **32** shows therefore some degree of charge-transfer interaction at high concentrations: it is symbolized as (■) in the following. It was already known in the literature that the BPDI unit shows stronger charge-transfer interactions than the HFDI unit (Figure 9).[22] The charge-transfer interactions are, however, significantly weaker than those of the the NDI-based (■) or the PMDI-based (■) homopolymers. Therefore, BPDI is in principle still usable as a non-binding unit. Besides the complexation shift, the BPDI-based homopolymer shows upon the addition of pyrene-d_{10} also a change in its *J*-coupling pattern (Figure 15). The adjacent diimide protons of the BPDI-based homopolymer are nearly equivalent in chemical shift and show very little coupling (top spectrum without pyrene-d_{10}) with minor outer lines. In the presence of pyrene-d_{10}, the two protons are chemically less equivalent and show a more pronounced coupling; moreover a pronounced roof effect is recognizable.

As expected from incorporation of the BPDA unit, the solubility of the biphthalimide homopolymer is poorer than that of the hexafluoroisopropylidene-diphthalimide analogue, which introduced later a further hurdle for complexation-sequencing, as the generally low solubility of NDI-based polymers is already a limiting factor anyway.

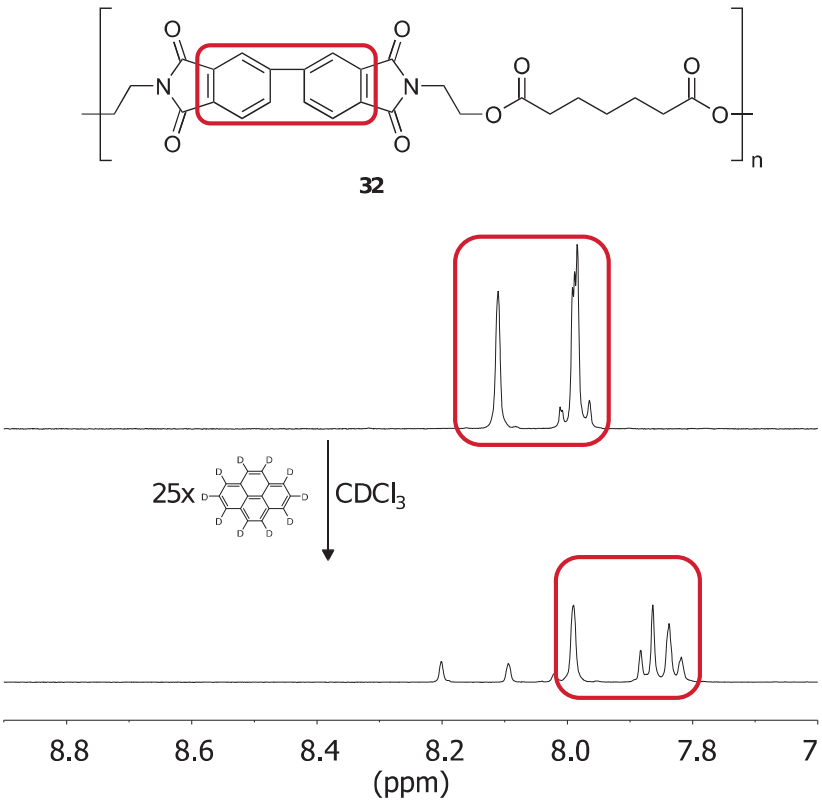

Figure 15: ^{1}H NMR spectrum of the BPDI-based homopolymer x = 5 in the absence (top) and presence (bottom) of a 25 fold excess of pyrene-d_{10}. The BPDI protons show a complexation shift of 0.11 ppm besides a more clearly exhibited proton-proton coupling.

For intercalation sequencing, a non-binding unit is incorporated into the copolymers to inhibit charge-transfer interactions and thus make neighbouring binding units in ^{1}H NMR distinguishable from other binding units by a reduced complexation shift. Since BPDI-based homopolymer (■) binds significantly less strongly than NDI-based (■) or PMDI-based (■) homopolymers, it can in principle be used as a non-binding unit, although it does not inhibit charge-transfer interactions so well as HFDI (□). In addition, the solubility of the BPDI unit is worse than the HFDI unit which limits the processability of the resulting polymers.

4.4. Obtaining sequence information: binding / non-binding copolymers

The above mentioned binding and non-binding monomers were used for the synthesis of various copolymers (Figure 16), each containing a binding (NDI ■ or PMDI ■) and a non-binding unit (BPDI ■ or HFDI □). In principle, the co-polymers could also comprise more than two co-monomers, but the resonances of binding and non-binding units in the ^{1}H NMR spectrum were not sufficiently well-resolved (far enough apart) that another binding unit would have been clearly distinguishable. For this reason, only binary copolymers were used in this study.

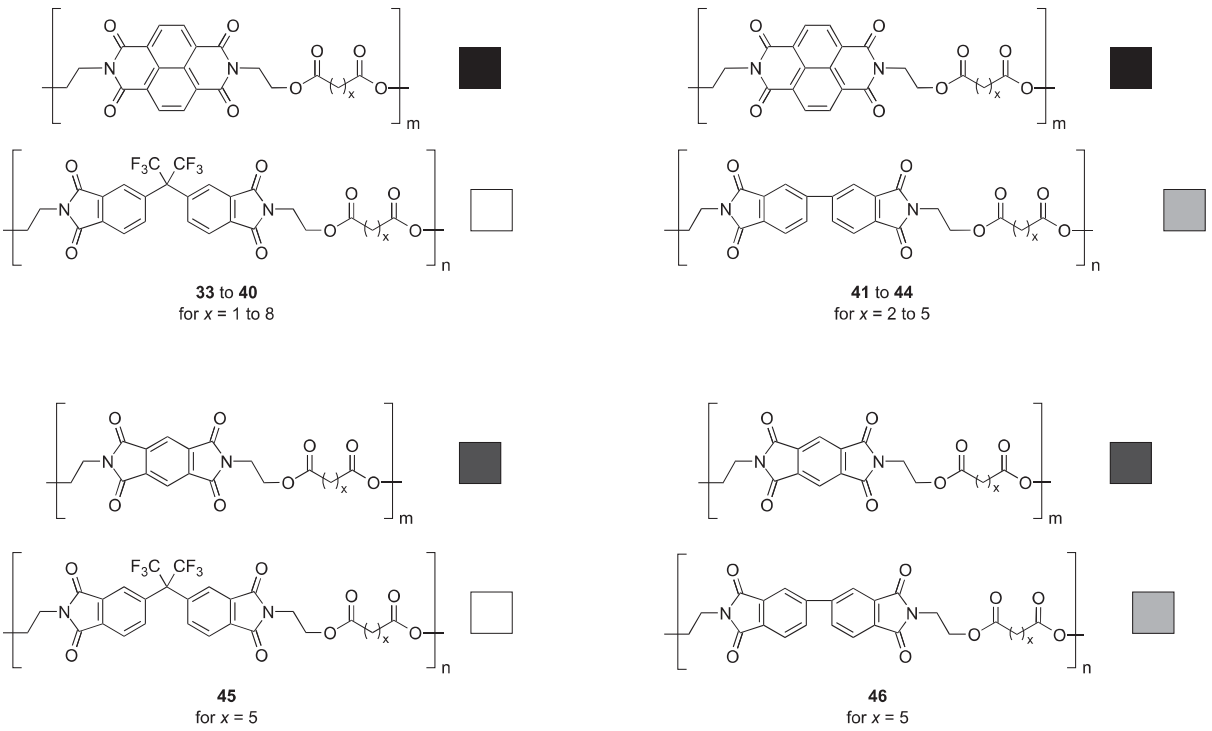

Figure 16: Above left: NDI / HFDI-based copolymers (**33** to **40**). Above right: NDI / BPDI-based copolymers (**41** to **44**). Below left: PMDI / HFDI-based copolymer (**45**). Below right: PMDI / BPDI-based copolymer (**46**). In case of polymers **33** to **44**, a range of polymers was obtained by varying the number of methylene groups *x*.

4.4.1. NDI / HFDI-based copolymers

NDI / HFDI-based copolymers (**33** to **40**, Figure 17, symbolized ■/□) have the largest difference in binding constant as the binding NDI (■) is, of the four diimide units, the one that shows the strongest binding and the non-binding HFDI (□) is the unit that shows the weakest binding. As described in section 4.2.2 it is thereby hypothesized that the most sequence information can be obtained from those polymers.

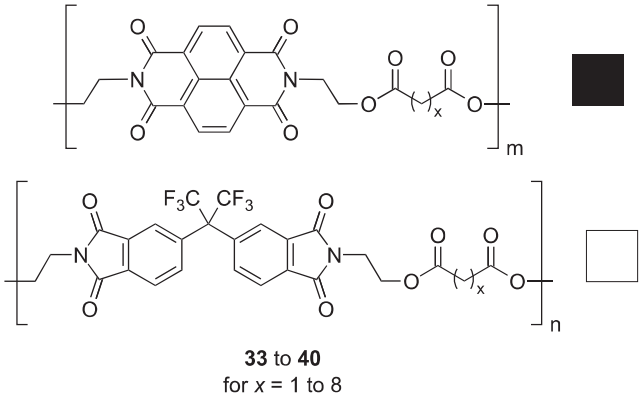

Figure 17: NDI / HFDI-based copolymers (**33** to **40**).

As described in Chapter 3, it was found that the binding strength of the homopolymer depends not only on the type of binding unit but additionally on the chain-length of the spacer (Figure 18). Since the NDI / HFDI-based copolymers were the most promising ones, a homologous series with varied binding strength was produced by systematic variation of the aliphatic spacers. Thus, 1:1 NDI / HFDI-based copolymers were synthesized with aliphatic spacers length in a range from $x = 8$ to $x = 1$. It was found that the NDI / HFDI-based copolymers with long spacers have the simplest splitting pattern, and these are therefore described first.

As is presented in the following, NDI-based copolymers with a high binding energy ($x = 2$ to 4, **33** to **36**) have a 'singlet / doublet / triplet' type splitting pattern, whereas NDI-based copolymers with a low binding energy ($x = 5$ to 8, **37** to **40**) show a 'triplet of triplets' type binding pattern. Based on this observation, two different binding models were applied (Figure 19), a chain-fold binding for polymers with high binding energy and a random binding for polymers with low binding energy.

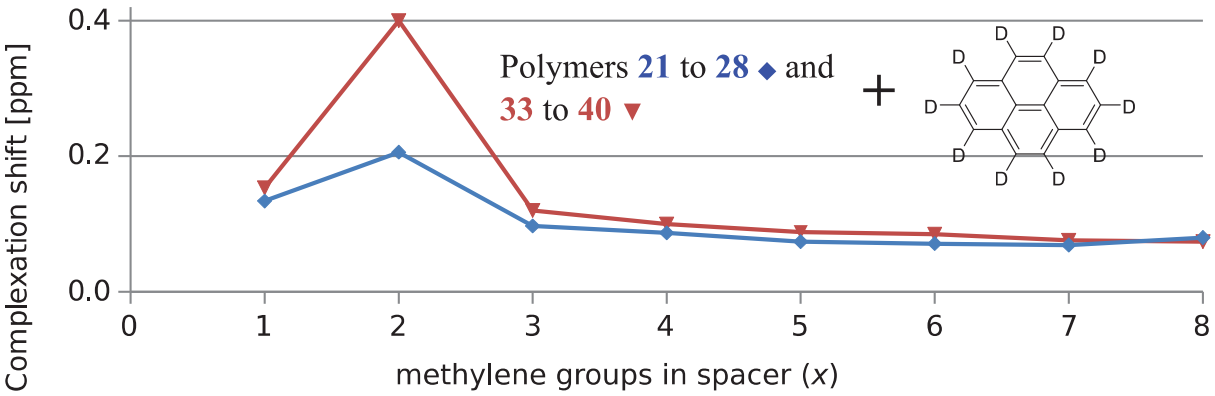

Figure 18: Comparison of complexation shifts (Δδ, ppm) of the aromatic imide protons in poly(ester imide)-pyrene complexes as a function of the spacer length from $x = 1$ to $x = 8$. The graphs show the complexation shift of the aromatic imide protons in the NDI-based homopolymers (◆, **21** to **28**) and in the NDI / HFDI-based copolymers (▼, **33** to **40**).

The chain-fold binding (Figure 19 a) assumed for polymers with a high binding energy ($x = 2$ to 4, **33** to **36**) has already been described in an earlier publication.[5] If no ordering forces are present, polymer chains are present in a non-ordered "random coil" conformation. In case of the NDI-based polymer, however, the entropic penalty of an ordered structure is compensated by the enthalpic gain of the attractive interaction between the NDI residues and pyrene. Thereby, a chain-fold binding is caused and a chain-folding conformation is formed in which NDI and pyrene are alternately stacked. This ordered region extends at least as far as it is detectable in ^{1}H NMR spectroscopy, i.e. as far as the ring-current shielding extends (in a time-averaged equilibrium structure).

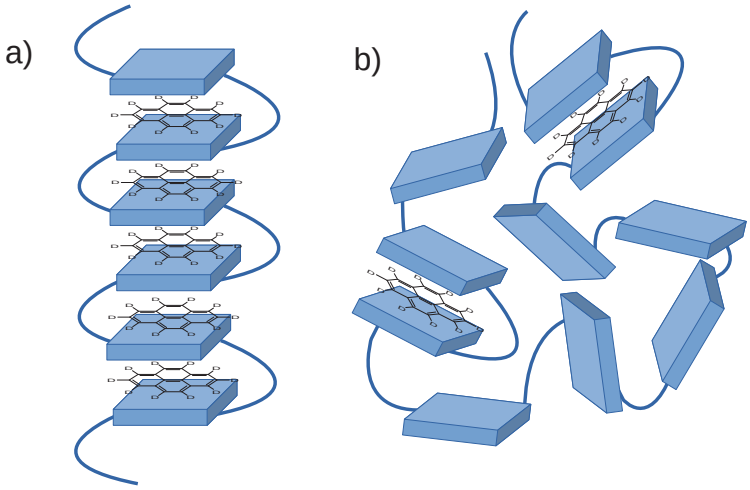

Figure 19: (a) Model showing possible binding conformations of NDI-based homopolymers (NDI residues represented by blue boxes and aliphatic spacer represented by blue lines) and pyrene-d_{10}. NDI-based homopolymers with short spacers and high binding energies (x = 2 to 4, 33 to 36) takes a conformation characterized by chain-fold binding, in which the NDI residues are alternatingly stacked with pyrene-d_{10}. (b) NDI-based homopolymers with long spacers and a low binding energy (x = 5 to 8, 37 to 40) take a less ordered conformation, in which a locally increased pyrene concentration is caused by transient pairwise binding.

In weakly binding polymers (x = 5 to 8, **37** to **40**), no chain-folding is assumed (Figure 19 b). Here, the weaker attractive pyrene-NDI interaction leads to a lesser degree of order. The smaller attractive pyrene-NDI interaction can be seen from the smaller complexation shift of the corresponding polymers in ^{1}H NMR spectroscopy at comparable pyrene concentrations. In the model, it is assumed that the pyrene concentration is locally increased by a delivery involving transient pairwise binding. Surrounding NDI units are presumed to be not in an ordered state.

4.4.1.1. NDI / HFDI-based copolymers with long spacers (x = 5 to 8)

The NDI resonance of NDI / HFDI-based copolymers with long spacers (x = 5 to 8, **37** to **40**) splits upon the addition of pyrene-d_{10} into an apparent ‘triplet of triplets’ (Figure 20). The shortening of the aliphatic spacer x does not affect the splitting pattern (comparing **37** and **38**) except for a minor improvement in resolution. This can be related to the fact that a shortening of the spacer length from x = 8 initially hardly leads to any change in binding energy (Figure 18).

Since the binding energy of these polymers is weak, the NDI / HFDI-based copolymers with long spacers (x = 5 to 8, **37** to **40**) are based on the weakly binding binding model, which has already been explained above in short. In the following, it is refined using a mathematical model in order to be able to approve the model and assign the sequences.

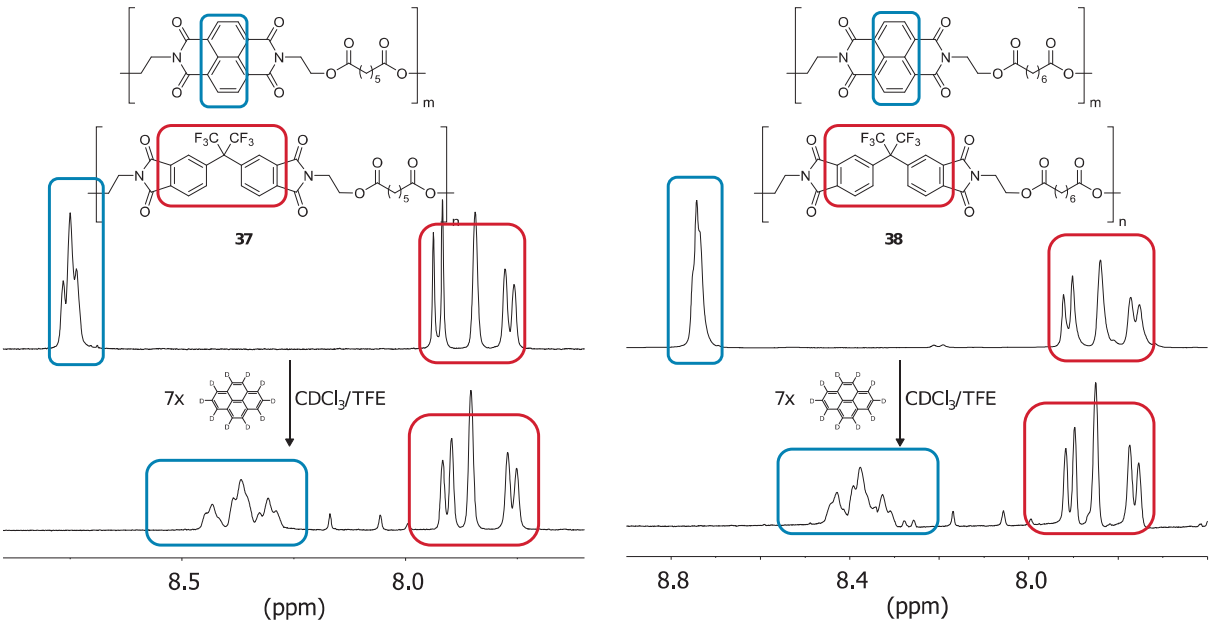

Figure 20: Expansion of the ^{1}H NMR spectrum of NDI / HFDI-based copolymer with a spacer-length of $x = 5$ (**37**, left) and $x = 6$ (**38**, right) upon the addition of a 7-fold molar excess of pyrene-d_{10}. The imide resonances of both polymers show a similar splitting pattern consisting of an apparent triplet of triplets.

Using a mathematical model, the sequence information contained in the splitting pattern can be assigned to the sequences present in the random copolymer. In a random high-molecular weight co-polymer all possible sequences exist (limited only by the molecular weight), and the frequency of each sequence can be calculated via a Bernoulli distribution. In this model, any NDI residue is located at the centre of its own specific sequence; other residues than the central one are also visible in the ^{1}H NMR spectrum, but are considered separately as part of a separate sequence. In the following, the NDI residue is abbreviated as I, the HFDI residue as F. The spacer between the two residues in any given copolymer is constant and can therefore be ignored in terms of sequence.

A cooperative complex formation between imide residues in spatial proximity is nevertheless observed. A possible explanation for the cumulative shielding in the present system is that "I" residues which are distant from the central observed **I** can "capture" pyrene molecules and "deliver" them to the central imide by the formation of a temporary chain-fold. If the central **I** is only surrounded by other Is (in the quintet -I-I-**I**-I-I-) an additional upfield shift is caused by pyrene bound to the adjacent Is. If the central **I** is only surrounded by Fs (in the quintet -F-F-**I**-F-F-) no additional shift is caused. As a result, the central diimide protons in the quintet -I-I-**I**-I-I- experiences the maximum total complexation shift and in the quintet -F-F-**I**-F-F- the weakest total complexation shift: the two sequences become thereby distinguishable. The

more distant the "capturing" residue is located from the observed "I" residue, the less likely will be formation of a random chain-fold that will bring the captured pyrene into the vicinity of the observed "**I**" residue. The complexation shift is thereby additionally dependent on the position of the adjacent Is in the sequence. The further the adjacent Is are away, the weaker is their contribution to the total complexation shift. The the sequence -I-I-**I**-I-F- has therefore a larger total complexation shift than the sequence -I-I-**I**-F-I-. The total complexation shift of each central imide residue depends thus on the number and proximity of other imide residues.

It can be shown that the nine resonances observed in the ^{1}H NMR spectrum (Figure 20) give information about *quintet* sequences, meaning about the adjacent and next-adjacent residues of the central imide unit. Since each of these residues can be either I or F, 2 x 2 x 2 x 2 = 2^4 = 16 possible sequences exist (Table 1). Since the total complexation shift of the central imide residue depends only on the number and proximity of the other imide residues, but not on their order, some sequences result in the same total shielding. For example, the sequences III**I**FF, FF**I**II and FI**I**FI all result in the same shielding; thus only 9 of the 16 sequences can be distinguished. The frequency of the sequences in Table 1 determines the intensity of the resonances in a ratio of 1:2:1 : 2:4:2 : 1:2:1.

Table 1: Possible quintet sequences and their associated shielding codes in a binary copolymer of monomers "F" and "I" ("rev" indicates the reverse sequence of the one shown).

	0	**1**	**2**	
1	100 FF**I**FF	110 FI**I**FF + rev	120 FI**I**IF	**0**
1	101 IF**I**FF + rev	111 III**I**FF + rev FI**I**FI + rev	121 FI**I**II + rev	**1**
1	102 IF**I**FI	112 III**I**FI + rev	122 III**I**I	**2**

To assign the sequences to the nine resonances, the total complexation shift of the resonances has to be calculated from a three-digit code (Table 1, codes shown in blue). The three-digit code indicates the number of other imide residues at a specific distance (i.e. number of monomer residues) from the central imide residue. Each of the observable sequences has a central imide residue, therefore all codes start with 1. The number of adjacent I residues can range between 0 and 2, as can the number of next-adjacent I residues. For example, the three-

digit code **101** is assigned to the sequence IF**I**FF (**1** central, **0** adjacent, **1** next-adjacent imide residue) and three-digit code **120** to sequence FI**I**IF (**1** central, **2** adjacent, **0** next-adjacent). Using this code, the total complexation shielding T can be summed using equation 1:

$$T = ac \sum_{k=1}^{3} N_k b^{-k} \qquad (1)$$

The previously empirically assigned[5] parameter b (a constant 4) corresponds to the factor by which the additional shielding diminishes with distance from the observed diimide. The value k = 1, 2 and 3 represents the distance (i.e. number of monomer residues) from the central imide unit and N_k the number of imide residues at such a distance. The pre-summation term ac represents the product of the ***a***ssociation constant and the ***c***oncentration of probe molecule (relative to diimide). While the formula could, in principle, describe sequences of infinite length, it was found in practice that taking the summation to k = 3 (quintet sequences) was sufficient to give a good prediction of the complexation shifts because of the very rapid decrease in b^{-k} as k increases.

Calculated values for a arbitrary association constant 1 and four different probe-molecule concentrations (c = 0.125 to 1) are given in Table 2. Based on these values, ^{1}H NMR spectra were simulated (at a fixed, 5 Hz line width, Figure 21).

Table 2: Total shielding parameters T, varying the molar concentration (c) of pyrene relative to "I" residues

c = 0.125	c = 0.25	c = 0.5	c = 1	Sequence	Degeneracy
0.03125	0.0625	0.125	0.25	FF**I**FF	1
0.033203125	0.06640625	0.1328125	0.265625	IF**I**FF + rev	2
0.03515625	0.0703125	0.140625	0.28125	IF**I**FI	1
0.0390625	0.078125	0.15625	0.3125	FI**I**FF + rev	2
0.041015625	0.08203125	0.1640625	0.328125	II**I**FF + rev FI**I**FI + rev	4
0.04296875	0.0859375	0.171875	0.34375	II**I**FI + rev	2
0.046875	0.09375	0.1875	0.375	FI**I**IF	1
0.048828125	0.09765625	0.1953125	0.390625	FI**I**I + rev	2
0.05078125	0.1015625	0.203125	0.40625	II**I**I	1

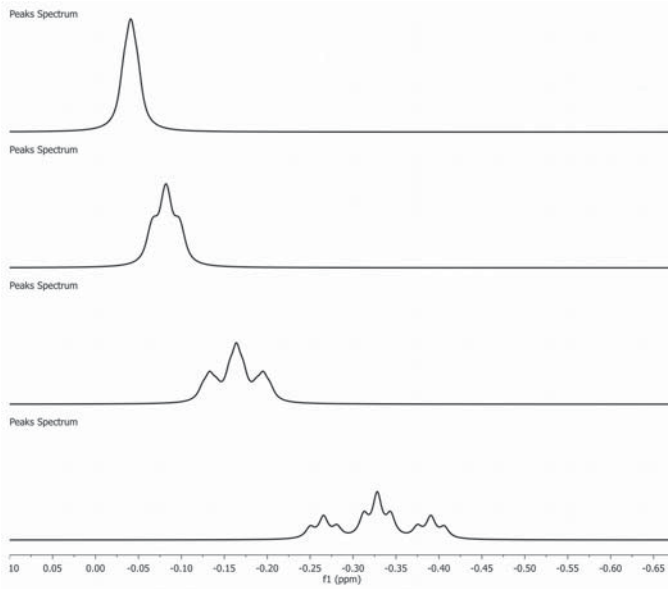

Figure 21: Simulated ^{1}H NMR spectra using the total shielding values from Table 2 using concentrations *c* of 0.125, 0.25, 0.5 and 1 (top to bottom).

The simulation shows a good agreement with the actual spectra (Figure 20 and 21). The minor deviations in the experimental integrals from the predicted ratio 1:2:1 : 2:4:2 : 1:2:1 can be attributed to incomplete randomization (data not shown). In Figure 22, the sequences were finally assigned to the experimental spectrum of copolymer **37** in the presence of a 7-fold excess of pyrene-d_{10} (Figure 20).

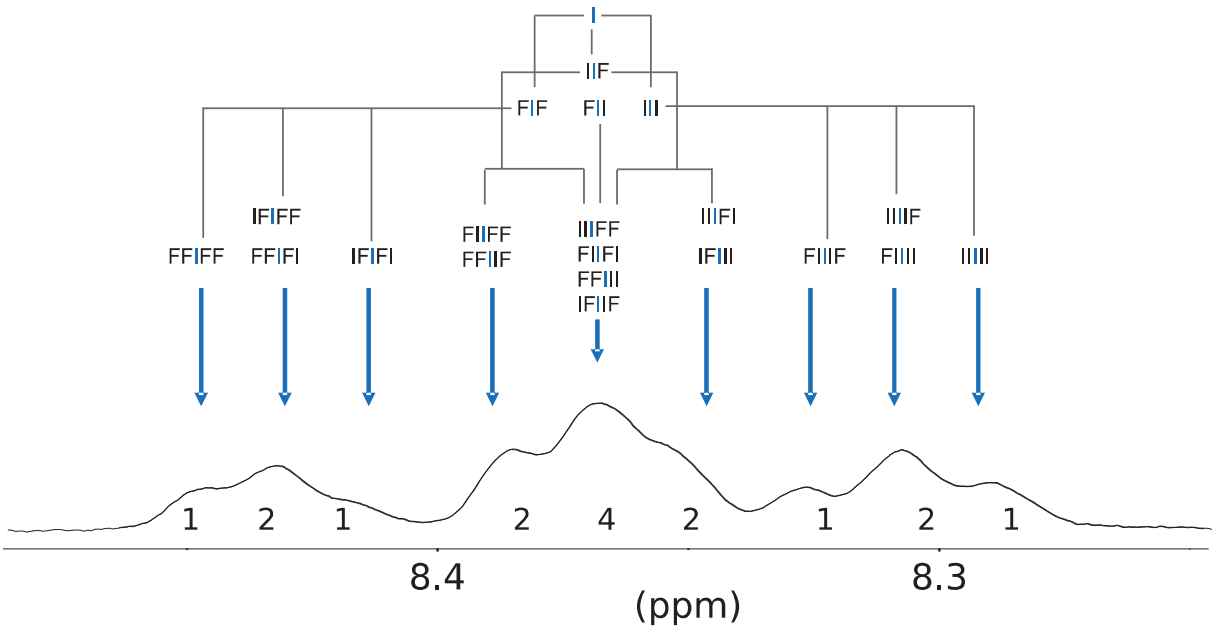

Figure 22: Expansion of the splitting pattern of the NDI / HFDI-based x = 5 copolymer (copolymer **37**, Figure 20), overlaid with a graphical model. Sequences with equal complexation shift are written above of one another.

As described above, the model is based on the assumption that the splitting pattern is not caused by *J*-coupling, often observed in NMR spectroscopy, but is composed of independent singlets which result from complexation shifts and statistical intensities which give, for example, an apparent triplet of triplets. This proposal was investigated using homonuclear (^{1}H-^{1}H decoupling) in the so-called JRES experiment.

JRES (*J*-resolved) NMR spectroscopy is a 2D homonuclear experiment that produces spectra in which the chemical shift is plotted on one axis (f2) and proton-proton coupling on the other axis (f1). JRES NMR spectroscopy helps to deconvolute spectra in which it is unclear if a multiplet is formed by various *J*-couplings of a single resonance or by overlapping of different resonances. *J*-coupled patterns collapse in the f2 dimension into one resonance while they split in the f1 dimension into a number of resonances according to the *J*-coupling (e. g. a triplet into three resonances).

The JRES (J-resolved) NMR spectrum of the NDI / HFDI-based x = 5 copolymer (**37**) is presented in Figure 23. The splitting pattern of the NDI repeat unit, an apparent triplet of triplets, shows in the f1 dimension indeed only a single line (blue box). There is thus no *J*-coupling involved in producing the NDI splitting pattern. Moreover, all nine lines can still be resolved in the f2 dimension. These results confirm the proposal that the individual lines in the observed pattern are true singlets, each arising from a specific NDI-centred quintet sequence. The HFDI repeat unit can serve as a reference for *J*-coupling; the two adjacent protons showing doublets in the ^{1}H NMR are clearly split into two regions in the f1 dimension (red box).

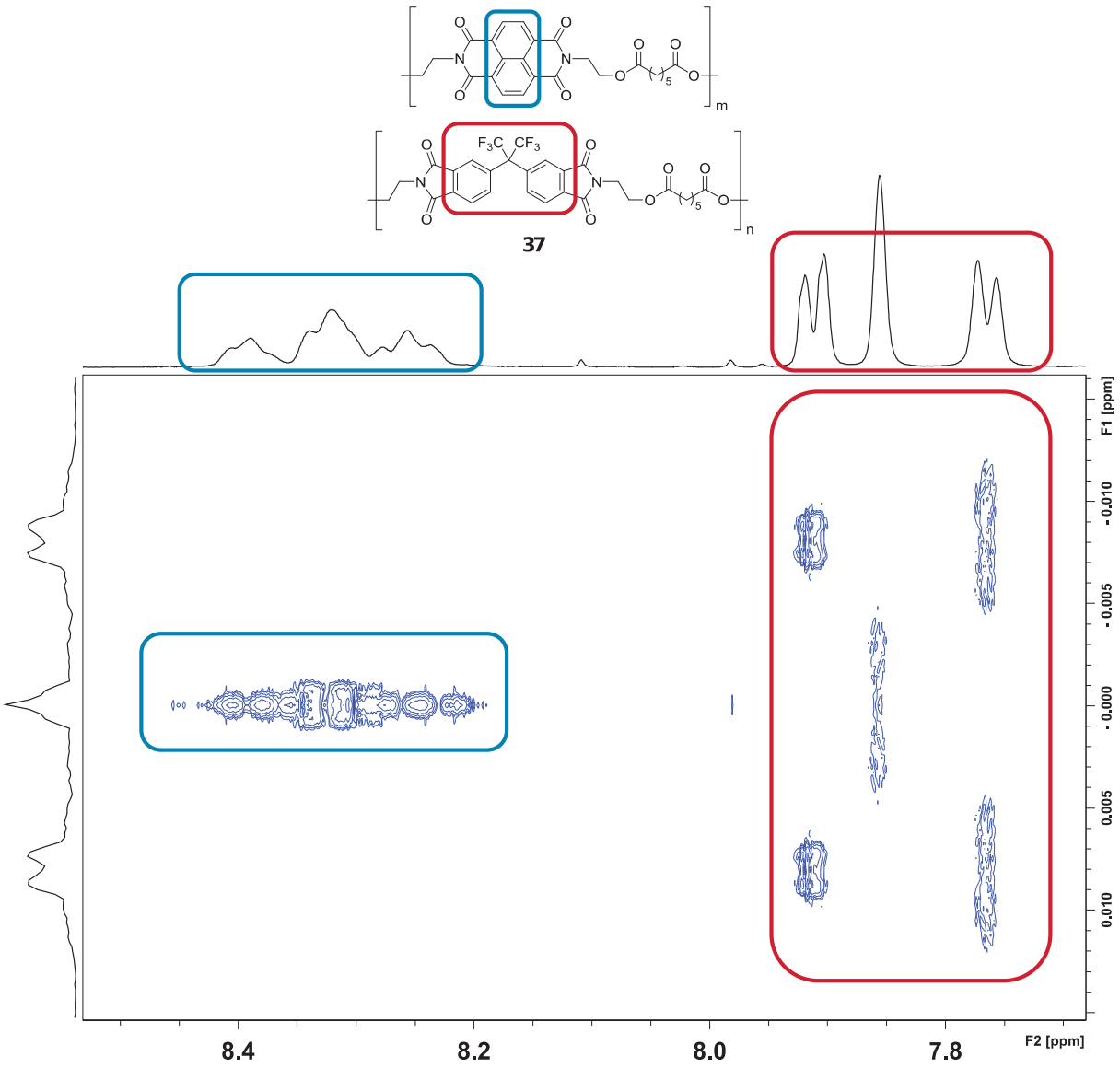

Figure 23: JRES ^{1}H NMR spectrum of the NDI / HFDI-based x = 5 copolymer (**37**) in the presence of an 8-fold molar excess of pyrene-d_{10} in $CDCl_3$ / TFE (6:1, *v:v*). The NDI resonances of the polymer (blue box) are a single line, indicating the absence of any *J*-coupling.

4.4.1.2. NDI / HFDI-based copolymers with short spacers (x = 2 to 4)

The NDI / HFDI-based copolymers with short spacers (x = 2 to 4) show a stronger association constant than the polymers with longer spacers, as it is apparent from the complexation shifts in Figure 18. While the NDI / HFDI-based copolymers with long spacers (x = 5 to 8) show uniformly a 'triplet of triplets' splitting pattern of the NDI resonance, other splitting patterns can be observed for the NDI / HFDI-based copolymers with short spacers (x = 2 to 4): The

splitting patterns NDI / HFDI-based copolymers $x = 3$ and $x = 4$ (**35** and **36**) have six clearly distinguishable resonances arranged in the aforementioned 'singlet / doublet / triplet' type splitting pattern (Figure 24).

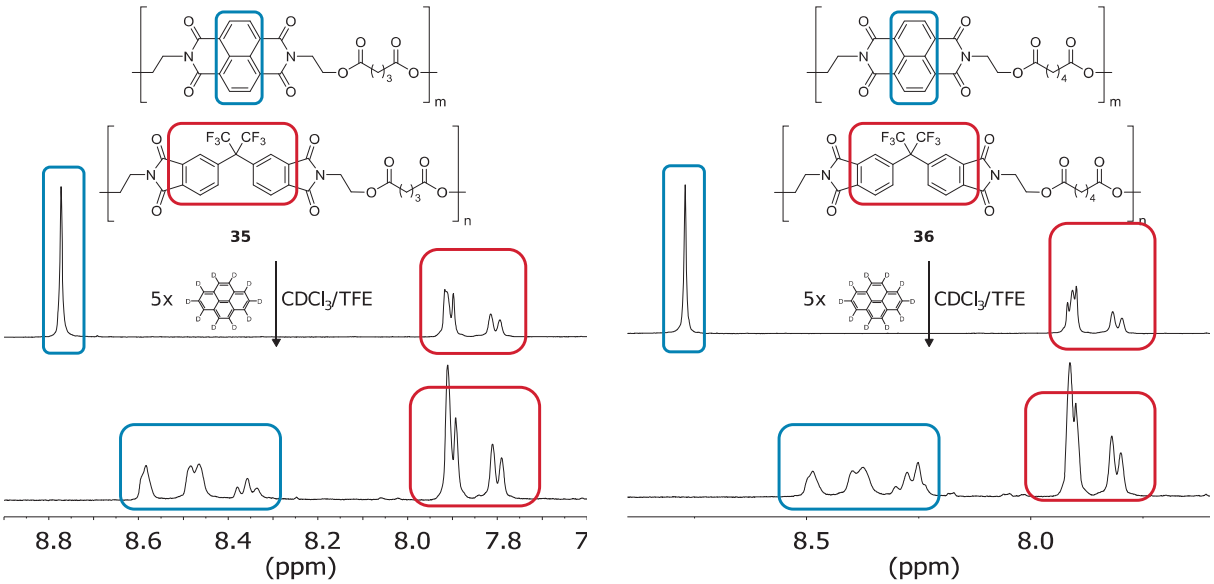

Figure 24: Expansion of the ^{1}H NMR spectrum of NDI / HFDI-based copolymer with a spacer-length of x = 3 (**35**, left) and x = 4 (**36**, right) upon the addition of a 5-fold molar excess of pyrene-d_{10}. The imide resonances of both polymers show a similar splitting pattern consisting of a the 'singlet / doublet / triplet' type pattern.

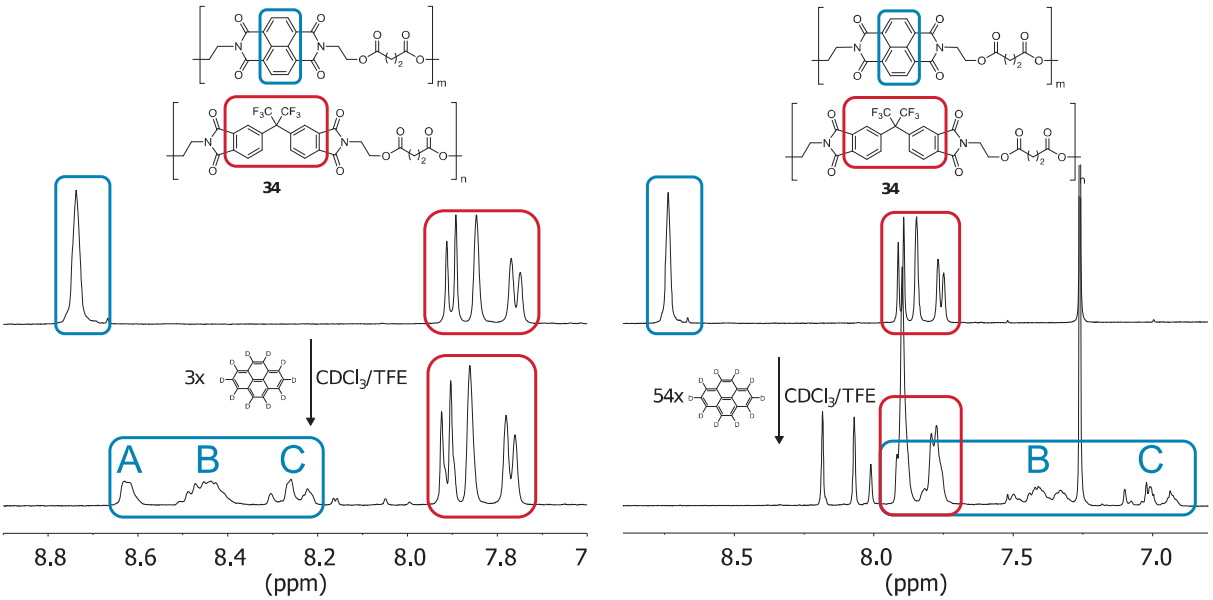

Figure 25: Expansion of the ^{1}H NMR spectrum of the NDI / HFDI-based copolymer with a spacer-length of $x = 2$ (**34**) upon the addition of a 3-fold molar excess of pyrene-d_{10} (left) or a 54-fold molar excess (right). The imide resonances' splitting pattern consistens of a single resonance A (obscured in case of 54-fold molar excess) an apparent triplet of triplets B and a 'singlet / doublet / triplet' type pattern C.

The intensity of the resonances is different between the two copolymers, but this is only based on of the different degree of randomization of the chain, as could be shown by transesterification subsequent to synthesis (data not shown). The 'singlet / doublet / triplet' splitting pattern can also be found in the literature in the splitting pattern of the chain-folding polymer (Figure 1, right side, spectra C and D, upfield resonances). The similarity of the splitting patterns of the NDI / HFDI-based copolymers $x = 3$ and $x = 4$ (**35** and **36**, Figure 24) suggests a similar conformation (Figure 19) as the chain-folding polymer from the literature (Figure 1), a chain-folding conformation is therefore also assumed for the polymers **35** and **36**.

The NDI / HFDI-based $x = 2$ copolymer has (measured by complexation shift) the highest association energy of all copolymers (Figure 18) and also shows the highest number of distinguishable resonances in intercalation sequencing (Figure 25).

The splitting pattern of the NDI / HFDI-based $x = 2$ copolymer can be divided into three sections A, B and C. Section C consists of the same 'singlet / doublet / triplet' splitting pattern as the NDI / HFDI-based copolymers $x = 3$ and $x = 4$ as well as the poly(ether imide) of the literature (Figure 1). Since the 'singlet / doublet / triplet' splitting pattern of the poly(ether imide) is obtained by chain folding, it is also assumed that the NDI / HFDI-based $x = 2$ has a chain-folding conformation in solution. Section B only deconvoluted at high concentration (a 54-fold molar excess of pyrene-d_{10}). This section has similarities to an apparent triplet of triplets. However, as shown in Chapter 5.4, there is evidence that the triplets are produced by overlapping doublets. A doublet is also found in the middle of the poly(ether imide) from the literature.[5] Section C is obscured at high concentration by overlapping with the HFDI resonances, at low concentrations only one resonance is clearly resolved. Also in case of the poly(ether imide) of the literature, only singlets are visible in low field position. In summary, there is a certain similarity with the splitting pattern of the poly(ether imide) from the literature. Therefore, a chain-fold binding is assumed for the NDI / HFDI-based $x = 2$ copolymer.

4.4.2. NDI / BPDI-based copolymers

NDI / BPDI-based copolymers are comprised of a strongly binding and a mostly non-binding unit (symbolized ■/■) and were investigated with spacers of $x = 2$ (**41**) to $x = 5$ (**44**). As can be seen for the representative polymers $x = 2$ (**41**) and $x = 5$ (**44,** Figure 26), the NDI / BPDI-based copolymers show upon the addition of pyrene-d_{10} splitting patterns similar to their NDI / HFDI-based counterparts (■/□) though with somewhat lower resolution. The NDI / BPDI-based copolymers $x = 5$ (**44**) shows the same triplet of triplets as the

NDI / HFDI-based copolymer x = 5 (**37**, Figure 20). The NDI / BPDI-based copolymer x = 2 (**41**) shows the 'singlet / doublet / triplet' splitting pattern, which has a strong similarity to the corresponding NDI / HFDI-based copolymer x = 2 (**34**, Figure 24).

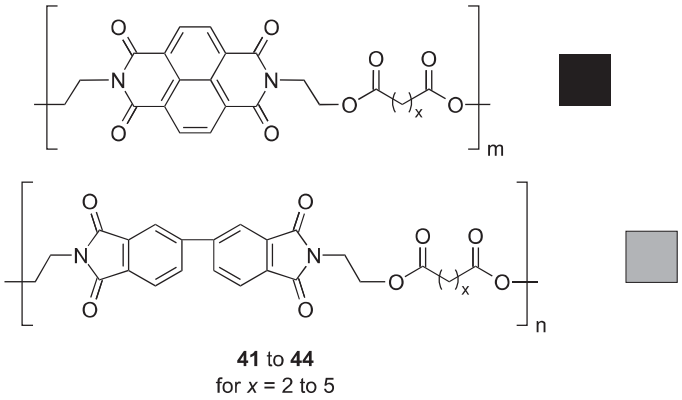

Figure 26: NDI / BPDI-based copolymers (**41** to **44**).

In contrast to HFDI (□), the BPDI unit (■) binds pyrene, albeit weakly, as was evident from complexation studies of the BPDI-based homopolymer (**32**, Chapter 4.3.2.2). It can be seen from the complexation shift and the splitting of the BPDI resonances that the same is also the case for the NDI / BPDI-based copolymer (Figure 27, resonances in the red box). The reason for the NDI resonances being less well-resolved than in the NDI / HFDI-based analogues (**34** to **36**) is presumably due to the difference in binding constant between the NDI units and the BPDI units, which is smaller than the difference in binding constant between the NDI unit and the HFDI unit. As the splitting patterns are the same as for the NDI / HFDI-based counterparts, the previously introduced models can be applied. The splitting pattern of the NDI / BPDI-based x = 5 copolymer is the same as for the NDI / HFDI-based x = 5 copolymer (**37**, Figure 20), and so the sequences are assigned accordingly (Figure 28).

Another disadvantage of the BPDI unit is reduced polymer solubility in comparison to HFDI-based polymers. It is well-known from the literature that the fluorinated HFDI improves the solubility,[26,30,31] and this was indeed also the case for the homopolymers and copolymers investigated in the current study. While HFDI acts as a solubilizer, the synthesis of the BPDI-based polymers was problematic due to the low solubility and a high proportion of fluorinated co-solvent had to be used during NMR spectroscopic analysis, which adversely affected the resolution and signal-to-noise ratio.

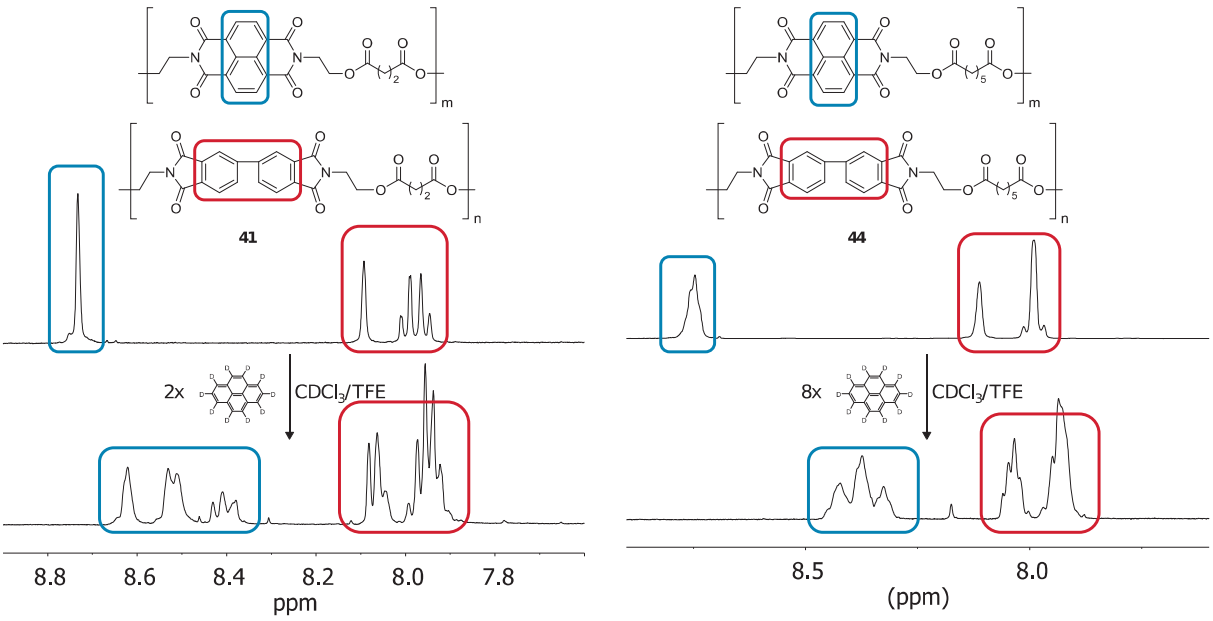

Figure 27: Expansion of the ^{1}H NMR spectrum of NDI / BPDI-based copolymer with a spacer-length of $x = 2$ (**41**, left) and $x = 5$ (**44**, right) upon the addition of a excess of pyrene-d_{10}.

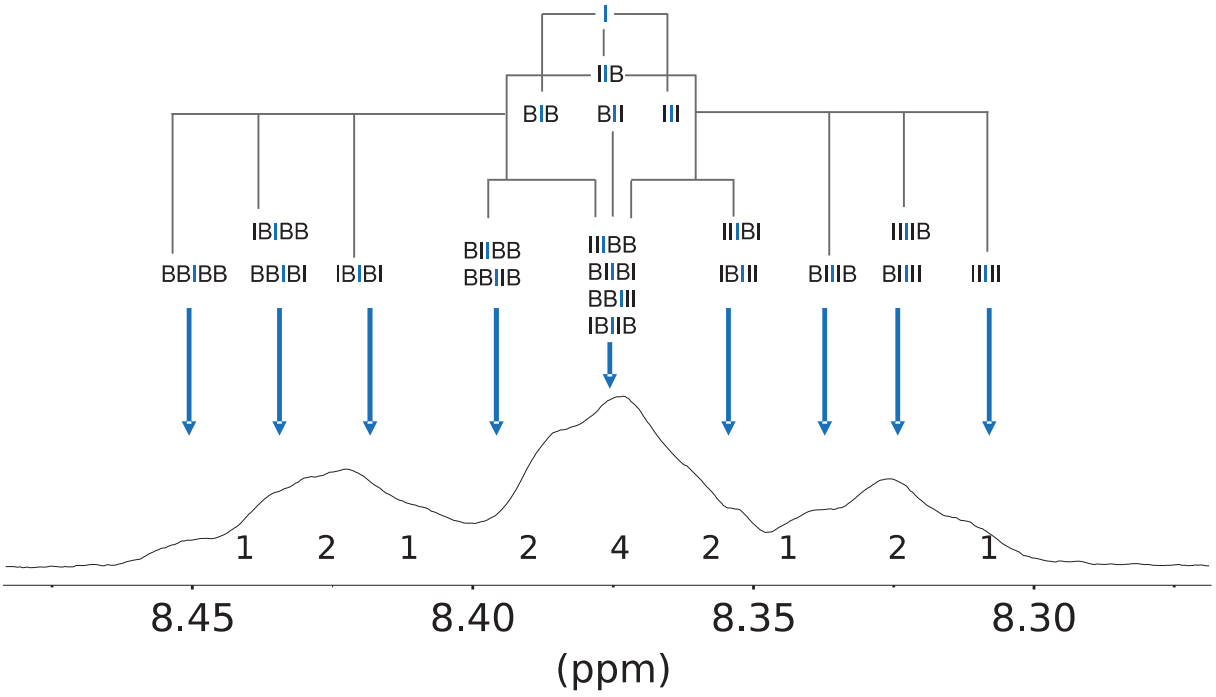

Figure 28: Expansion of the splitting pattern of the NDI / BPDI-based $x = 5$ copolymer (**44**). Sequences are assigned using the model described above for the analogous NDI / HFDI-based copolymers.

4.4.3. PMDI / HFDI-based copolymer

The PMDI / HFDI-based copolymer (**45**, Figure 29) is composed of a weakly binding and a non-binding co-monomer (■ / □). The copolymer with a spacer length of $x = 5$ shows only very slight sequence-related splitting of the aromatic imide resonance (Figure 30).

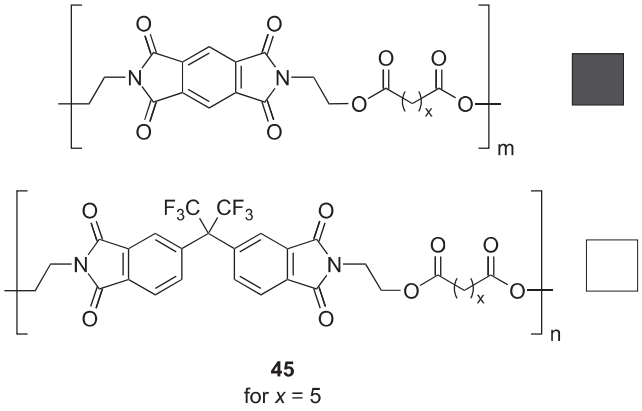

45
for $x = 5$

Figure 29: PMDI / HFDI-based copolymer (**45**).

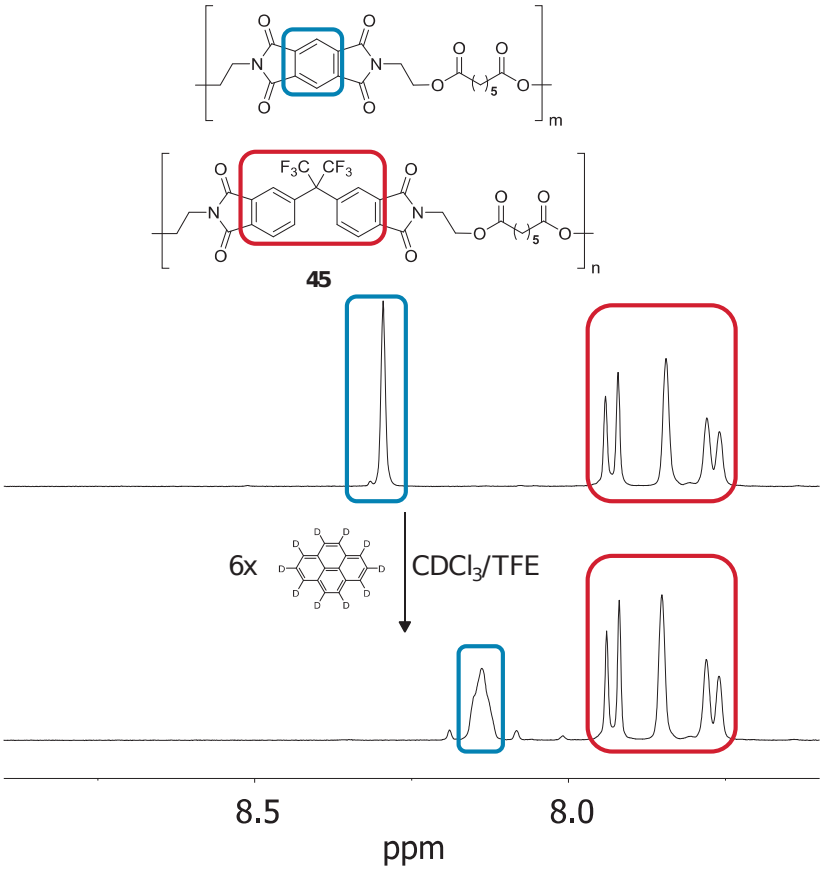

Figure 30: Splitting pattern of the PMDI / HFDI-based $x = 5$ (**45**) copolymer in the presence of pyrene-d_{10}: the polymer shows a small complexation shift and only faint splitting of the diimide resonance into a triplet.

However, even at high loadings of pyrene-d_{10} (8-fold excess) an apparent triplet is only indicated by two shoulders and no further structure is resolved. Since the aromatic imide resonance of the PMDI has a smaller chemical shift compared to NDI, only a comparably small complexation shift can be induced by the addition of pyrene-d_{10} before an overlap with the HFDI resonances is occurring. According to the model previously used, the three resonances that emerge as shoulders can be assigned as -HFDI-PMDI-HFDI-, -HFDI-PMDI-PMDI-/-PMDI-PMDI-HFDI- (possessing equal complexation shift) and -PMDI-PMDI-PMDI- (Figure 31).

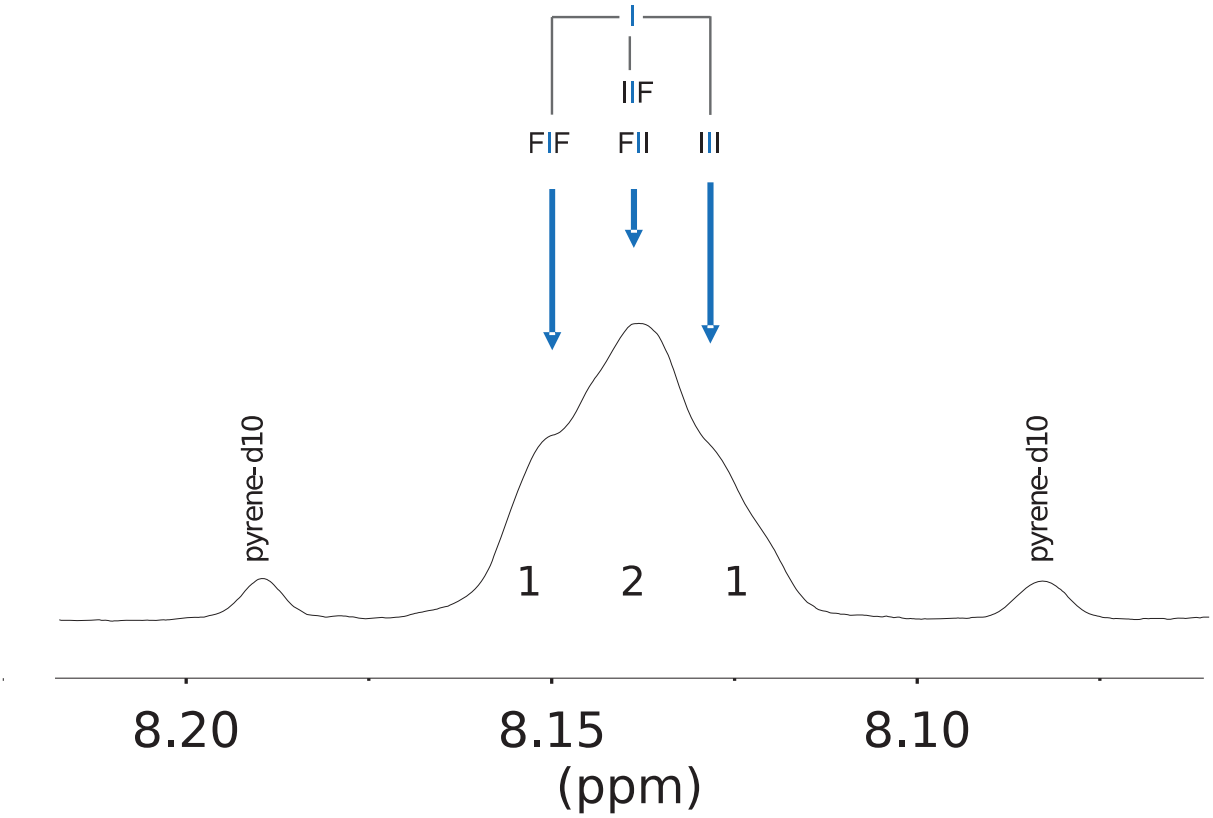

Figure 31: Expansion of the splitting pattern of the PMDI / HFDI-based x = 5 (**45**), overlaid with a graphical assignment. Sequences with equal complexation shift are written on top of one another.

4.4.4. PMDI / BPDI-based copolymers

The PMDI / BPDI-based copolymer (Figure 32, ■/■) is comprised of a weakly binding unit (PMDI, ■) and a mostly non-binding unit (BPDI, ■). The difference in binding constants is thereby smaller than in any other of the copolymers. Indeed, no splitting of the PMDI proton resonance and thereby no sequence information could be obtained from the ^{1}H NMR spectra in the presence of pyrene-d_{10} (Figure 33).

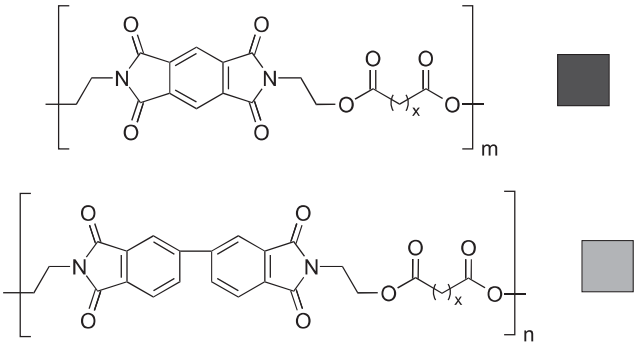

46
for $x = 5$

Figure 32: PMDI / BPDI-based copolymer (**46**).

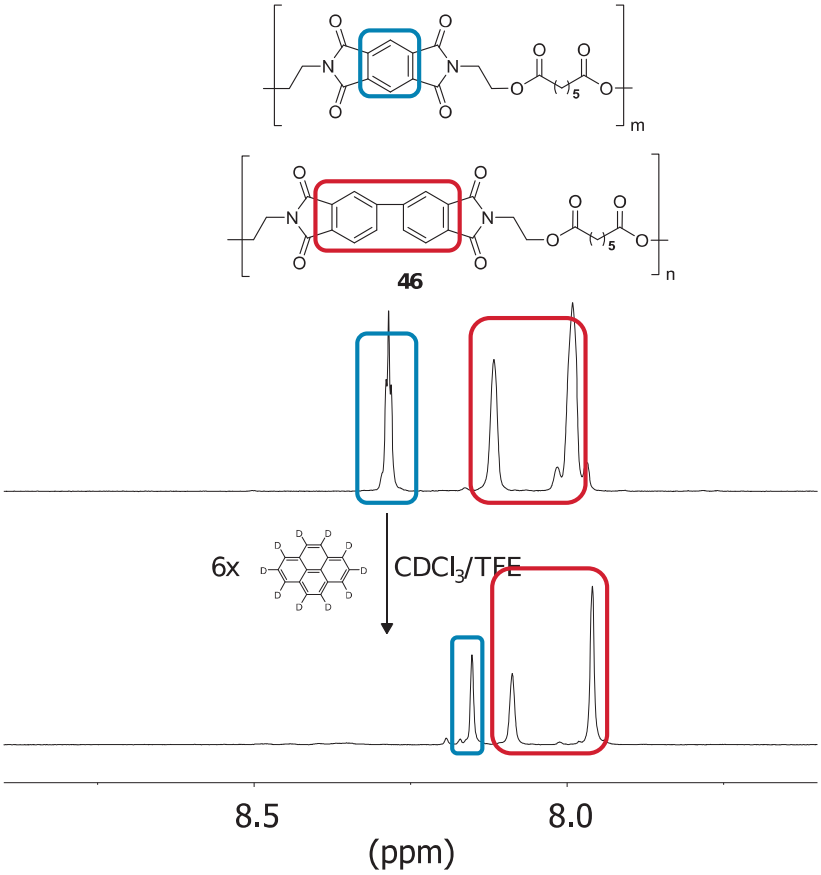

Figure 33: PMDI / BPDI-based $x = 5$ copolymer upon the addition of pyrene-d_{10}. No sequence information is obtained.

At low concentrations of pyrene, the difference in complexation shift between the -PMDI-BPDI- sequences (PMDI units attached to BPDI) and the -PMDI-PMDI- sequences is so small that the resonance remains a sharp singlet (Figure 33). At high concentrations of pyrene, the PMDI resonance (larger complexation shift and higher chemical shift than the PBDI resonance) has exactly the same overall chemical shift as one of the resonances of BPDI. There-

fore, no information can be extracted from the overlapping resonances. At even higher pyrene concentrations, both, the BPDI resonance and the PMDI resonances are found to split, but no well-defined sequence information could be extracted from the complex, overlapping pattern (not shown).

4.5. Titration concentration

In the copolymer/pyrene systems described so far, saturation occurs (only) at very high concentrations, where an equal increase in the pyrene concentration causes progressively smaller additional complexation shifts. This effect was used in Chapter 3 for the determination of the binding constants.[8] In order to obtain maximum deconvolution of splitting patterns, for every polymer-intercalator system numerous samples had to be prepared in which the polymer concentration was kept constant but the pyrene concentration was varied, usually up to a concentration of 32 mM (8-fold molar excess).

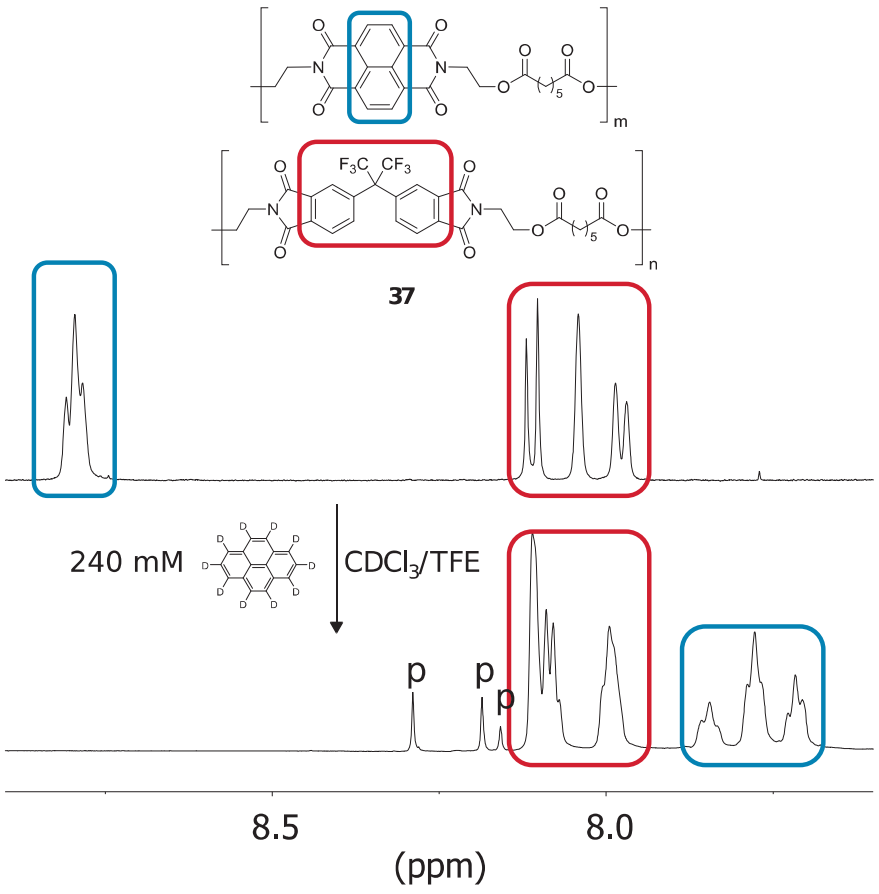

Figure 34: NDI / HFDI-based x = 5 copolymer (**37**) in the presence of a very high concentration of pyrene (240 mM, 60-fold molar excess). The high concentration of pyrene does not lead to additional splitting but only to a increased resolution of the existing pattern.

In order to obtain more sequence information, it was also attempted to increase the pyrene concentration very considerably (240 mM instead of 32 mM, Figure 34). Despite a much stronger complexation shift (compared to Figure 20), the number of distinguishable resonances remained same although the triplets are more clearly separated. However, as such sequence information could already be extracted with much less pyrene and such amounts of perdeuterated pyrene become very expensive, most other polymers were been only investigated at a pyrene concentration up to 32 mM (8-fold molar excess).

4.6. Titrations via ^{13}C NMR spectroscopy

Intercalation sequencing is based on π–π-stacking between the aromatic pyrene molecules and the diimide residues of the copolymer. The aromatic protons attached to the diimide residues experience ring-current shielding from both directly-bound pyrene and from pyrenes bound at adjacent diimide residues. The diimide residues can be distinguished as parts of different sequences as they experience a different total ring-current shielding depending on the number and distance of intercalator molecules.[5]

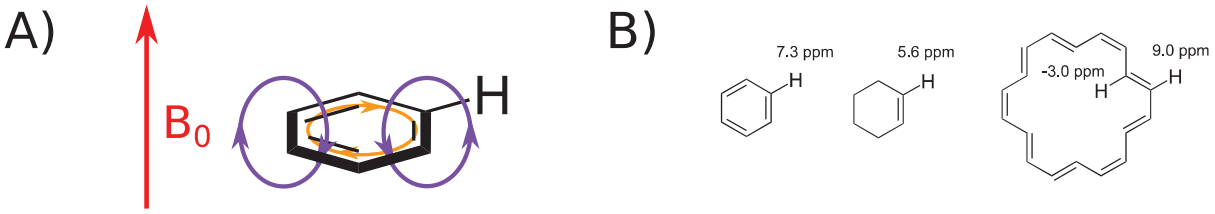

Figure 36: A) Benzene ring with exemplary ring-current in an external magnetic field (B_0). B) The aromatic protons of benzene have, at 7.3 ppm, a larger chemical shift than the unsaturated protons of cyclohexene. The protons at the inside of [18]-annulene experience a very large upfield shift, to 3.00 ppm above TMS, in ^1H NMR spectroscopy due to the ring-current.

The ring current is based on electron delocalization within the aromatic compound's π-system. The ring current induces a magnetic field that affects the chemical shift of protons bonded to the ring. Protons located outside of the aromatic ring are shifted down-field in comparison to alkenes; rarely present protons in the inside of the ring are shifted up-field (Figure 36).[48] The change in chemical shifts in ^1H NMR spectroscopy caused by the ring-current are thus used as an easily accessible measure of aromaticity.[49]

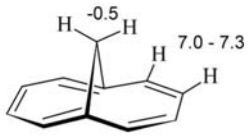

Figure 37: The protons at the bridge of 1,6-methano(10)annulene experience due to the ring-current a smaller chemical shift in ^{1}H NMR spectroscopy (-0.5 ppm) than in other sterically similar but non-aromatic annulenes.

The carbon atoms are usually not affected by the ring-current because they are exactly in the middle of it (e. g. in case of benzene). However, model studies comparing 1,6-methano(10)annulene (Figure 37) with other sterically similar but non-aromatic annulenes found that carbon atoms experience the same absolute magnitude of the ring-current effect when they occupy the same position in space with regard to the aromatic π-electron cloud.[50,51]

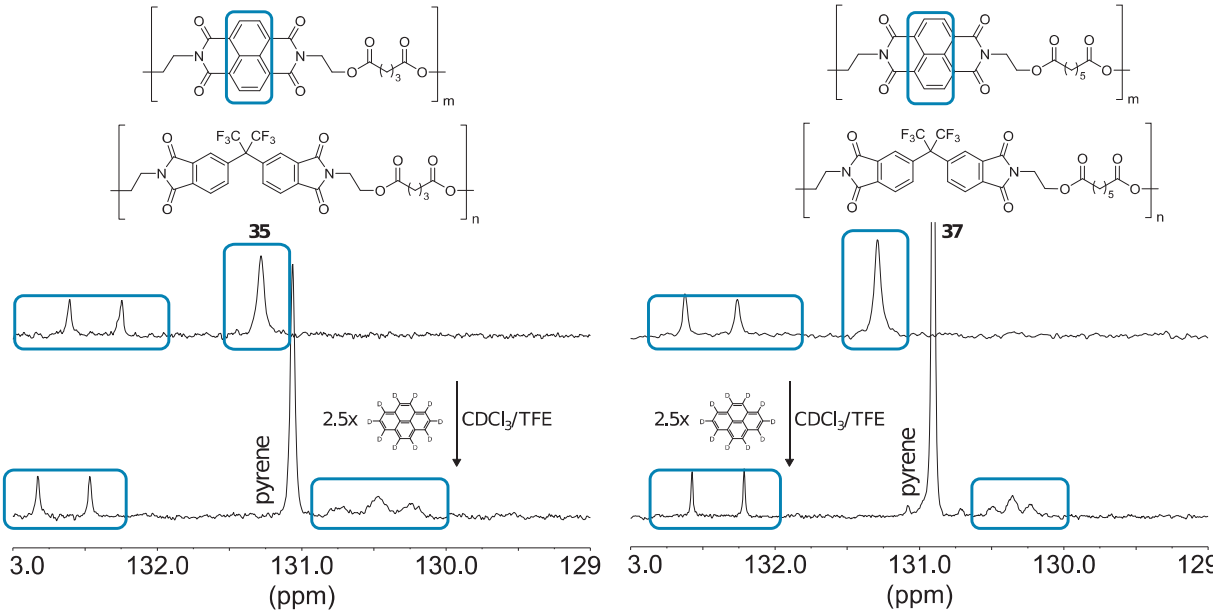

Figure 38: Expansion of the aromatic region of a ^{13}C NMR spectrum of the NDI / HDFI-based x = 3 copolymer (left, **35**) and the NDI / HDFI-based x = 5 copolymer (right, **37**). The carbon resonances do show sequence-related splitting upon the addition of pyrene (bottom spectra).

During intercalation sequencing, the diimide residues are π-stacked with, and are thus located above the aromatic pyrene residues. Although it should be thereby in principle possible to use ^{13}C NMR spectroscopy for intercalating sequencing, this has never been demonstrated experimentally. However, in the following study, an experimental proof is given. As it can be seen in Figure 38, the resonance at 131.3 ppm, corresponding to the "outer" (i.e. protonated) carbon

atoms of NDI in the co-poly(ester imide)s NDI / HFDI x = 3 and NDI / HFDI x = 5 show a complexation shift and a sequence-related splitting upon the addition of pyrene. The carbon resonances were assigned via HSQC (see Experimental Chapter).

Only the formation of an apparent triplet could be observed: The extracted sequence information is therefore considerably smaller than in the corresponding ^{1}H NMR spectra (Figure 20 and Figure 24). However, in the future this discovery could lead to more detailed investigations of the stacking geometry and provide further insights.

4.7. Conclusions

Using four types of homopolymers differing in binding strength and four derived types of copolymers, a potentially general method for the design and synthesis of sequenceable polymers was successfully developed.

The relative complexation strengths (with pyrene) of four diimide types was evaluated when incorporated in homopolymers, in particular NDI, PMDI, HFDI and BPDI. NDI and PMDI were used as strongly binding and less strongly binding units, HFDI and BPDI as non-binding and mostly non-binding units, respectively. The resolution of the splitting pattern of the aromatic diimide resonance was the higher the greater the difference in complexation strength between the binding and the non-binding unit. The most sequence information could thereby be extracted from NDI-based and HFDI-based copolymers (**33** to **40**). Using this principle, it has also been possible to produce a large number of polymers that show numerous sequence-assignable ^{1}H NMR resonances on complexation with pyrene ("splitting-resonances"). In the literature, usually only three splitting- resonances were found, in one case nine. In the current study, 12 further examples are described in which up to 15 such resonances could be distinguished. The imide units selected here are therefore promising for intercalation sequencing.

Since the complexation strengths of numerous other donors and acceptors is known in the literature, this could be a strategy for the development of a wide range of other sequenceable polymers.

4.8. References

1 Z. Zhu, C. J. Cardin, Y. Gan and H. M. Colquhoun, *Nat. Chem.*, 2010, **2**, 653–660.

2 H. M. Colquhoun and Z. Zhu, *Angew. Chem. Int. Ed.*, 2004, **43**, 5040–5045.

3 Z. Zhu, C. J. Cardin, Y. Gan, C. A. Murray, A. J. P. White, D. J. Williams and H. M. Colquhoun, *J. Am. Chem. Soc.*, 2011, **133**, 19442–19447.

4 H. M. Colquhoun, Z. Zhu, C. J. Cardin, Y. Gan and M. G. B. Drew, *J. Am. Chem. Soc.*, 2007, **129**, 16163–16174.

5 J. S. Shaw, R. Vaiyapuri, M. P. Parker, C. A. Murray, K. J. C. Lim, C. Pan, M. Knappert, C. J. Cardin, B. W. Greenland, R. Grau-Crespo and H. M. Colquhoun, *Chem. Sci.*, 2018, **9**, 4052–4061.

6 H. Colquhoun and J.-F. Lutz, *Nat. Chem.*, 2014, **6**, 455–456.

7 S. Nojoomi and P. Koehl, *BMC Bioinformatics*, 2017, **18**, 137.

8 P. Thordarson, *Chem. Soc. Rev.*, 2011, **40**, 1305–1323.

9 J. H. Williams, J. K. Cockcroft and A. N. Fitch, *Angew. Chem. Int. Ed.*, 1992, **31**, 1655–1657.

10 A. Das and S. Ghosh, *Angew. Chem. Int. Ed.*, 2014, **53**, 2038–2054.

11 H. M. Colquhoun, Z. Zhu and D. J. Williams, *Org. Lett.*, 2003, **5**, 4353–4356.

12 L. R. Hart, N. a. Nguyen, J. L. Harries, M. E. Mackay, H. M. Colquhoun and W. Hayes, *Polymer*, 2015, **69**, 293–300.

13 M. Yeh and H. Lin, *Phys. Chem. Chem. Phys.*, 2014, **16**, 24216–24222.

14 S. V Bhosale, C. H. Jani and S. J. Langford, *ChemInform*, 2008, **39**, 331–342.

15 S. Ghosh and S. Ramakrishnan, *Angew. Chem. Int. Ed.*, 2005, **44**, 5441–5447.

16 B. W. Greenland, M. B. Bird, S. Burattini, R. Cramer, R. K. O'Reilly, J. P. Patterson, W. Hayes, C. J. Cardin and H. M. Colquhoun, *Chem. Commun.*, 2013, **49**, 454–456.

17 C. Peebles, R. Piland and B. L. Iverson, *Chem. Eur. J.*, 2013, **19**, 11598–11602.

18 H. Mutlu and J.-F. Lutz, *Angew. Chem. Int. Ed.*, 2014, **53**, 13010–13019.

19 N. S. S. Kumar, M. D. Gujrati and J. N. Wilson, *Chem. Commun.*, 2010, **46**, 5464–5466.

20 P. E. Cassidy, T. M. Aminabhavi and V. S. Reddy, in *Kirk-Othmer Encyclopedia of Chemical Technology*, John Wiley & Sons, Inc., Hoboken, NJ, USA, 2000.

21 A. Susa, J. Bijleveld, M. Hernandez Santana and S. J. Garcia, *ACS Sustain. Chem. Eng.*, 2018, **6**, 668–678.

22 S. Ando, T. Matsuura and S. Sasaki, *Polym. J.*, 1997, **29**, 69–76.

23 M. Hegde, S. Shahid, B. Norder, T. J. Dingemans and K. Nijmeijer, *Polymer*, 2015, **81**, 87–98.

24 W. Ogieglo, Z. P. Madzarevic, M. J. T. Raaijmakers, T. J. Dingemans and N. E. Benes, *J. Polym. Sci. Part B Polym. Phys.*, 2016, **54**, 986–993.

25 M. Hasegawa and K. Horie, *Prog. Polym. Sci.*, 2001, **26**, 259–335.

26 M. Hasegawa, Y. Watanabe, S. Tsukuda and J. Ishii, *Polym. Int.*, 2016, **65**, 1063–1073.

27 M. Hasegawa, T. Ishigami, J. Ishii, K. Sugiura and M. Fujii, *Eur. Polym. J.*, 2013, **49**, 3657–3672.

28 F. La Terra, *Molecular Tweezers and Their Properties in Solution and on Surfaces*, PhD thesis, University of Reading, 2014.

29 M. Ding, *Prog. Polym. Sci.*, 2007, **32**, 623–668.

30 H. Behniafar and N. Sefid-Girandehi, *J. Fluor. Chem.*, 2011, **132**, 878–884.

31 B. Ghanem, N. Alaslai, X. Miao and I. Pinnau, *Polymer*, 2016, **96**, 13–19.

32 M. D. Damaceanu, C. P. Constantin, A. Nicolescu, M. Bruma, N. Belomoina and R. S. Begunov, *Eur. Polym. J.*, 2014, **50**, 200–213.

33 L. Yi, W. Huang and D. Yan, *J. Polym. Sci. Part A Polym. Chem.*, 2017, **55**, 533–559.

34 D. J. Liaw, K. L. Wang, Y. C. Huang, K. R. Lee, J. Y. Lai and C. S. Ha, *Prog. Polym. Sci.*, 2012, **37**, 907–974.

35 M. J. Croad, *Microporous Polymers for Carbon Dioxide Capture*, PhD thesis, Cardiff University, 2013.

36 A. Shimazu, T. Miyazaki and K. Ikeda, *J. Memb. Sci.*, 2000, **166**, 113–118.

37 B. Chun, *Polymer*, 1994, **35**, 4203–4208.

38 R. G. Bryant, in *Kirk-Othmer Encyclopedia of Chemical Technology*, John Wiley & Sons, Inc., Hoboken, NJ, USA, 2006.

39 S. H. Hsiao and Y. J. Chen, *Eur. Polym. J.*, 2002, **38**, 815–828.

40 S. B. Huang, Z. Y. Jiang, X. Y. Ma, X. P. Qiu, Y. F. Men, L. X. Gao and M. X. Ding, *Plast. Rubber Compos.*, 2013, **42**, 407–415.

41 M. Hasegawa, *Polymers*, 2017, **9**, 520.

42 J. Chang, H. Niu, M. He, M. Sun and D. Wu, *J. Appl. Polym. Sci.*, 2015, **132**, 1–8.

43 H. Lei, M. Zhang, H. Niu, S. Qi, G. Tian and D. Wu, *Polymer*, 2018, **149**, 96–105.

45 J. W. Steed and J. L. Atwood, *Supramolecular Chemistry*, John Wiley & Sons, Ltd, Chichester, UK, 2009.

46 D. Brynn Hibbert and P. Thordarson, *Chem. Commun.*, 2016, **52**, 12792–12805.

47 W. M. A. Niessen and R. A. Correa C., *Interpretation of MS-MS Mass Spectra of Drugs and Pesticides*, John Wiley & Sons, Inc., Hoboken, New Jersey, 2017.

48 P. M. Dewick, *Essentials of Organic Chemistry: For Students of Pharmacy, Medicinal Chemistry and Biological Chemistry*, Wiley, Hoboken, N.J., 2006.

49 P. Lazzeretti, *Prog. Nucl. Magn. Reson. Spectrosc.*, 2000, **36**, 1–88.

50 R. D. Vernet and V. Boekelheide, *Proc. Natl. Acad. Sci. U. S. A.*, 1974, **71**, 2961–2964.

51 H. Günther, H. Schmickler, H. Königshofen, K. Recker and E. Vogel, *Angew. Chem. Int. Ed.*, 1973, **12**, 243–245.

5 Sequence-recognition in all-aliphatic naphthalene diimide-based copolymers

5.1. Abstract

Intercalation sequencing is a technique for the determination of copolymer sequences via ^{1}H NMR spectroscopy and is based on the presence of a strongly binding and a non-binding repeat unit (with respect to electron-rich aromatic probe-molecules) in the polymer backbone. In the present chapter, the dependence of the binding strength on the spacer length in the imide chain fold (described in Chapter 3) was exploited successfully for the creation of sequenceable polymers; no additional imide-based non-binding unit is required.

This chapter reports the synthesis of so-called all-aliphatic naphthalene diimide-based copolymers by polymerizing a 1:1 mixture of two different diacyl chlorides with one NDI-based diol monomer, whereas previously (Chapter 4) one diacyl chloride was polymerized with a 1:1 mixture of two imide-based monomers. It is now shown that the sequence of the all-aliphatic polymers can successfully be determined by intercalation sequencing. As already shown for other co-polymers, a dependency of the amount of extractable information on the difference in binding energy was found. When compared to the NDI / HFDI-based copolymers, the all-aliphatic polymers also showed an improved solubility, which facilitated synthesis and analysis.

The successful sequencing of the all-aliphatic NDI-based copolymers shows that an all-aliphatic NDI-based chain-fold can be used as a new mostly non-binding structural unit. NDI can then be seen in intercalation sequencing as a sensing unit in otherwise fully aliphatic polymers. The results thus suggest a more general applicability of the intercalation sequencing.

5.2. Introduction

Every copolymer consisting of (at least) two differentiable repeat units can, in principle, represent elements of information. A binary copolymer can, for example, be seen as the logical equivalent of a string of ones and zeroes.[1] In the current study, the two repeat units are differentiable by possessing, or not possessing, the ability to bind pyrene. This distinguishability is possible because pyrene-binding monomers adjacent to non-binding monomers experience a lower complexation shift than binding monomers adjacent to binding monomers. These monomers differ only by their position in the sequence but their different complexation shifts make it possible to distinguish them in ^{1}H NMR spectra and therefore allows analysis of the copolymer's sequence. This type of analysis may in future support the synthesis of sequence-controlled polymers, which may potentially allow a more effective control of material properties.[2] In addition, the monomer sequences of copolymers may be used in perspective as the basis for information-storage at a molecular level.[1]

Non-binding repeating units in a polymer are essential for intercalation sequencing. In other fields of supramolecular chemistry, non-binding units are generally regarded as useless and trivial to achieve because supramolecular chemistry, as it was coined by Lehn,[3] is understood as the chemistry of intramolecular interactions[4]. For sequenceable polymers, however, the non-binding units must meet certain requirements regarding polymerizability, synthetic accessibility and potentially also regarding the chain conformation. Therefore, at the beginning of the current study, non-binding monomers were used which were already known in the literature[5] (HFDI) or which seemed promising according to the findings of previous doctoral students[6] (BPDI). Furthermore, the literature includes several systematic investigations for the mitigation of charge-transfer complexation in polyimides via the incorporation of fluorinated or aliphatic moieties[7] in the polymer backbone to prevent the otherwise intrinsically present charge-transfer colour.[8,9] Such coloration can be problematic in optical or consumer applications. This chapter presents a new approach to the design and synthesis of non-binding units.

There are some copolymers described in the literature, which allowed, at least to a limited extent, to read out their sequence. As basis of the current study, these copolymers contained pyrene-binding and non-binding elements (even though strongly binding pyrene-based tweezers and not pyrene itself was used in most cases). The non-binding units utilized were biphenylenedisulfone[5] or HFDI[10]; also BPDI[6] was suggested. Other studies used weakly binding instead of non-binding units, where complexation of the binding unit was mitigated either by

the presence of sterically-hindering methyl groups[11] (Figure 1) or by a unfavourable torsion angles introduced into the polymer backbone by the presence of a ketone linkage[12]. A mitigation of pyrene-binding was sufficient to differentiate parts of the polymer in ^{1}H NMR spectra which had otherwise the same chemical shift. In Chapter 4 of this thesis, non-binding elements were used for the creation of sequenceable polymers. This chapter presents a novel concept for the mitigation of pyrene binding to differentiate the two repeat units in a copolymer and thereby read out sequence information.

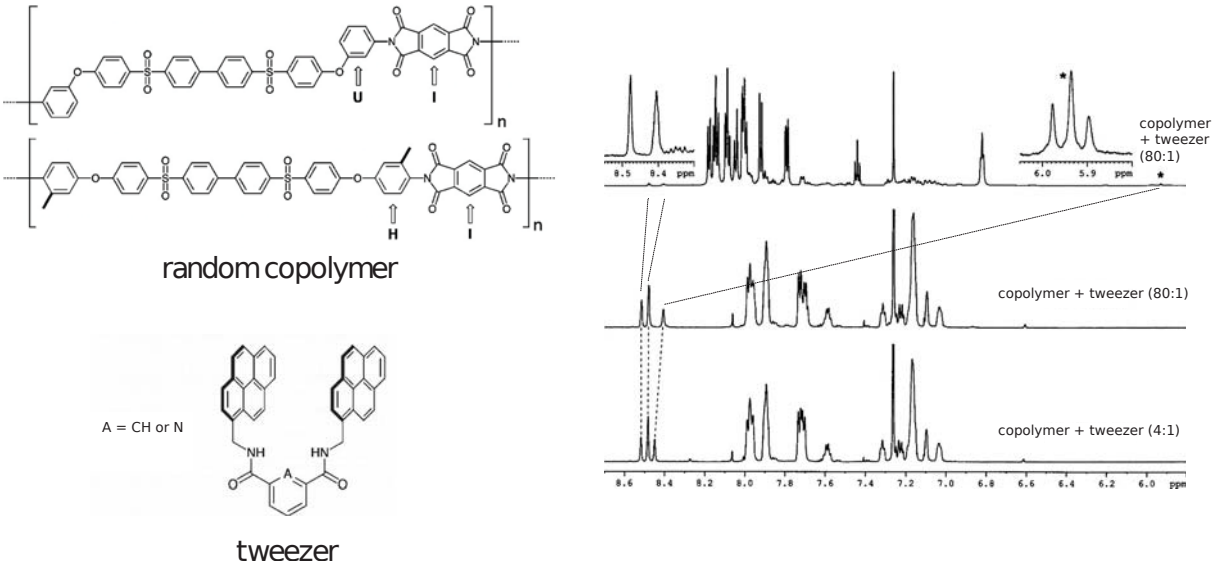

Figure 1: Previously observed splitting patterns of a sterically hindered co-polymer using a tweezer-molecule (used with permission).[13] Right: ^{1}H NMR spectrum of copolymer presented on the left upon addition of the tweezer presented on the left.

As described in Chapter 3, it was found that the complexation strength (as measured by the change in chemical shift Δδ upon addition of a aromatic donor) of a homologous series of poly(ester imide)s with aromatic donors (e. g. pyrene) depends on the length *x* of the aliphatic spacer contained in the polymer chain (Figure 2). For example, the poly(ester imide)s with a short spacer of $x = 2$ (**22** and **34**) bind pyrene strongly but the binding strength decreases for longer spacers (**23** to **28** and **35** to **40**, respectively); the polymers with the longest spacer investigated ($x = 8$, **28** and **40**) showed the weakest binding. This effect is used in the current chapter for the creation of sequenceable polymers by using NDI-based units with short spacers as strongly binding elements and NDI-based units with long spacers as weakly binding elements.

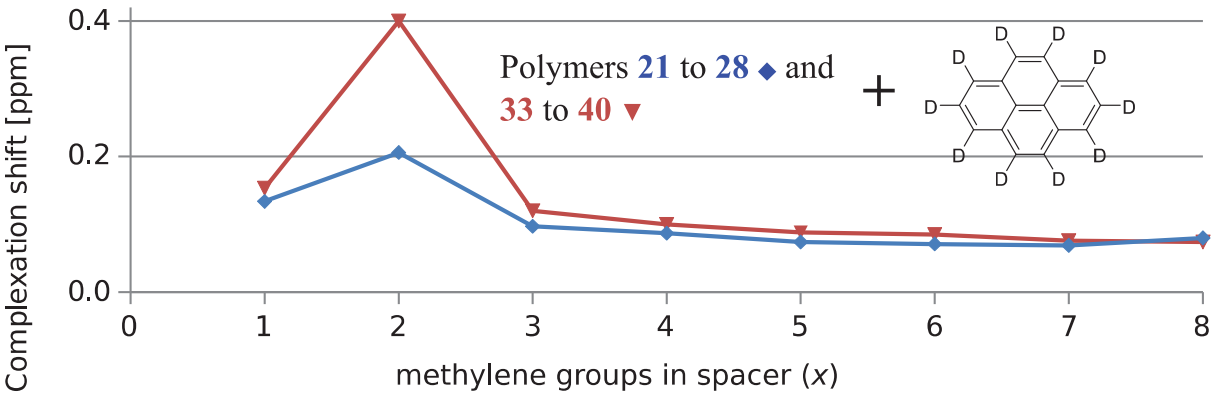

Figure 2: Comparison of complexation shifts (Δδ, ppm) of the aromatic imide protons in poly(ester imide)-pyrene complexes as a function of the spacer length x = 1 to x = 8; using solutions comprising 3 mM intercalator and 4 mM polymers (see Chapter 8.11.1). The graphs show the complexation shift of the aromatic imide protons in the NDI-based homopolymers (◆, **21** to **28**) and in the NDI / HFDI-based copolymers (▼, **33** to **40**).

The intercalation sequenceability of poly(ester imide)s can be optimized when the difference in binding strength between binding and non-binding units is maximised, as was clearly demonstrated in Chapter 4. Binding strength is a fundamental parameter in supramolecular chemistry:[14] it indicates to what extent host and guest attract each other. In Chapter 4, the sequence-related splitting pattern of the imide resonance was followed as a function of the binding strength. This was achieved by a permutation of four pyrene-binding and non-binding imide units in copolymers and the analysis of the resulting splitting patterns of the aromatic imide resonance.

The relative binding strengths of the different repeat units are indicated by graphical symbols: the strongly binding NDI is symbolized by (■), the less strongly binding PMDI unit by (■); the non-binding HFDI is symbolized as (□), the mostly non-binding BPDI as (■). A graphical sequence based on the symbol for the NDI / HFDI-based copolymers (■/□) is better identifiable than the PMDI / BPDI-based copolymer (■/■) due to the metaphorically higher contrast (Figure 3); accordingly a narrower resonance width was observed for the NDI / HFDI-based copolymer which possessed a larger difference in binding strength between the binding (■) and the non-binding unit (□).

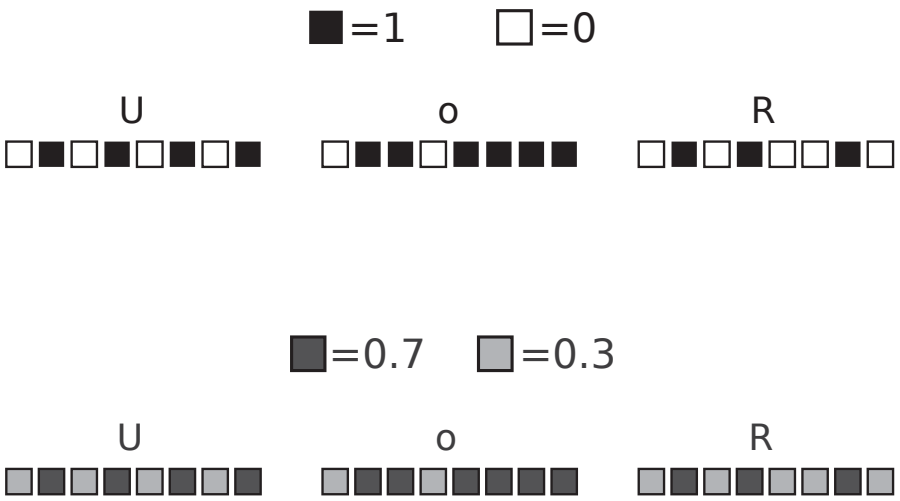

Figure 3: The ASCII code for the sequence UoR (University of Reading), top: made from a strongly binding monomer made from a strongly binding unit (1 or graphically ■) and non-binding unit (0 or □); bottom: made from a less strongly binding unit (0.7 or ■) and a mainly non-binding unit (0.3 or ■). The top row with a larger difference in binding constant has a higher contrast and is easier to read.

In Chapter 4, the theory was developed that maximising the binding strength difference between binding and non-binding units may serve as a general method for improving copolymer sequenceability. In the following, also the impact of the difference in binding strength between the strongly binding and weakly binding units in all-aliphatic NDI-based copolymers will be examined.

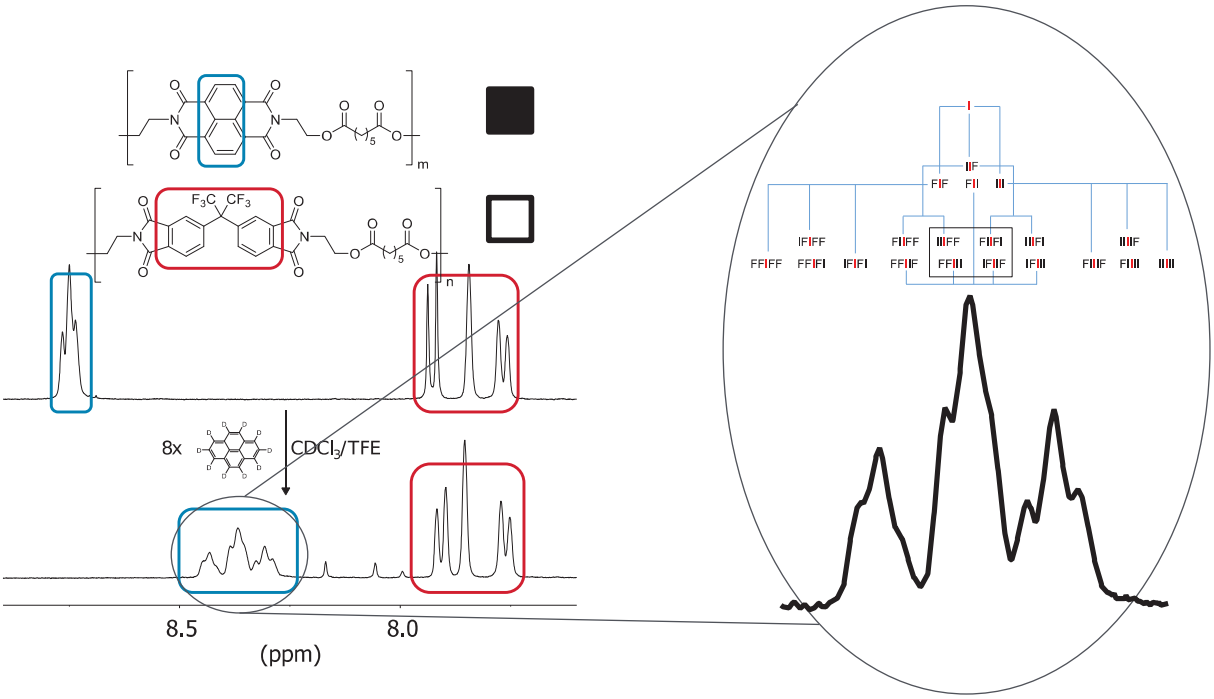

Figure 4: Splitting pattern of the NDI / HFDI-based x = 5 copolymer (**37**) upon the addition of pyrene (left) and expansion of the splitting pattern with overlayed model (right).

The splitting of the aromatic NDI resonance in the presence of pyrene gives information about the copolymer sequence that can be interpreted using a model. The decisive parameters that need to be predicted by the model are the relative complexation shifts of the resonances, their number and their intensity. The resonances represent the different sequences in the polymer backbone. The splitting pattern of the NDI / HFDI-based $x = 5$ copolymer was analysed in Chapter 4 using a detailed model; the sequences present in the polymer backbone could be assigned to the individual resonances (Figure 4). This or similar models will also be used to interpret potential splitting patterns of all-aliphatic NDI-based copolymers.

5.3. Concept and synthesis

The concept of the all-aliphatic NDI-based copolymers is based on the finding that NDIs in a polymer chain, linked by short spacers, bind pyrene more strongly than NDIs attached to long spacers. The all-aliphatic NDI-based copolymers contain both NDIs attached to long and to short spacers, as it is envisaged that the short aliphatic spacer will promote tight chain-folding and thereby enhance the binding of pyrene to adjacent NDI residues. NDIs attached to these spacers should become distinguishable in ^{1}H NMR spectra from the more weakly "single-site" binding NDIs by a different complexation shift and thereby reveal the co-polymers sequence. This new approach stands in contrast to the use of aromatic imide-containing non-binding repeat units, e. g. HFDI (Figure 5).

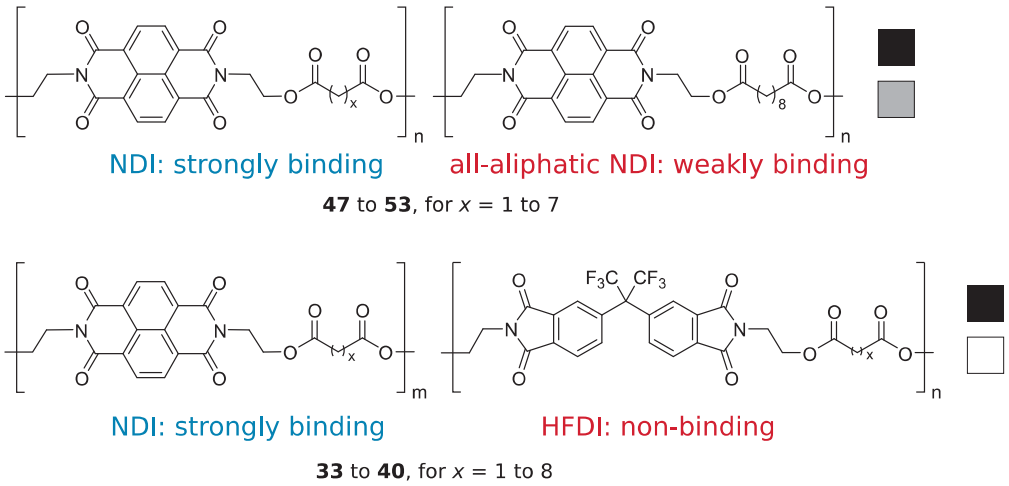

Figure 5: Comparison of the structure (and in particular the weakly binding unit) of all-aliphatic NDI-based copolymers (**47** to **53**) and NDI / HFDI-based polymers (**33** to **40**): The all-aliphatic NDI-based co-polymers are composed of strongly binding NDI units and weakly-binding NDI-units. The NDI / HFDI-based copolymers are composed of the strongly binding NDI unit and the non-binding HFDI-unit (below). In both cases, aromatic hydrocarbons such as pyrene serve as probe molecule, causing a distinguishable complexation shifts of the NDI structural units in different sequences.

The synthesis of the all-aliphatic NDI-based copolymers is shown in Scheme 1. The polymers are easily accessible since the monomers were already used in Chapter 2 and 3 and the same diacyl chloride-based single-step polyesterification could be applied. In case of the all-aliphatic NDI-based copolymers, a 1: 1 mixture of two different aliphatic acid chlorides is used instead of a 1:1 mixture of two bis(hydroxyethyl) diimides.

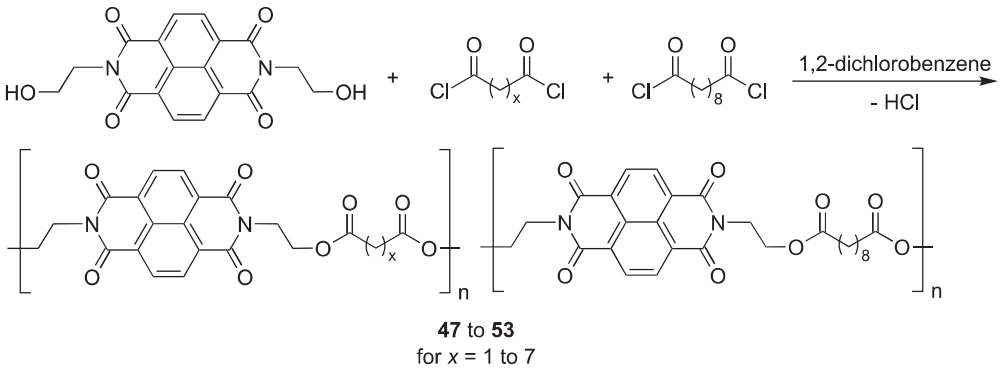

Scheme 1: General synthesis of the all-aliphatic NDI-based copolymers.

Copolymers with a spacer length of $x = 1$ to $x = 7$ were synthesized with a fixed, equimolar quantity of a known weakly-binding spacer having a length of 8 methylene groups in all polymers described here. All possible polymers of the homologous series of NDI-based polymers with a spacer length of $x/8$ were synthesized, from $x = 1$ up to $x = 7$. The polymer with a spacer length of $x = 8/8$ is a homopolymer again and contains thus by definition no information in its sequence. Table 1 shows the inherent viscosities of the polymers, the values all indicating a high molecular weight. ^{1}H NMR spectroscopy generally showed only the expected resonances and generally indicated the absence of side reactions. However, it was observed just as in Chapter 2 and 3 that the polymer with a spacer length of $x = 1$ showed a lower viscosity and a higher extent of side reactions or end groups in the ^{1}H NMR spectrum.

Table 1: Inherent viscosities (η_{inh}) of the polymers synthesized in this study.

x =	η_{inh}
1	0.43
2	0.76
3	0.64
4	3.09
5	1.76
6	1.65
7	1.31

The all-aliphatic NDI-based co-polymers were found to be readily soluble in chloroform/trifluoroethanol (6:1) and had a better solubility than the analogous NDI / HFDI-based copolymers of equal spacer length which generally required a higher fraction of fluorinated co-solvent for dissolution (depending on the spacer length). While it is expected that the trifluoromethyl group in HFDI increases the solubility, the stiffness of the aromatic structure in HFDI conversely reduces the polymer solubility. Apparently, the $x = 8$ spacer offers such good solubility that even the particularly low solubility of the NDI unit (observed in the NDI-based homopolymers **21** to **28**) is overcompensated.

5.4. ^{1}H NMR titrations

It was previously found (Chapter 4) that the greatest difference in binding strength between the binding and the non-binding unit yields the polymers with the most extractable sequence information as the aromatic imide resonances are more sharply resolved and a larger number of imide resonances is distinguishable. It was found on the one hand that the difference in binding strength and thereby the resolution could be maximised by a careful selection of binding imide and non-binding imide units. NDI (symbolized ■) is a stronger binding unit than PMDI (symbolized ■); HFDI (□) binds aromatic hydrocarbons even less than BPDI (■). Accordingly, it was observed that the NDI / HFDI-based copolymer (symbolized ■/□) gave in the presence of pyrene the highest number of distinguishable resonances, while the PMDI / BPDI-based (■/■) copolymer did not yield any sequence information at all. The NDI / BPDI (■/■) and the PMDI / HFDI-based copolymers (■/□) showed intermediate degrees of resolution. Resolution and splitting pattern could on the other hand be affected by the spacer length in the copolymer. For example, the co-poly(ester imide) based on NDI / HFDI $x = 2$ (**34**) shows a complex splitting pattern with a total of 15 distinguishable NDI resonances (Chapter 4, Figure 25). NDI-based units with longer spacers show weaker binding (Figure 2), so the aromatic NDI resonance of the NDI / HFDI-based $x = 5$ copolymer (**37**) splits into a triplet of triplets and only nine distinguishable resonances. It has therefore been expected that the sequenceability of the all-aliphatic NDI-based copolymers also depends on the spacer length of the strongly binding NDI-based unit.

The homologous series of the all-aliphatic NDI-based copolymers differs structurally only by the stronger-binding unit while the long weakly-binding NDI unit remains identical. The resolution depends therefore only on the spacer length of the more strongly binding NDI units.

The copolymer with the spacer length of x = 2 (**48**), which causes the strongest complexation shift, should therefore give the best-resolved and clearest sequence information. This is indeed the case. Figure 6 shows ^{1}H NMR spectra of the all-aliphatic NDI-based copolymer x = 2 (**48**) and, for comparison, the spectra of the NDI / HFDI-based copolymer of equal spacer length (x = 2, polymer **34**, described in detail in Chapter 4). Both polymers show a similar splitting pattern, consisting of of three sets of resonances each. The first is resolved as a singlet only (A), followed at higher field by a complex pattern (B) and an apparent triplet (C). The exact structure of the complex middle resonance pattern (B) is unclear, but it was observed that such structure deconvoluted at higher pyrene concentrations in case of the NDI / HFDI-based x = 2 copolymer (as described in Chapter 4) and as presented in the following.

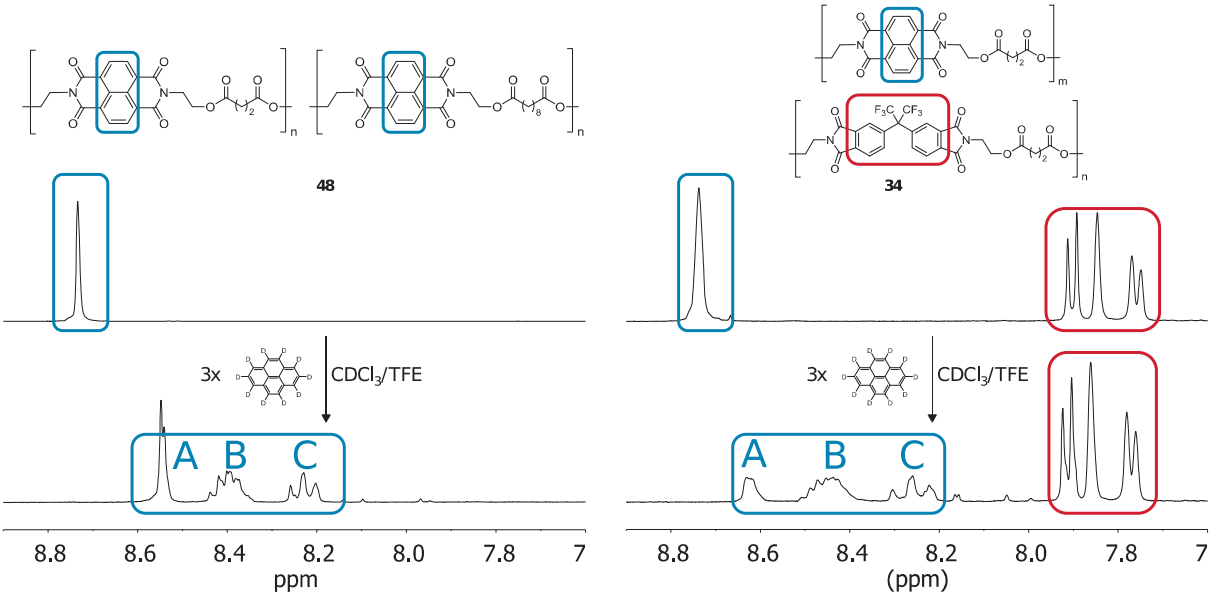

Figure 6: ^{1}H NMR spectra of the all-aliphatic NDI-based copolymer x = 2 (left, **48**) and NDI /HFDI-based copolymer x = 2 (right, **34**) in the absence (top) and presence (below) of pyrene-d_{10}. The splitting pattern of both the all-aliphatic NDI-based copolymer and the NDI / HFDI-based copolymer consists of an apparent doublet, a complex middle pattern and an apparent triplet, though the splitting pattern of the NDI / HFDI-based copolymer is slightly less resolved.

Figure 7 shows the ^{1}H NMR spectra of the same copolymers in the presence of a higher concentration of pyrene. It can be seen that the middle resonance pattern has indeed completely deconvoluted in both cases, for the all-aliphatic NDI-based copolymer as well as the NDI / HFDI-based copolymer. The splitting pattern of both polymers consists of two singlets (A, overlapped in case of the HFDI-based copolymer), a triplets of triplets (B) and a 'singlet / doublet / triplet' splitting pattern. However, the NDI / HFDI-based copolymer had to be measured at a different pyrene concentration because at the 12x molar excess used for the all-aliphatic NDI-based copolymer, central parts of the NDI resonances were overlapping with

the HFDI resonances. A very high pyrene concentration (54 molar excess) was necessary to cause a complexation shift which separates most resonances. It can thus be seen that both polymers, despite the different non-binding unit, have very similar splitting patterns.

As already described in Chapter 4.2.1, the 'singlet / doublet / triplet' splitting pattern (C) can also be found in the chain-folding poly(ether imide) (Figure 1c). It is therefore also assumed that the sequences forming the splitting pattern (C) are also oriented in a chain-folding conformation (see Chapter 4.4.1, Figure 19). Part (B) of the splitting pattern has a low complexation shift and thus lower binding energy. As splitting pattern (B) resembles the weakly binding NDI / HFDI-based x = 5 copolymer (**37**, Chapter 4, Figure 20) a similar less ordered binding is assumed (see Chapter Chapter 4.4.1, Figure 19).

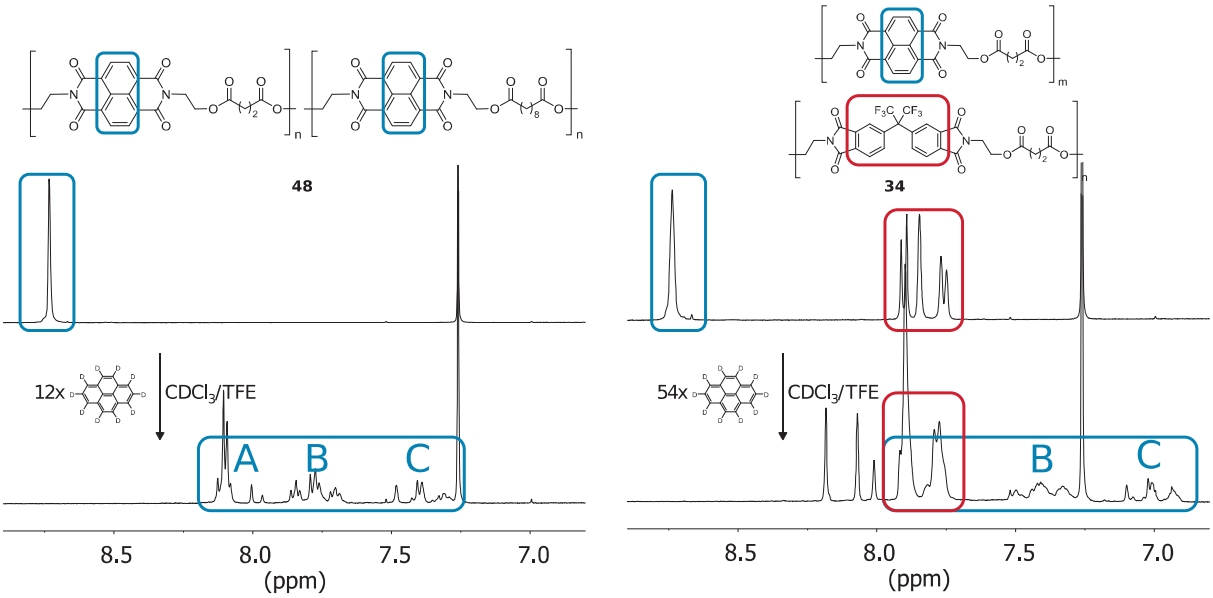

Figure 7: ^{1}H NMR spectra of the all-aliphatic NDI-based copolymer x = 2 (**48**, left) and the NDI / HFDI-based copolymer x = 2 (**34**, right) in the absence (top) and presence (below) of pyrene-d_{10}. The splitting pattern of both the aliphatic NDI polymer and the NDI / HFDI-based copolymer consists of an apparent doublet, an apparent triplet of triplets and triplets of triplets and a fractal-like singlet, doublet and triplet; the splitting pattern of the NDI / HFDI-based copolymer is again slightly less resolved.

To ensure that the complex splitting pattern of the all-aliphatic NDI-based copolymer x = 2 (**48**) is exclusively based on the polymer sequence, a JRES (*J*-resolved) NMR spectrum was measured. Intercalation sequencing does not cause *J*-coupling, therefore only one resonance would be expected in case of the f1 dimension for the NDI resonance (a line in the middle), if the NDI resonances are still singlets which are only separated by a different complexation shift. This expectation was confirmed for the NDI / HFDI x = 5 copolymer (**37**, Chapter 4). In case of the all-aliphatic NDI-based copolymer x = 2 (**48**, Figure 8), it can be seen that this is

the case for pattern C, a single line in the middle indicates that no *J*-coupling is involved. Pattern B, however, indicates *J*-coupling of the imide resonances as a doublet. The pattern in the ^{1}H NMR spectrum of the same resonances are apparent triplets. The width of the resonances in the JRES NMR spectrum could indicate that the apparent triplet results from a coupling with two entities that have the same coupling constant; the apparent triplets may thus result from two overlapping doublets. In region A there is an overlap with the weakly binding resonances, which show only very little complexation shift, therefore the intensity of the resonance is so high.

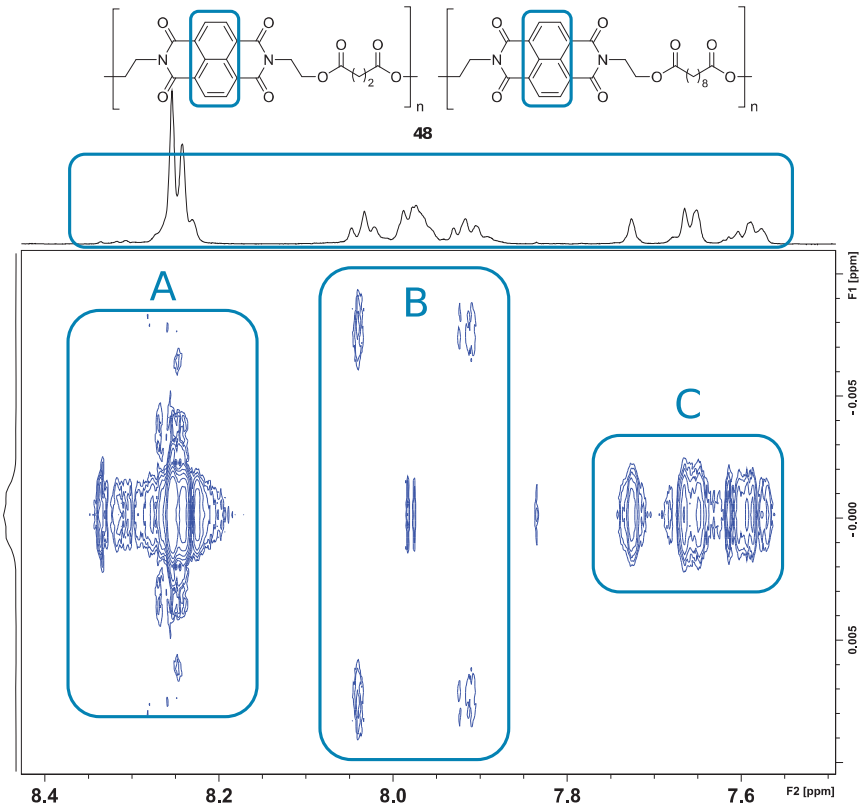

Figure 8: JRES ^{1}H NMR spectrum of the all-aliphatic NDI-based copolymer $x = 2$ (**48**). The spectrum indicates overlapping singlets in region A and a central singlet surrounded by overlapping doublets in region B. In the high field region C, the splitting pattern consists again only of singlets.

J-Coupling makes it difficult to interpret the splitting pattern with a model, but the occurrence of *J*-coupling in pattern B is at least consistent with the assignment of this group of resonances to unsymmetrical sequences centred on the triads 8-I-2 and 2-I-8. The unsymmetrical substitution about NDI is such sequences would make the two pairs of NDI protons inequivalent, so that their *J*-coupling could be expressed in the NMR spectrum. The splitting pattern of the all-aliphatic NDI-based copolymer $x = 3$ (**49**) can be seen in Figure 9, together with the splitting pattern of the NDI / HFDI-based copolymer $x = 3$ (**35**), both spectra measured with

the same molar excess of pyrene (5x excess). The measurement was carried out in the presence of a 5-fold molar excess of pyrene to avoid an overlap of the NDI resonances with the HFDI resonances or the pyrene resonances.

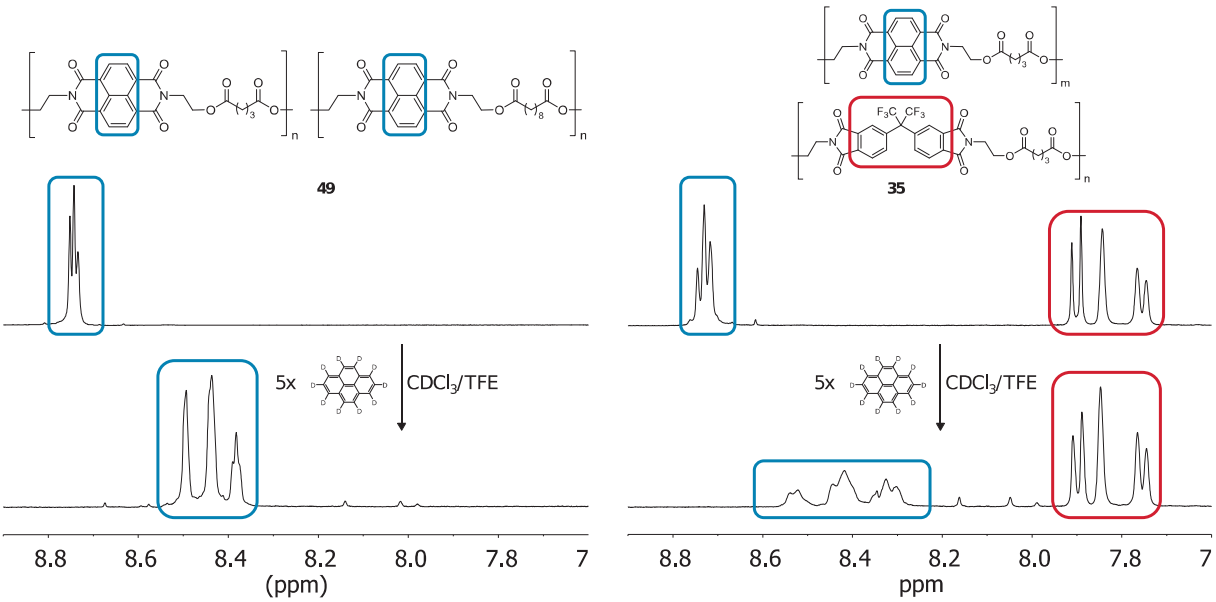

Figure 9: ^{1}H NMR spectra of the all-aliphatic NDI-based copolymer x = 3 (**49**, left) and the NDI / HFDI-based copolymer x = 3 (**35**, right) in the absence (top) and presence (below) of pyrene-d_{10}. The all-aliphatic splitting pattern closely resembles that shown by the copolyimide shown in Chapter 4, Figure 1 d, in the presence of just 0.12 equivalents of pyrene. This is indicative of a chain-folded binding geometry, but the binding in the present system is clearly very much weaker.

While the splitting pattern is somewhat similar, it is noticeable that the all-aliphatic NDI-based copolymer shows a much reduced resolution compared to the corresponding NDI / HFDI-based. The triplet with high complexation shift of the NDI / HFDI-based copolymer (**35**) at 8.3 ppm is still just about identifiable as a triplet in the all-aliphatic NDI-based copolymer (**49**). The resonance with intermediate complexation shift has in case of the all-aliphatic NDI-based copolymer still a faint shoulder, whereas the resonance with the smallest complexation shift is resolved as a singlet only. The difference in resolution between the all-aliphatic NDI-based copolymer and the NDI / HFDI-based copolymers is probably based on the difference in binding strength between the binding and non-binding moieties. As was presented in Figure 2, the binding energy of the NDI-spacer unit drops sharply with an increase in spacer length and approaches thus the binding energy of the weakly binding unit x = 8. As a result, the difference in binding strength between the binding x = 3 NDI structural units and the "non-binding" x = 8 NDI structural units is significantly smaller than in the all-aliphatic NDI-based copolymer x = 2 (**48**). When the difference in binding energy is smaller, both resonances move closer together and a greater overlap results in a reduced resolution.

While the HFDI unit has the advantage of a particularly low (essentially zero) binding constant, the binding of the "non-binding" unit in the all-aliphatic NDI-based copolymers is still significant, and this is a inherent disadvantage of the concept of an all-aliphatic NDI-based copolymer. The "binding" and the "weakly binding" NDI units show than only a comparatively small difference in binding constant. For example, in Chapter 2 it was calculated that the binding constant of $x = 2$ was $K_a = 220$, while the binding constant of $x = 5$ is 55. The binding constant of HFDI is close to zero, and no significant shift is detectable even at high concentrations. The maximum difference between the strongest binding and the non-binding unit is thus found in the NDI / HFDI copolymer system. The difference in case of the all-aliphatic NDI-based copolymers, however, decreases rapidly with decreasing binding strength of longer spacers in the binding unit. The smaller difference in binding constant leads to a lower resolution. The resolution becomes worse as the the spacer x becomes longer. Since Figure 2 shows also a saturation function, the spacer of the non-binding unit can not be made longer in order to decrease the binding any further.

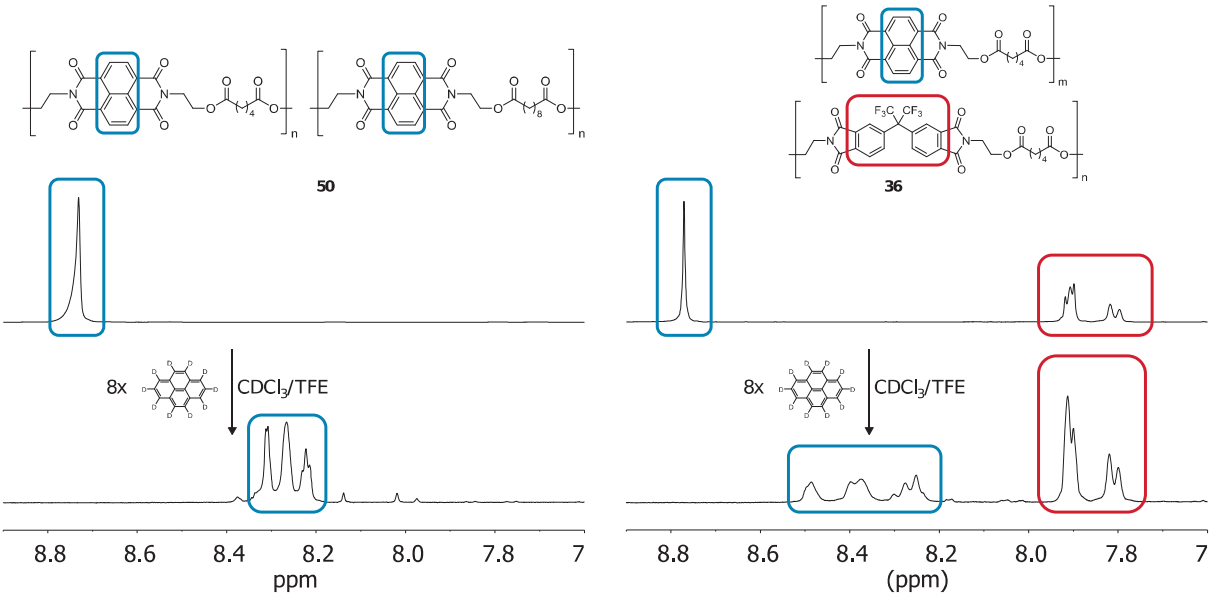

Figure 10: ^{1}H NMR spectra of the all-aliphatic NDI-based copolymer $x = 4$ (**50**, left) and the NDI / HFDI-based copolymer $x = 4$ (**36**, right) in the absence (top) and presence (below) of pyrene-d_{10}. The splitting pattern seems to consists of the 'singlet / doublet / triplet' splitting pattern which indicates a chain-folding conformation. The splitting pattern of the NDI / HFDI-based copolymer is much better resolved than that of the all-aliphatic NDI-based copolymer.

The all-aliphatic NDI-based copolymer $x = 4$ (**50**) shows a very similar splitting pattern as $x = 3$ (**49**), both somewhat resembling that of the NDI / HFDI-based copolymer $x = 4$ (**36,** Figure 10). The difference in the intensity of the NDI resonances of the NDI / HFDI-based copolymer results from the fact that this polymer could not be transesterified due to its reduced solubility, it has therefore no further significance, as it is described in Chapter 6.

Even longer spacers show a further decrease in binding energy (Figure 2), so it is obvious that an extension of the spacer must be accompanied by a further deterioration in resolution. The splitting pattern of the all-aliphatic NDI-based $x = 5$ copolymer is only one triplet, while the NDI / HFDI-based polymer shows a triplet of triplets (Figure 11). The reduced resolution is from here on followed by a remarkable loss of readable sequence information. The splitting pattern of the NDI / HFDI-based $x = 5$ copolymer has been assigned in Chapter 4, the nine resonances resulting from the 16 possible quintet sequences.

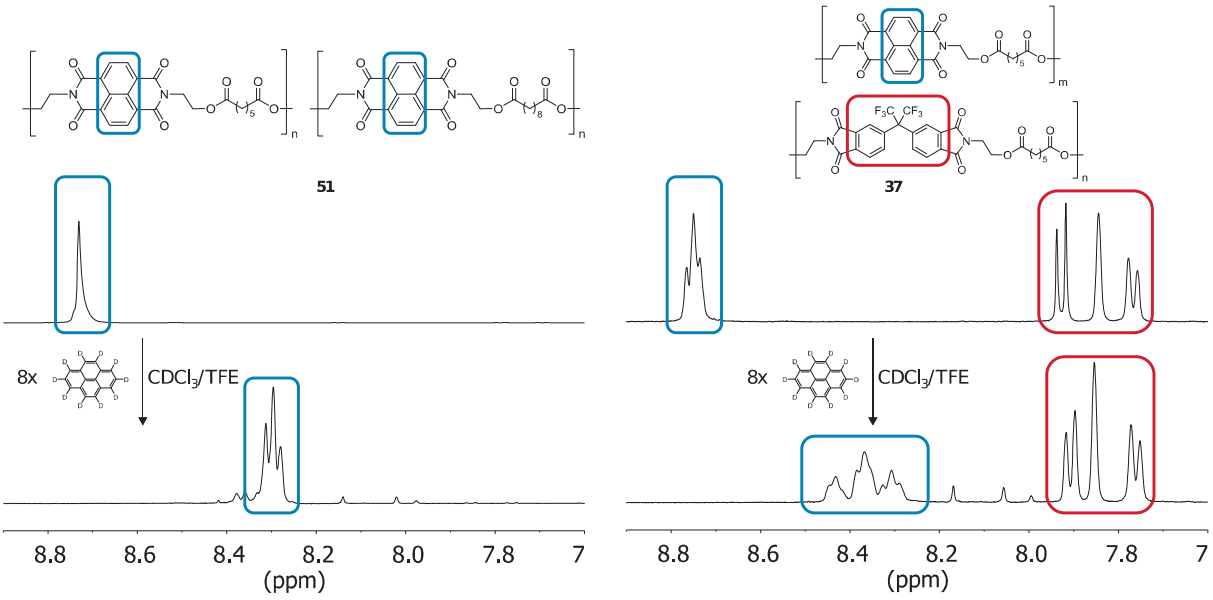

Figure 11: ^{1}H NMR spectra of the all-aliphatic NDI-based copolymer $x = 5$ (**51**, left) and the NDI / HFDI-based copolymer $x = 5$ (**37**, right) in the absence (top) and presence (below) of pyrene-d_{10}. While the splitting pattern of the NDI / HFDI-based copolymer shows a highly resolved apparent triplet of triplets, the all-aliphatic NDI-based copolymer shows only a triplet and therefore less sequence information.

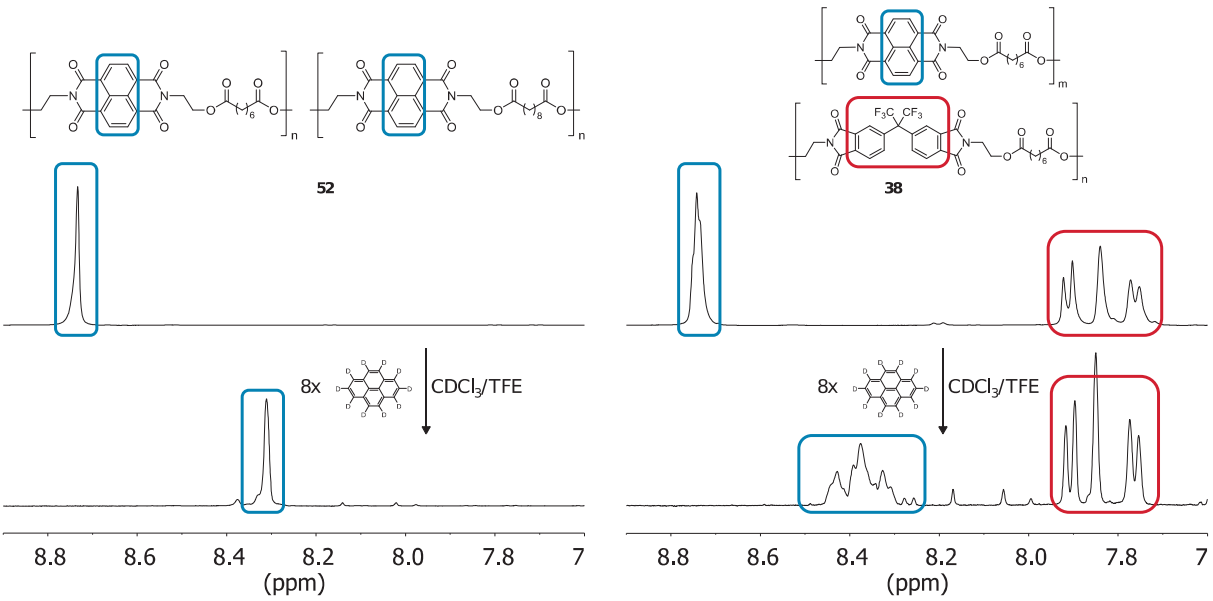

Figure 12: ^{1}H NMR spectra of the all-aliphatic NDI-based copolymer $x = 6$ (**52**, left) and NDI / HFDI-based copolymer $x = 6$ (**38**, right) in the absence (top) and presence (below) of pyrene-d_{10}. While the splitting pattern of the NDI / HFDI-based copolymer shows again a highly resolved apparent triplet of triplets, the all-aliphatic NDI-based copolymer shows only a singlet therefore gives no sequence information.

The all-aliphatic NDI-based copolymer shows much less sequence information, the three resonances reflecting the fact that only triplet sequences can be distinguished. A detailed assignment was, for example, carried out in Chapter 4 for the NDI / HFDI-based $x = 5$ copolymer: the three resonances are based on the sequences (from low-field to high field) -[weakly-binding]-[strongly-binding]-[weakly-binding]-, [weakly-binding]-[strongly-binding]-[strongly-binding]- (and reverse), and -[strongly-binding]-[strongly-binding]-[strongly-binding]-.

The NDI resonance of the all-aliphatic NDI-based copolymer $x = 6$ (**51**) remains a singlet upon the addition of pyrene (Figure 12). This means that the difference in binding energy is so low that no more sequence information can be read out. The splitting pattern of the corresponding NDI / HFDI-based copolymers is again a 'triplet of triplets', so that here relevant deterioration of the resolution is observed upon the extension of the spacers.

5.5. Evaluation and transfer of the concept

The extraction of sequence information from the polymer chain in the present, all-aliphatic system, is possible whenever the diimide resonance shows splitting upon the addition of pyrene or another aromatic probe molecule. The longer the spacer of the binding unit in the all-aliphatic NDI-based copolymer polymer, the less resolution and splitting can be observed. This decrease in resolution can be ascribed to the difference in binding strength between the

binding and "non-binding" unit. The all-aliphatic NDI-based copolymer with spacers from x = 1 to x = 5 are sequenceable. It is remarkable that the difference of only three methylene groups in the spacer of the all-aliphatic NDI-based copolymer x = 5 and its non-binding spacer is yet sufficient for the extraction of sequence information. This demonstrates a potentially broad applicability of the concept, since even fairly slight differences in binding energy seem sufficient.

The comparison of the ^{1}H NMR spectra demonstrates furthermore the advantages and disadvantages of the all-aliphatic NDI unit when compared to HFDI as non-binding units. HFDI has the advantage that it shows virtually no binding towards pyrene. As a result, the difference in binding between any binding unit and the non-binding unit HFDI is greater than with the weakly binding all-aliphatic NDI unit. This is the basis for a significantly higher resolution of the HFDI-based copolymers in most cases. All-aliphatic NDI copolymers, on the other hand, have the advantage of the absence of any resonances in the aromatic region which would overlap with the binding NDI resonances. The all-aliphatic NDI unit resonances show instead (by definition) in the presence of pyrene a weaker complexation shift than the binding NDIs and remain thus in the low field region of the spectrum. For the NDI / HFDI-based copolymer, however, comes inevitably the point when the increasing complexation shift causes (at least parts of) the NDI-resonance to overlap with the HFDI resonances. This overlapping obscures part of the splitting pattern. Another advantage of aliphatic NDI copolymers is their higher solubility when compared to HFDI. The polymers based thereon are thus easier to use, manufacture and process. So far, the solubility was usually a bottleneck for the HFDI-based polymers described in Chapter 2 and 4. Finally, the preparation of all-aliphatic NDI-based copolymers requires, in contrast to NDI / HFDI-based copolymers, only the synthesis of one solid diimide monomer. Instead, two diacyl chlorides are mixed, both of which are commercially available. The use of non-binding NDI slightly simplifies thereby the experimental setup.

As a further test, the concept of the weakly binding NDIs was applied to a different class of polymers by synthesizing new copolymers containing an already known structural binding unit[15] consisting of two NDI residues linked by the sharply chain-folding spacer 2,2′-(ethylenedioxy)bis(ethylamine) (EDEA, Figure 13). The copolymer (**55**) consisted of NDI / HFDI / EDEA units; HFDI served therefore as non-binding unit. The copolymer containing a weakly binding unit (**54**) used the concept of the all-aliphatic NDIs; 1,12-diaminododecane (DADD) was used as weakly binding long-chain aliphatic unit; the copolymer was

therefore based on NDI / DADD / EDEA. The synthesis of the NDI / *HFDI* / EDEA-based copolymer is given in Scheme 2, and the synthesis of the NDI / *DADD* / EDEA-based copolymer was carried out analogously. For the synthesis of the polymers, the anhydride(s) and *N*-methyl-2-pyrrolidone were dehydrated using a Dean–Stark apparatus and an azeotroping solvent (toluene) under reflux, after the amine(s) were added. The viscous solution was again dehydrated under reflux, and afterwards the solvent was removed at reduced pressure and 125 °C. In case of the polymer NDI / HFDI / EDEA, the same temperature sensitivity was observed as described for the poly(ester imide)s in Chapter 2: If imide formation took place at elevated temperature (150 instead of 125 °C), this led to a significantly reduced inherent viscosity, instead of 1.66 only 0.60 dLg^{-1} was obtained.

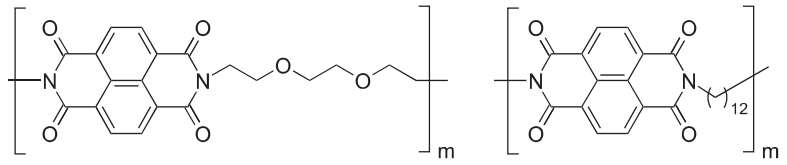

54

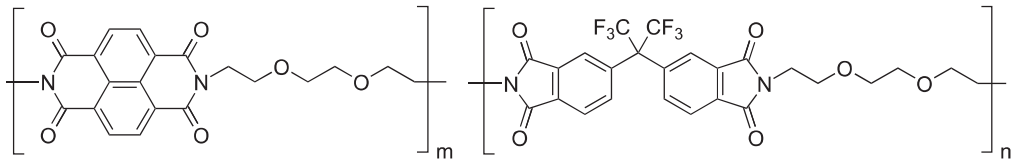

55

Figure 13: The NDI / *DADD* / EDEA-based copolymer (**54**) and NDI / *HFDI* / EDEA-based copolymer (**55**).

Figure 14 compares the ^{1}H NMR spectra of the all-aliphatic NDI-based and the HFDI-based copolymers in the presence of pyrene. The extensive splitting of the NDI resonance demonstrates that the information read-out via binding and not-binding co-monomers could be applied successfully to another class of poly(imide)s. The NDI / *DADD* / EDEA-based copolymer (**54**) and the NDI / *HFDI* / EDEA-based copolymer (**55**) show quite similar splitting patterns. This demonstrates furthermore that a weakly binding NDI-linker-NDI site is suitable as a replacement for HFDI as non-binding unit for the read-out of sequence information.

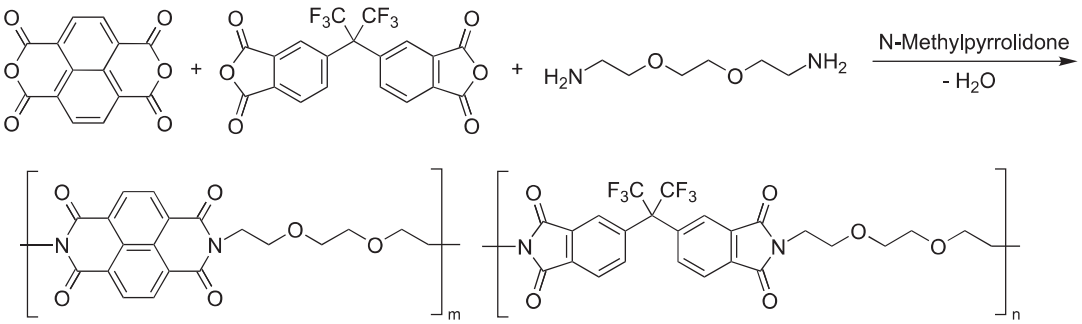

55

Scheme 2: Synthesis of the NDI / HFDI / EDEA-based copolymer (**55**).

The concept may work also in this case so well because the tightly-folding structural unit is very strongly binding (it produces with only a 2-fold excess of pyrene a complexation shift of 1.55 ppm). The transferability to another, related class of poly(imide)s shows that the concept of weakly binding NDIs could be potentially more broadly applicable.

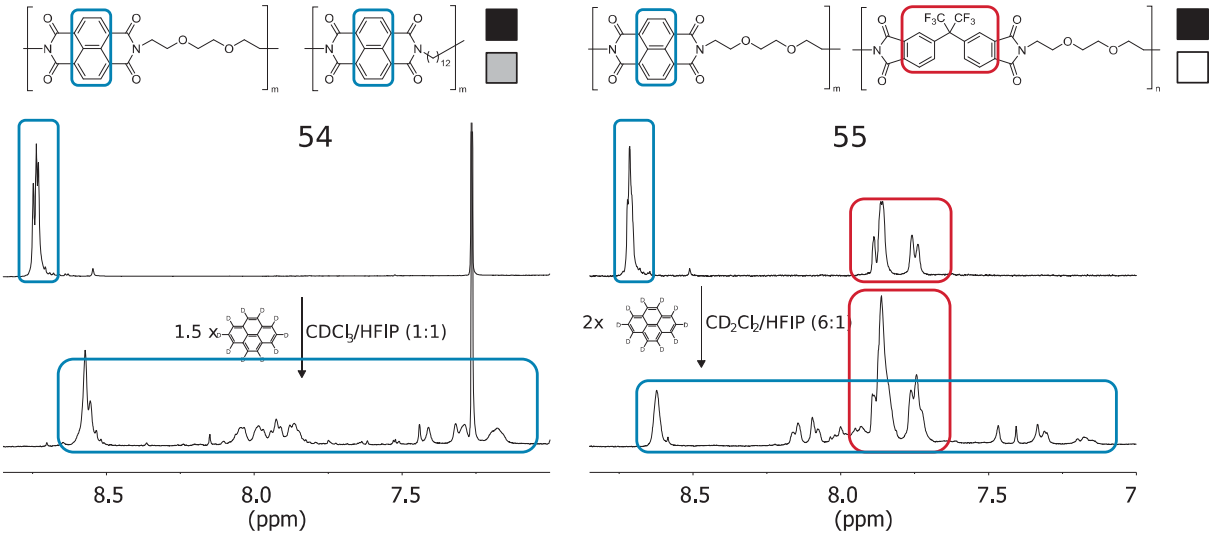

Figure 14: ^{1}H NMR spectra of the NDI / *DADD* / EDEA-based copolymer (**54**, left) and the NDI / *HFDI* / EDEA-based copolymer (**55**, right) in the absence (top) and presence (below) of pyrene-d_{10}. The right part of the splitting pattern is for both polymers similar to the splitting pattern shown in Figure 7 and consists of a triplet, a doublet and a singlet. The middle splitting pattern consists for both polymers of a set of four resonances. The left part of the splitting pattern shows again similarity with the resonances shown in Figure 4, consisting of a singlet or two overlapping singlets.

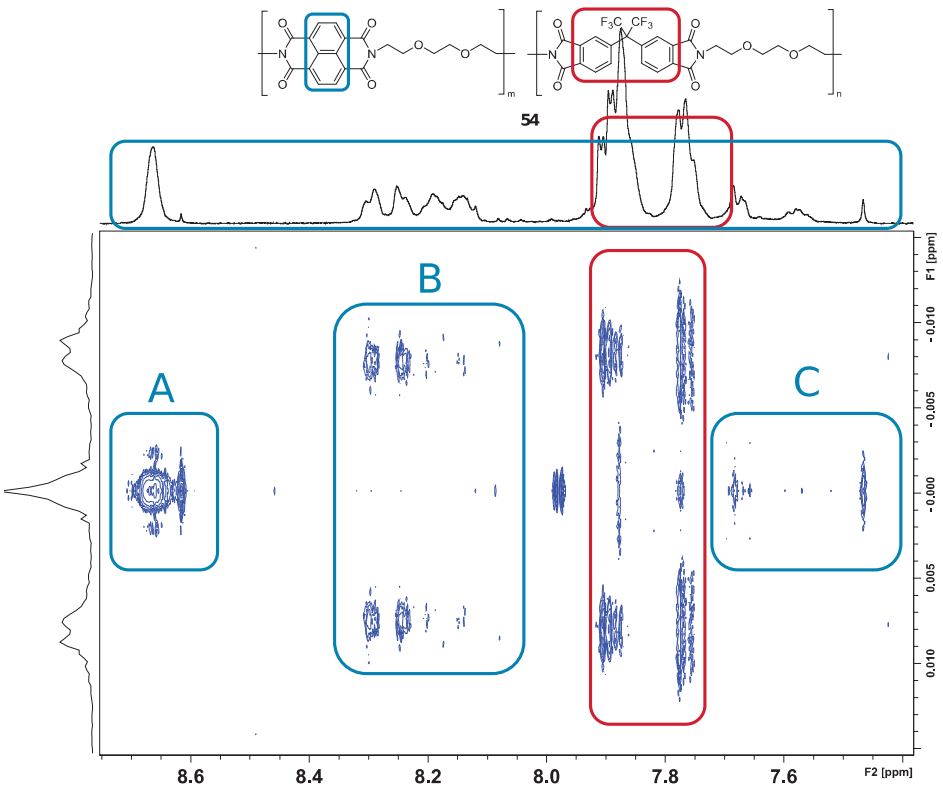

Figure 15: JRES ^{1}H NMR spectrum of the NDI / *DADD* / EDEA-based copolymer (**54**). The JRES indicates overlapping singlets in region A and overlapping doublets in region B. In the high field region C, the signal-to-noise ratio is so poor that only singlets and the right and left border can be clearly identified.

Also a JRES ^{1}H NMR spectrum of the NDI / *DADD* / EDEA-based copolymer was measured (Figure 15). The measurement was problematic because the solubility of the copolymer was limited, therefore it had to be dissolved in dichloromethane-d_2/HFIP (1:1, *v:v*). The high proportion of the co-solvent HFIP also degraded the signal-to-noise ratio. In addition, dichloromethane evaporated due to its high volatility within the time required for the measurement (13h), so that only a part of the data could be utilized and the signal-to-noise ratio deteriorated further. It can thus be seen that the poor solubility of the NDI-based polymers caused besides the problematic synthesis (in particular in case of the poly[ester imide]s) further limitations. It can be seen from the data with some certainty that splitting pattern B consists at least in parts of doublets. The only recognizable resonances of the splitting pattern A show singlets, but the resonances are only partially resolved. As far as it is possible to say, the JRES of the NDI / *HFDI* / EDEA-based copolymer (**55**) confirms the findings of the JRES NMR of the all-aliphatic NDI-based $x = 2$ copolymer, but data of higher quality would clearly be needed to clarify and account for the complexation-based splitting patterns of these systems.

5.6. Conclusions

In order to expand the applicability of intercalation sequencing, novel co-poly(ester imide)s comprising a strongly binding (NDI-based) and a weakly binding (all-aliphatic-based) unit were synthesized. These polymers are analogous to the NDI-based / HFDI-based copolymers of corresponding length. Supramolecular complexation studies demonstrated that the all-aliphatic NDI-based unit is under certain circumstances suitable as a weakly binding unit and can be used in place of the non-binding unit HFDI. The all-aliphatic units have the advantage of not possessing any resonances in the aromatic region. HFDI, on the other hand, has the advantage of a particularly low binding constant.

The splitting patterns of the NDI / HFDI-based copolymer and of the all-aliphatic NDI-based copolymers of equal spacer length are the same for some spacer lengths (as long as they are observable in the light of the reduced resolution of the all-aliphatic NDI-based copolymers). In any case, the two types of copolymers show the same complexation shift of the -III- unit. This indicates that the all-aliphatic NDI-based copolymers and the NDI / HFDI-based copolymers adopt closely related conformations in solution.

Furthermore, the principle of a preferably strong difference in binding between binding and non-binding unit for a high resolution (demonstrated in Chapter 4) was confirmed for the all-aliphatic NDI-based copolymers and could be transferred to poly(ether imide)s. This design principle will be of help for the further creation and expansion of the concept of information storing polymers. It may potentially allow the intercalation sequencing of otherwise fully aliphatic polymers using NDI as sensing unit. The concept shown here has the advantage that it is synthetically simply, which is advantageous for potential applications.

5.7. References

1 H. Colquhoun and J.-F. Lutz, *Nat. Chem.*, 2014, **6**, 455–456.

2 J.-F. Lutz, M. Ouchi, D. R. Liu and M. Sawamoto, *Science*, 2013, **341**, 1238149–1238149.

3 J.-M. Lehn, *Angew. Chem. Int. Ed.*, 1990, **29**, 1304–1319.

4 J. W. Steed, D. R. Turner and K. Wallace, *Core Concepts in Supramolecular Chemistry and Nanochemistry*, Wiley-Blackwell, Chichester, UK, 2007.

5 J. S. Shaw, R. Vaiyapuri, M. P. Parker, C. A. Murray, K. J. C. Lim, C. Pan, M. Knappert, C. J. Cardin, B. W. Greenland, R. Grau-Crespo and H. M. Colquhoun, *Chem. Sci.*, 2018, **9**, 4052–4061.

6 F. La Terra, *Molecular Tweezers and Their Properties in Solution and on Surfaces*, PhD thesis, University of Reading, 2014.

7 A. Susa, J. Bijleveld, M. Hernandez Santana and S. J. Garcia, *ACS Sustain. Chem. Eng.*, 2018, **6**, 668–678.

8 M. Hasegawa, Y. Watanabe, S. Tsukuda and J. Ishii, *Polym. Int.*, 2016, **65**, 1063–1073.

9 S. Ando, T. Matsuura and S. Sasaki, *Polym. J.*, 1997, **29**, 69–76.

10 Z. Zhu, C. J. Cardin, Y. Gan and H. M. Colquhoun, *Nat. Chem.*, 2010, **2**, 653–660.

11 H. M. Colquhoun and Z. Zhu, *Angew. Chem. Int. Ed.*, 2004, **43**, 5040–5045.

12 Z. Zhu, C. J. Cardin, Y. Gan, C. A. Murray, A. J. P. White, D. J. Williams and H. M. Colquhoun, *J. Am. Chem. Soc.*, 2011, **133**, 19442–19447.

13 H. M. Colquhoun, Z. Zhu, C. J. Cardin, Y. Gan and M. G. B. Drew, *J. Am. Chem. Soc.*, 2007, **129**, 16163–16174.

14 P. Thordarson, *Chem. Soc. Rev.*, 2011, **40**, 1305–1323.

15 L. R. Hart, J. H. Hunter, N. A. Nguyen, J. L. Harries, B. W. Greenland, M. E. Mackay, H. M. Colquhoun and W. Hayes, *Polym. Chem.*, 2014, **5**, 3680–3688.

6 Utilizing ^{1}H NMR spectroscopy-based intercalation sequencing to follow transesterification reactions

6.1. Abstract

The monomer-sequence of a copolymer is a fundamental parameter that affects numerous properties such as phase separation of incompatible polymer blends, mechanical properties like tensile strength or macroscopic properties like the structure of polymer foams. In the present Chapter, the ^{1}H NMR-based intercalation sequencing described in Chapter 4 and 5 is used to follow the formation of new sequences during the transesterification of two homopolymers. It was found that the splitting pattern intensity ratios of the aromatic imide resonances, which are followed by the intercalation sequencing, were during the transesterification process as expected in view of the intercalation sequencing theory. The observed intensity ratios were as expected for all polymers investigated, namely the NDI-based x = 5 homopolymer (**25**), a copolymer from a mixture of the NDI-based x = 3 homopolymer (**23**) and the HFDI-based x = 3 homopolymer (**29**) and a copolymer from a mixture of the NDI-based x = 5 homopolymer (**25**) and the HFDI-based x = 5 homopolymer (**30**). Furthermore, a lactone macrocycle (**58**) was inserted successfully into a homopolymer forming a random copolymer (**59**). Again, the formation of new sequences in the copolymer (**59**) was observed via intercalation sequencing. Using intercalation sequencing, it is thereby possible to follow a transesterification, determine the relative frequency of the sequences in the chain and observe the transesterification progress. Thus, it was shown that intercalation sequencing could be used as a tool to investigate the transesterification of industrially relevant polymers. In comparison to conventional NMR-based sequencing, which uses usually three resonances, intercalation sequencing allows to obtain by the observation of nine or more resonances more information and to distinguish sequences with significantly longer repeat units.

6.2. Introduction

The term ‘sequencing’ means analysing the defined order of distinct elements. In copolymers, the distinct elements are called repeat units: their arrangement has has consequences on a material’s properties and can be used for information storage as demonstrated by DNA. Polymer sequencing is thereby of general interest, it is in particular used in the field of sequence-controlled polymers (Figure 1).

For chemical investigations, information about the material under investigation is obtained by instrumental analysis; the sequence of non-natural polymers is analysed by ^{1}H or ^{13}C NMR spectroscopy, whereas the sequence of proteins by mass spectrometry. NMR spectroscopy is generally the most widely applied technique for polymer analysis, as the signals are narrow in relation to the width of a spectrum and identical atomic groups appear in the spectrum only once. This means that comparably much information can be obtained by NMR spectroscopy; apart from sequence, this can be chain defects and chain end groups, cyclic oligomers, and by-products present at small concentrations and even quantification of the structural features mentioned.[1]

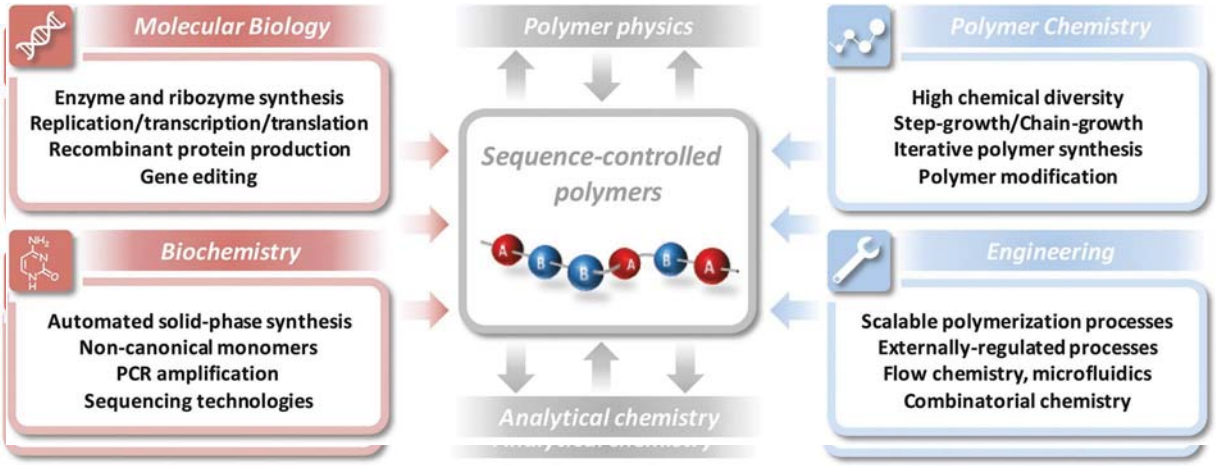

Figure 1: Sequence-controlled polymers are utilized in biology (red) and polymer science (blue). Sequence-controlled polymers are applied in materials science and nanotechnology applications: they are seen as bridge between evolutionary optimized biopolymers and conventional plastics.[2]

An example of how sequences are usually detected via ^{1}H NMR spectroscopy is presented in Figure 2, which shows the ^{1}H NMR spectrum of an copolymer from poly(ethylene terephthalate), a commodity plastic and poly(ethylene naphthalate), an "engineering" polymer with superior properties. The ethylene glycol units show different chemical shifts depending on whether they are attached to terephthalate, naphthalate or one of each, as this effects the chemical shift. Even though only three resonances can be distinguished and thereby only little information is obtained, this sequence information allows to follow the transesterification process and thereby control macroscopic structures and produce materials with tailored properties.[3] Without transesterification, phase separation is observed, when two polymers are insoluble in one another. With a small degree of transesterification, a copolymer is formed at the interface. This stabilized droplet-type structure causes improved mechanical properties.

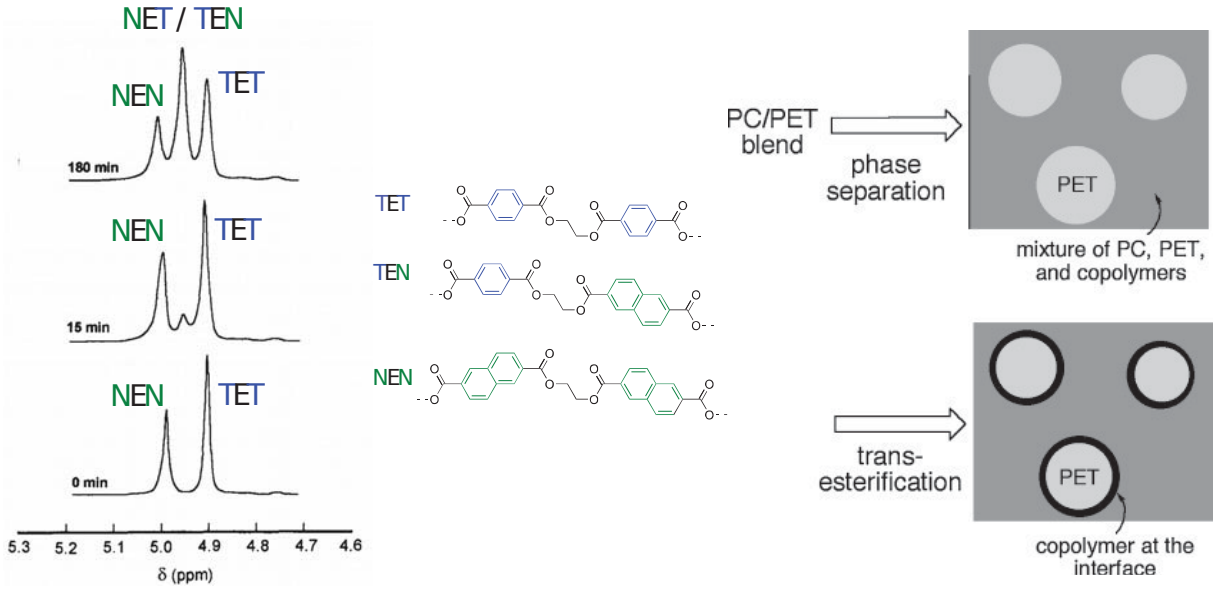

Figure 2: Left: ^{1}H NMR spectra of a mixture of two homopolymers (below left), which are reacted under transesterification conditions to a partially random copolymer (above left).[4] The ^{1}H NMR spectra allow determination of the ratios of the three sequences NEN, TEN, NET and TET (middle) and thereby follow the transesterification. TEN is only the reverse sequence of NET, the two have thereby the same chemical shift. Right: A droplet structure formed by blending two immiscible polymers (PET and PC) can be stabilized by transesterification via the creation of a copolymer at the interface.[3] Used with permission.

In previous chapters (Chapter 4 and 5), intercalation sequencing was described for different types of polymers. In each case, random copolymers were investigated, as for those, the relative abundance of each sequence in the chain can be calculated. The calculation of the relative abundance allowed to develop a mathematical model which could predict expected ratios and relative peak positions. Using the model, the individual resonances could be assigned to the sequences present in the chain.

In the current chapter, it was planned to extract further information from the already known sequence ratio of the random copolymers. Two general options were considered: Either, two homopolymers could be mixed and subjected to ester-exchange reaction. By the exchange reaction, random copolymers should be formed, which should show the same sequence patterns as the directly produced random copolymers. Another option would be to prepare and analyse polymers with a specific and controlled sequence. This would presumably make it possible to generate ^{1}H NMR spectra with any desired intensity ratios to test the theory of the assigned sequences to resonances more thoroughly, but such a synthesis would be extremely difficult. It was therefore decided to realise the first option. It is seen as a first advantage that the exchange reaction between two homopolymers requires less experimental effort than the synthesis of sequence defined polymers. Minimizing the experimental effort for a scientific

proof, i.e. achieving the goal as efficiently as possible, is an important aspect. Whitesides writes in his well-known paper about the significance of choosing suitable tasks.[5] The use of an exchange reaction between two homopolymers is advantageous in a second aspect as such exchange reaction is closer to the industrial practice. The analysis method would thus make a further step towards potential applications. A disadvantage of the method is, however, that the reaction is limited to the entropically favoured sequences and relationships. Thus, not any desired sequence ratios can be observed in ^{1}H NMR spectroscopy and the theory cannot be tested without restrictions.

The exchange reaction is based on ester bonds in the repeat units of the polymers, which are present in the homo- and co-poly(ester imide)s **13** to **53** reported in the previous chapters. It is known that when two homopolymers are mixed under exchangeable conditions, first homopolymers are formed, which are then further randomized into block copolymers of decreasing size until finally fully random copolymers are obtained (Figure 3).

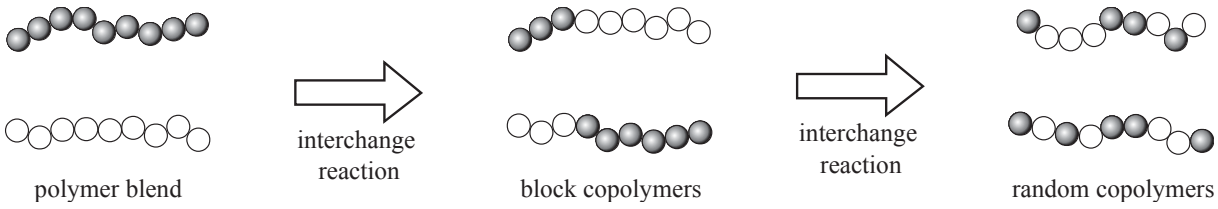

Figure 3: The interchange reaction of homopolymers, (left, e. g. transesterification) proceeds via the formation of block copolymers (middle). By further exchange reactions, the block size decreases until fully random copolymers are obtained (right).[3] Used with permission.

The exchange reaction generates new sequences that do not exist in the initial homopolymers. However, these new sequences are the same sequences as those present in the random copolymers produced via direct synthesis (polymerizing a mixture of two monomers as described in in Chapter 2). It is evident that the sequence-related splitting-patterns have the same chemical shift for co-polymers obtained via transesterification or via direct synthesis (in the presence of a equal concentration of intercalator). Upon continued transesterification, the ratios of the copolymers produced via transesterification should approach the ratios present in the directly produced copolymers. Once complete transesterification is achieved, the peak ratios should be identical.

In the presence of an intercalator, the imide resonance of the binding homopolymer shows only a single resonance, since all binding units have the same complexation shift. It is expected that the reaction of the homopolymer to an increasingly random copolymer will reveal initially unknown intermediate splitting patterns. By further transesterification, the splitting pat-

tern should approach the splitting pattern of the random copolymer via direct synthesis. Figure 4 shows the two questions that should therefore be answered in this chapter: First, is it actually possible to produce via transesterification the same splitting patterns of sequence-related splitting-resonances as by transesterification? This is symbolised by question mark "?A" in Figure 4. Second, what do the intermediate stages look like? This is represented by question mark "?B". The splitting patterns are planned to be be compared to the predictions of the theory.

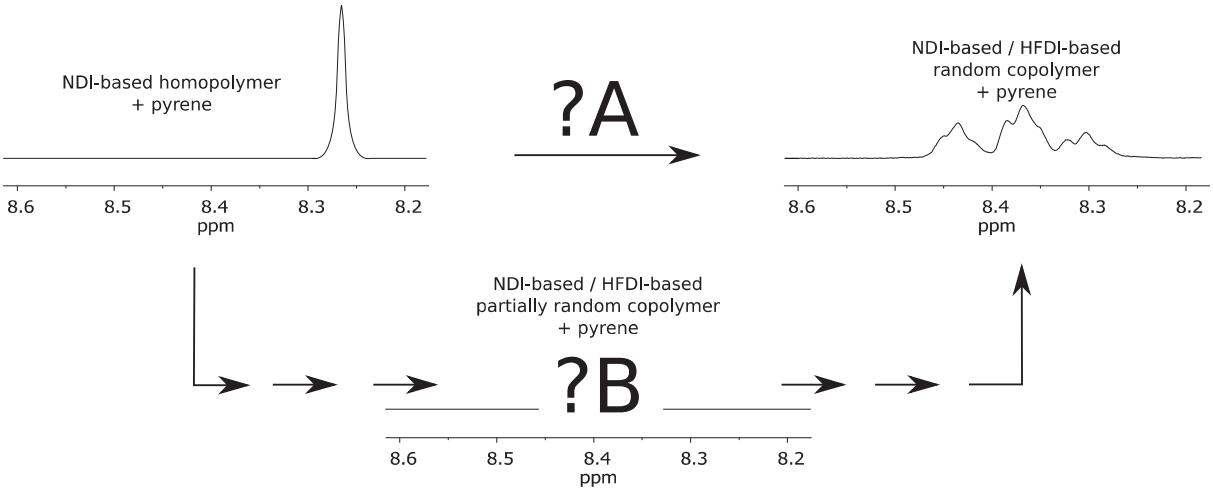

Figure 4: The figure shows a schematic view of the assumed intercalation sequencing splitting patterns during the course of the reaction. The aromatic imide resonance of an imide-based homopolymer consists of a single resonance (above left). Question mark ?A symbolizes the question if a random copolymer can be synthesized via full transesterification, which has the same splitting pattern as the directly synthesized random copolymer (above right). By stepwise transesterification intermediate splitting patterns should be observable, this is symbolized by question mark ?B (below).

6.3. Transesterification of NDI / HFDI-based homopolymers

In the following it is described how a randomization via transesterification can be followed by intercalation sequencing. Initially, two homopolymers are transesterified, specifically a binding and a non-binding homo-poly(ester imide) (**23** and **29** or **25** and **30**, Figure 5, above). After the transesterification reaction, intercalation sequencing is applied by measuring a ^{1}H NMR spectrum of the polymer mixture in the presence of the intercalator pyrene-d_{10}. The directly synthesized binding / non-binding co-poly(ester imide)s, for which a sequencing was described in Chapter 4, are intended to be synthesized in the current chapter via full transesterification and subsequently to be analysed. In a later step, a binding homopolymer and an ester-bearing cyclic small molecule (lactone macrocycle **58**) were transesterified yielding a binding / weakly binding co-poly(ester imide) (**59**) which was deduced from the concept of

the weakly binding unit introduced in Chapter 5 (Figure 5, below). For all reactions, fully randomised copolymers were produced and sequenced at first. Subsequently, the transesterification reaction was followed by successively taking intermediate samples. The fully transesterified samples could be compared to the copolymers directly synthesized and analysed in Chapter 4 and 5.

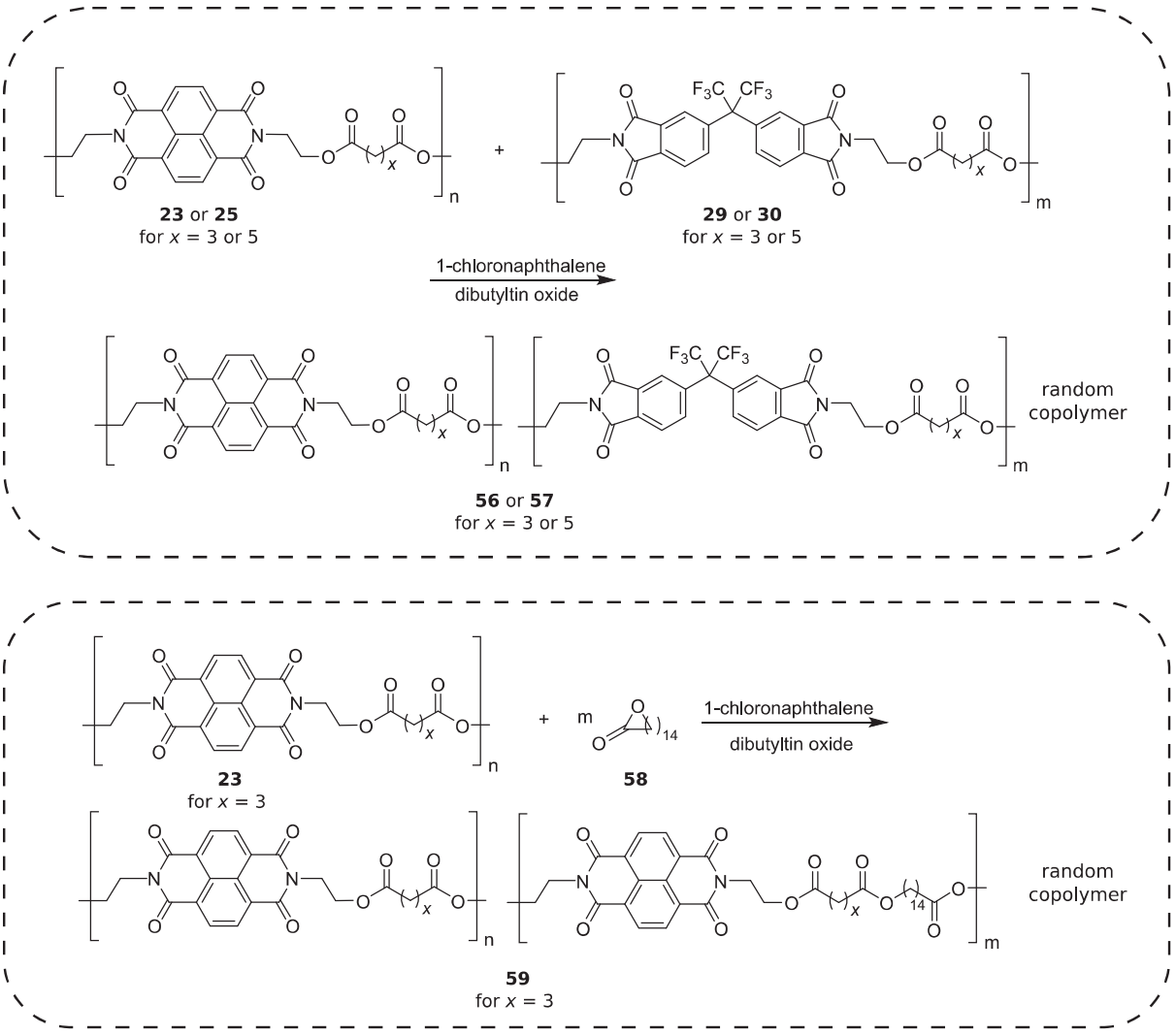

Figure 5: In this chapter, sequencing is used to follow two reactions. A binding NDI-based homopolymer (**23** or **25**) and a non-binding HFDI-based homopolymer (**29** or **30**) are converted to a sequenceable copolymer (**56** or **57**, above). Furthermore, a non-binding lactone **59** is inserted into a binding NDI-based homopolymer **23** to obtain a binding / weakly binding copolymer **59**.

6.3.1. Full Transesterification

For the transesterification reaction, an NDI-based homopolymer and a HFDI-based homopolymer were mixed in a 1:1 molar ratio and 2 mol% dibutyl tin oxide (DBTO) (with regard to the repeat units) was added as transesterification catalyst. For complete randomization, the

mixture was heated in dichlorobenzene for 24 hours at 170 °C. It is known from the literature that transesterification occurs in polymers under these conditions.[6] Of all the copolymers produced in Chapter 4, the NDI / HFDI-based copolymers were selected as target because these polymers revealed the most sequence information. They also showed an improved solubility over the NDI / BPDI-based copolymers. The NDI-based and HFDI-based homopolymers were selected with a chain length of $x = 3$ and $x = 5$. On the one hand, the NDI / HFDI-based $x = 3$ and NDI / HFDI-based $x = 5$ copolymers showed different splitting patterns. On the other hand, copolymers containing odd-numbered spacers showed showed again an improved solubility. The NDI / HFDI-based $x = 4$ copolymer, on the contrary, precipitates during synthesis and can not be redissolved in refluxing dichlorobenzene, the same applies to the NDI / HFDI-based $x = 2$ copolymer. The remaining bonds were all the same as for the copolymers via direct synthesis. After the transesterification reaction, the sample was treated in the same way as the copolymers from direct synthesis and reprecipitated from halogenated solvents in methanol for solvent removal. Also the intercalation sequencing carried out as in Chapters 4 and 5 by mixing concentrated solutions of polymer and pyrene-d_{10} in different ratios with micropipettes and followed by measuring ^{1}H NMR spectra of the mixtures. Again, deuterated pyrene was used to avoid resonance overlapping.

The splitting pattern of the NDI / HFDI-based $x = 5$ copolymer via direct synthesis (**37**) consists of a triplet of triplets (Figure 6) as shown in Chapter 4 (Chapter 4, Figure 19). It was already shown in Chapter 4 that copolymers but not homopolymers show sequence-related splitting in the presence of pyrene-d_{10} (as only copolymers have many different sequences). A mixture of initially homopolymers was expected to show after complete randomization the same splitting pattern as the directly synthesized copolymers. A mixture of the binding NDI-based $x = 5$ homopolymer (**25**) and the non-binding HFDI-based $x = 5$ homopolymer (**30**) was therefore heated with a catalyst (DBTO) in 1,2-dichlorobenzene for 6 hours at 170 °C. Numerous examples for aromatic polyesters that can be transesterified at similar temperatures and catalysts within 2 hours are known from the literature,[7–11] a reaction time of 6 hours in the current system was supposed to ensure full randomization. The polymer mixture was freed from solvent by precipitation. A direct comparison of the ^{1}H NMR spectrum of the NDI / HFDI-based $x = 5$ copolymer (**37**) *versus* the ^{1}H NMR spectrum of the NDI / HFDI $x = 5$ polymer mixture after transesterification (**57**) shows complete agreement.

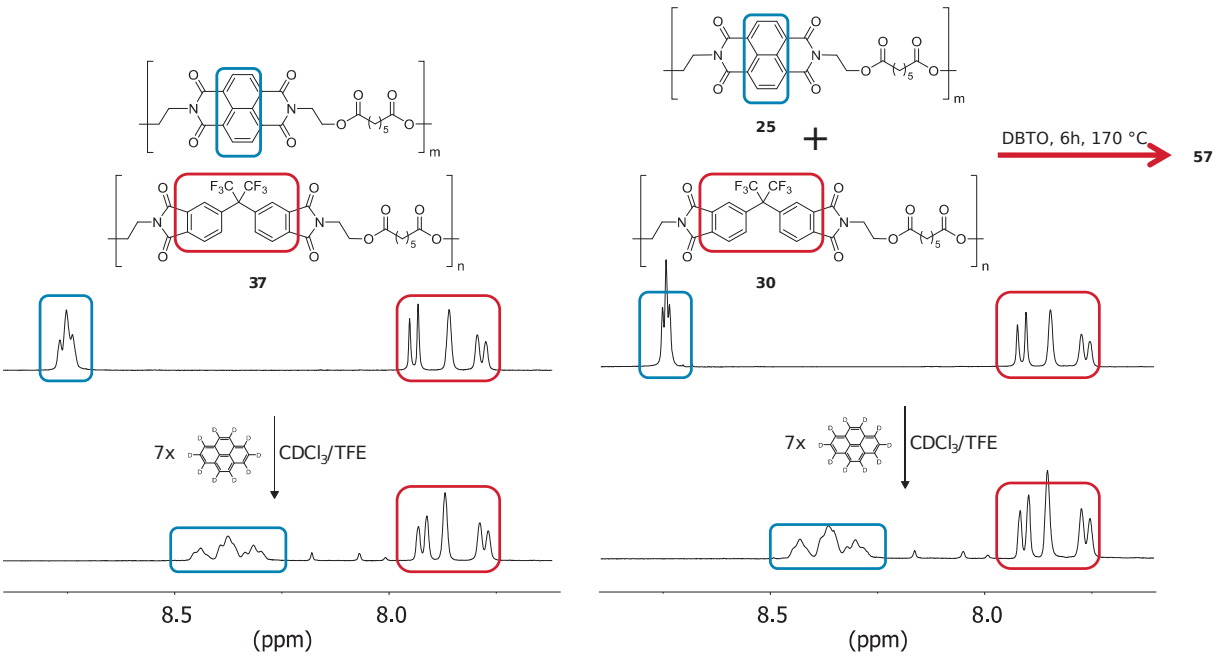

Figure 6: Comparison of the ^{1}H NMR spectra of the NDI / HFDI-based x = 5 copolymer (**37**) via direct synthesis and NDI / HFDI-based x = 5 polymer mixture after transesterification (**57**) analysed by intercalation sequencing: Left: The aromatic imide resonance of the NDI / HFDI-based x = 5 copolymer (**37**) via direct synthesis splits upon the addition of pyrene-d_{10} into an apparent triplets of triplets. Right: The aromatic imide resonance of the NDI / HFDI-based x = 5 polymer mixture after transesterification (**57**) equally splits upon the addition of pyrene-d_{10} into an apparent triplets of triplets.

In order to validate the result, a control sample was prepared analogue to the previous samples: The NDI-based x = 5 homopolymer (**25**) and the non-binding HFDI x = 5 homopolymer (**30**) were physically mixed with the transesterification catalyst and dichlorobenzene using a mortar, but not heated. No interchange reaction should take place in the absence of the required activation energy and the polymers should remain homopolymers. After the solvent had been removed in the sample by precipitation, a ^{1}H NMR spectrum was obtained (Figure 7). The ^{1}H NMR spectrum shows the aromatic imide resonances of the NDI-based x = 5 homopolymer (**25**) and the non-binding HFDI x = 5 homopolymer (**30**), the NDI resonance remains upon addition of pyrene-d_{10} a singlet and shows no sequence related splitting. It was therefore concluded that the randomization with the transesterification proceeds as expected and the same random sequences are obtained as via direct synthesis. This result is also a further indication that the resonance splitting observed in intercalation sequencing shows shows indeed the random sequence of the copolymer.

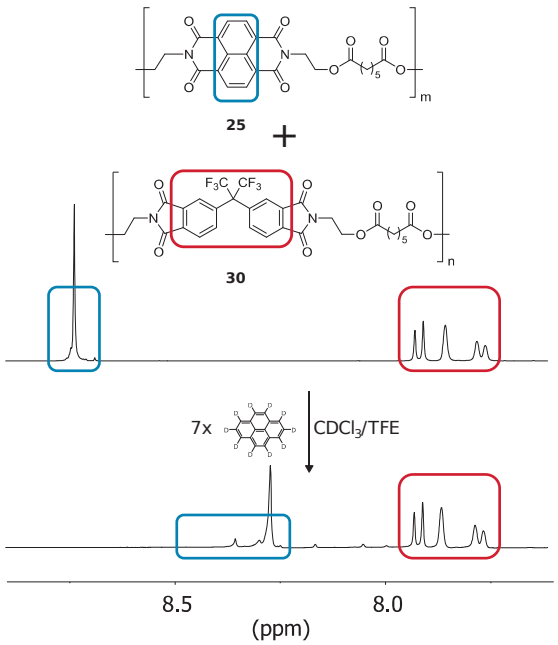

Figure 7: Control sample for the intercalation sequencing. The top and bottom ^{1}H NMR spectra are from a physical mixture of the NDI-based x = 5 homopolymer (**25**) and the HFDI x = 5 homopolymer (**30**) equally treated like the transesterified samples only without heating. No sequence-related splitting is observed upon the addition of pyrene-d_{10}.

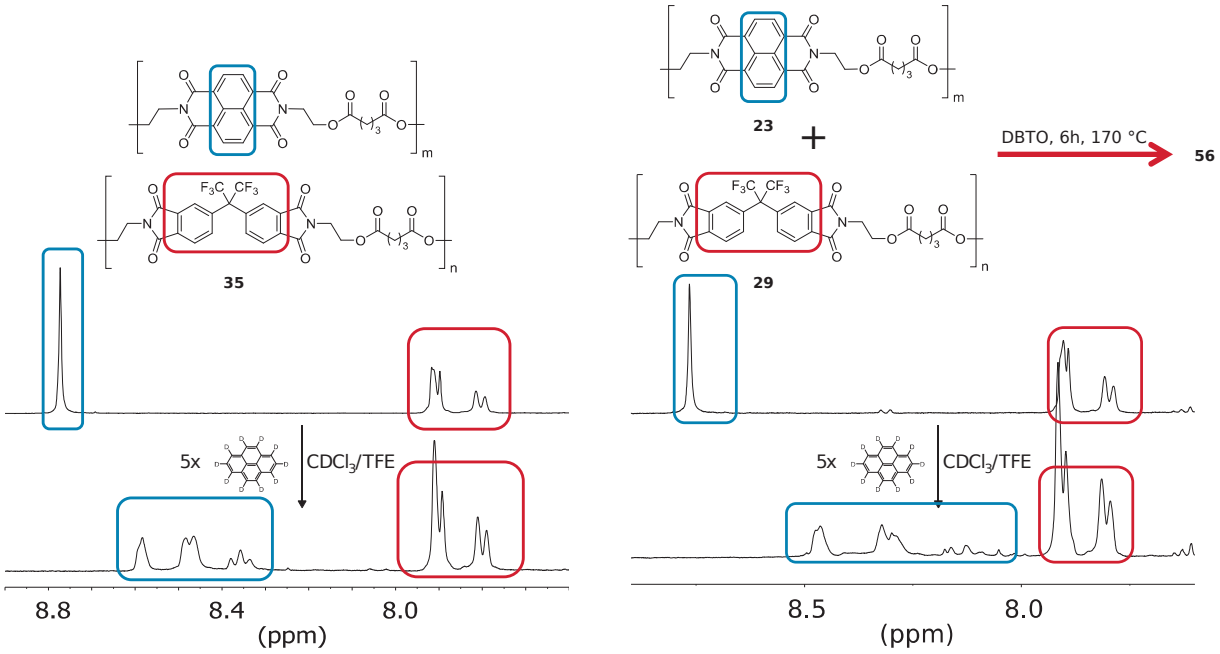

Figure 8: Comparison of the ^{1}H NMR spectra of the NDI / HFDI-based x = 3 copolymer via direct synthesis (**35**) and the NDI / HFDI x = 3 polymer mixture after transesterification (**56**) analysed by intercalation sequencing. Left: The aromatic imide resonance of the NDI / HFDI-based x = 3 copolymer (**35**) via direct synthesis splits upon the addition of pyrene-d_{10} into an apparent singlet, doublet and triplet. Right: The aromatic imide resonance of NDI / HFDI x = 3 polymer mixture after transesterification (**56**) equally splits upon the addition of pyrene-d_{10} into an apparent singlet, doublet and triplet.

The NDI / HFDI-based x = 3 copolymer (**35**) was selected as the second model system. Analogously to the above, a mixture of the NDI x = 3 homopolymer (**23**) and HFDI x = 3 homopolymer (**29**) was transesterified for 6 hours and the formed reaction mixture analysed after purification via intercalation sequencing. The splitting pattern of the directly synthesized NDI / HFDI x = 3 (**35**) polymer observed by intercalation sequencing consists of an apparent singlet, a doublet and a triplet (Figure 8). The NDI / HFDI x = 3 polymer mixture after transesterification (**56**) shows a rather similar spectrum, thereby indicating that the reaction mixture again consists of a mixture of fully random copolymers.

6.3.2. Stepwise transesterification

In Section 6.2.1 it was demonstrated successfully by intercalation sequencing that random copolymers can be produced via transesterification of NDI- and HFDI-comprising homopolymers and that the reaction can be observed via intercalation sequencing. In the following, the course of the reaction is to be investigated by observing the order in which resonances gain intensity. This was intended to confirm the assignment of sequences to the resonances by the models presented in Chapter 4. This is symbolized in Figure 4 by the first question mark.

For the stepwise transesterification, a larger amount of polymer (about 5 g) was mixed with the transesterification catalyst DBTO and the high-boiling solvents dichlorobenzene or 1-chloronaphthalene. Aliquots were taken at regular intervals and individually purified and analysed as described in Chapter 6.2.1.

At the beginning of the transesterification reaction, the only polymeric entities present are the NDI homopolymer and the HFDI homopolymer. Since the range of the ring current shielding is limited, the full NDI homopolymer itself cannot be investigated by intercalation sequencing but only the pentamer -IIIII- present in the NDI homopolymer; the NDI homopolymer itself obviously contains substantially more than five consecutive I-units. In the course of transesterification, the sequences I-I and H-H undergo entropically driven an exchanged forming I-H sequences (note: I = NDI; H = HFDI). An exchange of I-I sequences with other I-I sequences would not have any effect. The transesterification thus results in the unit -IIIII- decreasing in concentration, whereas I-H-containing sequences are generated and increase in concentration. Thus, in the ^{1}H NMR spectrum the -IIIII- resonance should proportionally decrease in intensity, whereas the 8 other resonances of the apparent triplet of triplets (e. g. Figure 6) should become visible in the spectrum and increase in intensity. The more reaction steps are required for the formation of a sequence, the later it should gain intensity in the ^{1}H NMR spectrum.

Thus, the sequences with a high H proportion (resonances at lower field) should tend to become visible later. As it can be seen in Figure 9, the ^{1}H NMR spectra of the intercalation sequenced reaction mixture do indeed show the predicted trends.

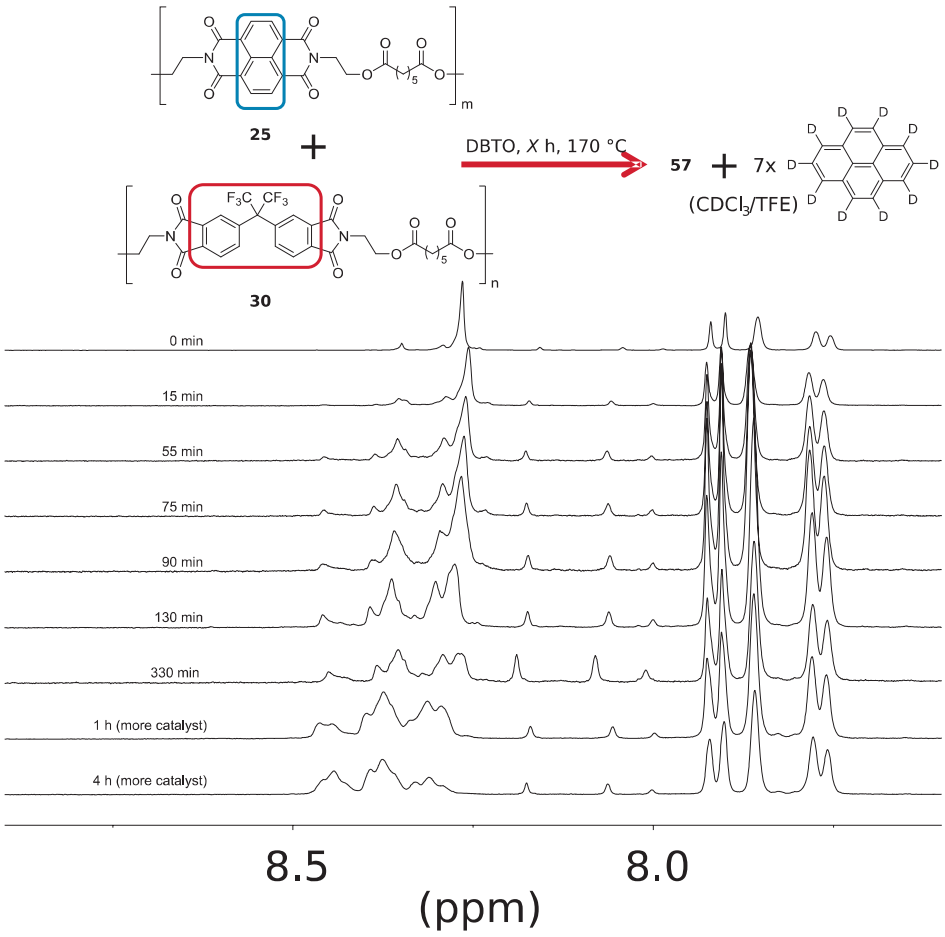

Figure 9: Stepwise transesterification of a mixture of the NDI x = 5 homopolymer (**25**) and the HFDI x = 5 homopolymer (**30**). The stacked ^{1}H NMR spectra are measured in the presence of a constant concentration of pyrene-d_{10}. In the scope of the transesterification reaction, the resonance related to the NDI homopolymer decreases in intensity (the resonance with highest upfield chemical shift) while all other resonances of the splitting pattern of the aromatic imide resonance increase in intensity. The HFDI-related resonances are unaffected.

The HFDI units are only indirectly detected by intercalation sequencing insofar as they are affecting the intercalator binding Is. The HFDI units themselves do not show in the presence intercalators any measurable complexation shift. Therefore, the HFDI units do not reveal any sequence information and are not considered in the sequence analysis.

Also the stepwise synthesis of the NDI / HFDI-based x = 3 copolymer by transesterification (**56**) was investigated (Figure 10). While the HFDI-based homopolymers showed an excellent solubility, the solubility of the NDI-based homopolymers was a limiting factor. The NDI-based x = 5 homopolymer (**25**) has a long spacer and, as it is relatively soluble, it could be re-

acted in 1,2-dichlorobenzene. The NDI-based x = 3 copolymer (**23**) has a comparably worse solubility, so that 1-chloronaphthalene had to be used as solvent, which has a higher boiling point and thereby allows a higher reaction temperature. As presented in Chapter 4 and in this chapter in Figure 8, the splitting pattern of the NDI / HFDI-based x = 3 copolymer by direct synthesis (**35**) consists of a singlet, an apparent doublet and an apparent triplet. It can be seen between 10 and 20 minutes that a second resonance is appearing in the region of the apparent triplet. At the same time, a resonance is appearing in the singlet region and the -IIIII- resonance is losing intensity. At the next step, after 30 minutes, the transesterification has already been fully achieved and the splitting pattern corresponds in intensity to the splitting pattern of the directly synthesized random copolymer. No further intermediate steps could be observed.

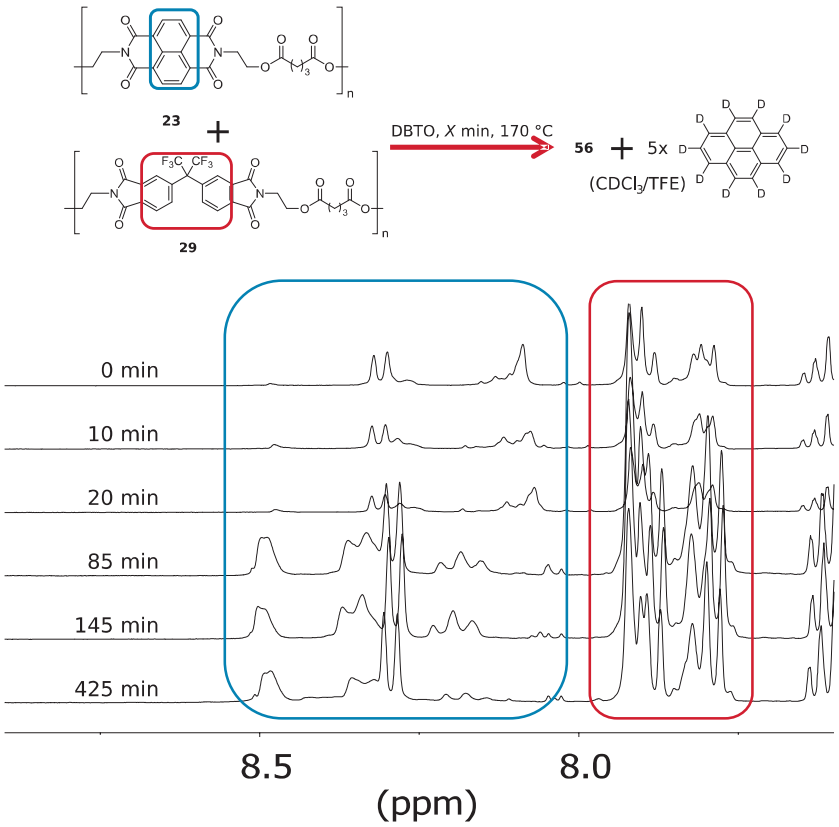

Figure 10: Stepwise transesterification of a mixture of the NDI-based x = 3 homopolymer (**23**) and the HFDI-based x = 3 homopolymer (**29**). The stacked ^{1}H NMR spectra were measured in the presence of a constant concentration of pyrene-d_{10}. In the scope of the transesterification reaction, the resonance related to the NDI homopolymer decreases in intensity (the resonance with highest upfield chemical shift) while all other resonances of the splitting pattern of the aromatic imide resonance increase in intensity. The first three ^{1}H NMR spectra from 0 to 20 minutes show a stepwise transesterification while from 85 minutes on, the splitting pattern is similar to the fully randomized polymer. The resonances at 8.29 ppm, 7.88 to 7.76 ppm and 7.59 to 7.39 ppm correspond to residual solvent (1-chloronaphthalene).

It was thereby shown that also in case of the NDI / HFDI-based $x = 3$ copolymer the transesterification can be followed incrementally in principle. Two resonances of the final splitting pattern could be clearly identified. However, in comparison to the NDI / HFDI-based $x = 5$ copolymer (**57**) the data quality is worse as fewer ^{1}H NMR spectra are available in the relevant time period. From spectrum four on (85 minutes), the transesterification is almost complete. In addition, the 1-chloronaphthalene was not completely removed from the samples, so that resonance overlap occurred. The removal of the 1-chloronaphthalene and the acquiring of more relevant spectra is in principle a resolvable problem as only more samples have to be purified via more precipitation steps.

6.4. Insertion reaction of a lactone

In the previous section it was shown that the directly synthesized NDI / HFDI-based copolymers described in Chapter 4 can also be obtained via stepwise transesterification of the homopolymers thereby allowing the creation of new sequences. In this section, copolymers similar to the binding / weakly binding copolymers of Chapter 5 are investigated. The intercalation sequencing of these polymers is based on the principle that the binding strength of NDI-based copolymers depends on the length of the aliphatic spacer. To create such a copolymer it was decided to insert an aliphatic macrocycle as an aliphatic chain extension into an NDI-based homopolymer with short aliphatic spacers. The insertion of the macrocycle at random positions should create a sequenceable binding / weakly binding copolymer. It is known from the literature that a concentration dependent equilibrium between polymers and macrocycles exists.[7] This has been used in the past for the synthesis of macrocyles by exposing polymers to exchange reactions (high temperature in the presence of a catalyst) under high dilution. However, the equilibrium has also been used for the entropically driven synthesis of polymers from macrocyles by exposing the macrocycles in bulk to a chain-exchanging catalyst.

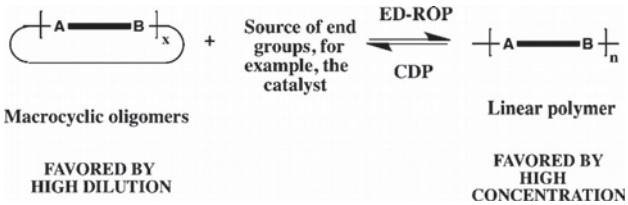

Figure 11: The equilibrium between macrocyclic oligomers and linear polymers is known from the literature. The equilibrium is driven by the concentration.[7]

However, in the experiments described in the literature, only one type of repeat unit or monomer was used, no binary sequence was thereby formed. In the present experiment, a macrocycle is supposed to be inserted into a homopolymer, forming a mixture of copolymers and (mainly cyclic) oligomers.

In the current experiment, cyclopentadecanolide was chosen as a macrocyclic as it is a fully aliphatic lactone and commercially available. The NDI-based $x = 3$ homopolymer was chosen as it was the NDI-based polymer showing in Chapter 5 the most information and still being soluble in 1-chloronaphthalene, unlike the NDI-based $x = 4$ or $x = 6$ homopolymers. As for transesterification of the two homopolymers, the macrocycle was mixed in the current experiment with the homopolymer, the transesterification catalyst DBTO and 1-chloronaphthalene. After heating to 150 °C, the mixture liquified and aliquots were taken at regular time intervals.

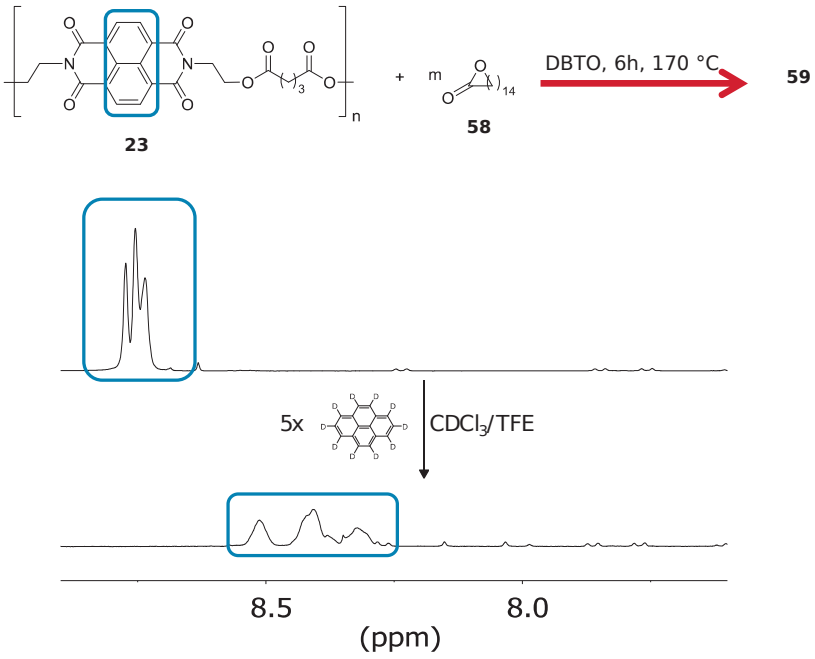

Figure 12: The aromatic imide resonance of a reaction mixture (**59**) of the NDI-based $x = 5$ homopolymer (**23**) and the lactone cyclopentadecanolide (**58**) splits upon the addition of pyrene-d_{10} into an apparent triplet.

6.4.1. Full transesterification

It is known that the NDI homopolymer in the presence of an intercalator shows only a singlet ^{1}H NMR resonance (Figure 7), since all sequences have the same complexation shift. On the contrary, the reaction product of the NDI-based $x = 3$ homopolymer and macrocycle shows three resonances with intercalator. These resonances can also be distinguished to a certain de-

gree without any intercalator. Furthermore, the two higher field resonances show a fine structure in the form of shoulders, which are, however, not sufficiently resolved to be investigated further. In any case, the formation of at least three resonances shows that a random copolymer has formed.

6.4.2. Stepwise transesterification

Subsequently, a stepwise transesterification was investigated, analogous to the previous reactions (Figure 13). It can be seen that the expected 1:2:1 ratio of the three resonances was already achieved at the time of the first measurement (45 minutes). After this first ^{1}H NMR spectrum, no further change in the splitting pattern was observed up to 675 minutes. The smoothing of the three resonances at 675 minutes has already been observed for the NDI / HFDI x = 5 copolymer (**37**) after 24 hours heating, it is presumably caused by decomposition of the polymer into oligomers by thermal degradation; thereby longer range sequence information is lost. Another hurdle is the presence of residual 1-chloronaphthalene, which partly obscures the ^{1}H NMR spectrum and changes the concentration of polymer or the ratio of polymer to pyrene, so that the complexation shift is not constant in every spectrum. However, neither of these is a fundamental problem but should be solvable by taking samples at shorter reaction times and by multiple purifications.

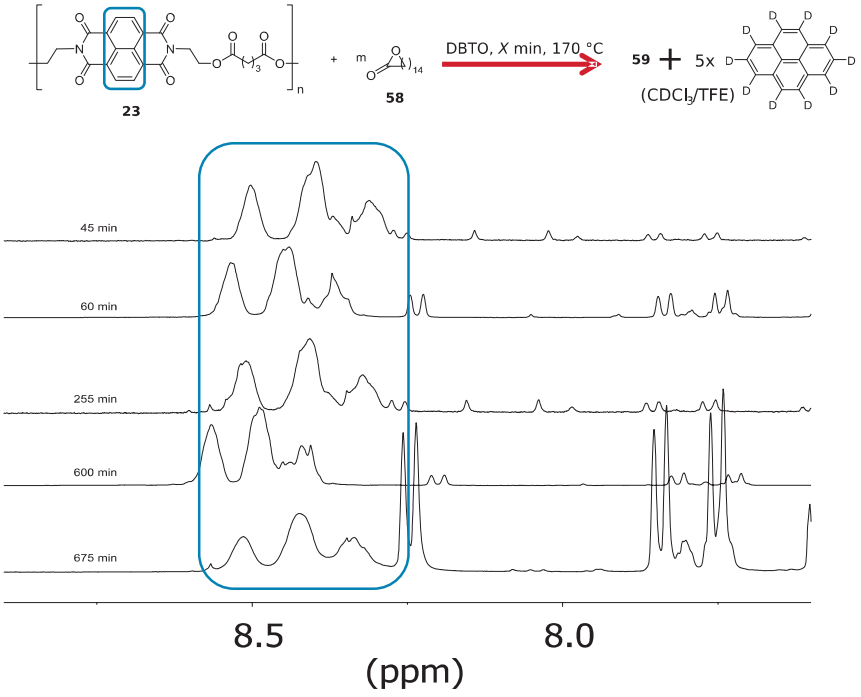

Figure 13: Stepwise transesterification of a mixture of the NDI-based x = 3 homopolymer (**23**) and the macrocyle cyclopentadecanolide (**58**). The stacked ^{1}H NMR spectra are measured in the presence of a constant concentration of pyrene-d_{10}. Already the first spectrum at 45 minutes shows the apparent triplet expected for the fully randomized polymer. No change occurs upon longer reaction times, only

the fine structure of the resonances is lost at 675 minutes. The resonances at 8.29 ppm and 7.88 to 7.76 ppm correspond to residual solvent (1-chloronaphthalene).

The formation of a copolymer from a homopolymer by the insertion of an lactone was observed. However, the current reaction proceeds much faster than the transesterification of NDI-based and HFDI-based homopolymers. Shorter reaction times would have to be applied for the observation of the transesterification process.

6.5. Conclusions

In this chapter the technique of intercalation sequencing was applied to random copolymers formed by a transesterification of homopolymers. It was observed that the same random copolymers could be produced by transesterification of homopolymers as by direct synthesis of random copolymers. A control experiment confirmed that the splitting pattern is indeed caused by sequences generated via transesterification: a physical mixing of homopolymers showed no splitting in the presence of pyrene. This is a further confirmation that the splitting patterns are caused by the polymer sequence. Furthermore, by taking samples stepwise, the increase of different sequences could be followed over time. This confirmed the intercalation theory from Chapter 4, as it predicts the probabilities of formation of the different sequences.

For the sequence-exchange reaction, a 1:1 molar ratio of homopolymers and 2 mol% DBTO were heated in 1,2-dichlorobenzene or 1-chloronaphthalene to 170 °C. Initially, the same sequence pattern as the directly synthesized NDI / HFDI-based copolymers (**35** and **37**) were obtained by heating the mixture of the NDI-based homopolymers (**23** and **25**) and the HFDI homopolymers (**29** and **30**) of different spacer length for 24 hours. This indicates in combination with a control experiment that transesterification of the homopolymers is possible and that the new sequences can be observed by intercalator sequencing. In later experiment, mixtures of the homopolymers were transesterified under the above conditions and samples were taken at regular intervals, thus a stepwise evolution of the sequences could be observed. This allowed the progressive formation of different sequences to be observed and compared with the theoretical predictions of the intercalation sequencing theory. A complete agreement was found.

This experiments allowed a novel application of the theory of intercalation sequencing and thus validated it. Furthermore, intercalation sequencing was successfully be applied to a problem of potential significance to industry.

6.6. References

1 A. M. de Ilarduya and S. Muñoz-Guerra, *Macromol. Chem. Phys.*, 2014, **215**, 2138–2160.

2 J.-F. Lutz, *Macromol. Rapid Commun.*, 2017, **38**, 1700582.

3 T. Maeda, H. Otsuka and A. Takahara, *Prog. Polym. Sci.*, 2009, **34**, 581–604.

4 S. C. Lee, K. H. Yoon, I. H. Park, H. C. Kim and T. W. Son, *Polymer*, 1997, **38**, 4831–4835.

5 G. M. Whitesides, *Adv. Mater.*, 2004, **16**, 1375–1377.

6 S. Collins, A. M. Kenwright, C. Pawson, S. K. Peace, R. W. Richards, W. A. MacDonald and P. Mills, *Macromolecules*, 2000, **33**, 2974–2980.

7 P. Hodge, *Chem. Rev.*, 2014, **114**, 2278–2312.

8 Y. Wang and A. S. Hay, *Macromolecules*, 1997, **30**, 182–193.

9 S. Salhi, M. Tessier, R. El Gharbi and A. Fradet, *Polymer*, 2014, **55**, 73–82.

10 P. Hodge, Z. Yang, A. Ben-Haida and C. S. McGrail, *J. Mater. Chem.*, 2000, **10**, 1533–1537.

11 M. Nelißen, H. Keul and H. Höcker, *Macromol. Chem. Phys.*, 1995, **196**, 1645–1661.

7 Conclusions and Future work

7.1. Conclusions

The main aim of this research project was to expand the field of intercalation sequencing of polymers by a better understanding of its fundamental principles. This has been successfully achieved by producing different model poly(ester imide)s and analysing them by intercalation sequencing.

Using diacyl chloride-based polyesterification, various NDI-based, PMDI-based, BPDI-based and HFDI-based potentially intercalation-sequenceable model polymers were prepared. The length of the aliphatic polymers backbone was varied systematically by using the corresponding diacyl chlorides. For the synthesis, a particular significance for mild polymerization conditions was found. The use of low reaction temperatures and short reaction times yielded polymers with an average inherent viscosity η_{inh} of 0.70 dL g^{-1}; this is considerably higher than the average inherent viscosity reported in the literature of η_{inh} of 0.50 dL g^{-1}.

To optimize the chain fold's binding strength, homologous series' of polymers were produced which differed only in the number of methylene groups in the aliphatic diacid residue, which ranged between 1 and 8. The complexation shifts in ^{1}H NMR spectroscopy of the aromatic imide protons of the various homo- and co-poly(ester imide)s were measured with different intercalators under otherwise identical conditions to obtain comparable values. A weak binding was found for polymers comprising long spacers (5 to 8 methylene groups), but a stronger binding for short spacers (1 to 4 methylene groups) with a resonance in binding strength for polymers comprising only 2 methylene groups. For six representative complexes, the binding strength was quantified by the determination of binding constants, whereby a maximum binding constant of K_a of 270 M^{-1} was found (NDI-based homopolymer $x = 2$ [**22**] with the guest perylene).

In intercalation sequencing of the different model co-poly(ester imide)s (based on NDI, PMDI, HFDI and BPDI) it was found that the resolution of the splitting pattern of the aromatic diimide resonance was the higher the greater the difference in complexation strength between the binding and the non-binding unit. This relationship was found for said dependency of binding strength on the spacer length (copolymers containing the strongest binding spacer, with 2 methylene groups showed the highest resolution) as well as for the known differences in binding between NDI and PMDI or HFDI and BPDI, respectively. Using this principle, it was possible to produce a large number of polymers that show numerous sequence-

assignable ^{1}H NMR resonances on complexation with pyrene ("splitting-resonances"). In the literature, usually only three splitting-resonances were found, though in one case[1] nine. In the current study, 12 further sequenceable polymers are described in which up to 15 splitting-resonances could be distinguished.

Based on the dependency of the binding strength on the spacer length, intercalation sequenceable NDI-based co-poly(ester imide)s were produced successfully, in which the difference in binding strength, which is required for sequencing, was produced by two polymer backbones of different length ("all-aliphatic NDI-based copolymers") by using spacers of different lengths in the polymer backbone. This made it possible to produce polymers in which HFDI as a non-binding unit could be dispensed with and weakly binding NDI was used instead. However, this is only successful if the difference in spacer length and thus in binding energy is large enough. The all-aliphatic units have the advantage of not possessing any resonances in the aromatic region, and the advantage of improved solubility. This principle could also be transferred successfully to a new poly(ether imide). This made it possible to produce polymers in which HFDI as a non-binding unit could be avoided and weakly binding NDI was used instead.

Finally, intercalation sequencing was applied to sequences on co-poly(esterimide)s produced by the reaction of a binding homopolymer with a non-binding homopolymer. On the one hand, it could be confirmed that the splitting patterns in ^{1}H NMR spectra are actually caused by sequence-related splitting. On the other hand, it was observed that the same random copolymers could be produced by transesterification of homopolymers as by direct synthesis of random copolymers, as identical splitting patterns were produced. A control test confirmed that the splitting pattern is indeed caused by sequences generated via transesterification. In later experiments, samples were taken at regular intervals from the transesterifying polymer mixture, thus a stepwise transesterification could be observed. This allowed to determine a succession of the formation of the different sequences and to compare it with the theoretical predictions of the intercalation sequencing theory. Complete agreement was found.

7.2. Future Work

Whilst principles for the design of intercalation sequenceable polymers have been developed within this study, further investigations could extend the application of intercalator sequencing to industrially relevant polymers. This could be used for the production of polymers with tailored sequence and thereby tailored properties. As described in Chapter 1.4.2, it is known that changing the sequence of a polymer can modify its macroscopic properties, such as forming microspheres,[2] creating polymer foams of variable structure,[3] controlling and maximising tensile strength,[4] or forming of a compatibiliser between matrix and particles to ensure the stress transfer in the sample under mechanical load.[5] Influencing the sequence of a polymer, at least to some extent, can thereby provide materials with desirable properties.

Step-growth polymerizations can be efficiently used for the synthesis of sequence-controlled polymers, in particular of controlled randomness (“blockiness) and periodic structures[6]. With higher experimental effort, sequence-defined copolymers can also be produced via multistep-growth mechanisms (using protective groups or solid support).[7]

However, the degree of sequence control cannot simply be derived from the synthesis method used, as it can be distorted by interfering factors. For example, due to different solubility of co-monomers, phase separation may occur and the polymerization may proceed in part as homopolymerization, thereby lowering the degree of randomness.[8] By applying intercalation sequencing, however, the degree of randomness (or the "blockiness") can be directly measured and can be made comparable. Thus, it might be possible to correlate the degree of randomness determined by intercalation sequencing with polymer properties.

In order to make intercalation sequencing applicable to industrial applications, polymers which could be potentially analysed by intercalation sequencing could be identified in the future work. Fundamentally, intercalation sequencing requires a intercalator binding and a intercalator non-binding unit. As described in the conclusion part, sequence information was successfully obtained from copolymers comprising the binding PMDI or NDI unit. PMDI is already a known structural unit in commercially used polyimides.[9] To achieve sequenceability, PMDI would then have to be combined with a non-binding unit. Non-binding units used successfully in this study are another imide (Chapter 4), a fluorinated imide (Chapter 4) and aliphatic units (Chapter 5). Asymmetric imides,[10] fluorinated imides[11] and aliphatic[12] co-monomers are already known from the literature as “non-binding units” for the suppression of CT-induced coloration, as described in Chapter 5.2. It is therefore reasonable to use other

units that have been used to suppress CT interactions as potentially non-binding units. Also the diphenyl sulfone unit (Figure 1 a), which was used successfully for sequencing,[1] has been described previously for the suppression of CT intercations.[13] Three more potentially non-binding units described to suppress CT interactions are listed in Figure 1 b – 1 d. Polyimides based on such non-binding units with a binding unit (e.g. PMDI) could potentially be sequenced. This result in a large number of potentially intercalation sequenceable polymers.

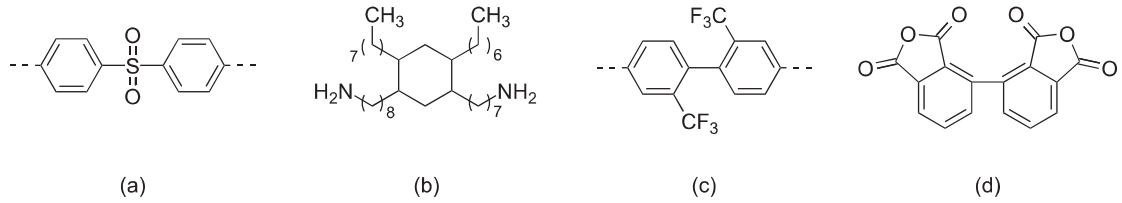

Figure 1: The diphenyl sulfone unit (a) was described for the suppression of CT intercations[13] and was used successfully in intercalation sequencing[1]. Compounds b (a dimer fatty diamine),[12] c (2,2'-bis (trifluoromethyl)benzidine)[13] and d (3,3'-BPDA)[10] were described for the suppression of CT interactions in polyimides and could be used in the future as non-binding units.

Intercalation sequencing could thereby ultimately be used for improved polymers of industrial significance, as it might help to control the copolymers' sequence, which is a fundamental parameter and affects many properties.

It was found In the present thesis that pyrene-based intercalation sequencing of a copolymer based on the weakly binding PMDI-based unit and the mostly non-binding BPDI-based unit was not feasible as the difference in binding energy was not sufficiently large (Chapter 4, Figure 33). It was found in the literature, however, that a PMDI-based polymer could be sequenced using tweezers instead of pyrene, in which there was only a minor difference in binding between the binding and the non-binding unit (binding strength only modified by a neighbouring methyl group, see Chapter 5, Figure 1).[14] The two polymers and the used intercalators are compared in Figure 2. The use of molecular tweezers could therefore be a strategy to sequence polymers showing a small difference in binding between the binding and the non-binding unit. By using tweezers instead of pyrene, the number of sequenceable polymers could be considerably extended, this could be tested on suitable PMDI-based polymers.

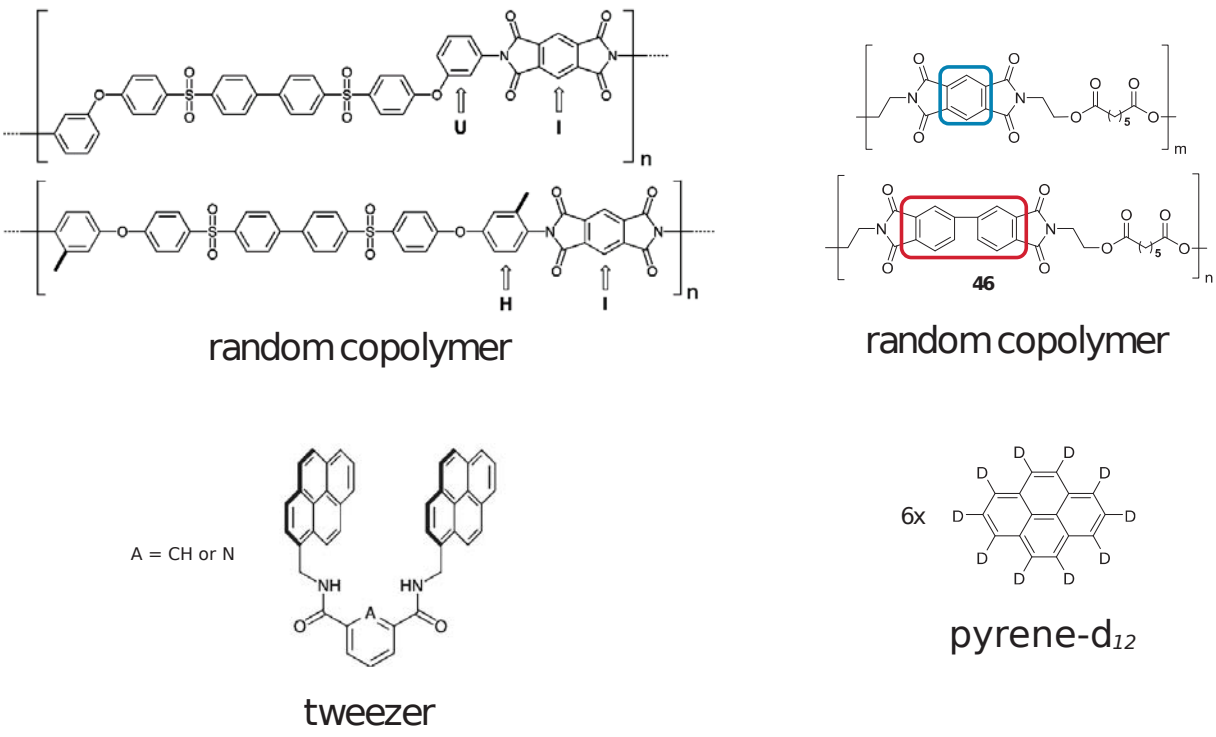

Figure 2: In the poly(sulfone imide), the binding and non-binding units differ only by a neighbouring methyl group (left), the polymer can be sequenced using a tweezer. In the polymer of the present study (**46**, right), the binding and the non-binding unit differ by an additional benzene ring; it cannot be sequenced with pyrene-d_{10}.

As described in the Conclusion, a novel naphthalene diimide-based structural unit (Figure 3) with particularly high binding strength for electron-rich aromatic molecules (perylene, pyrene, anthracene) was discovered in Chapter 3 which was used successfully for intercalation sequencing and might be used for applications. Unfortunately, the solubility of the corresponding homopolymer and thus of the chain fold itself is low, which may limit the further use of the structural unit.

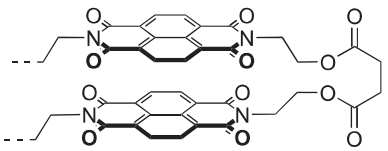

Figure 3: The naphthalene diimide-based structural unit, being present for example in the homopoly(ester imide) **22**.

The solubility of the chain-fold could be modified using solubilizing pendant groups. In principle, a modification is possible at the diimide core itself or at the surrounding groups.[15] In case of a substitution at the diimide core itself, however, it would be likely, however, that the

binding constant of the structural unit would be reduced. Accordingly, the aliphatic spacer might be modified instead, for example by introducing methoxy groups. A possible synthesis is from 2,3-dihydroxybutanedioic acid (Tartaric acid) is proposed in Figure 4.

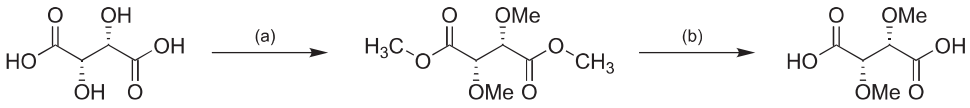

Figure 4: A possible synthesis for 2,3-dimethoxybutanedioic acid. (a): Dimethyl sulfate, acetone. (b): KOH, methanol/water.

In this way, a soluble but strongly binding structural unit could possibly be created that can also improve other systems or applications.

In the present thesis several different splitting patterns were observed. So far, all resonances of the triplet of triplets pattern (present in the NDI / HFDI-based x = 5 polymer, **37** and the NDI / BPDI-based x = 5 copolymer, **44**) and of the triplet pattern (present in the PMDI / HFDI-based x = 5 copolymer, **45**) could be assigned to the sequences present in the polymer by means of a mathematical model. Such a mathematical model would also be needed for the singlet / doublet / triplet pattern (which occurs in the NDI / HFDI-based x = 3 polymer, **35**) and for the complex splitting pattern of the NDI / HFDI-based x = 2 polymer (**34**).

The analysis of splitting patterns which were not subject to ^{1}H-^{1}H decoupling was complicated as sequence-related splitting and *J*-coupling were observed simultaneously. Sequence-related splitting and *J*-coupling could be distinguished by *J*-resolved NMR spectroscopy as demonstrated successfully in Chapters 5.4 and 5.5. To simplify a spectrum showing both *J*-coupling and sequence-related splitting, a PSYCHE pure shift ^{1}H NMR spectrum could be measured. In the case of NDI / HFDI-based x = 5 polymer (**37**) it was shown that the technique eliminates *J*-coupling but leaves sequence-related splitting unchanged (Figure 5). In this way, the analysis of the complex splitting pattern could be simplified considerably, although very long accumulation times would be necessary to overcome the reduction in signal-to-noise ratio.

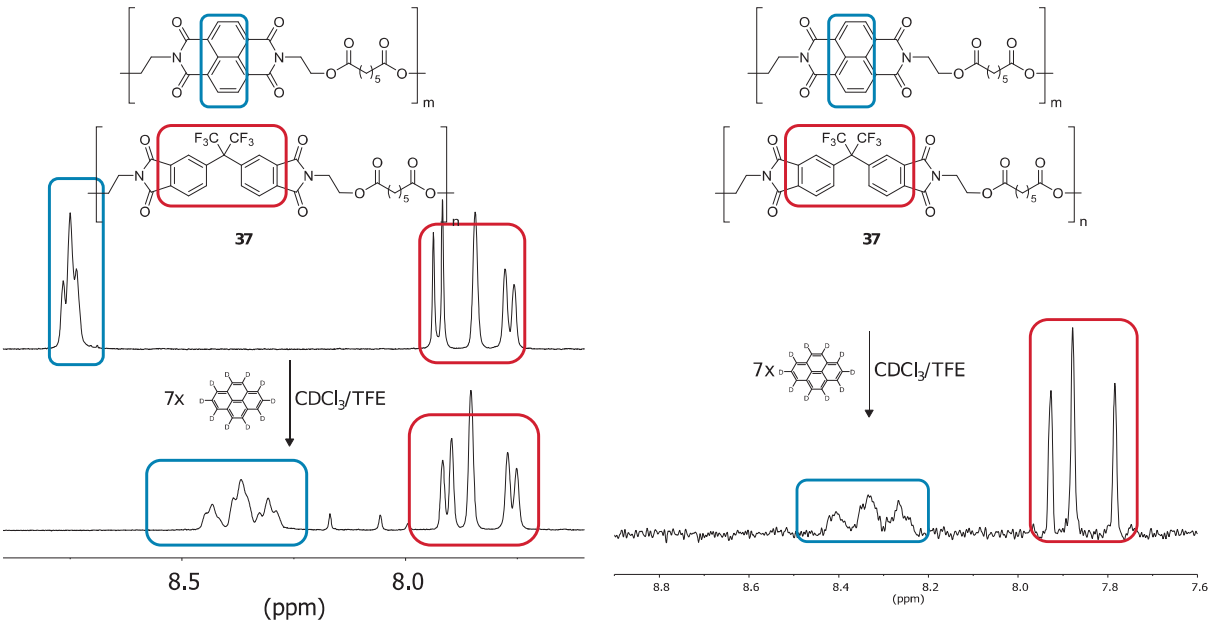

Figure 5: Conventional ^{1}H NMR spectrum of the NDI HFDI-based x = 5 copolymer (**37**). After addition of pyrene-d_{10}, the resonance splits into a triplet of triplets. The HFDI resonances remain unchanged doublets. Right: PSYCHE ^{1}H NMR spectrum of the same polymer again after addition of pyrene-d_{10}. While the J-coupled HFDI resonances collapse into singlets, the triplet of triplets pattern remains unchanged, proving that the splitting pattern is not based on J-coupling.

As already described in the summary, similar splitting patterns have been found repeatedly for different polymers. For example, the singlet / doublet / triplet structure, characteristic of tight, chain-folding and strong binding of pyrene to pairs of NDI residues, could be found for the NDI / HFDI-based poly(ester imide)s (Chapter 4), for the all-aliphatic NDI-based poly(ester imide)s (Chapter 5), for the poly(ether imide)s (Chapter 5) and for a poly(ether sulfone imide) from the literature[1]. Thus, similar splitting patterns were found despite different chemical structures and repeat units of different lengths. It is thereby assumed that the recurring similarities are based on a similar conformation of the different polymer chains in solution. By further analysing the given splitting patterns with mathematical models, fundamental laws about the intercalation sequencing of arbitrary copolymers might possibly be discovered.

One potential technical application of the current system is similar to the already realized applications of artificial DNA: Silica-encapsulated DNA was used as artificial data storage in molecular barcoding to identify counterfeits of high-priced olive oil[16], to identify the supply chain of milk and dairyproducts[17], or in biological research to mark animals in food webs[18]. Transferred to the current system the information storage in artificial polymers could help to mark plastics in commodity flows. Counterfeits could be detected more easily if a machines

plastic components contain information at the molecular level. Components or particles found after an aircraft crash could be unambiguously assigned when the identity of the component is coded in the material itself.

The technical use of DNA also has some inherent limitations which could be overcome with the current polyimide-based system. DNA is chemically and mechanically fragile (unlike e. g. aromatic polyimides[19]), the molecular machinery very complex (thus hard to modify) and it is highly charged which makes the use of other solvents than water or the use in nano electronic devices unlikely.[20] Artificial polymers could also be more easily modulated at the molecular level for a specific application and produced at lower costs at a high scale.[21]

Another potential application is the long-term storage of information with low expectation of extensive access, e. g. government or historical records[22,23] as molecular information storage has the advantage of a high information density.[20] The advantage of polymer based data storage would be that no maintenance would be required, unlike for magnetic tapes (currently used) which have to be rewritten at fixed intervals.

The use of a molecular barcode requires polymers or oligomers with a defined sequence. In principle, a certain degree of sequence control can be achieved by a specific degree of exchange reaction between homopolymers as demonstrated in Chapter 6 of the current work. However, it is also known that step-growth polymers with repeating sequences can be produced with modest synthetic effort. Also the introduction the information into the polymer chain is to use a template in which the information is already predefined.[7] It is also possible to introduce information into the polymer chain by using a template in which the information is already given.[24]

7.3. References

1 J. S. Shaw, R. Vaiyapuri, M. P. Parker, C. A. Murray, K. J. C. Lim, C. Pan, M. Knappert, C. J. Cardin, B. W. Greenland, R. Grau-Crespo and H. M. Colquhoun, *Chem. Sci.*, 2018, **9**, 4052–4061.

2 H. Yoon, Y. Feng, Y. Qiu and C. C. Han, *J. Polym. Sci. B*, 1994, **32**, 1485–1492.

3 P. Gong and M. Ohshima, *Polym. Eng. Sci.*, 2015, **55**, 375–385.

4 C. Wu, C. D. Han, Y. Suzuki and M. Mizuno, *Macromolecules*, 2006, **39**, 3865–3877.

5 Y. Guo, J. He, X. Zhang, S. Sun and H. Zhang, *J. Macromol. Sci. Part B*, 2015, **54**, 823–835.

6 J.-F. Lutz, J.-M. Lehn, E. W. Meijer and K. Matyjaszewski, *Nat. Rev. Mater.*, 2016, **1**, 16024.

7 J.-F. Lutz, *Macromol. Rapid Commun.*, 2017, **38**, 1700582.

8 Q. Guan, B. Norder, L. Chu, N. A. M. Besseling, S. J. Picken and T. J. Dingemans, *Macromolecules*, 2016, **49**, 8549–8562.

9 R. G. Bryant, in *Kirk-Othmer Encyclopedia of Chemical Technology*, John Wiley & Sons, Inc., Hoboken, NJ, USA, 2006.

10 M. Ding, *Prog. Polym. Sci.*, 2007, **32**, 623–668.

11 M. Hasegawa, Y. Watanabe, S. Tsukuda and J. Ishii, *Polym. Int.*, 2016, **65**, 1063–1073.

12 A. Susa, J. Bijleveld, M. Hernandez Santana and S. J. Garcia, *ACS Sustain. Chem. Eng.*, 2018, **6**, 668–678.

13 M. Hasegawa, *Polymers*, 2017, **9**, 520.

14 H. M. Colquhoun, Z. Zhu, C. J. Cardin, Y. Gan and M. G. B. Drew, *J. Am. Chem. Soc.*, 2007, **129**, 16163–16174.

15 S. V. Bhosale, C. H. Jani and S. J. Langford, *ChemInform*, 2008, **39**, 331–342.

16 M. Puddu, D. Paunescu, W. J. Stark and R. N. Grass, *ACS Nano*, 2014, **8**, 2677–2685.

17 M. S. Bloch, D. Paunescu, P. R. Stoessel, C. A. Mora, W. J. Stark and R. N. Grass, *J. Agric. Food Chem.*, 2014, **62**, 10615–10620.

18 C. A. Mora, D. Paunescu, R. N. Grass and W. J. Stark, *Mol. Ecol. Resour.*, 2015, **15**, 231–241.

19 H. M. Colquhoun and Z. Zhu, *Angew. Chem. Int. Ed.*, 2004, **43**, 5040–5045.

20 H. M. Colquhoun and J.-F. Lutz, *Nat. Chem.*, 2014, **6**, 455–456.

21 S. Varghese, J. A. A. W. Elemans, A. E. Rowan and R. J. M. Nolte, *Chem. Sci.*, 2015, **6**, 6050–6058.

22 N. Goldman, P. Bertone, S. Chen, C. Dessimoz, E. M. LeProust, B. Sipos and E. Birney, *Nature*, 2013, **494**, 77–80.

23 R. N. Grass, R. Heckel, M. Puddu, D. Paunescu and W. J. Stark, *Angew. Chem. Int. Ed.*, 2015, **54**, 2552–2555.

24 J.-F. Lutz, M. Ouchi, D. R. Liu and M. Sawamoto, *Science*, 2013, **341**, 1238149–1238149.

8 Experimental

8.1. Experimental methods

8.1.1. Infrared spectroscopy

IR spectra were recorded on a Perkin-Elmer Spectrum 100 FT-IR spectrometer with a Universal Attenuated Total Reflectance accessory. Monomer samples were analysed as powders whereas polymers were analysed in compressed pellet form.

8.1.2. Differential scanning calorimetry

Differential scanning calorimetry (DSC) was carried out using a Mettler Toledo DSC23e instrument. Weighed samples of around 5 mg of monomer or 10 mg of polymer were heated twice from 30 °C to 325 °C and back at a scan rate of 10 °C min^{-1}. A nitrogen flow rate of 50 mL min^{-1} and aluminium pans were used.

8.1.3. Gel permeation chromatography

Gel permeation chromatography (GPC) was conducted using an Agilent Technologies 1260 Infinity system and the data were processed using Agilent GPC/SEC software; polystyrene was used as the calibrant. Samples for GPC analysis were dissolved in analytical grade THF (2 mg mL^{-1}) with butylated hydroxytoluene stabiliser, and run using the same solvent as the mobile phase, eluting through two Agilent PLgel 5 μm MIXED-D 300 × 7.5 mm columns in series.

8.1.4. Solution inherent viscosity

Inherent viscosity (η_{inh}) was determined for 0.1 wt% polymer solutions in chloroform (and a co-solvent in some cases) with a Schott-Geräte CT-52 auto-viscometer, using glass capillary No. 53103 in a water bath at 25 °C. The viscosity was calculated from the following equation:

$$\eta_h = \left(\frac{\ln\left[\frac{t_2}{t_1}\right]}{c} \right)$$

where η_{inh} is the inherent viscosity (dL·g^{-1}), t_1 and t_2 are the flow times of pure solvent and polymer solution respectively and c is the concentration of the polymer solution (g·dL^{-1}). The inherent viscosity was calculated as average of 5 measurements of the same solution.

8.1.5. NMR spectroscopy

^{1}H, ^{19}F and ^{13}C NMR spectra were obtained on a Bruker Nanobay 400 MHz spectrometer and referenced to residual solvent resonances or tetramethylsilane. Samples were dissolved in various deuterated solvents at room temperature. All values representing chemical shifts.

PSYCHE (^{1}H-^{1}H-decoupled) NMR spectra were obtained on a B500 Bruker Avance II+ 500 MHz spectrometer at the NMR department of the University of Manchester.

8.1.6. Computational methods

Computational simulations of pyrene-polymer intercalation were carried out by Dr Ricardo Grau-Crespo and Scott Midgley (University of Reading), as described below:

The pyrene intercalation energies were obtained using the self-consistent charge density functional tight-binding (SCC-DFTB) approach, as implemented within the DFTB+ code [1]. Parameters for all atoms and pairs including elements C, H, N, O were taken from the "mio" Slater-Koster library [2]. Dispersion corrections based on a Lennard-Jones potential were applied in all simulations [3]. The polymers were represented by 7 linked monomers and the intercalation of pyrene was evaluated at the central chain-fold. Intercalation energies (E_i) were then derived using the equation:

$$E_i = E_{complex} - \left(E_{pyrene} + E_{polymer}\right)$$

where $E_{complex}$, E_{pyrene} and $E_{polymer}$ are the minimised energies of the polymer/pyrene complex, the single pyrene molecule and non-intercalated polymer, respectively.

8.2. Monomer synthesis

N,N'-Bis-(2-hydroxyethyl)-biphthalimide

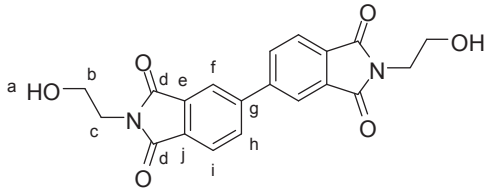

N,N'-Bis(2-hydroxyethyl)-biphthalimide was received from Dupont-Teijin Films. The white powder was recrystallized from DMF/water (8.01 g in 140 mL/50 mL) affording the pure product (6.33 g, 79% overall yield).

^{1}H NMR (400 MHz, DMSO-d_6) δ_H 8.34 – 8.16 (m, 4H$_{f/i}$), 8.02 – 7.90 (m, 2H$_h$), 4.86 (t, J = 6.0 Hz, 2H$_a$), 3.67 (t, J = 5.6 Hz, 4H$_c$), 3.63 – 3.54 (m, 4H$_b$). ^{13}C NMR (101 MHz, DMSO-d_6) δ_C 167.5 (C$_d$), 144.1 (C$_q$), 133.2 (C$_{f/i}$), 132.8 (C$_q$), 131.5 (C$_q$), 123.6 (C$_h$), 121.74 (C$_{f/i}$), 57.9 (C$_b$), 40.5 (C$_c$).

FTIR ν_{max} ATR (cm^{-1}): 1699 (imide -CO-N-CO-), 1377 (imide C-N stretch), 1066 (imide ring deformation), 739 (imide ring deformation).

Melting point (DSC): = 285 °C

ESI MS m/z = 381.1088 [M + H$^+$], calculated 381.1081; 403.0903 [M + Na$^+$], calculated 403.0901.

N,N'-Bis-(2-hydroxyethyl)-naphthalene tetracarboxylic diimide

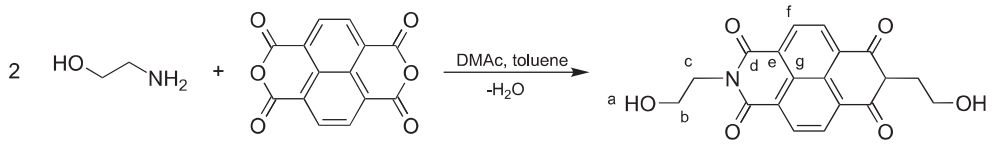

Naphthalene tetracarboxylic dianhydride (50.61 g, 188.7 mmol) was added to a mixture of *N,N*-dimethylacetamide (250 mL), 2-aminoethanol (25.03 g, 409.8 mmol) and toluene (30 mL). The solution was heated under reflux for 16 hours. After cooling to room temperature, the precipitated crystals were filtered and washed with water, acetone and methanol 3 times each. The crystals were dried in the oven at 100 °C for 24 hours to afford the crude product. The crude product was recrystallized in several batches: 5.97 g of the crude product were re-crystallised from *N,N*-dimethylformamide (145 mL), *N,N*-dimethylacetamide (75 mL) and H_2O (5 mL). The crystals were stored at 5 °C over night, filtered and washed with water and ethanol 3-4 times. Drying in the oven at 100 °C for up to 24 hours afforded the pure product (58.8 g, 88% overall yield).

^{1}H NMR (400 MHz, DMSO-d_6) δ_H (ppm) = 8.59 (s, 4H, C-H, f), 4.86 (t, J = 6.1 Hz, 2H, a), 4.16 (t, J = 6.4 Hz, 4H$_c$), 3.66 (q, J = 6.3 Hz, 4H$_b$). ^{13}C NMR (100 MHz, DMSO-d_6) δ_C (ppm) = 162.3 (d), 130.2 (f), 125.9 (e/g), 125.6 (e/g), 57.6 (b), 42.2 (c).

Melting point (DSC): > 290 °C (no melting observed up to the stated temperature)

FTIR ν_{max} ATR (cm^{-1}): 3516 (O-H stretch), 3068.77 (aromatic C-H), 1643 (imide -CO-N-CO), 1362 (imide C-N stretch), 1177 (imide ring deformation), 764 (imide ring deformation).

ESI MS m/z = 377.0744 [M + Na], calculated 377.0749.

8.2.1. *N,N'*-Bis-(2-hydroxyethyl)-pyromellitimide

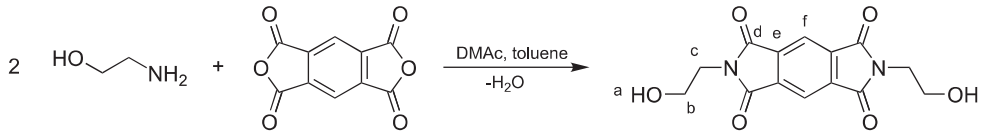

2-Aminoethanol (4.0114 g, 65.7 mmol) was added to a mixture of *N,N*-dimethylacetamide (15 mL), toluene (35 mL) and pyromellitic dianhydride (7.1066 g, 32.6 mmol). The solution was heated under reflux for 16 hours, and the water formed in the reaction was removed by azeotropic distillation using a Dean-Stark apparatus. Afterwards, the system was cooled to room temperature and the product was precipitated in deionised water, filtered off, and washed three times with water and methanol and dried in an oven at 100 °C for 24 hours to afford a white product (6.730 g, 68%). The crude product was recrystallised from a mixture of *N,N*-dimethylformamide (22.5 mL) and water (22.5 mL). After cooling overnight, the product was filtered off and washed three times each with water and ethanol. It was finally dried in an oven at 100 °C for 24 hours to afford a pure, crystalline product (4.953 g, 50% overall yield).

^{1}H NMR (400 MHz, DMSO-d_6) δ_H 8.21 (s, 2H, H_f), 4.89 (t, J = 6.1 Hz, 2H_a), 3.71 (t, J = 5.7 Hz, 4H_c), 3.63 (q, J = 5.7 Hz, 4H_b). ^{13}C NMR (100 MHz, DMSO-d_6) δ_C (ppm) = 166.4 (C_d), 137.0 (C_e), 117.0 (C_f), 57.8 (C_b), 40.9 (C_c).

Melting point (DSC): = 282 °C

FTIR ν_{max} ATR (cm^{-1}): 3312 (O-H stretch), 3030 (aromatic νC-H), 1696 (imide -CO-N-CO-), 1353 (imide C-N stretch), 1130 (imide ring deformation), 729 (imide ring deformation).

ESI MS m/z = 305.0767 [M + H$^+$], calculated 305.0768; 327.0587 [M + Na$^+$], calculated 327.0588.

8.2.2. *N,N'*-Bis-(2-hydroxyethyl)-hexafluoroisopropylidene biphthalimide

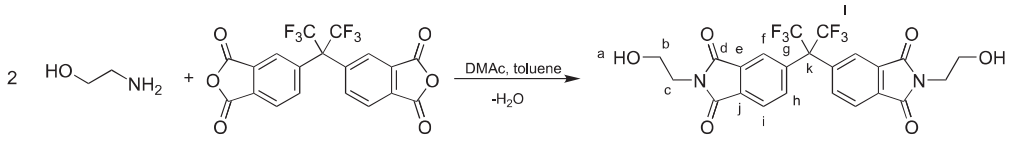

4,4'-(Hexafluoroisopropylidene) diphthalic dianhydride (25.32 g, 57.0 mmol) was added to a mixture of *N,N*-dimethylacetamide (50 mL), 2-aminoethanol (7.38 g, 120.8 mmol) and toluene (30 mL). The solution was heated under reflux for 17 hours with Dean-Stark removal of

water. After being cooled to room temperature, the solution was precipitated into 350 mL water, filtered and dried for 24 hours at 100 °C, affording the crude product (27.51 g, 91%). The crude product was recrystallised from *n*-butanol (53 mL) and the solution was stored at 5 °C for several weeks until crystals had formed. The product was filtered off, washed with water and ethanol 3-4 times and dried in the oven at 100 °C for 24 hours to afford the pure product (25.69 g, 85% overall yield).

^{1}H NMR (400 MHz, DMSO-d_6) δ_H 8.07 (d, J = 8.0 Hz, 2H$_i$), 7.89 (d, J = 8.1 Hz, 2H$_h$), 7.65 (s, 2H$_f$), 4.83 (t, J = 6.1 Hz, 2H$_a$), 3.66 (t, J = 5.5 Hz, 4H$_c$), 3.59 (m, 4H$_b$). ^{13}C NMR (101 MHz, DMSO-d_6) δ_C 167.0 (C$_d$), 166.86 (C$_d$), 137.0 (C$_{e/j}$), 135.5 (C$_h$), 133.1 (C$_g$), 132.6 (C$_{e/j}$), 123.8 (C$_i$), 123.1 (C$_f$), 57.8 (C$_b$), 40.7 (C$_c$). ^{19}F NMR (400 MHz, DMSO-d_6) δ_F -63.5 (CF_3).

FTIR ν_{max} ATR (cm^{-1}): 3513 (O-H stretch), 1701 (imide -CO-N-CO-), 1386 (imide C-N stretch), 1191 (vs, C–F), 1130.95 (imide ring deformation), 742 (imide ring deformation).

M.P. 212 °C (DSC). ESI MS m/z = 531.0968 [M + H$^+$], calculated 531.0985; 553.0782 [M + Na$^+$], calculated 553.0805.

8.2.3. Heptanedioyl dichloride

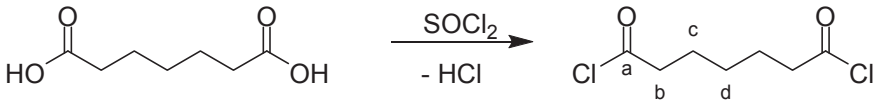

Heptanedioic acid (65.52 g, 409.07 mmol) was added into thionyl chloride (400 mL, 5507 mmol) and the mixture was refluxed for 4 hours. The excess of thionyl chloride was removed under reduced pressure and the residual brown oil was purified by distillation at reduced pressure (2.0 mbar) affording heptanedioyl dichloride as a colourless liquid (57.23 g, 71% yield).

^{1}H NMR (400 MHz, Chloroform-*d*) δ_H (ppm) = 2.91 (t, *J* = 7.2 Hz, 4H, H$_b$), 1.73 (m, 4H, H$_c$), 1.49 – 1.36 (m, 2H, H$_d$). ^{13}C NMR (100 MHz, Chloroform-*d*) δ_C (ppm) = 173.6 (C$_a$), 46.7 (C$_b$), 27.2 (C$_c$), 24.6 (C$_d$).

8.3. NDI-based homo-poly(ester imide)s

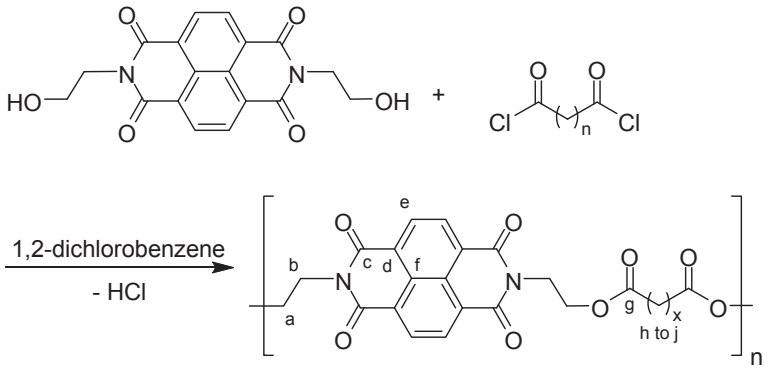

1,2-Dichlorobenzene (4.5 mL, distilled from CaH_2), *N,N′*-bis-(2-hydroxyethyl)-naphthalene tetracarboxylic diimide (dried at 120 °C for 24 hours) and an acid chloride (*n* = 1 to 8) were mixed at room temperature. The mixture was heated to 170 °C for 24 hours under N_2 atmosphere. After cooling to room temperature, the solidified product mixture was dissolved in 30 mL dichloromethane/hexafluoroisopropanol (1:1, v/v) and precipitated dropwise into an excess of methanol (~ 400 mL). The precipitate was filtered and dried at 80 °C for up to 24 hours. The reprecipitation was repeated three times to afford the pure polymer.

Propanedioyl-based homopolymer

Monomers used: *N,N′*-bis-(2-hydroxyethyl)-naphthalene tetracarboxylic diimide (0.702 g, 1.98 mmol), propanedioyl chloride (0.282 g, 2.00 mmol). Yield: (0.32 g, 38%).

^{1}H NMR (400 MHz, Chloroform-*d*/TFA 9:1, *v:v*) δ 8.81 (s, 4H), 4.65 – 4.34 (m, 8H), 3.47 (s, 2H). ^{13}C NMR (101 MHz, Chloroform-*d*) δ_C 168.1 (C_g), 164.0 (C_c), 131.7 (C_e), 126.7 ($C_{d/f}$), 126.2 ($C_{d/f}$), 63.1 (C_a) , 60.9 (C_b), 39.2 (C_h).

FTIR ν_{max} ATR (cm^{-1}): 2965 (aromatic νC-H), 1732 (imide -CO-N-CO-), 1704 (ester νC=O), 1371 (imide C-N stretch), 1188 (ester C-O-C), 1144 (imide ring deformation), 766 (imide ring deformation).

Inherent viscosity (η_{inh}, $CHCl_3$/HFIP 1:1, *v:v*): 0.17 $dL \cdot g^{-1}$.

Butanedioyl-based homopolymer

Monomers used: *N,N′*-bis-(2-hydroxyethyl)-naphthalene tetracarboxylic diimide (0.876 g, 2.47 mmol), butanedioyl chloride (0.392 g, 2.50 mmol) Yield: (0.67 g, 62%).

^{1}H NMR (400 MHz, Chloroform-*d*/TFA 9:1, *v:v*) δ_H 8.82 (s, 4H, C-H), 4.53 (m, 8H, N-C-H_2, O-C-H_2), 2.64 (m, 4H, C-H_2). ^{13}C NMR (100 MHz, Dichloromethane-d_2/HFIP 3:1, *v:v*) δ_C 174.6 (C_g), 164.2 (C_c), 131.9 (C_e), 127.2 ($C_{d/f}$), 126.7 ($C_{d/f}$), 62.6 (C_a), 39.7 (C_b), 29.0 (C_h).

FTIR ν_{max} ATR (cm^{-1}): 2966 (aromatic νC-H), 1732 (imide -CO-N-CO-), 1703 (ester νC=O), 1371 (imide C-N stretch), 1188 (ester C-O-C), 1146 (imide ring deformation), 765 (imide ring deformation).

T_g (DSC): 239 °C. T_m (DSC): Not observed.

Inherent viscosity (η_{inh}, $CHCl_3$/HFIP 1:1, *v:v*): 0.56 $dL \cdot g^{-1}$.

Pentanedioyl-based homopolymer

Monomers used: *N,N′*-bis-(2-hydroxyethyl)-naphthalene tetracarboxylic diimide (2.005 g, 5.66 mmol), pentanedioyl chloride (0.967 g, 5.72 mmol) Yield: (1.450 g, 56%).

^{1}H NMR (400 MHz, Chloroform-d/TFA 9:1, *v:v*) δ_H 8.82 (s, $4H_e$), 4.68 – 4.48 (m, $8H_{a/b}$), 2.39 (t, $4H_h$), 1.86 (m, $2H_i$). ^{13}C NMR (100 MHz, Dichloromethane-d_2/HFIP 6:1, *v:v*) δ_C 175.4 (C_g), 163.98 (C_c), 131.8 (C_e), 127.2 ($C_{d/f}$), 126.7 ($C_{d/f}$), 62.4 (C_a), 39.8 (C_b), 33.3 (C_h), 19.5 (C_i).

FTIR ν_{max} ATR (cm^{-1}): 2963 (aromatic νC-H), 1731 (imide -CO-N-CO-), 1703 (ester νC=O), 1372 (imide C-N stretch), 1189 (ester C-O-C), 1142 (imide ring deformation), 765 (imide ring deformation).

T_g (DSC): 132 °C. T_m (DSC): -

Inherent viscosity (η_{inh}, $CHCl_3$/HFIP 1:1, *v:v*): 1.54 $dL \cdot g^{-1}$.

Hexanedioyl-based homopolymer

Monomers used: *N,N′*-bis-(2-hydroxyethyl)-naphthalene tetracarboxylic diimide (2.090 g, 5.90 mmol), hexanedioyl chloride (1.091 g, 5.96 mmol) Yield: (2.101 g, 76%).

^{1}H NMR (400 MHz, Chloroform-*d*/TFA 9:1, *v:v*) δ_H 8.83 (s, $4H_e$), 4.57 (m, $4H_b$), 4.54 (m, $4H_a$), 2.34 (t, $4H_h$), 1.57 (t, $4H_i$). ^{13}C NMR (100 MHz, Dichloromethane-d_2/HFIP 6:1, *v:v*) δ_C 175.9 (C_g), 163.9 (C_c), 131.8 (C_e), 127.2 ($C_{d/f}$), 126.8 ($C_{d/f}$), 62.2 (C_a), 39.8 (C_b), 33.9 (C_h), 24.1 (C_i).

FTIR ν_{max} ATR (cm^{-1}): 2959 (aromatic νC-H), 1731 (imide -CO-N-CO-), 1703 (ester νC=O), 1372 (imide C-N stretch), 1192 (ester C-O-C), 1138 (imide ring deformation), 766 (imide ring deformation).

T_g (DSC): 116 °C. T_m (DSC): Not observed.

Inherent viscosity (η_{inh}, $CHCl_3$/HFIP 1:1, *v:v*): 0.75 $dL \cdot g^{-1}$.

Heptanedioyl-based homopolymer

Monomers used: *N,N′*-bis-(2-hydroxyethyl)-naphthalene tetracarboxylic diimide (2.0052 g, 5.66 mmol), heptanedioyl chloride (1. 134 g, 6.80 mmol) Yield: (2.125 g, 78%).

^{1}H NMR (400 MHz, Chloroform-*d*/TFA 9:1, *v:v*) δ_H 8.83 (s, 4H$_e$), 4.57 (m, 4H$_b$), 4.54 (m, 4H$_a$), 2.32 (t, 4H$_h$), 1.54 (p, 4H$_i$), 1.37 – 1.17 (m, 2H$_j$). ^{13}C NMR (100 MHz, Dichloromethane-d_2/HFIP 6:1, *v:v*) δ_C 176.5 (C$_g$), 164.0 (C$_c$), 131.8 (C$_e$), 127.2 (C$_{d/f}$), 126.8 (C$_{d/f}$), 62.2 (C$_a$), 39.8 (C$_b$), 34.1 (C$_h$), 28.5 (C$_i$), 24.4 (C$_j$).

FTIR ν_{max} ATR (cm^{-1}): 2950 (aromatic νC-H), 1731.72 (imide -CO-N-CO-), 1703 (ester νC=O), 1372 (imide C-N stretch), 1192 (ester C-O-C), 1160 (imide ring deformation), 766 (imide ring deformation).

T_g (DSC): 90 °C. T_m (DSC): Not observed.

Inherent viscosity (η_{inh}, $CHCl_3$/TFE 6:1, *v:v*): 0.58 dL·g^{-1}.

Octanedioyl-based homopolymer

Monomers used: *N,N′*-bis-(2-hydroxyethyl)-naphthalene tetracarboxylic diimide (2.079 g, 5.87 mmol), octanedioyl chloride (1.238 g, 5.87 mmol). Yield: (2.11 g, 73%).

^{1}H NMR (400 MHz, Chloroform-*d*/TFA 9:1, *v:v*) δ_H 8.83 (s, 4H$_e$), 4.57 (m, 4H$_b$), 4.54 (m, 4H$_a$), 2.32 (t, 4H$_h$), 1.52 (m, 4H$_i$), 1.33 – 1.10 (m, 4H$_j$). ^{13}C NMR (100 MHz, Dichloromethane-d_2/HFIP 6:1, *v:v*) δ_C 176.13 (C$_g$), 163.6 (C$_c$), 131.7 (C$_e$), 127.0 (C$_{d/f}$), 126.6 (C$_{d/f}$), 62.0 (C$_a$), 40.0 (C$_b$), 34.2 (C$_h$), 28.6 (C$_i$), 24.4 (C$_j$).

FTIR ν_{max} ATR (cm^{-1}): 2935 (aromatic νC-H), 1731 (imide -CO-N-CO-), 1703 (ester νC=O), 1373 (imide C-N stretch), 1161 (ester C-O-C), 1154 (imide ring deformation), 766 (imide ring deformation).

T_g (DSC): 73 °C. T_m (DSC): Not observed.

Inherent viscosity (η_{inh}, $CHCl_3$/HFIP 1:1, *v:v*): 0.19 dL·g^{-1}.

Nonanedioyl-based homopolymer

Monomers used: *N,N′*-bis-(2-hydroxyethyl)-naphthalene tetracarboxylic diimide (2.121 g, 5.99 mmol), nonanedioyl chloride (1.362 g, 6.05 mmol) Yield: (2.47 g, 81%).

^{1}H NMR (400 MHz, Chloroform-*d*/TFA 9:1, *v:v*) δ_H 8.83 (s, 4H$_e$), 4.58 (m, 4H$_b$), 4.55 (m, 4H$_a$), 2.34 (t, 4H$_h$), 1.60 – 1.42 (m, 4H$_i$), 1.22 (m, 6H$_j$). ^{13}C NMR (100 MHz, Dichloromethane-d_2/HFIP 6:1, *v:v*) δ_C 176.7 (C$_g$), 163.9 (C$_c$), 131.8 (C$_e$), 127.2 (C$_{d/f}$), 126.8 (C$_{d/f}$), 62.1 (C$_a$), 39.8 (C$_b$), 34.4 (C$_h$), 29.0 (C$_i$), 24.8 (C$_j$).

FTIR ν_{max} ATR (cm^{-1}): 2933 (aromatic νC-H), 1732 (imide -CO-N-CO-), 1704 (ester νC=O), 1373 (imide C-N stretch), 1156 (ester C-O-C), 1154 (imide ring deformation), 766 (imide ring deformation).

T_g (DSC): 76 °C. T_m (DSC): Not observed.

Inherent viscosity (η_{inh}, $CHCl_3$/TFE 6:1, *v:v*): 1.20 dL·g^{-1}.

Decanedioyl-based homopolymer

Monomers used: *N,N′*-bis-(2-hydroxyethyl)-naphthalene tetracarboxylic diimide (2.081 g, 5.88 mmol), decanedioyl chloride (1.420 g, 5.94 mmol), yield: (2.79 g, 91%).

^{1}H NMR (400 MHz, Chloroform-*d*/TFA 9:1, *v:v*) δ_H 8.83 (s, 4H$_e$), 4.58 (m, 4H$_b$), 4.55 (m, 4H$_a$), 2.33 (t, 4H$_h$), 1.73 – 1.40 (m, 4H$_i$), 1.22 (m, 8H$_j$). ^{13}C NMR (100 MHz, Dichloromethane-d_2/HFIP 6:1, *v:v*) δ_C 178.3 (C$_g$), 165.4 (C$_c$), 133.3 (C$_e$), 128.7 (C$_{d/f}$), 128.3 (C$_{d/f}$), 63.6 (C$_a$), 41.3 (C$_b$), 36.0 (C$_h$), 30.7 (C$_i$), 26.4 (C$_j$).

FTIR ν_{max} ATR (cm^{-1}): 2929 (aromatic νC-H), 1732 (imide -CO-N-CO-), 1704 (ester νC=O), 1373 (imide C-N stretch), 1156 (ester C-O-C), 1154 (imide ring deformation), 766 (imide ring deformation).

T_g (DSC): 50 °C. T_m (DSC): Not observed.

Inherent viscosity (η_{inh}, $CHCl_3$/TFE 6:1, *v:v*): 0.93 dL·g^{-1}.

8.4. PMDI-based homo-poly(ester imide)s

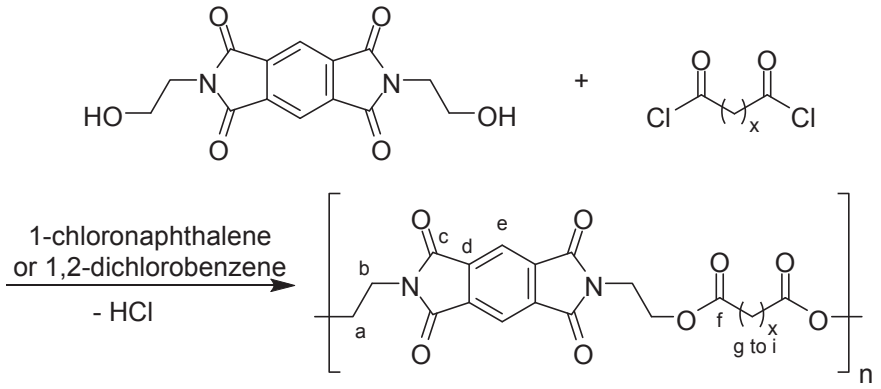

1,2-Dichlorobenzene or 1-chloronaphthalene (4.5 mL, distilled from CaH_2), *N,N'*-bis-(2-hydroxyethyl)-pyromellitic diimide (dried at 100 °C for up to 24 hours) and a diacid chloride (from **a** to **h**) were combined and heated to 170 °C for up to 24 hours under N_2 atmosphere. After cooling to room temperature, the solidified product mixture was dissolved in 25 mL chloroform/1,1,1,3,3,3-hexafluoroisopropanol (4:1 *v/v*) and then precipitated dropwise into an excess of methanol (~ 400 mL). The precipitate was filtered off and dried at 80 °C for up to 24 hours. The reprecipitation was repeated three times to afford the pure polymer.

Propanedioyl-based homopolymer

Monomers used: *N,N'*-bis-(2-hydroxyethyl)-pyromellitic diimide (2.020 g, 6.64 mmol), propanedioyl chloride (0.9853 g, 6.991 mmol). Yield: (1.6998 g, 68%).

^{1}H NMR (400 MHz, Chloroform-*d*/TFA 9:1, v:v) δ_H 8.34 (s, $2H_e$), 4.36 – 4.15 (m, $4H_b$), 3.82 (t, $4H_a$), 3.58 (s, $2H_g$). ^{13}C NMR (100 MHz, Chloroform-*d*/TFE 10:1, v:v) δ_C 172.6 (C_f), 166.4 (C_c), 137.2 (C_d), 118.3 (C_e), 65.0 (C_a), 38.1 (C_b), 25.7 (C_g).

FTIR ν_{max} ATR (cm^{-1}): 2949 (aromatic νC-H), 1696 (imide -CO-N-CO-, ester νC=O), 1397 (imide C-N stretch), 1154 (ester C-O-C), 1048 (imide ring deformation), 728 (imide ring deformation).

T_g (DSC): Not observed. T_m (DSC): 194 °C.

Inherent viscosity (η_{inh}, $CHCl_3$/TFE 6:1, v:v): 0.48 $dL \cdot g^{-1}$.

Butanedioyl-based homopolymer

Monomers used: *N,N'*-bis-(2-hydroxyethyl)-pyromellitic diimide (2.099 g, 6.90 mmol), butanedioyl chloride (1.080 g, 6.97 mmol) Yield: (2.2456 g, 84%).

^{1}H NMR (400 MHz, Chloroform-*d*/TFA 9:1, v:v) δ_H 8.34 (s, 2H$_e$), 4.21 (t, 4H$_b$), 3.88 – 3.74 (m, 4H$_a$), 2.74 (s, 2H$_g$). ^{13}C NMR (100 MHz, Chloroform-*d*/TFE 9:1, v:v) δ_C 173.1 (C$_f$), 166.5 (C$_c$), 137.2 (C$_d$), 118.3 (C$_e$), 61.9 (C$_a$), 38.2 (C$_b$), 28.9 (C$_g$).

FTIR ν_{max} ATR (cm^{-1}): 2948 (aromatic νC-H), 1698 (imide -CO-N-CO-, ester νC=O), 1397 (imide C-N stretch), 1155 (ester C-O-C), 1050 (imide ring deformation), 727 (imide ring deformation).

T_g (DSC): Not observed. T_m (DSC): 233 °C.

Inherent viscosity (η_{inh}, $CHCl_3$/TFE 6:1, v:v): 0.36 dL·g^{-1}.

Pentanedioyl-based homopolymer

Monomers used: *N,N'*-bis-(2-hydroxyethyl)-pyromellitic diimide (1.991 g, 6.54 mmol), pentanedioyl chloride (1.119 g, 6.621 mmol) Yield: (2.331 g, 88%).

^{1}H NMR (400 MHz, Chloroform-*d*/TFA 9:1, v:v) δ_H 8.35 (s, 2H$_e$), 4.41 (t, 4H$_b$), 4.08 (t, 4H$_a$), 2.45 – 2.31 (m, 4H$_g$), 1.87 (m, 2H$_h$). ^{13}C NMR (100 MHz, Dichloromethane-d_2/TFE 6:1, v:v) δ_C 174.0 (C$_f$), 166.7 (C$_c$), 137.5 (C$_d$), 118.7 (C$_e$), 61.9 (C$_a$), 37.9 (C$_b$), 33.1 (C$_g$), 19.8 (C$_h$).

FTIR ν_{max} ATR (cm^{-1}): 2953 (aromatic νC-H), 1702 (imide -CO-N-CO-, ester νC=O), 1388 (imide C-N stretch), 1155 (ester C-O-C), 1032 (imide ring deformation), 724 (imide ring deformation).

T_g (DSC): Not observed. T_m (DSC): 223 °C.

Inherent viscosity (η_{inh}, $CHCl_3$/TFE 6:1, v:v): 0.60 dL·g^{-1}.

Hexanedioyl-based homopolymer

Monomers used: *N,N'*-bis-(2-hydroxyethyl)-pyromellitic diimide (2.061 g, 6.77 mmol), hexanedioyl chloride (1.240 g, 6.77 mmol) Yield: (2.7503 g, 96%).

^{1}H NMR (400 MHz, Chloroform-*d*) δ 8.36 (s, 2H$_e$), 4.43 (t, J = 4.8 Hz, 4H$_b$), 4.09 (t, J = 4.9 Hz, 4H$_a$), 2.37 (m, 4H$_g$), 1.67 – 1.49 (m, 4H$_h$). ^{13}C NMR (151 MHz, Chloroform-*d*) δ 176.6 (C$_f$), 166.6 (C$_c$), 137.1 (C$_d$), 119.1 (C$_e$), 62.6 (C$_a$), 37.7 (C$_b$), 33.6 (C$_g$), 23.7 (C$_h$).

FTIR ν_{max} ATR (cm^{-1}): 2951 (aromatic νC-H), 1699 (imide -CO-N-CO-, ester νC=O), 1387 (imide C-N stretch), 1155 (ester C-O-C), 1252 (imide ring deformation), 759 (imide ring deformation).

T_g (DSC): 77 T_m (DSC): 253 °C.

Inherent viscosity (η_{inh}, $CHCl_3$/TFE 6:1, v:v): 0.55 $dL \cdot g^{-1}$.

Heptanedioyl-based homopolymer

Monomers used: *N,N'*-bis-(2-hydroxyethyl)-pyromellitic diimide (2.101 g, 6.91 mmol), heptanedioyl chloride (1.374 g, 6.97 mmol) Yield: (2.4415 g, 82%).

^{1}H NMR (600 MHz, Chloroform-*d*) δ 8.38 (s, $2H_e$), 4.45 (t, J = 5.1 Hz, $4H_b$), 4.10 (t, J = 5.1 Hz, $4H_a$), 2.36 (t, J = 7.6 Hz, $4H_g$), 1.58 (p, J = 7.7 Hz, $4H_h$), 1.40 – 1.20 (m, $2H_i$). ^{13}C NMR (151 MHz, Chloroform-*d*) δ_C 177.2 (C_f), 166.6 (C_c), 137.1 (C_d), 119.1 (C_e), 62.5 (C_a), 37.7 (C_b), 33.8 (C_g), 28.0 (C_h), 23.9 (C_i).

FTIR ν_{max} ATR (cm^{-1}): 2944 (aromatic νC-H), 1698 (imide -CO-N-CO-, ester νC=O), 1397 (imide C-N stretch), 1155 (ester C-O-C), 1051 (imide ring deformation), 727 (imide ring deformation).

T_g (DSC): Not observed. T_m (DSC): 190 °C.

Inherent viscosity (η_{inh}, $CHCl_3$/TFE 6:1, v:v): 0.59 $dL \cdot g^{-1}$.

Octanedioyl-based homopolymer

Monomers used : *N,N'*-bis-(2-hydroxyethyl)-pyromellitic diimide (2.065 g, 6.79 mmol), octanedioyl chloride (1.447 g, 6.856 mmol) Yield: (2.64 g, 88%).

^{1}H NMR (400 MHz, Chloroform-*d*/TFA 9:1, v:v) δ_H 8.37 (s, $2H_e$), 4.43 (t, $4H_b$), 4.09 (t, $4H_a$), 2.34 (t, $4H_g$), 1.63 – 1.46 (m, $4H_h$), 1.27 (m, $4H_i$). ^{13}C NMR (101 MHz, Chloroform-*d*/TFA 9:1, v:v) δ_C 174.4 (C_f), 166.1 (C_c), 137.1 (C_d), 118.6 (C_e), 61.4 (C_a), 37.7 (C_b), 33.8 (C_g), 28.5 (C_h), 24.3 (C_i).

FTIR ν_{max} ATR (cm^{-1}): 2938 (aromatic C-H), 1712 (imide -CO-N-CO-, ester C=O), 1386 (imide C-N stretch), 1153 (ester C-O-C), 1030 (imide ring deformation), 723 (imide ring deformation).

T_g (DSC): Not observed. T_m (DSC): 217 °C.

Inherent viscosity (η_{inh}, $CHCl_3$/TFE 6:1, v:v): 0.62 $dL \cdot g^{-1}$.

Nonanedioyl-based homopolymer

Monomers used: *N,N'*-bis-(2-hydroxyethyl)-pyromellitic diimide (2.029 g, 6.67 mmol), nonanedioyl chloride (1.516 g, 6.735 mmol) Yield: (2.64 g, 85%).

^{1}H NMR (400 MHz, Chloroform-*d*/TFA 9:1, v:v) δ_H 8.37 (s, 2H$_e$), 4.44 (t, 4H$_b$), 4.10 (t, 4H$_a$), 2.35 (t, 4H$_{g)}$, 1.62 – 1.49 (m, 4H$_h$), 1.25 (m, 6H$_i$). ^{13}C NMR (100 MHz, Chloroform-*d*) δ_C 173.50 (C$_f$), 165.9 (C$_c$), 137.2 (C$_d$), 118.5 (C$_e$), 61.1 (C$_a$), 37.9 (C$_b$), 33.9 (C$_g$), 28.8 (C$_h$), 24.5 (C$_i$).

FTIR ν_{max} ATR (cm^{-1}): 2931 (aromatic νC-H), 1712 (imide -CO-N-CO-, ester νC=O), 1386 (imide C-N stretch), 1155 (ester C-O-C), 1032 (imide ring deformation), 724 (imide ring deformation).

T_g (DSC): Not observed. T_m (DSC): 203 °C.

Inherent viscosity (η_{inh}, $CHCl_3$/TFE 6:1, v:v): 0.37 dL·g^{-1}.

Decanedioyl-based homopolymer

Monomers used: *N,N'*-bis-(2-hydroxyethyl)-pyromellitic diimide (2.148 g, 7.06 mmol), decanedioyl chloride (1.705 g, 7.13 mmol) Yield: (3.2305 g, 97%).

^{1}H NMR (400 MHz, Chloroform-*d*/TFA 9:1, v:v) δ_H 8.37 (s, 2H$_e$), 4.44 (t, 4H$_b$), 4.10 (t, 4H$_a$), 2.35 (t, 4H$_g$), 1.66 – 1.45 (m, 4H$_h$), 1.24 (m, 8H$_i$).^{13}C NMR (100 MHz, Chloroform-*d*/TFE 10:1, v:v) δ_C 174.6 (C$_f$), 166.1 (C$_c$), 137.1 (C$_d$), 118.6 (C$_e$), 61.2 (C$_a$), 37.7 (C$_b$), 33.9 (C$_g$), 28.9 (C$_h$), 24.5 (C$_i$).

FTIR ν_{max} ATR (cm^{-1}): 2929 (aromatic νC-H), 1709 (imide -CO-N-CO-, ester νC=O), 1386 (imide C-N stretch), 1155 (ester C-O-C), 1032 (imide ring deformation), 723 (imide ring deformation).

T_g (DSC): Not observed. T_m (DSC): 207 °C.

Inherent viscosity (η_{inh}, $CHCl_3$/TFE 6:1, v:v): 0.59 dL·g^{-1}.

8.5. HFDI-based homo-poly(ester imide)s

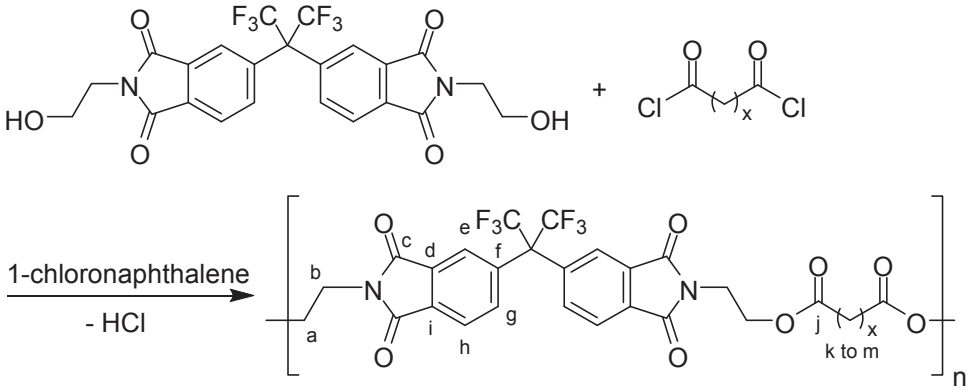

1-Chloronaphthalene (1.5 mL, distilled from CaH_2), *N,N′*-bis-(2-hydroxyethyl)-hexafluoroisopropylidene biphthalimide (dried at 120 °C for up to 24 hours) and a diacid chloride were combined at room temperature. The mixture was heated to 120 °C for 4 hours under N_2 atmosphere. After cooling to room temperature, the homogeneous product was dissolved in 20 mL chloroform and precipitated dropwise into an excess of methanol (~ 400 mL). The precipitate was filtered off and dried at 80 °C for up to 24 hours. The reprecipitation was repeated three times to afford the pure polymer.

HFDI Pentanedioyl-based homopolymer

FTIR ν_{max} ATR (cm^{-1}): 2961 (aromatic νC-H), 1779 (imide -CO-N-CO-), 1708 (ester νC=O), 1387 (imide C-N stretch), 1188 (vs, C–F), 1163 (ester C-O-C), 1139 (imide ring deformation), 745 (imide ring deformation).

GPC: M_n = 30,100 g/mol ; M_w = 62,300 g/mol; $Đ$ = 2.07

T_g (DSC): 109 °C. T_m (DSC): Not observed.

Inherent viscosity (η_{inh}, $CHCl_3$/TFE 6:1, v:v): 0.83 $dL \cdot g^{-1}$.

HFDI Heptanedioyl-based homopolymer

Monomers used: *N,N′*-bis-(2-hydroxyethyl)-hexafluoroisopropylidene biphthalimide (1.25 g, 2.35 mmol), heptanedioyl dichloride (0.46 g, 2.36 mmol), yield: (1.29 g, 84%).

^{1}H NMR (400 MHz, Chloroform-*d*) δ 7.93 (d, *J* = 8.0 Hz, $2H_{g/h}$), 7.85 (s, $2H_e$), 7.77 (d, *J* = 8.0 Hz, $2H_{g/h}$), 4.31 (t, *J* = 5.2 Hz, $4H_b$), 3.96 (t, J = 5.1 Hz, $4H_a$), 2.26 (t, J = 7.5 Hz, $4H_k$), 1.65 – 1.50 (m, $8H_l$), 1.37 – 1.25 (m, $2H_m$). ^{13}C NMR (101 MHz, Chloroform-*d*/TFE 9:1, *v:v*) δ_C 174.5 (C_j), 167.4 (C_c), 139.2 ($C_{d/i}$), 136.2 ($C_{g/h}$) , 132.8 (C_f), 132.5 ($C_{d/i}$), 125.1 (C_e), 124.0 ($C_{g/h}$), 61.2 (C_b), 37.5 (C_a), 33.9 (C_k), 28.5 (C_m), 24.3 (C_l). ^{19}F NMR (400 MHz, Chloroform-*d*/TFE 9:1, *v:v*) δ_F -62.9 (CF_3).

FTIR ν_{max} ATR (cm^{-1}): 2958 (aromatic νC-H), 1779 (imide -CO-N-CO-), 1709 (ester νC=O), 1387 (imide C-N stretch), 1188 (vs, C–F), 1164 (ester C-O-C), 1136 (imide ring deformation), 708 (imide ring deformation).

GPC: M_n = 20,400 g/mol ; M_w = 39,200 g/mol; $Đ$ = 1.92.

T_g (DSC): 72 °C. T_m (DSC): Not observed.

Inherent viscosity (η_{inh}, $CHCl_3$/TFE 6:1, v:v): 0.56 $dL \cdot g^{-1}$.

8.6. BPDI-based homo-poly(ester imide)s

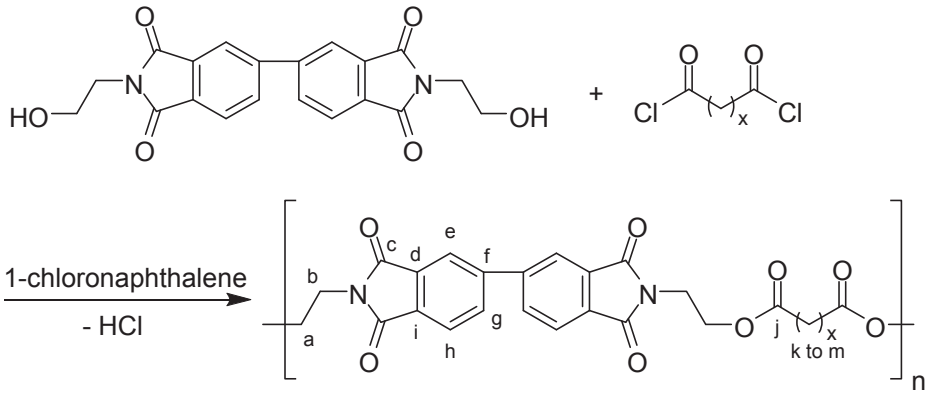

1-Chloronaphthalene (15 mL, distilled from CaH_2), *N,N′*-bis-(2-hydroxyethyl)-biphthalimide (dried at 120 °C for up to 24 hours) and an acid chloride were combined at room temperature. The mixture was heated to 170 °C for up to 24 hours under N_2 atmosphere. After cooling to room temperature, the solidified product mixture was dissolved in 20 mL of chloroform and precipitated dropwise into an excess of methanol (~ 400 mL). The precipitate was filtered and dried at 80 °C for up to 24 hours. The reprecipitation was repeated three times to afford the pure polymer.

BPDI Pentanedioyl-based homopolymer

Monomers used: *N,N′*-bis-(2-hydroxyethyl)-biphthalimide (2.01 g, 13.61 mmol), pentanedioyl dichloride (0.96 g, 13.60 mmol). Yield: (2.08 g, 87%).

^{1}H NMR (400 MHz, Chloroform-*d*) δ_H 8.11 (s, $2H_e$), 8.06 – 7.88 (m, $4H_{h/g}$), 4.33 (t, J = 5.2 Hz, 4H), 3.98 (t, J = 5.2 Hz, 4H), 2.25 (t, J = 7.5 Hz, 4H), 1.56 (m, 4H), 1.37 – 1.17 (m, 2H). ^{13}C NMR (101 MHz, Chloroform-*d*/TFE 9:1, *v:v*) δ 174.0 (C_j), 168.0 (C_c), 145.3 ($C_{d/f/i}$), 133.3 ($C_{d/f/i}$), 132.9 ($C_{g/h}$), 131.5 ($C_{d/f/i}$), 124.3 ($C_{g/h}$), 122.9 (C_e), 61.6 (C_a), 37.1 (C_b), 33.5 (C_k), 23.8 (C_l).

FTIR ν_{max} ATR (cm^{-1}): 2947 (aromatic νC-H), 1770 (imide -CO-N-CO-), 1702 (ester νC=O), 1384 (imide C-N stretch), 1187 (ester C-O-C), 1143 (imide ring deformation), 740 (imide ring deformation).

T_g (DSC): 109 °C. T_m (DSC): Not observed

Inherent viscosity (η_{inh}, $CHCl_3$): 1.08 $dL \cdot g^{-1}$.

BPDI Heptanedioyl-based homopolymer

Monomers used: *N,N′*-bis-(2-hydroxyethyl)-biphthalimide (2.68 g, 7.05 mmol), heptanedioyl dichloride (1.3882 g, 7.03 mmol). Yield: (2.02 g, 67%).

^{1}H NMR (400 MHz, Chloroform-*d*) δ_H 8.11 (s, $2H_e$), 8.06 – 7.88 (m, $4H_{h/g}$), 4.33 (t, J = 5.2 Hz, $4H_b$), 3.98 (t, J = 5.2 Hz, $4H_a$), 2.25 (t, J = 7.5 Hz, $4H_k$), 1.56 (m, $4H_l$), 1.37 – 1.17 (m, $2H_m$). ^{13}C NMR (101 MHz, Chloroform-*d*) δ_C 173.3 (C_j), 167.5 (C_c), 145.2 ($C_{d/f/i}$), 133.2 ($C_{d/f/i}$), 133.1 ($C_{g/h}$), 131.8 ($C_{d/f/i}$), 124.2 ($C_{g/h}$), 122.3 (C_e), 61.3 (C_a), 37.4 (C_b), 33.7 (C_j), 28.4 (C_l), 24.3 (C_k).

FTIR ν_{max} ATR (cm^{-1}): 2942 (aromatic νC-H), 1771 (imide -CO-N-CO-), 1702 (ester νC=O), 1383 (imide C-N stretch), 1158 (ester C-O-C), 1137 (imide ring deformation), 739 (imide ring deformation).

T_g (DSC): 68 °C. T_m (DSC): Not observed.

Inherent viscosity (η_{inh}, $CHCl_3$): 0.51 $dL \cdot g^{-1}$.

8.7. NDI/HFDI-based *co*-poly(ester-imide)s

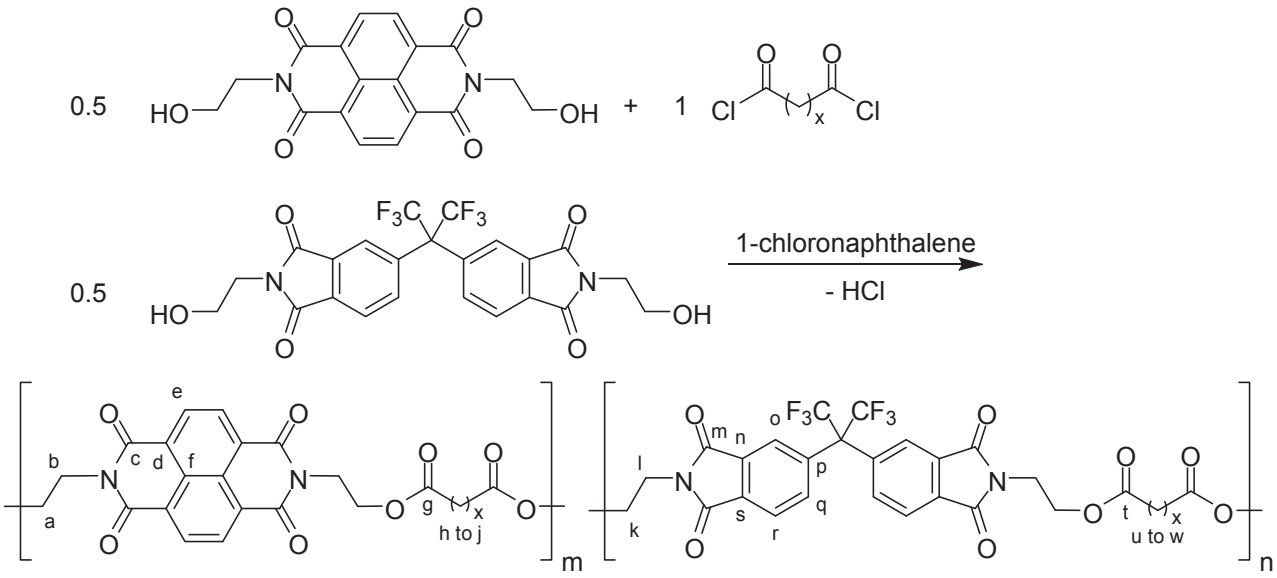

1-Chloronaphthalene (2.5 mL, distilled from CaH_2), *N,N′*-bis-(2-hydroxyethyl)-naphthalene-tetracarboxylic diimide (dried at 100 °C for up to 24 hours), *N,N′*-bis(2-hydroxyethyl)-hexa-fluoroisopropylidene-diphthalic diimide (dried at 100 °C for up to 24 hours) and an acid chloride were combined at room temperature. The mixture was heated to 160 °C for up to 24 hours under N_2 atmosphere, unless specified otherwise. After cooling to room temperature, the solidified product mixture was dissolved in 30 mL dichloromethane/hexafluoroisopro-panol (4:1, v/v) and precipitated dropwise into an excess of methanol (~ 400 mL). The precip-itate was filtered and dried at 80 °C for up to 24 hours. The reprecipitation was repeated three times to afford the pure polymer.

8.7.1. NDI/HFDI Propanedioyl-based copolymer

N,N′-bis-(2-hydroxyethyl)-naphthalenetetracarboxylic diimide (0.7076 g, 1.99 mmol), *N,N′*-bis(2-hydroxyethyl)-hexafluoroisopropylidene-diphthalic diimide (1.0445 g, 1.97 mmol), pro-panedioyl dichloride (0.5612 g, 3.98 mmol). Yield: (1.8342 g, 90%).

FTIR ν_{max} ATR (cm^{-1}): 2956 (aromatic νC-H), 1706 (imide -CO-N-CO-), 1665 (ester νC=O), 1390 (imide C-N stretch), 1190 (vs, C–F), 1142 (ester C-O-C), 1104 (imide ring deformation), 768 (imide ring deformation).

Inherent viscosity (η_{inh}, $CHCl_3$/TFE 6:1, *v:v*): 0.81 $dL \cdot g^{-1}$.

8.7.2. NDI/HFDI Butanedioyl-based copolymer

N,N′-bis-(2-hydroxyethyl)-naphthalenetetracarboxylic diimide (1.011 g, 2.82 mmol), *N,N′*-bis(2-hydroxyethyl)-hexafluoroisopropylidene-diphthalic diimide (1.513 g, 2.82 mmol), butanedioyl dichloride (0.902 g, 5.82 mmol). Yield: (1.8525 g, 60%).

^{1}H NMR (400 MHz, Chloroform-*d*/TFA 9:1, v:v) δ_H 8.83 (s, 4H, -CH- NDI), 7.98 (d, J = 8.0 Hz, 2H, -CH- HFDI), 7.92 – 7.79 (m, 4H, CH, CH HFDI), 4.83 – 3.87 (m, 16H, N-CH_2, O-CH_2), 2.64 (m, 8H, -CO-CH_2). ^{13}C NMR (101 MHz, Chloroform-*d*/TFE 9:1, *v:v*) δ_C 172.9 ($C_{g/t}$), 172.8 ($C_{g/t}$), 163.3 (C_m), 163.3 (C_c), 139.0 ($C_{n/s}$), 136.0 ($C_{q/r}$), 133.6 (C_p), 132.3 ($C_{n/s}$), 131.2 (C_e), 126.8 ($C_{d/f}$), 126.4 ($C_{d/f}$), 124.9 ($C_{q/r}$), 61.8 ($C_{a/k}$), 39.4 (C_b), 37.1 (C_l), 28.6 (C_h).

FTIR ν_{max} ATR (cm^{-1}): 2973 (aromatic νC-H), 1779 (imide -CO-N-CO-), 1707 (ester νC=O), 1388 (imide C-N stretch), 1189 (vs, C–F), 1146 (ester C-O-C), 1100 (imide ring deformation), 768 (imide ring deformation).

T_g (DSC): 130 °C. T_m (DSC): Not observed.

Inherent viscosity (η_{inh}, $CHCl_3$/TFE 6:1, *v:v*): 0.20 dL·g^{-1}.

8.7.3. NDI/HFDI Pentanedioyl-based copolymer

Monomers used: *N,N′*-bis-(2-hydroxyethyl)-naphthalenetetracarboxylic diimide (1.001 g, 2.8 mmol), *N,N′*-bis(2-hydroxyethyl)-hexafluoroisopropylidene-diphthalic diimide (1.517 g, 2.9 mmol), pentanedioyl dichloride (0.980 g, 5.8 mmol). Yield: (1.2210 g, 38%).

^{1}H NMR (400 MHz, Chloroform-*d*/TFA 9:1, v:v) δ_H 8.82 (s, 4H, -CH- NDI), 7.98 (d, J = 8.0 Hz, 2H, -CH- HFDI), 7.92 – 7.79 (m, 4H, CH HFDI), 4.73 – 3.96 (m, 16H, N-CH_2, O-CH_2), 2.51 – 2.33 (m, 8H, CO-CH_2), 1.95 – 1.81 (m, 4H, CO-CH2-CH_2). ^{13}C NMR (101 MHz, Chloroform-*d*/TFE 6:1, *v:v*) δ_C 173.8 ($C_{g/t}$), 173.7 ($C_{g/t}$), 167.3 (C_m), 163.2 (C_c), 139.0 ($C_{n/s}$), 136.0 ($C_{q/r}$), 132.6 (C_p), 132.2 ($C_{n/s}$), 131.3 (C_e), 126.4 ($C_{d/f}$), 124.9 ($C_{d/f}$), 123.8 ($C_{q/r}$), 61.7 ($C_{a/k}$), 39.5 (C_b), 37.2 (C_l), 32.8 (C_h), 19.4 (C_u).

FTIR ν_{max} ATR (cm^{-1}): 2958 (aromatic νC-H), 1779 (imide -CO-N-CO-), 1701 (ester νC=O), 1388 (imide C-N stretch), 1189 (vs, C–F), 1163 (ester C-O-C), 1140 (imide ring deformation), 768 (imide ring deformation).

T_g (DSC): 99 °C. T_m (DSC): Not observed.

Inherent viscosity (η_{inh}, $CHCl_3$/TFE 6:1, *v:v*): 0.26 dL·g^{-1}.

8.7.4. NDI/HFDI Hexanedioyl-based copolymer

N,N′-bis-(2-hydroxyethyl)-naphthalenetetracarboxylic diimide (0.502 g, 1.4 mmol), *N,N′*-bis(2-hydroxyethyl)-hexafluoroisopropylidene-diphthalic diimide (0.762 g, 1.4 mmol), hexanedioyl dichloride (0.533 g, 2.91 mmol). Yield: (1.025 g, 62%).

^{1}H NMR (400 MHz, Chloroform-*d*/TFA 9:1, *v:v*) δ_H 8.83 (s, 4H$_e$), 7.98 (d, *J* = 8.0 Hz, 2H$_{q/r}$), 7.92 – 7.79 (m, 4H$_{q/r/o}$), 4.63 – 4.48 (m, 8H$_{a/b}$), 4.39 (t, J = 5.3 Hz, 4H$_l$), 4.02 (q, J = 8.7, 7.3 Hz, 4H$_k$), 2.52 – 2.19 (m, 8H$_{h/u}$), 1.59 (m, 8H$_{i/v}$). ^{13}C NMR (101 MHz, Chloroform-*d*/TFE 6:1, v:v) δ_C 175.2 (C$_{g/t}$), 175.1 (C$_{g/t}$), 167.6 (C$_m$), 163.4 (C$_c$), 139.3 (C$_{n/s}$), 136.2 (C$_{q/r}$), 132.9 (C$_p$), 132.5 (C$_{n/s}$), 131.5 (C$_e$), 126.7 (C$_{d/f}$), 125.2 (C$_{d/f}$), 124.1 (C$_{q/r}$), 61.7 (C$_{a/k}$), 39.8 (C$_b$), 37.5 (C$_l$), 34.3 (C$_h$), 34.2 (C$_u$), 29.1 (C$_{i/v}$), 24.8 (C$_{j/w}$).

FTIR ν_{max} ATR (cm^{-1}): 2958 (aromatic νC-H), 1780 (imide -CO-N-CO-), 1708 (ester νC=O), 1389 (imide C-N stretch), 1190 (vs, C–F), 1163 (ester C-O-C), 1140 (imide ring deformation), 769 (imide ring deformation).

T_g (DSC): 96 °C. T_m (DSC): Not observed.

Inherent viscosity (η_{inh}, $CHCl_3$/TFE 6:1, *v:v*): 1.09 dL·g^{-1}.

8.7.5. NDI/HFDI Heptanedioyl-based copolymer

N,N′-bis-(2-hydroxyethyl)-naphthalenetetracarboxylic diimide (0.8688 g, 2.45 mmol), *N,N′*-bis(2-hydroxyethyl)-hexafluoroisopropylidene-diphthalic diimide (1.3262 g, 2.50 mmol), heptanedioyl dichloride (0.9986 g, 5.07 mmol). Yield: (1.63 g, 56%).

^{1}H NMR (400 MHz, Chloroform-*d*/TFA 9:1, *v:v*) δ 8.75 (s, 4H$_e$), 7.93 (d, *J* = 8.0 Hz, 2H$_{q/r}$), 7.84 (s, 2H$_o$), 7.77 (d, *J* = 8.1 Hz, 2H$_{q/r}$), 4.58 – 4.36 (m, 8H$_{a/b}$), 4.37 – 4.21 (m, 4H$_l$), 4.08 – 3.86 (m, 4H$_k$), 2.38 – 2.11 (m, 8H$_{h/u}$), 1.68 – 1.42 (m, 8H$_{i/v}$), 1.42 – 1.11 (m, 6 H$_{j/w}$). ^{13}C NMR (101 MHz, Chloroform-*d*/TFE 6:1, *v:v*) δ 174.7 (C$_{g/t}$), 167.3 (C$_m$), 163.1 (C$_c$), 139.0 (C$_{n/s}$), 136.0 (C$_{q/r}$), 132.6 (C$_p$), 132.3 (C$_{n/s}$), 131.3 (C$_e$), 126.8 (C$_{d/f}$), 126.4 (C$_{d/f}$), 124.9 (C$_o$), 123.8 (C$_{q/r}$), 61.5 (C$_{a/k}$), 39.5 (C$_b$), 37.2 (C$_l$), 33.7 (C$_h$), 33.7 (C$_u$), 28.2 (C$_{i/v}$), 24.1 (C$_{j/w}$).

FTIR ν_{max} ATR (cm^{-1}): 2942 (aromatic νC-H), 1780 (imide -CO-N-CO-), 1708 (ester νC=O), 1389 (imide C-N stretch), 1190 (vs, C–F), 1163 (ester C-O-C), 1140 (imide ring deformation), 769 (imide ring deformation).

T_g (DSC): 91 °C. T_m (DSC): Not observed.

Inherent viscosity (η_{inh}, $CHCl_3$/TFE 6:1, *v:v*): 0.61 dL·g^{-1}.

8.7.6. NDI/HFDI Octanedioyl-based copolymer

N,N′-bis-(2-hydroxyethyl)-naphthalenetetracarboxylic diimide (0.6059 g, 1.71 mmol), *N,N′*-bis(2-hydroxyethyl)-hexafluoroisopropylidene-diphthalic diimide (0.9224 g, 1.73 mmol), octanedioyl dichloride (0.7309 g, 3.46 mmol). Synthesized by heating for 45 minutes at 130 °C. Yield: (1.85 g, 92%).

^{1}H NMR (400 MHz, Chloroform-*d*/TFA 9:1, *v:v*) δ 8.84 (s, $4H_e$), 7.99 (d, *J* = 7.8 Hz, $2H_{q/r}$), 7.94 – 7.79 (m, $4H_{q/r/o}$), 4.74 – 4.47 (m, $8H_{a/b}$), 4.47 – 4.29 (m, $4H_l$), 4.16 – 3.91 (m, $4H_k$), 2.46 – 2.23 (m, $8H_{h/u}$), 1.63 – 1.41 (m, $8H_{i/v}$), 1.41 – 1.13 (m, $8H_{j/w}$). ^{13}C NMR (101 MHz, Chloroform-*d*/TFE 9:1, *v:v*) δ 174.8 ($C_{g/t}$), 174.7 ($C_{g/t}$), 167.3 (C_m), 163.1 (C_c), 139.0 ($C_{n/s}$), 136.0 ($C_{q/r}$) , 132.6 (C_p) , 132.3 ($C_{n/s}$), 131.3 (C_e), 126.8 ($C_{d/f}$), 126.4 ($C_{d/f}$) , 124.8 (C_o), 123.8 ($C_{q/r}$), 61.5 ($C_{a/k}$), 39.5 (C_b), 37.2 (C_l), 33.9 (C_h), 33.8 (C_u), 28.5 ($C_{i/v}$), 24.3 ($C_{j/w}$).

FTIR ν_{max} ATR (cm^{-1}): 2936 (aromatic νC-H), 1780 (imide -CO-N-CO-), 1704 (ester νC=O), 1387 (imide C-N stretch), 1189 (vs, C–F), 1164 (ester C-O-C), 1138 (imide ring deformation), 770.01 (imide ring deformation).

T_g (DSC): 79 °C. T_m (DSC): Not observed.

Inherent viscosity (η_{inh}, $CHCl_3$/TFE 6:1, *v:v*): 1. 26 $dL \cdot g^{-1}$.

8.7.7. NDI/HFDI Nonanedioyl-based copolymer

N,N′-bis-(2-hydroxyethyl)-naphthalenetetracarboxylic diimide (1.6051 g, 4.53 mmol), *N,N′*-bis(2-hydroxyethyl)-hexafluoroisopropylidene-diphthalic diimide (2.4450 g, 4.61 mmol), nonanedioyl dichloride (2.0541 g, 9.12 mmol). Synthesized by heating for 60 minutes at 120 °C. Yield: (2.14 g, 38%).

^{1}H NMR (400 MHz, Chloroform-*d*/TFA 9:1, *v:v*) δ_H 8.84 (s, $4H_e$), 7.99 (d, *J* = 8.0 Hz, $2H_{q/r}$), 7.94 – 7.79 (m, $4H_{q/r/o}$), 4.71 – 4.46 (m, $8H_{a/b}$), 4.39 (t, *J* = 4.9 Hz, $4H_l$), 4.04 (t, *J* = 5.0 Hz, $4H_k$), 2.44 – 2.23 (m, $8H_{h/u}$), 1.71 – 1.37 (m, $8H_{i/v}$), 1.37 – 1.06 (m, $12H_{j/w}$). ^{13}C NMR (101 MHz, Chloroform-*d*/TFE 9:1, *v:v*) δ_C 175.2 ($C_{g/t}$), 175.1 ($C_{g/t}$), 167.6 (C_m), 163.4 (C_c), 139.3 ($C_{n/s}$), 136.3 ($C_{q/r}$), 132.9 (C_p), 132.5 ($C_{n/s}$), 131.5 (C_e), 127.1 ($C_{d/f}$), 126.7 ($C_{d/f}$), 125.2 (C_o), 124.1 ($C_{q/r}$), 61.7 ($C_{a/k}$), 39.8 (C_b), 37.5 (C_l) , 34.3 (C_h), 34.2 (C_u), 29.0 ($C_{i/v}$), 24.7 ($C_{j/w}$). ^{19}F NMR (400 MHz, Chloroform-*d*/TFE 9:1, *v:v*) δ_F -63.52 (CF_3).

FTIR ν_{max} ATR (cm^{-1}): 2930 (aromatic νC-H), 1780 (imide -CO-N-CO-), 1706 (ester νC=O), 1387 (imide C-N stretch), 1189 (vs, C–F), 1161 (ester C-O-C), 1141 (imide ring deformation), 770 (imide ring deformation).

T_g (DSC): 80 °C. T_m (DSC): Not observed.

Inherent viscosity (η_{inh}, $CHCl_3$/TFE 6:1, v:v): 1. 20 $dL \cdot g^{-1}$.

8.7.8. NDI/HFDI Decanedioyl-based copolymer

N,N′-bis-(2-hydroxyethyl)-naphthalenetetracarboxylic diimide (1.6103 g, 4.54 mmol), *N,N′*-bis(2-hydroxyethyl)-hexafluoroisopropylidene-diphthalic diimide (2.4645 g, 4.65 mmol), decanedioyl dichloride (2.2019 g, 9.21 mmol). Synthesized by heating for 90 minutes at 120 °C. Yield: (2.86 g, 50%).

^{1}H NMR (400 MHz, Chloroform-*d*) δ 8.84 (s, $4H_e$), 8.11 – 7.95 (m, $2H_{q/r}$), 7.94 – 7.79 (m, $4H_{q/r/o}$), 4.70 – 4.47 (m, $8H_{a/b}$), 4.40 (t, *J* = 4.9 Hz, $4H_l$), 4.05 (t, *J* = 4.9 Hz, $4H_k$), 2.56 – 2.24 (m, $8H_{h/u}$), 1.75 – 1.42 (m, $8H_{i/v}$), 1.40 – 1.02 (m, $16H_{j/w}$). ^{13}C NMR (101 MHz, Chloroform-*d*/TFE 9:1, *v:v*) δ_C 174.8 $C_{g/t}$, 174.6 ($C_{g/t}$), 167.2 (C_m), 163.1 (C_c), 139.0 ($C_{n/s}$), 135.9 ($C_{q/r}$), 132.7 (C_p), 132.3 ($C_{n/s}$), 131.2 (C_e), 126.8 ($C_{d/f}$), 126.4 ($C_{d/f}$), 124.9 (C_o), 123.8 ($C_{q/r}$), 61.4 ($C_{a/k}$), 39.6 (C_b), 37.3 (C_l), 34.0 (C_h), 34.0 (C_u) , 28.9 ($C_{i/v}$), 24.5 ($C_{j/w}$).

FTIR ν_{max} ATR (cm^{-1}): 2928 (aromatic νC-H), 1780 (imide -CO-N-CO-), 1718 (ester νC=O), 1373 (imide C-N stretch), 1190 (vs, C–F), 1162 (ester C-O-C), 1152 (imide ring deformation), 771 (imide ring deformation).

T_g (DSC): 65 °C. T_m (DSC): Not observed.

Inherent viscosity (η_{inh}, $CHCl_3$/TFE 6:1, v:v): 1.37 $dL \cdot g^{-1}$.

8.8. NDI / BPDI-based copolymers

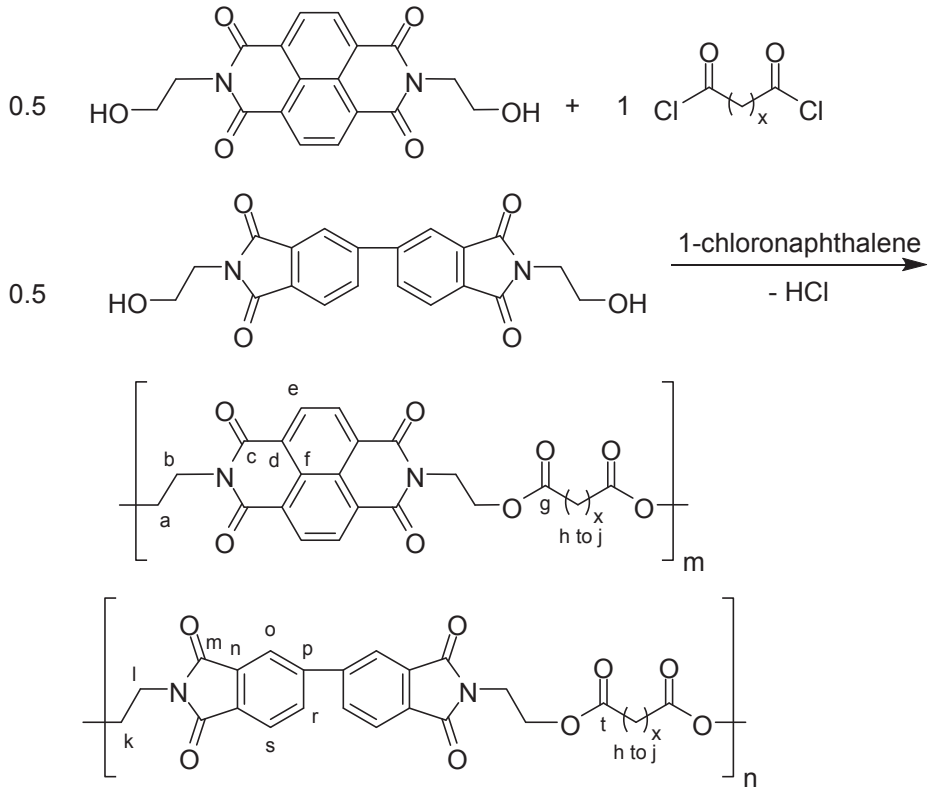

1-Chloronaphthalene (15 mL, distilled from CaH_2), *N,N′*-bis(2-hydroxyethyl)-naphthalene-tetracarboxylic diimide (dried at 100 °C for up to 24 hours), *N,N′*-bis(2-hydroxyethyl)-biphthalimide (dried at 120 °C for up to 24 hours) and a diacid chloride were combined at room temperature. The mixture was heated to 170 °C for 24 hours under N_2 atmosphere. After cooling to room temperature, the solidified product mixture was dissolved in 20 mL chloroform and precipitated dropwise into an excess of methanol (~ 400 mL). The precipitate was filtered off and dried at 80 °C for up to 24 hours. The reprecipitation was repeated three times to afford the pure polymer.

8.8.1. NDI/BPDI Butanedioyl-based copolymer

Monomers used: *N,N′*-bis-(2-hydroxyethyl)-naphthalenetetracarboxylic diimide (1.001 g, 2.8 mmol), *N,N′*-bis-(2-hydroxyethyl)-biphthalimide (1.0774 g, 2.8 mmol), butanedioyl dichloride (0.8946 g, 5.8 mmol). Yield: (1.9367 g, 75%).

^{1}H NMR (400 MHz, Chloroform-*d*/TFE 9:1 *v:v*) δ_H 8.82 (s, 4H), 8.18 (m, 2H$_o$), 8.15 – 7.91 (m, 4H$_{r/s}$), 4.65 – 4.21 (m, 12H$_{a/k/l}$), 4.04 (m, 4H$_b$), 2.66 (m, 8H$_h$). ^{13}C NMR (101 MHz, Chloroform-*d*/TFE 6:1 *v:v*) δ_C 173.0 (C$_g$), 172.8 (C$_u$), 168.1 (C$_m$), 163.3 (C$_c$), 145.5 (C$_{n/p/t}$), 133.4 (C$_e$), 133.1 (C$_{n/p/t}$), 131.7 (C$_{r/s}$), 131.4 (C$_{n/p/t}$), 127.0 (C$_{d/f}$), 126.6 (C$_{d/f}$), 124.5 (C$_{r/s}$), 122.5 (C$_e$), 74.6 (C$_a$), 62.0 (C$_k$), 39.6 (C$_b$), 37.2 (C$_l$), 28.8 (C$_h$).

FTIR ν_{max} ATR (cm^{-1}): 2958 (aromatic νC-H), 1772 (imide -CO-N-CO-), 1705 (ester νC=O), 1386 (imide C-N stretch), 1189 (ester C-O-C), 1151 (imide ring deformation), 769 (imide ring deformation).

T_g (DSC): 125 °C. T_m (DSC): Not observed.

Inherent viscosity (η_{inh}, $CHCl_3$/TFE 6:1): 0.98 d·Lg^{-1}.

8.8.2. NDI/BPDI Pentanedioyl-based copolymer

Monomers used: *N,N′*-bis-(2-hydroxyethyl)-naphthalenetetracarboxylic diimide (1.0000 g, 2.82 mmol), *N,N′*-bis-(2-hydroxyethyl)-biphthalimide (1.0735 g, 2.82 mmol), pentanedioyl dichloride (0.9773 g, 5.78 mmol). Yield: (1.6243 g, 61%).

^{1}H NMR (400 MHz, Chloroform-*d*/TFE 9:1 *v:v*) δ_H 9.00 – 8.57 (m, 4H$_e$), 8.17 (m, 2H$_o$), 8.03 (s, 4H$_{r/s}$), 4.72 – 4.27 (m, 12H$_{a/k/l}$), 4.20 – 3.85 (m, 4H$_b$), 2.54 – 2.19 (m, 8H$_h$), 1.87 (s, 4H$_i$). ^{13}C NMR (101 MHz, Chloroform-*d*/TFE 9:1 *v:v*) δ_C 173.6 (C$_g$), 173.5 (C$_u$), 167.9 (C$_m$), 163.1 (C$_c$), 145.3 (C$_{n/p/t}$), 133.3 (C$_e$), 132.9 (C$_{n/p/t}$), 131.5 (C$_{r/s}$), 131.2 (C$_{n/p/t}$), 126.7 (C$_{d/f}$), 126.4 (C$_{d/f}$), 124.3 (C$_{r/s}$), 122.3 (C$_e$), 77.2 (C$_a$), 74.4 (C$_k$), 39.5 (C$_b$), 37.1 (C$_l$), 32.8 (C$_h$), 19.4 (C$_i$).

FTIR ν_{max} ATR (cm^{-1}): 2958 (aromatic νC-H), 1772 (imide -CO-N-CO-), 1706 (ester νC=O), 1387 (imide C-N stretch), 1191 (ester C-O-C), 1148 (imide ring deformation), 769 (imide ring deformation).

T_g (DSC): 96 °C. T_m (DSC): not observed.

Inherent viscosity (η_{inh}, $CHCl_3$/TFE 6:1): 1.31 dL·g^{-1}.

8.8.3. NDI/BPDI Hexanedioyl-based copolymer

Monomers used: *N,N′*-bis-(2-hydroxyethyl)-naphthalenetetracarboxylic diimide (1.0045 g, 2.84 mmol), *N,N′*-bis-(2-hydroxyethyl)-biphthalimide (1.0763 g, 2.83 mmol), hexanedioyl dichloride (1.0583 g, 5.78 mmol). Yield: (1.94 g, 70%).

^{1}H NMR (400 MHz, Chloroform-*d*/TFA 9:1, *v:v*) δ 8.83 (s, 4H$_e$), 8.19 (s, 2H$_o$), 8.05 (s, 4H$_{r/s}$), 4.55 (m, 12H$_{a/k/l}$), 4.19 – 3.92 (m, 4H$_b$), 2.37 (m, 8H$_h$), 1.59 (m, 8H$_i$). ^{13}C NMR (101 MHz, Chloroform-*d*/TFE 9:1 *v:v*) δ$_C$ 174.3 (C$_g$), 174.2 (C$_u$), 168.1 (C$_m$), 163.3 (C$_c$), 145.5 (C$_{n/p/t}$), 133.5 (C$_e$), 133.1 (C$_{n/p/t}$), 131.7 (C$_{r/s}$), 131.5 (C$_{n/p/t}$), 127.0 (C$_{d/f}$), 126.6 (C$_{d/f}$), 124.5 (C$_{r/s}$), 122.5 (C$_e$), 74.6 (C$_a$), 61.8 (C$_k$), 39.7 (C$_b$), 37.4 (C$_l$), 33.7 (C$_h$), 24.1 (C$_i$).

FTIR ν$_{max}$ ATR (cm^{-1}): 2962 (aromatic νC-H), 1773 (imide -CO-N-CO-), 1708 (ester νC=O), 1387 (imide C-N stretch), 1192 (ester C-O-C), 1164 (imide ring deformation), 770 (imide ring deformation).

T$_g$ (DSC): 95 °C. T$_m$ (DSC): Not observed.

Inherent viscosity (η$_{inh}$, $CHCl_3$/TFE 6:1): 0.84 dL.g^{-1}.

8.8.4. NDI/BPDI Heptanedioyl-based copolymer

Monomers used: *N,N'*-bis-(2-hydroxyethyl)-naphthalenetetracarboxylic diimide (1.1107 g, 3.13 mmol), *N,N'*-bis-(2-hydroxyethyl)-biphthalimide (1.1989 g, 3.15 mmol), heptanedioyl dichloride (1.3058 g, 6.62 mmol). Yield: (2.1597 g, 47%).

^{1}H NMR (400 MHz, Chloroform-d/TFA 9:1, *v:v*) δ$_H$ 8.82 (s, 4H$_e$), 8.26 – 8.13 (m, 2H$_o$), 8.13 – 7.94 (m, 4H$_{r/s}$), 4.71 – 4.32 (m, 12H$_{a/k/l}$), 4.19 – 3.96 (m, 4H$_b$), 2.46 – 2.20 (m, 8H$_h$), 1.78 – 1.43 (m, 8H$_i$), 1.43 – 1.14 (m, 4H$_j$). ^{13}C NMR (101 MHz, Chloroform-*d*/TFE 9:1 *v:v*) δ$_C$ 174.5 (C$_g$), 174.4 (C$_u$), 168.1 (C$_m$), 163.2 (C$_c$), 145.5 (C$_{n/p/t}$), 133.5 (C$_e$), 133.8 (C$_{n/p/t}$), 131.7 (C$_{r/s}$), 131.4 (C$_{n/p/t}$), 127.0 (C$_{d/f}$), 126.6 (C$_{d/f}$), 124.5 (C$_{r/s}$), 122.5 (C$_e$), 77.4 (C$_a$), 74.5 (C$_k$), 39.7 (C$_b$), 37.4 (C$_l$), 33.9 (C$_h$), 28.5 (C$_i$), 24.3 (C$_j$).

FTIR ν$_{max}$ ATR (cm^{-1}): 2938 (aromatic νC-H), 1772 (imide -CO-N-CO-), 1705 (ester νC=O), 1385 (imide C-N stretch), 1191 (ester C-O-C), 1160 (imide ring deformation), 769 (imide ring deformation).

T$_g$ (DSC): 90 °C. T$_m$ (DSC): Not observed.

Inherent viscosity (η$_{inh}$, $CHCl_3$/TFE 6:1): 0.19 dL·g^{-1}.

PMDI-based *co*-poly(ester-imide)s

PMDI/BPDI heptanedioyl-based *co*-poly(ester-imide)s

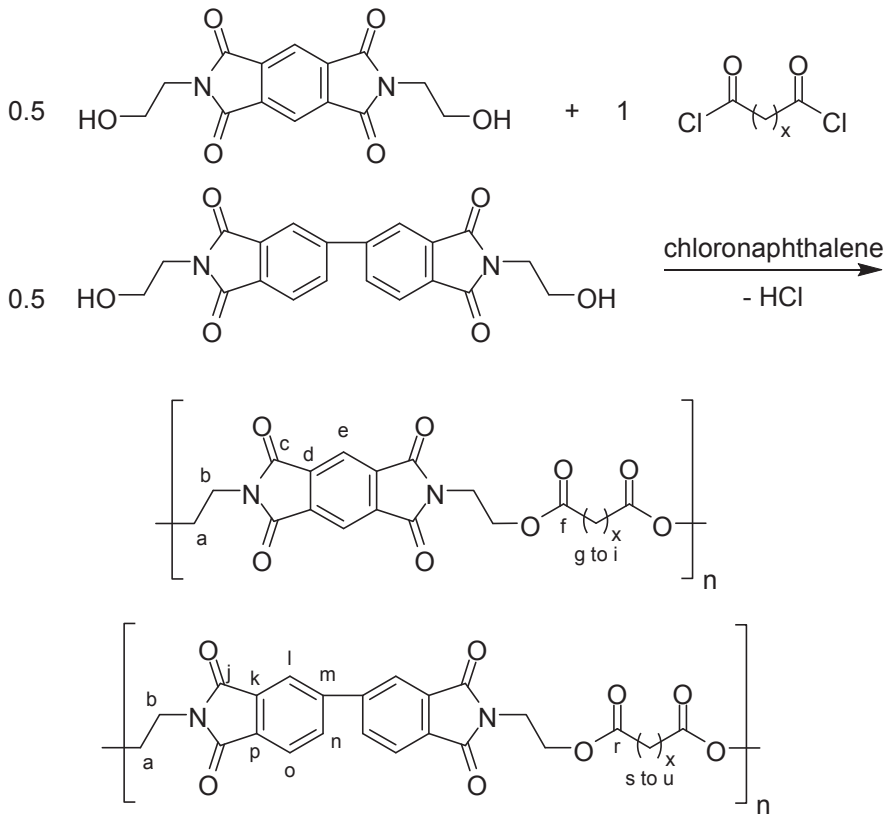

1-Chloronaphthalene (4.5 mL, distilled from CaH_2), *N,N′*-bis(2-hydroxyethyl)pyromellitic diimide (1.05 g, 3.46 mmol, dried at 120 °C for up to 24 hours before use), *N,N′*-bis-(2-hydroxyethyl)-biphthalimide (1.31 g, 3.46 mmol, dried at 120 °C for up to 24 hours before use) and heptanedioyl dichloride (1.39 g, 7.05 mmol) were mixed at room temperature. The mixture was heated to 170 °C for 24 hours under N_2 atmosphere. After cooling to room temperature, the solidified product mixture was dissolved in 20 mL of chloroform and precipitated dropwise into an excess of methanol (~ 400 mL). The precipitate was filtered and dried at 80 °C for up to 24 hours. The reprecipitation was repeated three times to afford the pure polymer. Yield: 2.49 g, 75%.

^{1}H NMR (400 MHz, Chloroform-*d*/TFA 9:1, *v:v*) δ_H 8.36 (s, 2H), 8.19 (s, 2H), 8.05 (m, 4H), 4.43 (m, 8H), 4.08 (m, 8H), 2.35 (m, 9H), 1.61 (m, 8H), 1.30 (m, 8.2 Hz, 4H). ^{13}C NMR (101 MHz, Chloroform-*d*) δ 174.3 (C_jB/P), 168.1 (C_cB), 166.3 (C_cP), 145.5 ($C_{d/f/i}B$), 137.3 (C_dP), 133.5 ($C_{d/f/i}B$), 133.1 ($C_{g/h}B$), 131.7 ($C_{d/f/i}B$), 124.5 ($C_{g/h}B$), 122.5 (C_eB), 118.7 (C_eP), 61.6 (C_aB/P), 37.9 (C_bB), 37.4 (C_bP), 33.9 (C_g), 28.4 (C_lB), 24.3 (C_iP).

FTIR ν_{max} ATR (cm^{-1}): 2941 (aromatic νC-H), 1773 (imide -CO-N-CO-), 1708 (ester νC=O), 1385 (imide C-N stretch), 1191 (ester C-O-C), 1156 (imide ring deformation), 741 (imide ring deformation).

Inherent viscosity (η_{inh}, $CHCl_3$): 0.36 $dL \cdot g^{-1}$.

8.8.5. PMDI/HFDI heptanedioyl-based copolymer

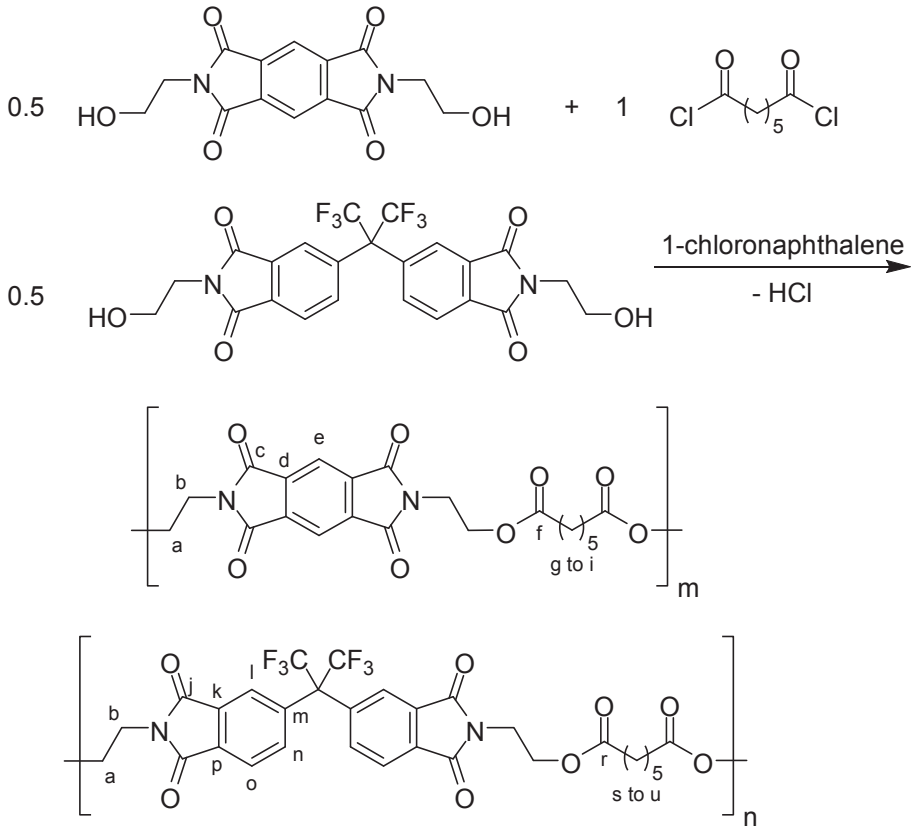

1-Chloronaphthalene (6 mL, distilled from CaH_2), *N,N′*-bis(2-hydroxyethyl)pyromellitic diimide (0.78 g, 2.56 mmol, dried at 120 °C for up to 24 hours before use), *N,N′*-bis(2-hydroxyethyl)-hexafluoroisopropylidene diphthalic diimide (1.34 g, 2.52 mmol, dried at 120 °C for up to 24 hours before use) and heptanedioyl dichloride (1.00 g, 5.09 mmol) were mixed at room temperature. The mixture was heated to 170 °C for 24 hours under N_2 atmosphere. After

cooling to room temperature, the solidified product mixture was dissolved in 15 mL chloroform and precipitated dropwise into an excess of methanol (~ 400 mL). The precipitate was filtered and dried at 80 °C for up to 24 hours. The reprecipitation was repeated three times to afford the pure polymer. Yield: 2.45 g, 86%.

^{1}H NMR (400 MHz, Chloroform-*d*) δ_H 8.29 (s, 2H$_e$), 8.12 (s, 2H$_l$), 8.00 (m, 4H$_{n/o}$), 4.34 (m, 8H$_b$), 3.99 (m, 8H$_a$), 2.25 (m, 8H$_{g/s}$), 1.55 (m, 8H$_{h/t}$), 1.28 (m, 4H$_{i/u}$). ^{13}C NMR (101 MHz, Chloroform-*d*) δ_C 173.3 (C$_{f/r}$), 173.3 (C$_{f/r}$), 167.5 (C$_j$), 165.9 (C$_c$), 145.2 (C$_{k/p}$), 137.2 (C$_d$), 133.1 (C$_{n/o}$), 133.1 (C$_m$), 131.8 (C$_{k/p}$), 124.2 (C$_{n/o}$), 122.3 (C$_l$), 118.5 (C$_e$), 61.3 (C$_b$), 61.1 (C$_b$), 37.9 (C$_a$), 37.4 (C$_a$), 33.7 (C$_{g/s}$), 28.4 (C$_{h/t}$), 24.2 (C$_{i/u}$).

Inherent viscosity (η_{inh}, $CHCl_3$): 0.27 dL·g^{-1}.

8.9. All-aliphatic *co*-poly(ester-imide)s

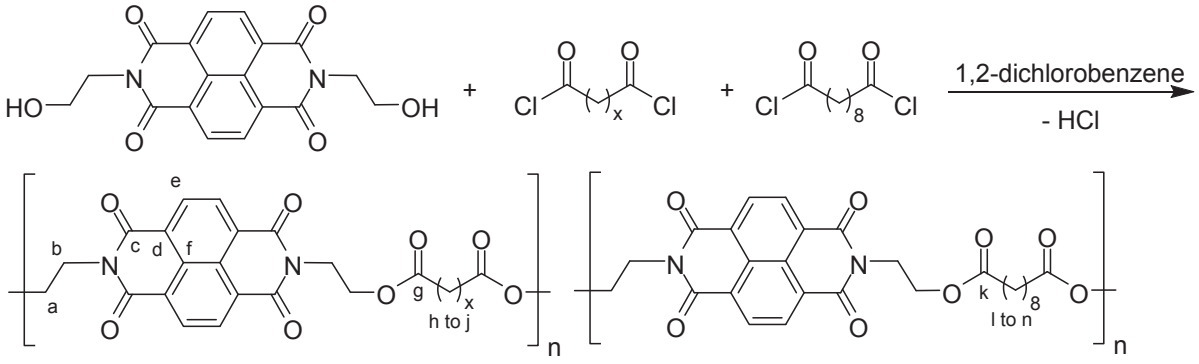

1,2-Dichlorobenzene (1.5 mL, distilled from CaH_2), *N,N′*-bis-(2-hydroxyethyl)-naphthalenetetracarboxylic diimide (dried at 100 °C for up to 24 hours) and an acid chloride were mixed at room temperature. The mixture was heated under N_2 atmosphere (temperature and time given below). After cooling to room temperature, the product was dissolved in 20 mL dichloromethane/hexafluoroisopropanol (2:1, *v/v*) and precipitated dropwise into an excess of methanol (~ 400 mL). The precipitate was filtered and dried at 80 °C for 24 hours. The reprecipitation was repeated three times to afford the pure polymer.

8.9.1. NDI *x* = 1/8 copolymer

Monomers used: *N,N′*-bis-(2-hydroxyethyl)-naphthalenetetracarboxylic diimide (0.6855 g, 1.9 mmol), propanedioyl dichloride (0.1374 g, 1.0 mmol), decanedioyl dichloride (0.2358 g, 1.0 mmol). Heated for 120 minutes to 110 °C. Yield: (0.63 g, 69%).

^{1}H NMR (400 MHz, Chloroform- *d*/TFA 9:1 *v:v*) δ_H 8.83 (s, 8H$_e$), 4.78 – 4.36 (m, 16H$_{a/b}$), 3.47 (s, 2H$_h$), 2.34 (t, *J* = 7.6 Hz, 4H$_m$), 1.67 – 1.43 (m, 4H$_n$), 1.21 (m, 8H$_m$). ^{13}C NMR (101 MHz, Chloroform-/TFE 6:1) δ_C 176.4 (C$_g$), 167.5 (C$_k$), 163.5 (C$_c$), 131.5 (C$_e$), 126.8 (C$_{d/f}$), 126.3 (C$_{d/f}$), 63.0 (C$_a$), 61.7 (C$_a$), 39.5 (C$_b$), 39.2 (C$_b$), 34.0 (C$_l$), 28.7 (C$_h$), 24.4 (C$_m$).

FTIR ν_{max} ATR (cm^{-1}): 2929 (aromatic C-H), 1736 (imide -CO-N-CO-), 1704 (ester C=O), 1373 (imide C-N stretch), 1191 (ester C-O-C), 1164 (imide ring deformation), 768 (imide ring deformation).

T_g (DSC): 72 °C. T_m (DSC): Not observed.

Inherent viscosity (η_{inh}, $CHCl_3$/TFE 6:1, *v:v*): 0.43 dL·g^{-1}.

8.9.2. NDI *x* = 2/8 copolymer

Monomers used: *N,N′*-bis-(2-hydroxyethyl)-naphthalenetetracarboxylic diimide (0.9932 g, 2.8 mmol), butanedioyl dichloride (0.2165 g, 1.4 mmol), decanedioyl dichloride (0.3375 g, 1.4 mmol). Heated for 35 minutes to 130 °C. Yield: (0.91 g, 68%).

^{1}H NMR (400 MHz, Chloroform-*d*/TFA 9:1 *v:v*) δ_H 8.83 (s, 8H$_e$), 4.71 – 4.37 (m, 16H$_{a/b}$), 2.65 (s, 4H$_h$), 2.33 (t, *J* = 7.7 Hz, 4H$_m$), 1.66 – 1.43 (m, 4H$_n$), 1.23 (m, 8H$_m$). ^{13}C NMR (101 MHz, Chloroform-*d*/TFE 6:1) δ_C 175.0 (C$_g$), 172.9 (C$_k$), 163.1 (C$_c$), 131.2 (C$_e$), 126.7 (C$_{d/f}$), 126.4 (C$_{d/f}$), 61.8 (C$_a$), 61.4 (C$_a$), 39.5 (C$_b$), 39.4 (C$_b$), 34.0 (C$_l$), 28.9 (C$_h$), 28.7 (C$_m$), 24.5 (C$_n$).

FTIR ν_{max} ATR (cm^{-1}): 2930 (aromatic νC-H), 1735 (imide -CO-N-CO-), 1706 (ester νC=O), 1372 (imide C-N stretch), 1188 (ester C-O-C), 1156 (imide ring deformation), 767 (imide ring deformation).

T_g (DSC): 107 °C. T_m (DSC): Not observed.

Inherent viscosity (η_{inh}, $CHCl_3$/TFE 6:1, *v:v*): 0.53 dL·g^{-1}.

8.9.3. NDI *x* = 3/8 copolymer

Monomers used: *N,N′*-bis-(2-hydroxyethyl)-naphthalenetetracarboxylic diimide (0.9805 g, 2.8 mmol), pentanedioyl dichloride (0.2338 g, 1.4 mmol), decanedioyl dichloride (0.3309 g, 1.4 mmol). Heated for 60 minutes to 130 °C. Yield: (1.25 g, 93%).

^{1}H NMR (400 MHz, Chloroform-*d*/TFA 9:1 *v:v*) δ_H 8.85 (s, 8H$_e$), 4.79 – 4.37 (m, 16H$_{a/b}$), 2.41 (t, *J* = 7.4 Hz, 8H$_h$), 2.34 (t, *J* = 7.7 Hz, 8H$_l$), 1.88 (m, 2H$_i$), 1.54 (m, 4H$_m$), 1.22 (m, 8H$_n$). ^{13}C NMR (101 MHz, Chloroform-*d*/TFE 6:1) δ_C 174.0 (C$_g$), 173.1 (C$_k$), 162.8 (C$_c$), 131.1 (C$_e$), 126.7 (C$_{d/f}$), 126.4 (C$_{d/f}$) , 61.3 (C$_a$), 61.0 (C$_a$), 39.6 (C$_b$), 34.0 (C$_l$), 32.9 (C$_h$), 29.0 (C$_m$), 24.6 (C$_i$), 19.5 (C$_n$).

FTIR ν_{max} ATR (cm^{-1}): 2929 (aromatic νC-H), 1736 (imide -CO-N-CO-), 1706 (ester νC=O), 1372 (imide C-N stretch), 1193 (ester C-O-C), 1164 (imide ring deformation), 768 (imide ring deformation).

T_g (DSC): 71 °C. T_m (DSC): Not observed.

Inherent viscosity (η_{inh}, $CHCl_3$/TFE 6:1, *v:v*): 0.64 dL·g-1.

8.9.4. NDI *x* = 4/8 copolymer

Monomers used: *N,N′*-bis-(2-hydroxyethyl)-naphthalenetetracarboxylic diimide (0.7349 g, 2.0 mmol), hexanedioyl dichloride (0.1873 g, 1.0 mmol), decanedioyl dichloride (0.2488 g, 1.0 mmol). Heated for 40 minutes to 160 °C. Yield: (0.86 g, 84%).

^{1}H NMR (400 MHz, Chloroform-*d*/TFA 9:1 *v:v*) δ_H 8.83 (s, 8H$_e$), 4.69 – 4.41 (m, 16H$_{a/b}$), 2.54 – 2.11 (m, 8H$_{h/l}$), 1.74 – 1.41 (m, 8H$_{i/m}$), 1.36 – 1.10 (m, 8H$_{j/n}$). ^{13}C NMR (101 MHz, Chloroform-*d*/TFE 6:1) δ_C 175.0 (C$_g$), 174.2 (C$_k$), 163.1 (C$_c$), 131.3 (C$_e$), 126.8 (C$_{d/f}$), 126.4 (C$_{d/f}$), 61.8 (C$_a$), 61.4 (C$_a$), 39.5 (C$_b$), 34.0 (C$_l$), 33.5 (C$_h$), 28.9 (C$_m$), 24.5 (C$_n$), 23.8 (C$_j$).

FTIR ν_{max} ATR (cm^{-1}): 2930 (aromatic νC-H), 1731 (imide -CO-N-CO-), 1703 (ester νC=O), 1372 (imide C-N stretch), 1190 (ester C-O-C), 1145 (imide ring deformation), 768 (imide ring deformation).

T_g (DSC): 73 °C. T_m (DSC): Not observed.

Inherent viscosity (η_{inh}, $CHCl_3$/TFE 6:1, *v:v*): 3.09 dL·g^{-1}.

8.9.5. NDI *x* = 5/8 copolymer

Monomers used: *N,N′*-bis-(2-hydroxyethyl)-naphthalenetetracarboxylic diimide (0.7574 g, 2.1 mmol), heptanedioyl dichloride (0.2134 g, 1.1 mmol), decanedioyl dichloride (0.2560 g, 1.1 mmol). Heated for 60 minutes to 130 °C. Yield: (0.91 g, 86%).

^{1}H NMR (400 MHz, Chloroform-*d*/TFA 9:1 *v:v*) δ_H 8.84 (s, 8H$_e$), 4.66 – 4.44 (m, 16H$_{a/b}$), 2.33 (t, *J* = 7.5 Hz, 8H$_{h/l}$), 1.64 – 1.46 (m, 8H$_{i/m}$), 1.35 – 1.13 (m, 10H$_{j/n}$). ^{13}C NMR (101 MHz, Chloroform-*d*) δ_C 175.3 (C$_g$), 174.9 (C$_k$), 163.4 (C$_c$), 131.5 (C$_e$), 127.0 (C$_{d/f}$), 126.7 (C$_{d/f}$), 61.8 (C$_a$), 61.7 (C$_a$), 39.8 (C$_b$), 34.3 (C$_l$), 34.0 (C$_h$), 29.1 (C$_m$), 28.5 (C$_i$), 24.8 (C$_n$), 24.4 (C$_j$).

FTIR ν_{max} ATR (cm^{-1}): 2929 (aromatic νC-H), 1732 (imide -CO-N-CO-), 1705 (ester νC=O), 1372 (imide C-N stretch), 1189 (ester C-O-C), 1159 (imide ring deformation), 766 (imide ring deformation).

T_g (DSC): 68 °C. T_m (DSC): Not observed.

Inherent viscosity (η_{inh}, $CHCl_3$/TFE 6:1, *v:v*): 1.76 dL·g^{-1}.

8.9.6. NDI *x* = 6/8 copolymer

Monomers used: *N,N′*-bis-(2-hydroxyethyl)-naphthalenetetracarboxylic diimide (1.1170 g, 3.1 mmol), octanedioyl dichloride (0.3357 g, 1.6 mmol), decanedioyl dichloride (0.3770 g, 1.6 mmol). Heated for 40 minutes to 160 °C. Yield: (1.58 g, 99%).

^{1}H NMR (400 MHz, Chloroform-*d*/TFA 9:1 *v:v*) δ_H 8.83 (s, 8H$_e$), 4.68 – 4.42 (m, 16H$_{a/b}$), 2.43 – 2.23 (m, 8H$_{h/l}$), 1.64 – 1.43 (m, 8H$_{i/m}$), 1.34 – 1.12 (m, 12H$_{j/n}$). ^{13}C NMR (101 MHz, Chloroform-*d*/TFE 6:1 *v:v*) δ_C 175.0 (C$_g$), 174.8 (C$_k$), 163.1 (C$_c$), 131.2 (C$_e$), 126.8 (C$_{d/f}$), 126.4 (C$_{d/f}$), 61.4 (C$_a$), 39.5 (C$_b$), 34.0 (C$_l$), 33.9 (C$_h$), 28.9 (C$_m$), 28.5 (C$_i$), 24.5 (C$_n$), 24.3 (C$_j$).

FTIR ν_{max} ATR (cm^{-1}): 2935 (aromatic νC-H), 1734 (imide -CO-N-CO-), 1704 (ester νC=O), 1372 (imide C-N stretch), 1196 (ester C-O-C), 1146 (imide ring deformation), 771 (imide ring deformation).

T_g (DSC): 72 °C. T_m (DSC): 222 °C.

Inherent viscosity (η_{inh}, $CHCl_3$/TFE 6:1, *v:v*): 1.65 dL·g^{-1}.

8.9.7. NDI *x* = 7/8 copolymer

Monomers used: *N,N′*-bis-(2-hydroxyethyl)-naphthalenetetracarboxylic diimide (2.0915 g, 5.9 mmol), nonanedioyl dichloride (0.6694 g, 2.9 mmol), decanedioyl dichloride (0.7058 g, 2.9 mmol). Heated for 60 minutes to 120 °C. Yield: (2.62 g, 86%).

^{1}H NMR (400 MHz, Chloroform-*d*/TFA 9:1 *v:v*) δ_H 8.83 (s, 8H$_e$), 4.56 (m, 16H$_{a/b}$), 2.32 (m, 8H$_{h/l}$), 1.52 (m, 8H$_{i/m}$), 1.21 (m, 14H$_{j/n}$). ^{13}C NMR (101 MHz, Chloroform-*d*/TFE 6:1 *v:v*) δ_C 174.9 (C$_g$), 174.8 (C$_k$), 163.2 (C$_c$), 131.4 (C$_e$), 126.9 (C$_{d/f}$), 126.6 (C$_{d/f}$), 61.6 (C$_a$), 39.8 (C$_b$), 34.2 (C$_l$), 34.1 (C$_h$), 29.1 (C$_m$), 28.9 (C$_i$), 24.7 (C$_n$), 24.6 (C$_j$).

FTIR ν_{max} ATR (cm^{-1}): 2927 (aromatic νC-H), 1733 (imide -CO-N-CO-), 1703 (ester νC=O), 1372 (imide C-N stretch), 1196 (ester C-O-C), 1059 (imide ring deformation), 768 (imide ring deformation).

T_g (DSC): 58 °C. T_m (DSC): Not observed.

Inherent viscosity (η_{inh}, $CHCl_3$/TFE 6:1, *v:v*): 1.31 dL·g^{-1}.

8.10. Poly(ether imide)s

8.10.1. NDI / HFDI / EDEA-based copolymer

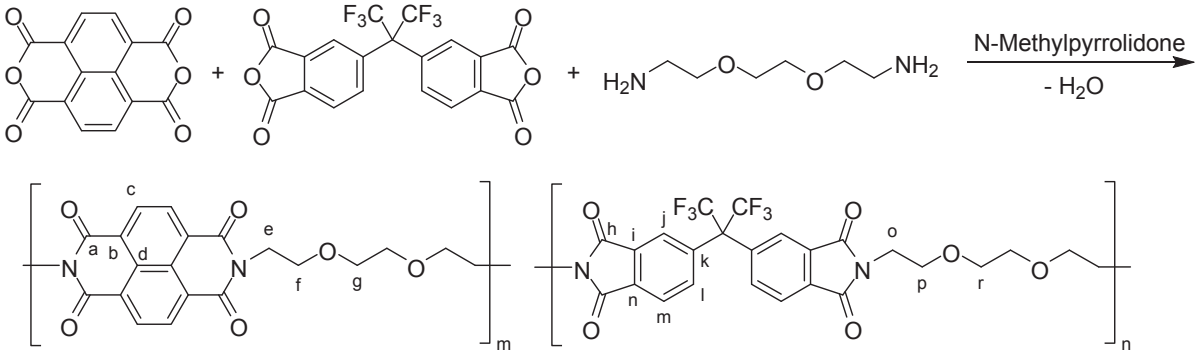

N-Methyl-2-pyrrolidone (40 mL), toluene (15 mL), 1,4,5,8-naphthalenetetracarboxylic dianhydride (2.6834 g, 10.01 mmol) and 4,4′-(hexafluoroisopropylidene)diphthalic anhydride (4.4700 g, 10.06 mmol) were dehydrated using a Dean–Stark apparatus under reflux. After cooling to room temperature, 2,2′-(ethylenedioxy)bis(ethylamine) (2.9746 g, 20.07 mmol) was added and the brown solution stirred at 40 °C for 8 h. The viscous solution was again dehydrated under reflux using the Dean–Stark apparatus for 16 h. The whole process was carried out under nitrogen atmosphere. The solvent was removed at reduced pressure and 125 °C within 30 minutes. The product was dissolved in 40 mL dichloromethane/hexafluoroisopropanol (6:1, *v/v*) and precipitated dropwise into an excess of methanol (~ 400 mL). Yield: 8.05 g, 85%.

^{1}H NMR (400 MHz, Chloroform-*d*) δ_H 8.78 (s, 4H), 7.93 (m, 2H$_c$), 7.86 (s, 2H), 7.79 (d, J = 8.2 Hz, 2H), 4.49 (m, 4H), 4.16 – 3.59 (m, 8H). ^{13}C NMR (101 MHz, Chloroform-*d*/HFIP 1:1) δ_C 178.5, 169.0, 164.2, 132.1, 131.7, 131.5, 126.2, 125.7, 124.9, 75.0, 73.2, 67.6, 50.7, 39.4, 37.0, 30.5, 29.2, 16.7.

FTIR ν_{max} ATR (cm^{-1}): 2867 (aromatic νC-H), 1704 (imide -CO-N-CO-), 1388 (aliphatic C-H rocking), 1331 (imide C-N stretch), 1242 (imide ring deformation), 1208 (C-O-C stretch), 766 (imide ring deformation).

8.10.2. NDI / DADD / EDEA-based copolymer

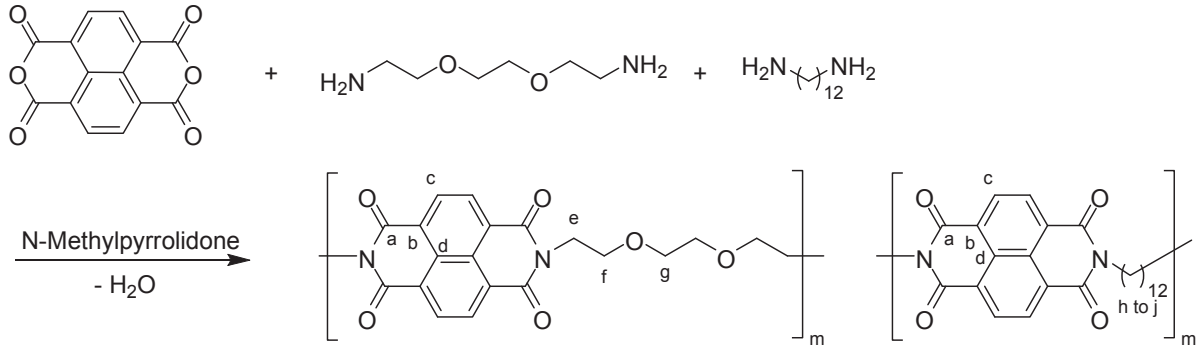

N-Methyl-2-pyrrolidone (20 mL), toluene (15 mL) and 1,4,5,8-naphthalenetetracarboxylic dianhydride (1.7356 g, 6.47 mmol) were dehydrated using a Dean–Stark apparatus under reflux. After cooling to room temperature, a solution of 20 mL NMP containing 2,2′-(ethylenedioxy)bis(ethylamine) (0.4878 g, 3.29 mmol) and 1,12-diaminododecane (0.6482 g, 3.24 mmol) was added and the brown solution stirred at 40 °C for 8 hours. The viscous solution was again dehydrated under reflux using the Dean–Stark apparatus for 16 hours. The whole process was carried out under nitrogen atmosphere. The solvent was removed at reduced pressure and 125 °C within 30 minutes. The product was precipitated into methanol, dissolved in 40 mL dichloromethane/hexafluoroisopropanol (1:1, *v/v*) and precipitated dropwise into an excess of methanol (~ 400 mL) again. Yield: 2.09 g, 74%.

^{1}H NMR (400 MHz, Chloroform-*d*) δ 8.96 – 8.50 (m, 8H$_c$), 4.47 (m, 4H$_e$), 4.21 (m, 4H$_h$), 3.95 (m, 4H$_f$), 3.86 (s, 4H$_g$), 1.74 (t, J = 7.9 Hz, 4H$_i$), 1.28 (s, 16H$_j$). ^{13}C NMR (101 MHz, Chloroform-*d*/HFIP 1:1) δ_C 164.2, 131.6, 126.7, 126.2, 120.7, 117.0, 69.5, 67.6, 39.4, 29.2, 29.0, 27.7, 26.7.

FTIR ν_{max} ATR (cm^{-1}): 2923 (aromatic C-H), 1705 (imide -CO-N-CO-), 1374 (aliphatic C-H rocking), 1333 (imide C-N stretch), 1243 (imide ring deformation), 1191 (C-O-C stretch), 767 (imide ring deformation).

Inherent viscosity (η_{inh}, $CHCl_3$/TFE 6:1, *v:v*): 1.66 $dL \cdot g^{-1}$.

8.11. Titrations

8.11.1. Titrations using pyrene

The following method has been adapted from the publication: J. S. Shaw, R. Vaiyapuri, M. P. Parker, C. A. Murray, K. J. C. Lim, C. Pan, M. Knappert, C. J. Cardin, B. W. Greenland, R. Grau-Crespo and H. M. Colquhoun, *Chem. Sci.*, 2018, **9**, 4052–4061.

In the following, an exemplary procedure is described. Equimolar stock solutions with exact concentrations of pyrene-d_{10} (24 mM) and a polymer (24 mM) with respect to the binding unit (see below) in $CDCl_3$/hexafluoropropan-2-ol (6 : 1 v/v) were prepared by weighing an approximate amount of pyrene-d_{10} or polymer, respectively, and adding the required volume of solvent via a micropipette. Copolymer solution (100 µL) was added to each NMR tube using a micropipette and varying volumes of pyrene solution were then added to the tubes (*e.g.* 100 µL for 1 : 1 molar ratio of pyrene to diimide). The NMR tubes were all then filled to 600 µL total volume with the required volume of solvent (*e.g.* 400 µL to the 1 : 1 solution) and were well-mixed, thus affording a constant diimide concentration of 4 mM in each tube.

In some cases, ratios higher than 1:5 (pyrene-d_{10} to polymer) were required. These were not obtainable by the above described procedure, and in this case a pyrene-d_{10} stock solution of higher concentration was used.

The molecular weight of the polymer binding unit was assumed to be two NDI-containing repeat units in the case of the homopolymers and a NDI-containing unit and a non-binding unit in case of the copolymers.

8.11.2. Titrations using perylene and anthracene

The solubility of perylene and anthracene in $CDCl_3$ and in $CDCl_3$ with co-solvents was found to be limited (about 3.5 mM for perylene in $CDCl_3$/HFIP, 1:1, *v:v*), and so a different titration method was developed which allowed solutions near the solubility limit of the aromatic hydrocarbon to be used. In the following, an exemplary procedure is described.

For a 3 mM solution of polymer and perylene each, a 3 mM solution of perylene was prepared by adding $CDCl_3$/HFIP (1:1, *v:v*) to an appropriate amount of perylene. Complete dissolution was observed after 16 h. In case of the NDI-based x = 5 homopolymer (478.457 g/mol per repeat unit, 956.914 g/mol per binding unit) an abitrary amount of the homopolymer was weighed in (e.g. 1.7 mg) and an appropriate amount of the 3 mM perylene solution was added (592 µL in this case) to obtain a 3 mM solution of polymer and perylene each. If a higher amount of polymer was weighed in (e. g. 1.9 mg) this was compensated by adding a larger amount of the 3 mM perylene solution (in this case 662 µL) so that a 3 mM solution of polymer and perylene each was still obtained. This method prevented the need for exact weighing of very small quantities of polymer.

Again, the molecular weight of the polymer binding unit was assumed to be two NDI-containing repeat units in case of the homopolymers and a NDI-containing unit and a non-binding unit in case of the copolymers.

8.12. Transesterification reactions

8.12.1. Transesterification of NDI homopolymer *x* = 3 / pentadecanolide

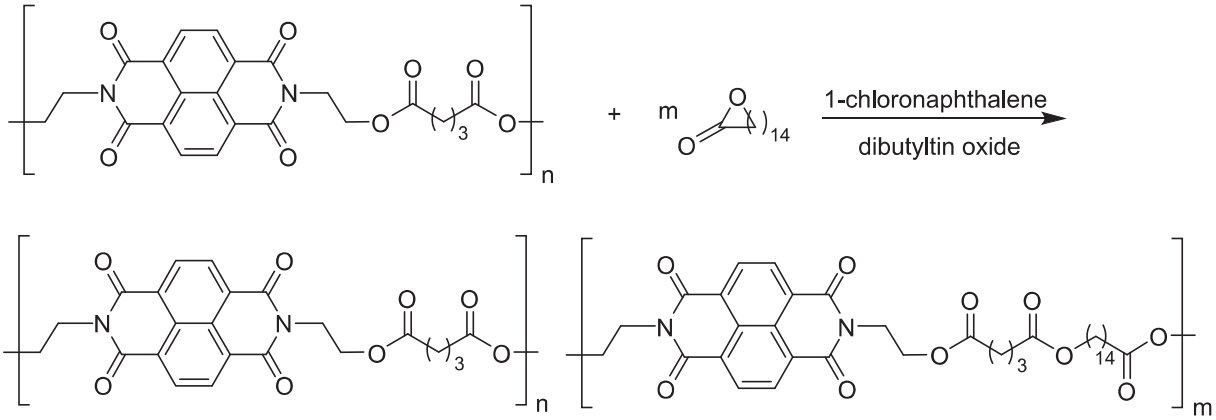

The NDI-based homopolymer (0.2103 g, 0.233 mmol repeat units, 900.806 g/mol per repeat unit), pentadecanolide (0.0561 g, 0.233 mmol, 240.38 g/mol), dibutyltin oxide (0.0054 g, 2 w %). and 1-chloronaphthalene (0.6 mL) were heated in a flask to 180 °C under nitrogen atmosphere. The reaction temperature was measured next to the flask at the heating block and confirmed with an external thermometer. The mixture was slowly stirred once the mixture had dissolved, as was apparent by liquifaction. Aliquots were taken at regular intervals under a nitrogen counterstream.

Each aliquot was treated separately as follows: Chloroform/trifluoroethanol (6:1 *v:v*, 4 mL) was added to the sample. Once dissolved, the mixture was precipitated into 100 mL cold methanol and filtered. The polymer was dried for 24 hours at room temperature. The precipitation was repeated until no 1-chloronaphthalene was detected by ^{1}H NMR.

The samples were individually analysed by ^{1}H NMR spectroscopy by a titration with pyrene (see 7.9).

8.12.2. Transesterification of NDI-based homopolymer / HFDI-based homopolymer

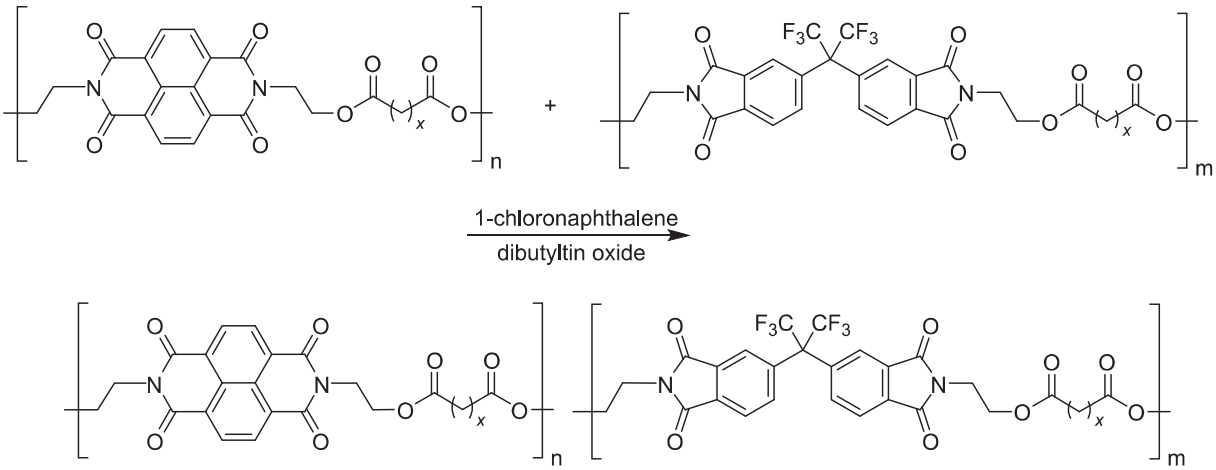

The homopolymer *NDI-homo x = 3* (2.03 g, 900.806 g/mol per repeat unit), the homopolymer *HFDI-homo x = 3* (2.7804 g, 1252.92 g/mol per repeat unit), dibutyltin oxide (0.09 g, 2 wt%). and 1-chloronaphthalene (10 mL) were partially homogenized in a mortar and then heated in a flask to 170 °C under nitrogen atmosphere. Once the mixture had liquified, it was slowly stirred.

Each aliquot was treated separately as follows: Chloroform/trifluoroethanol (6:1 *v:v*, 4 mL) was added to the sample. Once dissolved, the mixture was precipitated into 100 mL cold methanol and filtered. The polymer was dried for 24 hours at room temperature. The precipitation was repeated until no 1-chloronaphthalene was detected by ^{1}H NMR spectroscopy.

The samples were individually analysed by ^{1}H NMR spectroscopy by a titration with pyrene (see 7.11).

[1] Aradi, B., Hourahine, B., & Frauenheim, T. DFTB+, a sparse matrix-based implementation of the DFTB method. *J. Phys. Chem. A* 111 (2007) 5678–5684.

[2] Elstner, M., Porezag, D., Jungnickel, G., Elsner, J., Haugk, M., Frauenheim, T., & Seifert, G. Self-consistent-charge density-functional tight-binding method for simulations of complex materials properties. *Phys. Rev. B*, 58 (1998) 7260–7268.

[3] Zhechkov L., Heine, T., Patchkovskii, S., Seifert, G., & Duarte, H. A. An Efficient a Posteriori Treatment for Dispersion Interaction in Density-Functional-Based Tight Binding *J. Chem. Theory Comput.* 1 (2005) 841-847.

9 Appendix: IR data

9.1. NDI-based homo-poly(ester imide)s

9.1.1. Propanedioyl-based homopolymer

FTIR ν_{max} ATR (cm^{-1}): 2965 (aromatic νC-H), 1732 (imide -CO-N-CO-), 1704 (ester νC=O), 1371 (imide C-N stretch), 1188 (ester C-O-C), 1144 (imide ring deformation), 766 (imide ring deformation).

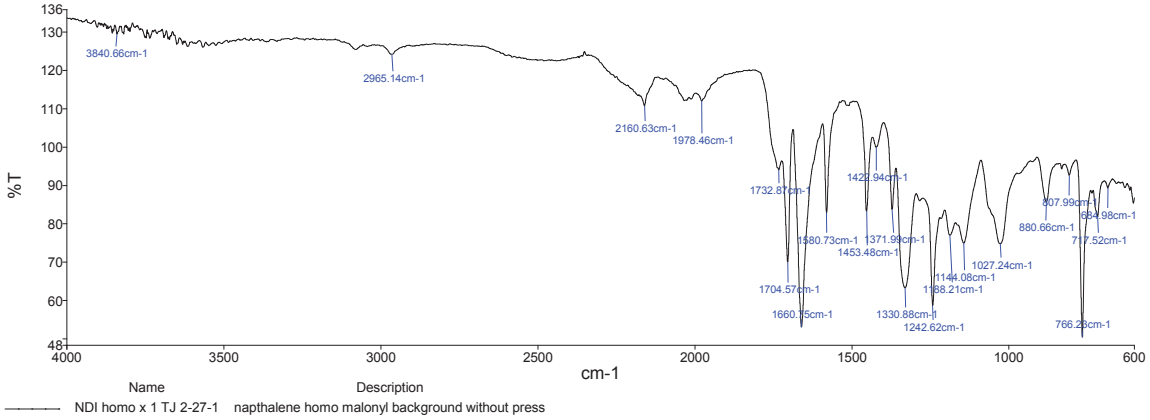

9.1.2. Butanedioyl-based homopolymer

FTIR ν_{max} ATR (cm^{-1}): 2966 (aromatic νC-H), 1732 (imide -CO-N-CO-), 1703 (ester νC=O), 1371 (imide C-N stretch), 1188 (ester C-O-C), 1146 (imide ring deformation), 765 (imide ring deformation).

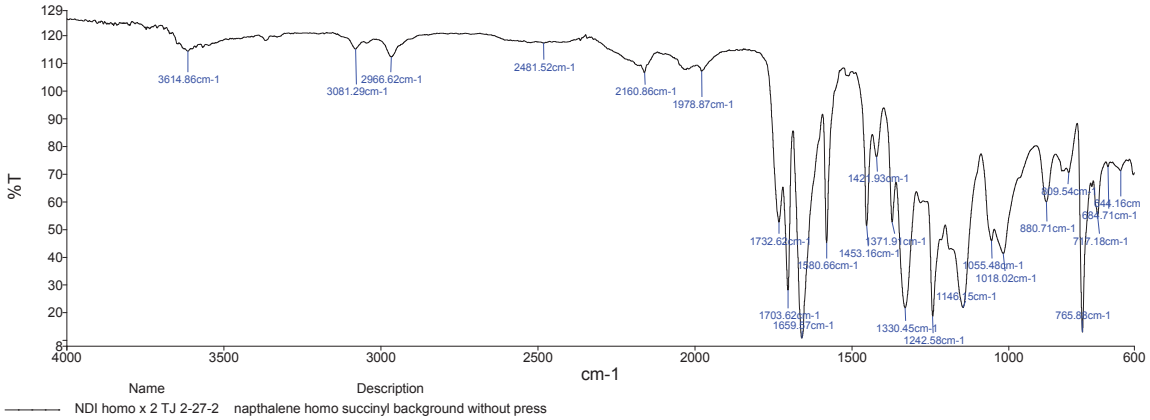

9.1.3. Pentanedioyl-based homopolymer

FTIR ν_{max} ATR (cm^{-1}): 2963 (aromatic νC-H), 1731 (imide -CO-N-CO-), 1703 (ester νC=O), 1372 (imide C-N stretch), 1189 (ester C-O-C), 1142 (imide ring deformation), 765 (imide ring deformation).

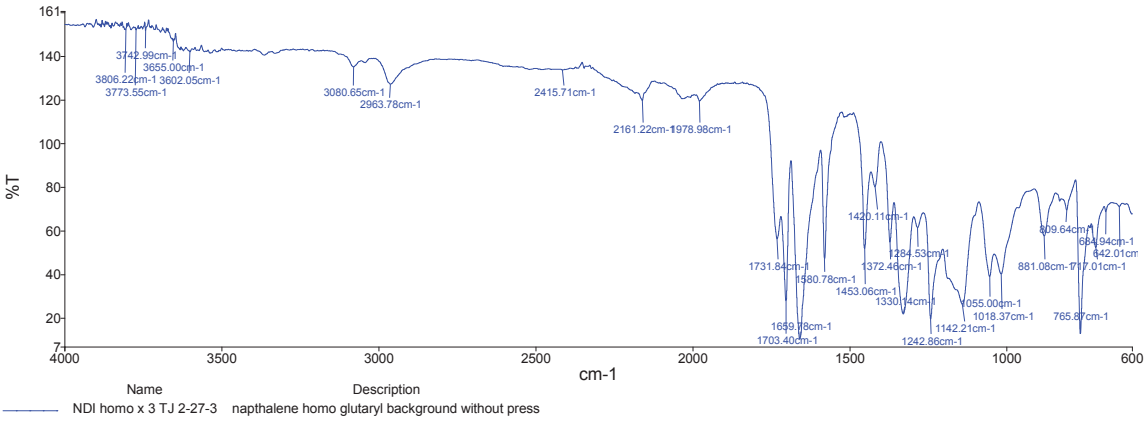

9.1.4. Hexanedioyl-based homopolymer

FTIR ν_{max} ATR (cm^{-1}): 2959 (aromatic νC-H), 1731 (imide -CO-N-CO-), 1703 (ester νC=O), 1372 (imide C-N stretch), 1192 (ester C-O-C), 1138 (imide ring deformation), 766 (imide ring deformation).

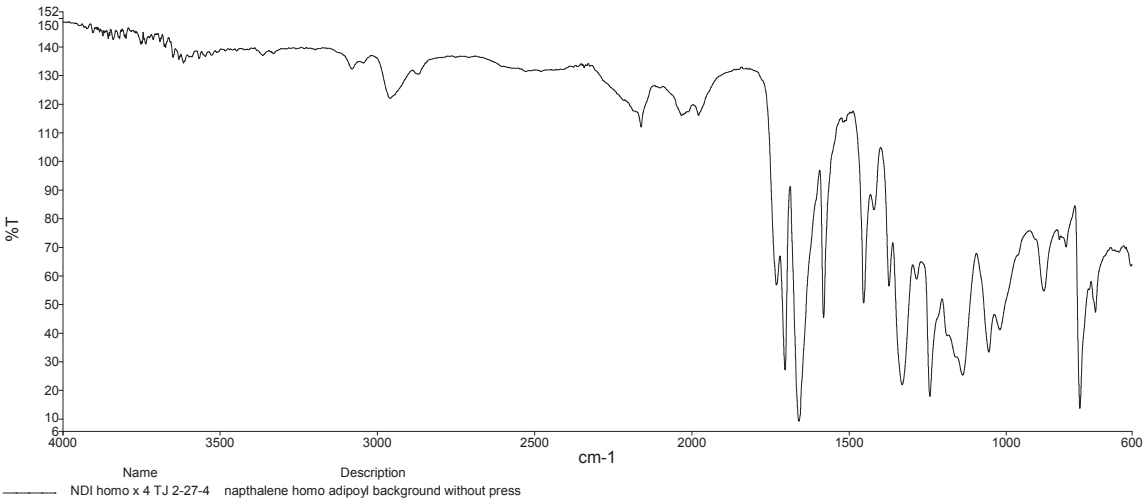

9.1.5. Heptanedioyl-based homopolymer

FTIR ν_{max} ATR (cm^{-1}): 2950 (aromatic νC-H), 1731.72 (imide -CO-N-CO-), 1703 (ester νC=O), 1372 (imide C-N stretch), 1192 (ester C-O-C), 1160 (imide ring deformation), 766 (imide ring deformation).

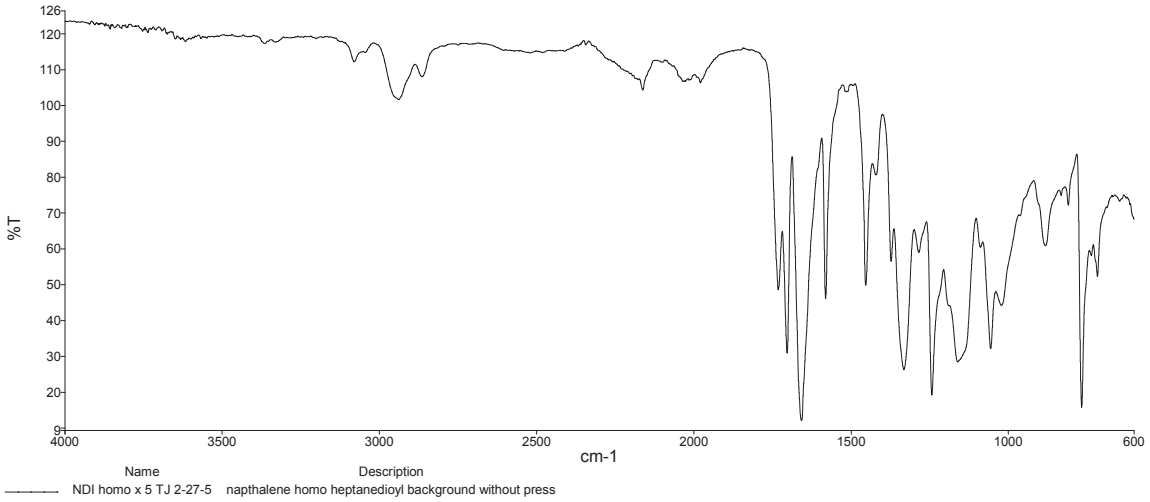

9.1.6. Octanedioyl-based homopolymer

FTIR ν_{max} ATR (cm^{-1}): 2935 (aromatic νC-H), 1731 (imide -CO-N-CO-), 1703 (ester νC=O), 1373 (imide C-N stretch), 1161 (ester C-O-C), 1154 (imide ring deformation), 766 (imide ring deformation).

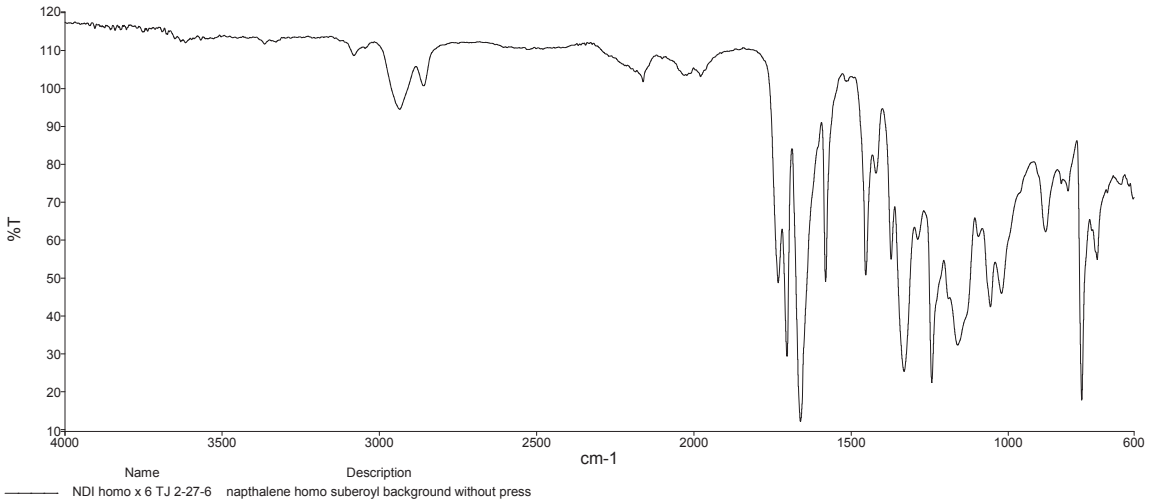

9.1.7. Nonanedioyl-based homopolymer

FTIR ν_{max} ATR (cm^{-1}): 2933 (aromatic νC-H), 1732 (imide -CO-N-CO-), 1704 (ester νC=O), 1373 (imide C-N stretch), 1156 (ester C-O-C), 1154 (imide ring deformation), 766 (imide ring deformation).

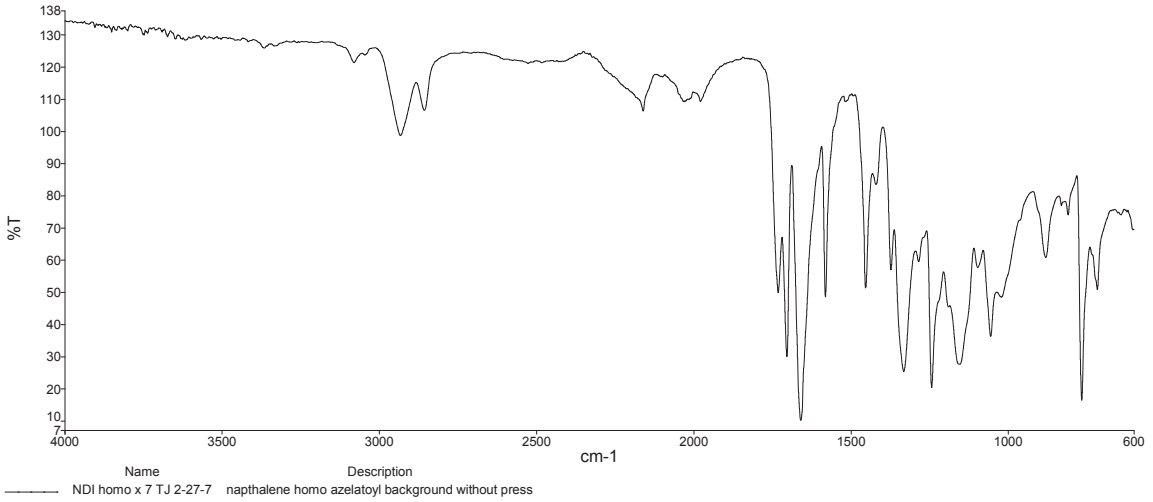

9.1.8. Decanedioyl-based homopolymer

FTIR ν_{max} ATR (cm^{-1}): 2929 (aromatic νC-H), 1732 (imide -CO-N-CO-), 1704 (ester νC=O), 1373 (imide C-N stretch), 1156 (ester C-O-C), 1154 (imide ring deformation), 766 (imide ring deformation).

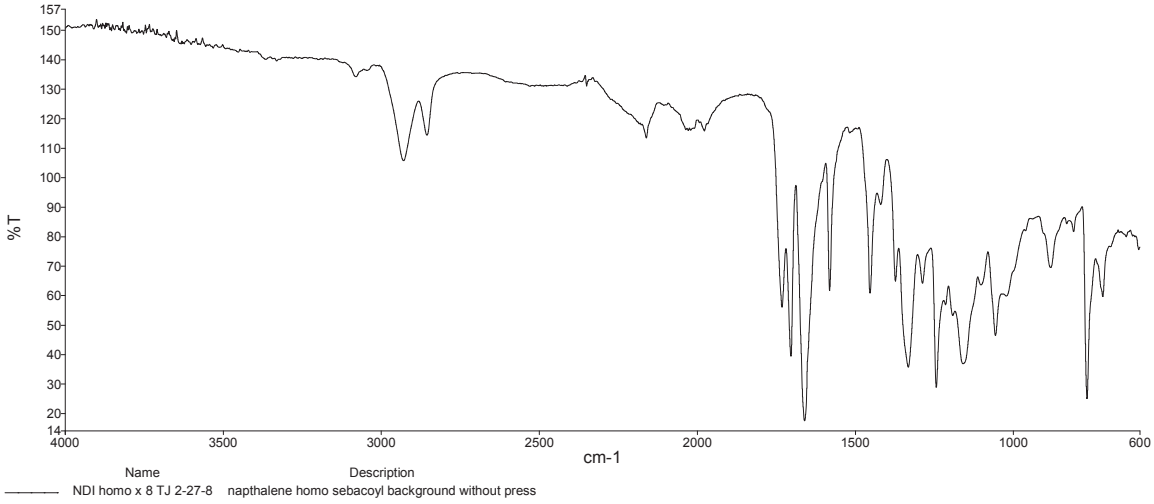

9.2. PMDI-based homo-poly(ester imide)s

9.2.1. Propanedioyl-based homopolymer

FTIR ν_{max} ATR (cm^{-1}): 2949 (aromatic νC-H), 1696 (imide -CO-N-CO-, ester νC=O), 1397 (imide C-N stretch), 1154 (ester C-O-C), 1048 (imide ring deformation), 728 (imide ring deformation).

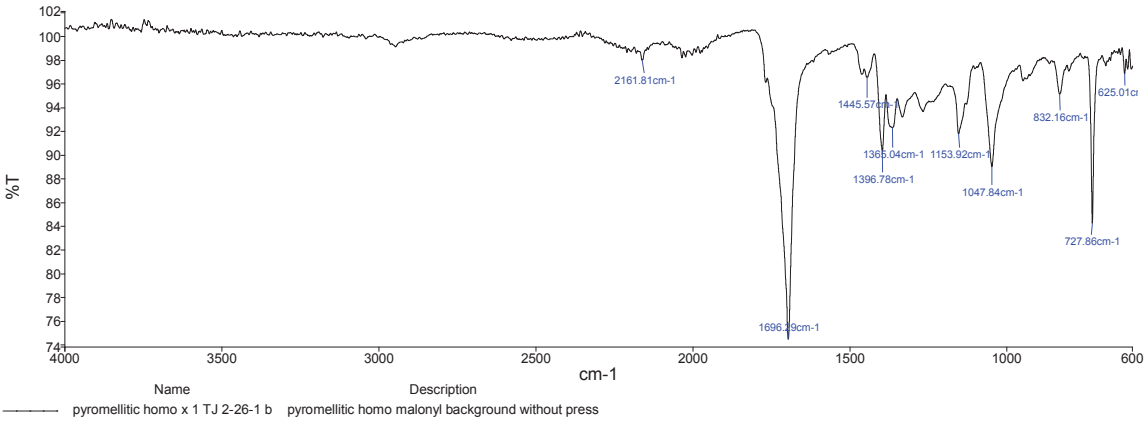

9.2.2. Butanedioyl-based homopolymer

FTIR ν_{max} ATR (cm^{-1}): 2948 (aromatic νC-H), 1698 (imide -CO-N-CO-, ester νC=O), 1397 (imide C-N stretch), 1155 (ester C-O-C), 1050 (imide ring deformation), 727 (imide ring deformation).

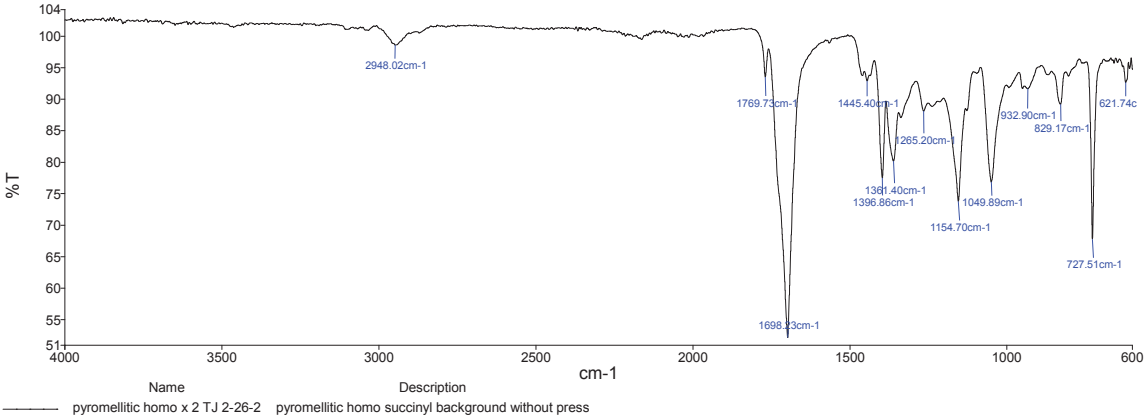

9.2.3. Pentanedioyl-based homopolymer

FTIR ν_{max} ATR (cm^{-1}): 2953 (aromatic νC-H), 1702 (imide -CO-N-CO-, ester νC=O), 1388 (imide C-N stretch), 1155 (ester C-O-C), 1032 (imide ring deformation), 723 (imide ring deformation).

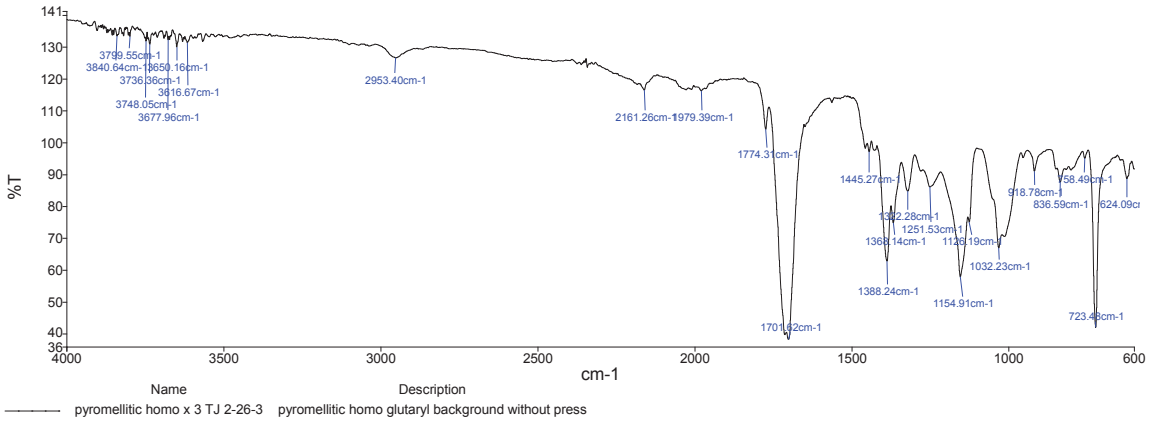

9.2.4. Hexanedioyl-based homopolymer

FTIR ν_{max} ATR (cm^{-1}): 2951 (aromatic νC-H), 1699 (imide -CO-N-CO-, ester νC=O), 1387 (imide C-N stretch), 1155 (ester C-O-C), 1252 (imide ring deformation), 759 (imide ring deformation).

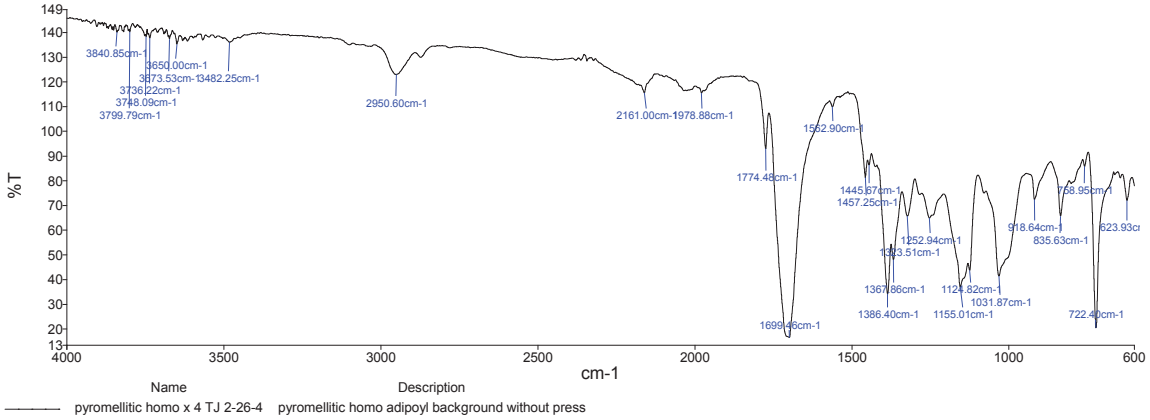

9.2.5. Heptanedioyl-based homopolymer

FTIR ν_{max} ATR (cm^{-1}): 2944 (aromatic νC-H), 1698 (imide -CO-N-CO-, ester νC=O), 1397 (imide C-N stretch), 1155 (ester C-O-C), 1051 (imide ring deformation), 727 (imide ring deformation).

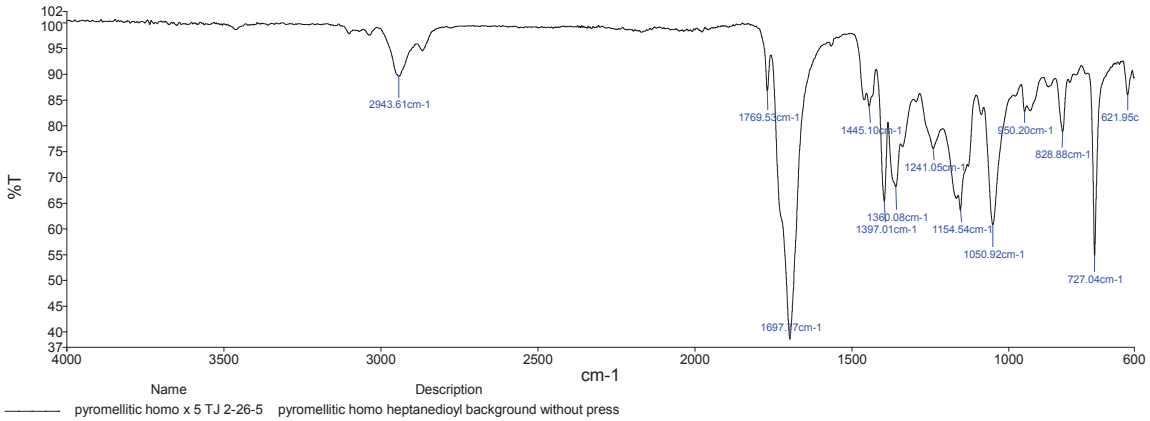

9.2.6. Octanedioyl-based homopolymer

FTIR ν_{max} ATR (cm^{-1}): 2938 (aromatic C-H), 1712 (imide -CO-N-CO-, ester C=O), 1386 (imide C-N stretch), 1154 (ester C-O-C), 1030 (imide ring deformation), 724 (imide ring deformation).

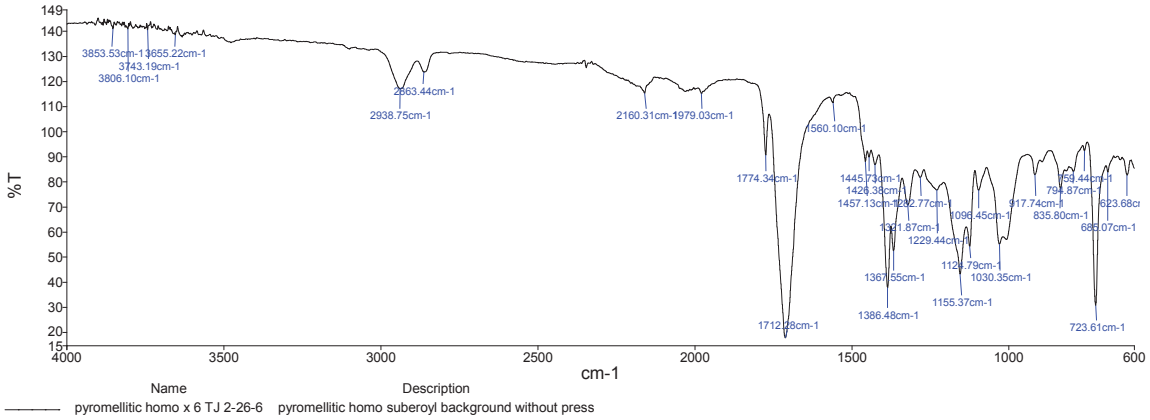

9.2.7. Nonanedioyl-based homopolymer

FTIR ν_{max} ATR (cm^{-1}): 2931 (aromatic νC-H), 1712 (imide -CO-N-CO-, ester νC=O), 1386 (imide C-N stretch), 1155 (ester C-O-C), 1032 (imide ring deformation), 724 (imide ring deformation).

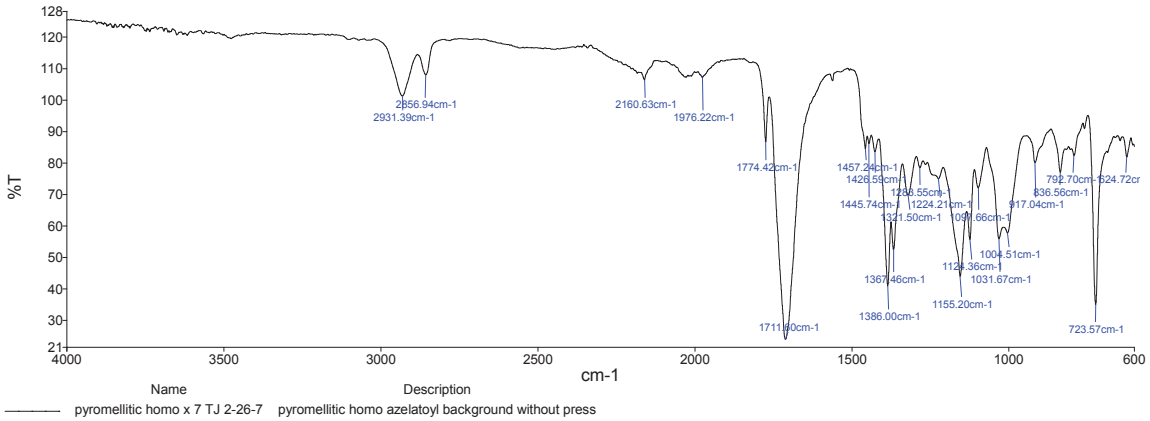

9.2.8. Decanedioyl-based homopolymer

FTIR ν_{max} ATR (cm^{-1}): 2929 (aromatic νC-H), 1709 (imide -CO-N-CO-, ester νC=O), 1386 (imide C-N stretch), 1155 (ester C-O-C), 1032 (imide ring deformation), 723 (imide ring deformation).

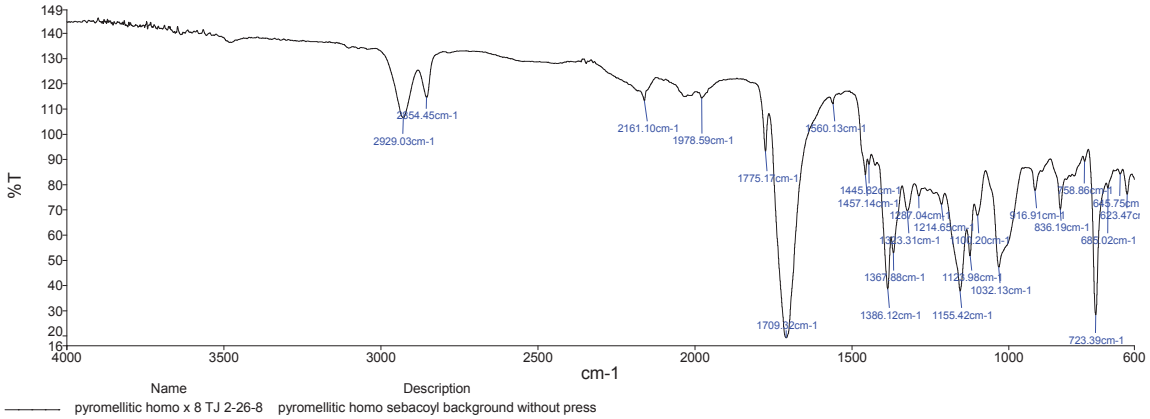

9.3. HFDI-based homo-poly(ester imide)s

HFDI Pentanedioyl-based homopolymer

FTIR ν_{max} ATR (cm^{-1}): 2961 (aromatic νC-H), 1779 (imide -CO-N-CO-), 1708 (ester νC=O), 1387 (imide C-N stretch), 1188 (vs, C–F), 1163 (ester C-O-C), 1139 (imide ring deformation), 745 (imide ring deformation).

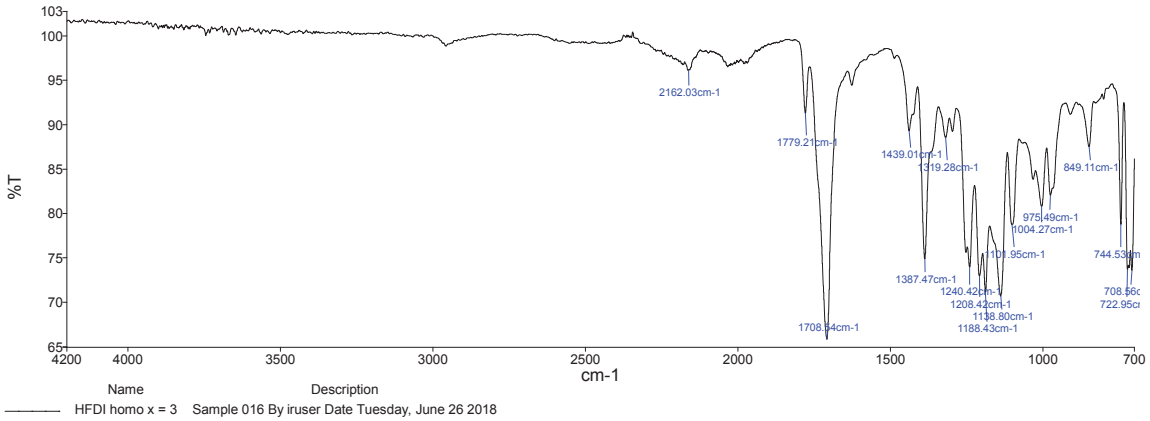

HFDI Heptanedioyl-based homopolymer

FTIR ν_{max} ATR (cm^{-1}): 2958 (aromatic νC-H), 1779 (imide -CO-N-CO-), 1709 (ester νC=O), 1387 (imide C-N stretch), 1188 (vs, C–F), 1164 (ester C-O-C), 1136 (imide ring deformation), 708 (imide ring deformation).

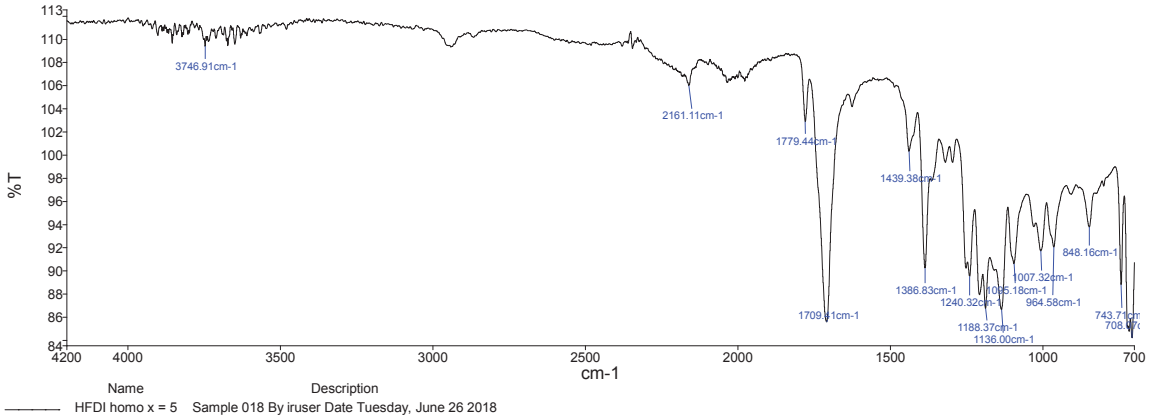

9.4. BPDI-based homo-poly(ester imide)s

BPDI Pentanedioyl-based homopolymer

FTIR ν_{max} ATR (cm^{-1}): 2947 (aromatic νC-H), 1770 (imide -CO-N-CO-), 1702 (ester νC=O), 1384 (imide C-N stretch), 1187 (ester C-O-C), 1143 (imide ring deformation), 740 (imide ring deformation).

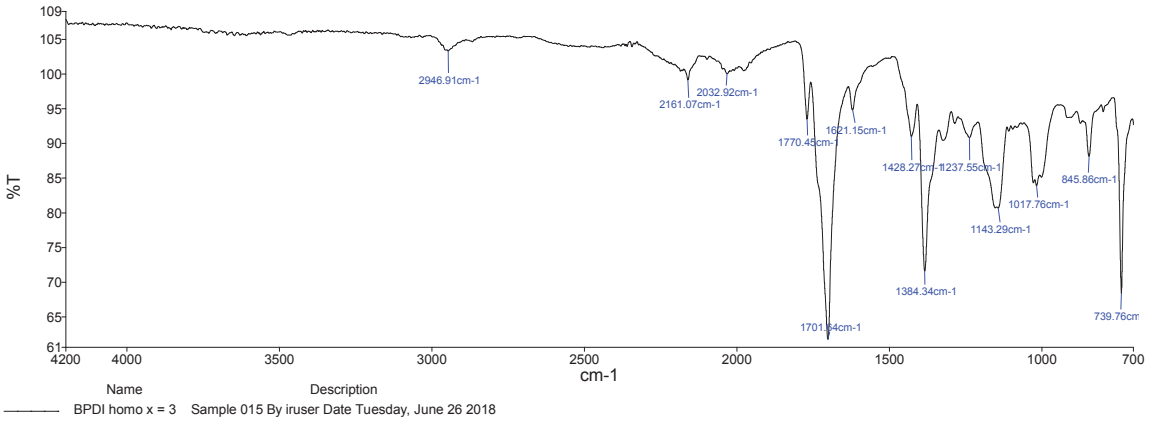

BPDI Heptanedioyl-based homopolymer

FTIR ν_{max} ATR (cm^{-1}): 2942 (aromatic νC-H), 1771 (imide -CO-N-CO-), 1702 (ester νC=O), 1383 (imide C-N stretch), 1158 (ester C-O-C), 1137 (imide ring deformation), 739 (imide ring deformation).

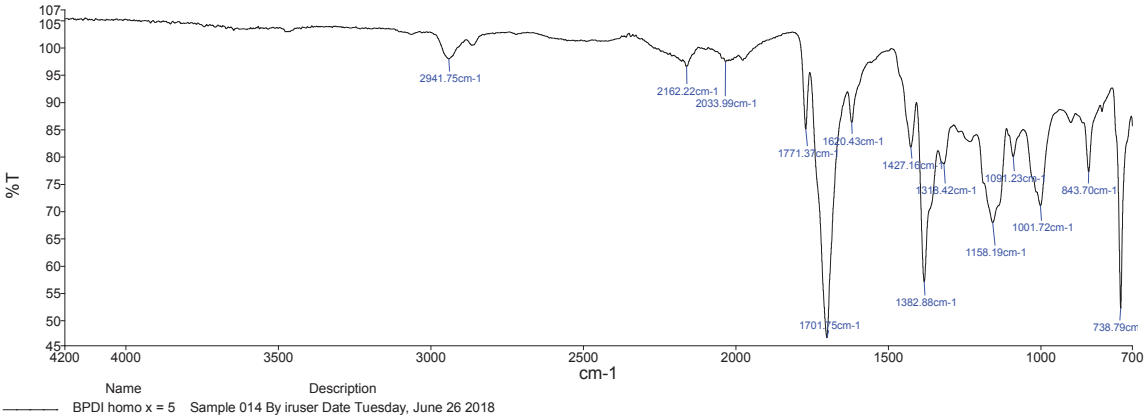

NDI/HFDI-based *co*-poly(ester-imide)s

9.4.1. NDI/HFDI Propanedioyl-based copolymer

FTIR ν_{max} ATR (cm^{-1}): 2956 (aromatic νC-H), 1706 (imide -CO-N-CO-), 1665 (ester νC=O), 1390 (imide C-N stretch), 1190 (vs, C–F), 1142 (ester C-O-C), 1104 (imide ring deformation), 768 (imide ring deformation).

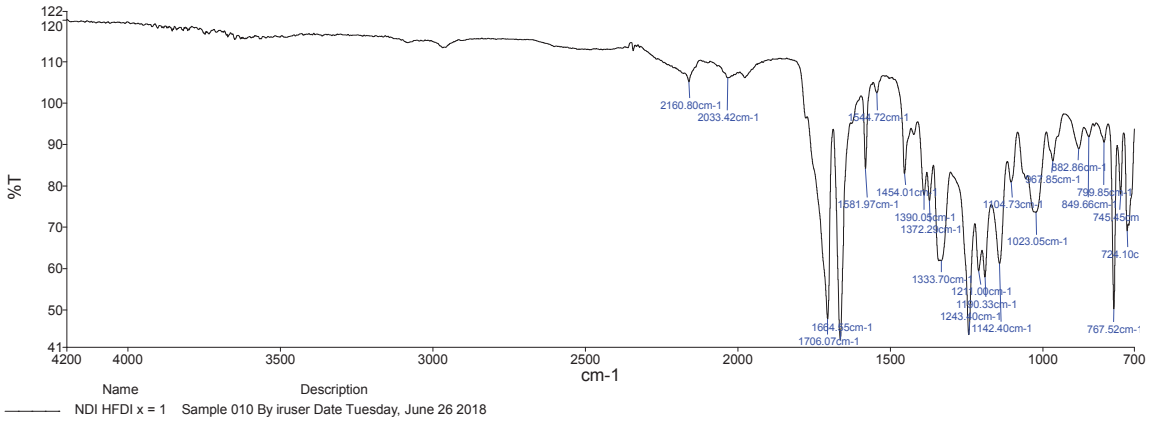

9.4.2. NDI/HFDI Butanedioyl-based copolymer

FTIR ν_{max} ATR (cm^{-1}): 2973 (aromatic νC-H), 1779 (imide -CO-N-CO-), 1707 (ester νC=O), 1388 (imide C-N stretch), 1189 (vs, C–F), 1146 (ester C-O-C), 1100 (imide ring deformation), 768 (imide ring deformation).

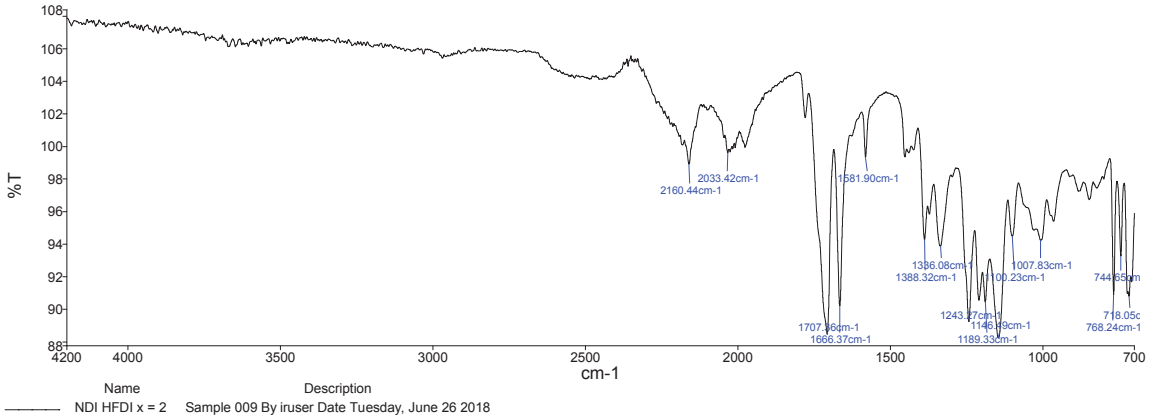

9.4.3. NDI/HFDI Pentanedioyl-based copolymer

FTIR ν_{max} ATR (cm^{-1}): 2958 (aromatic νC-H), 1779 (imide -CO-N-CO-), 1701 (ester νC=O), 1388 (imide C-N stretch), 1189 (vs, C–F), 1163 (ester C-O-C), 1140 (imide ring deformation), 768 (imide ring deformation).

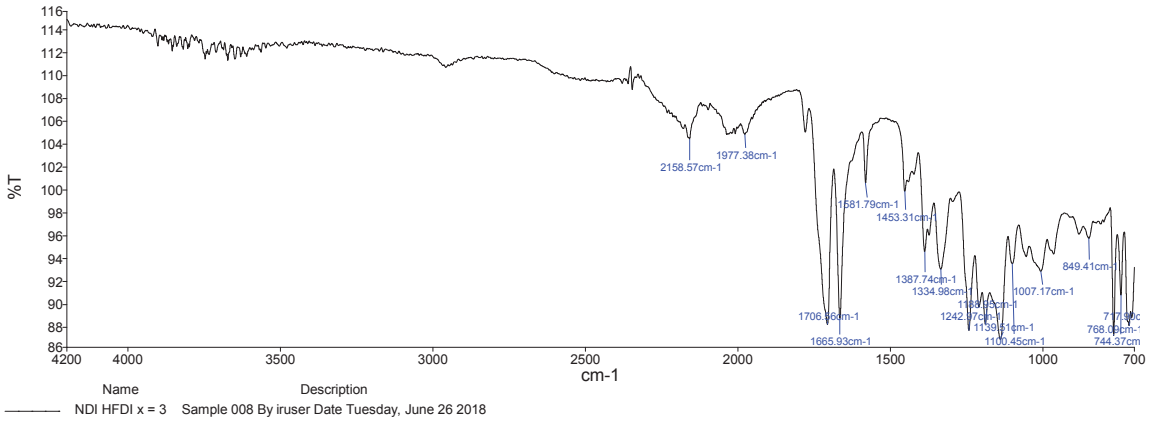

9.4.4. NDI/HFDI Hexanedioyl-based copolymer

FTIR ν_{max} ATR (cm^{-1}): 2958 (aromatic νC-H), 1780 (imide -CO-N-CO-), 1708 (ester νC=O), 1389 (imide C-N stretch), 1190 (vs, C–F), 1163 (ester C-O-C), 1140 (imide ring deformation), 769 (imide ring deformation).

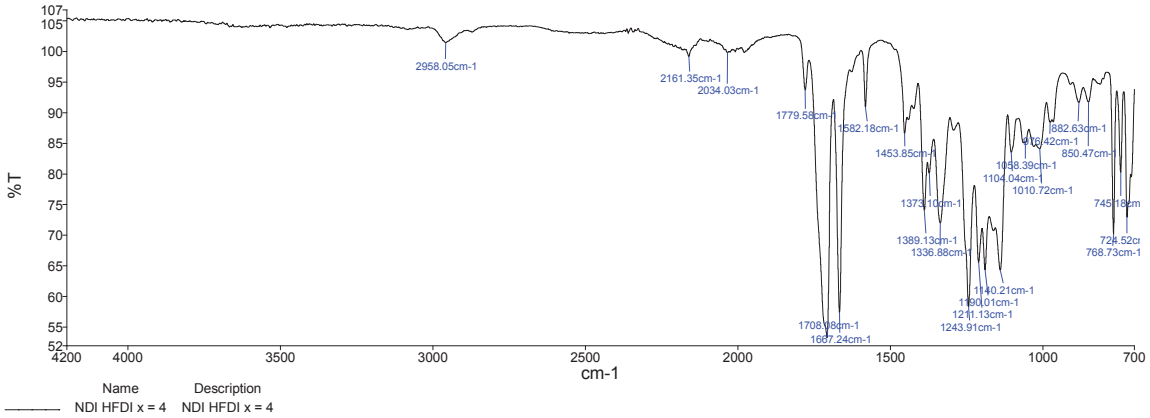

9.4.5. NDI/HFDI Heptanedioyl-based copolymer

FTIR ν_{max} ATR (cm^{-1}): 2942 (aromatic νC-H), 1780 (imide -CO-N-CO-), 1708 (ester νC=O), 1389 (imide C-N stretch), 1190 (vs, C–F), 1163 (ester C-O-C), 1140 (imide ring deformation), 769 (imide ring deformation).

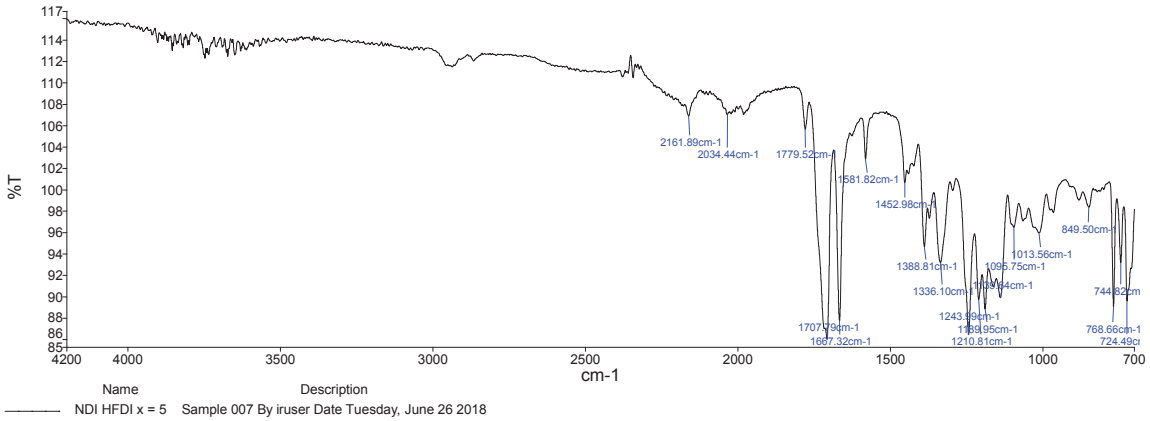

NDI/HFDI Octanedioyl-based copolymer

FTIR ν_{max} ATR (cm^{-1}): 2936 (aromatic νC-H), 1780 (imide -CO-N-CO-), 1704 (ester νC=O), 1387 (imide C-N stretch), 1189 (vs, C–F), 1164 (ester C-O-C), 1138 (imide ring deformation), 770 (imide ring deformation).

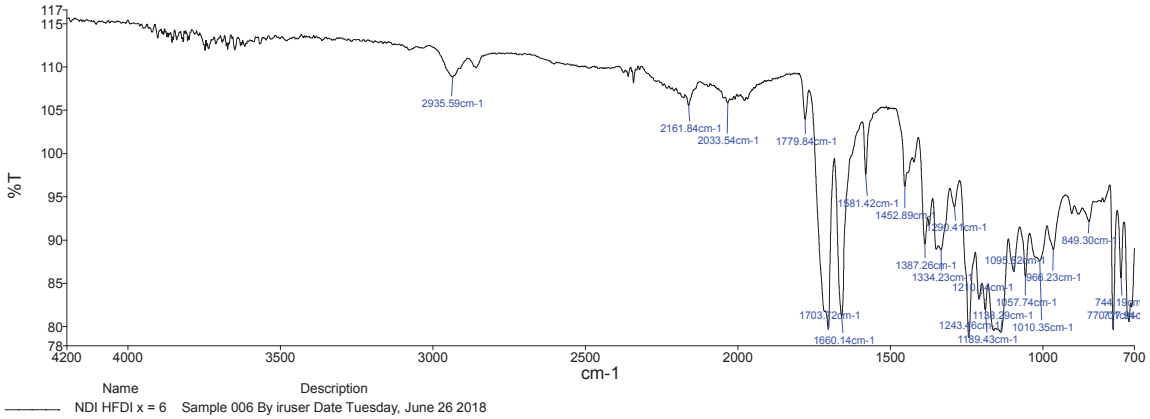

9.4.6. NDI/HFDI Nonanedioyl-based copolymer

FTIR ν_{max} ATR (cm^{-1}): 2930 (aromatic νC-H), 1780 (imide -CO-N-CO-), 1706 (ester νC=O), 1387 (imide C-N stretch), 1189 (vs, C–F), 1161 (ester C-O-C), 1141 (imide ring deformation), 770 (imide ring deformation).

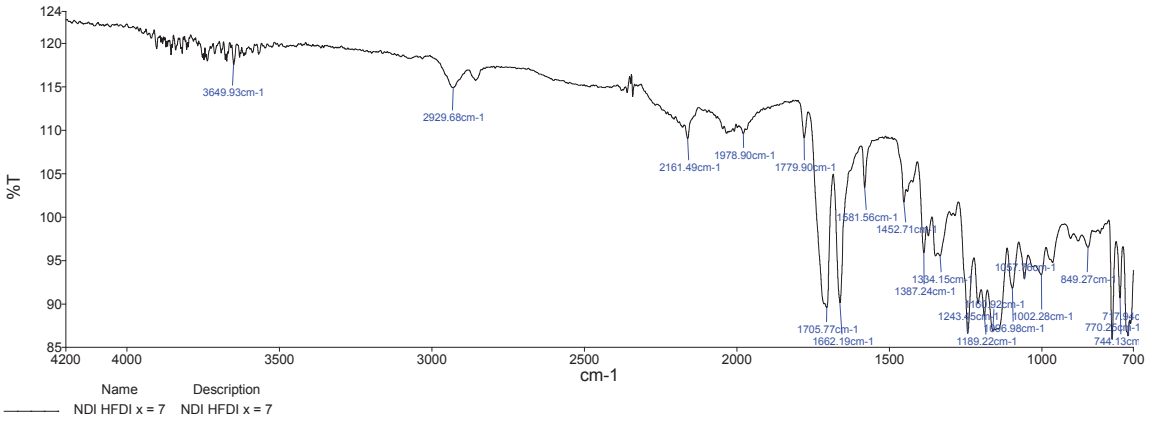

9.4.7. NDI/HFDI Decanedioyl-based copolymer

FTIR ν_{max} ATR (cm^{-1}): 2928 (aromatic νC-H), 1780 (imide -CO-N-CO-), 1718 (ester νC=O), 1373 (imide C-N stretch), 1190 (vs, C–F), 1162 (ester C-O-C), 1152 (imide ring deformation), 771 (imide ring deformation).

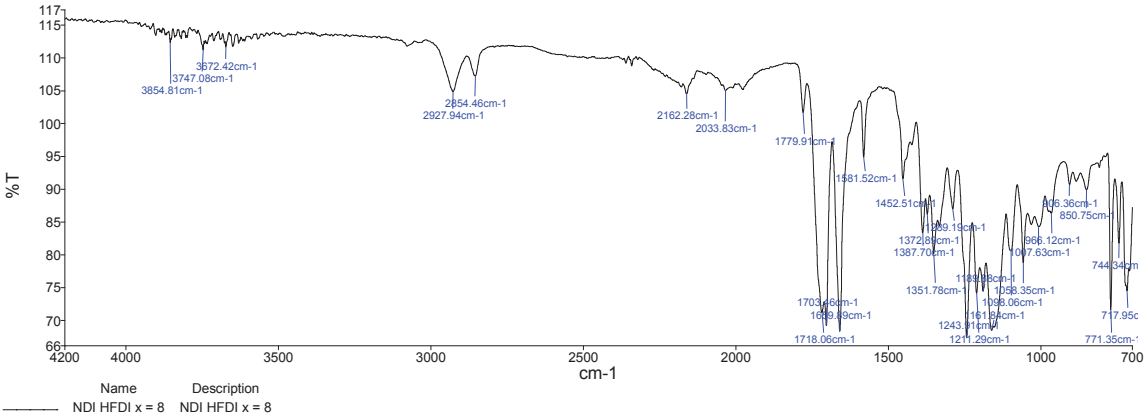

9.5. NDI / BPDI-based copolymers

9.5.1. NDI/BPDI Butanedioyl-based copolymer

FTIR ν_{max} ATR (cm^{-1}): 2958 (aromatic νC-H), 1772 (imide -CO-N-CO-), 1705 (ester νC=O), 1386 (imide C-N stretch), 1189 (ester C-O-C), 1151 (imide ring deformation), 769 (imide ring deformation).

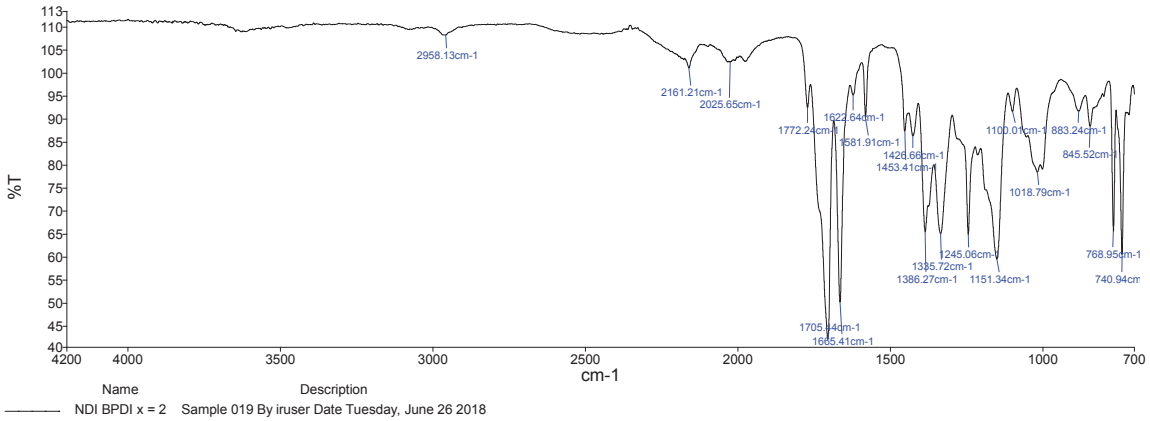

9.5.2. NDI/BPDI Pentanedioyl-based copolymer

FTIR ν_{max} ATR (cm^{-1}): 2958 (aromatic νC-H), 1772 (imide -CO-N-CO-), 1706 (ester νC=O), 1387 (imide C-N stretch), 1191 (ester C-O-C), 1148 (imide ring deformation), 769 (imide ring deformation).

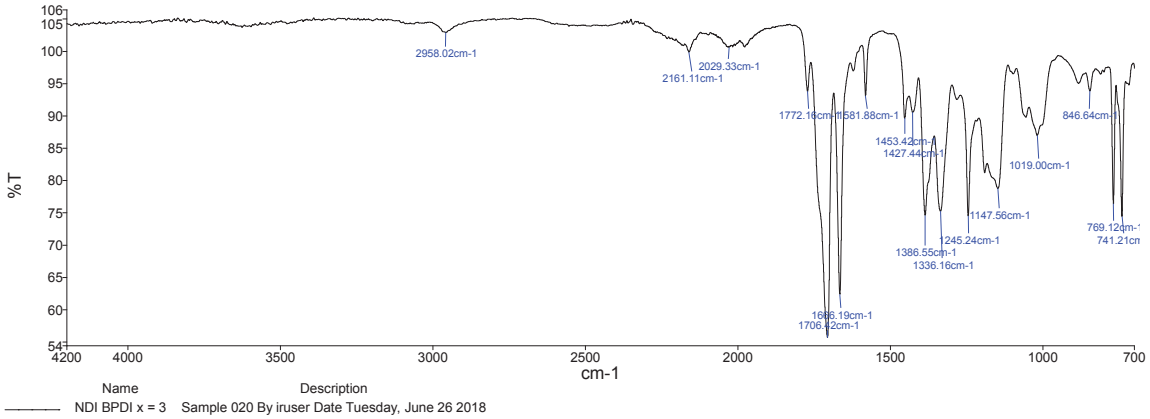

9.5.3. NDI/BPDI Hexanedioyl-based copolymer

FTIR ν_{max} ATR (cm^{-1}): 2962 (aromatic νC-H), 1773 (imide -CO-N-CO-), 1708 (ester νC=O), 1387 (imide C-N stretch), 1192 (ester C-O-C), 1164 (imide ring deformation), 770 (imide ring deformation).

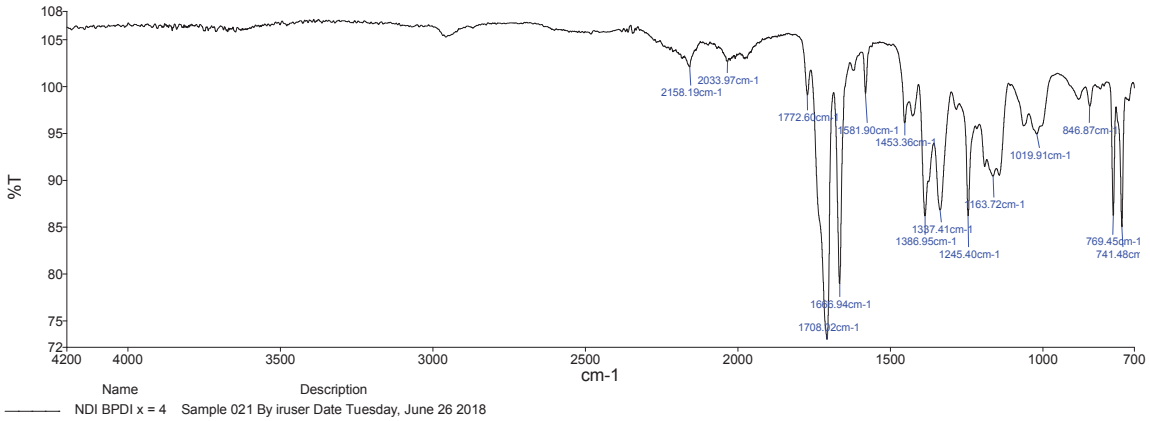

9.5.4. NDI/BPDI Heptanedioyl-based copolymer

FTIR ν_{max} ATR (cm^{-1}): 2938 (aromatic νC-H), 1772 (imide -CO-N-CO-), 1705 (ester νC=O), 1385 (imide C-N stretch), 1191 (ester C-O-C), 1160 (imide ring deformation), 769 (imide ring deformation).

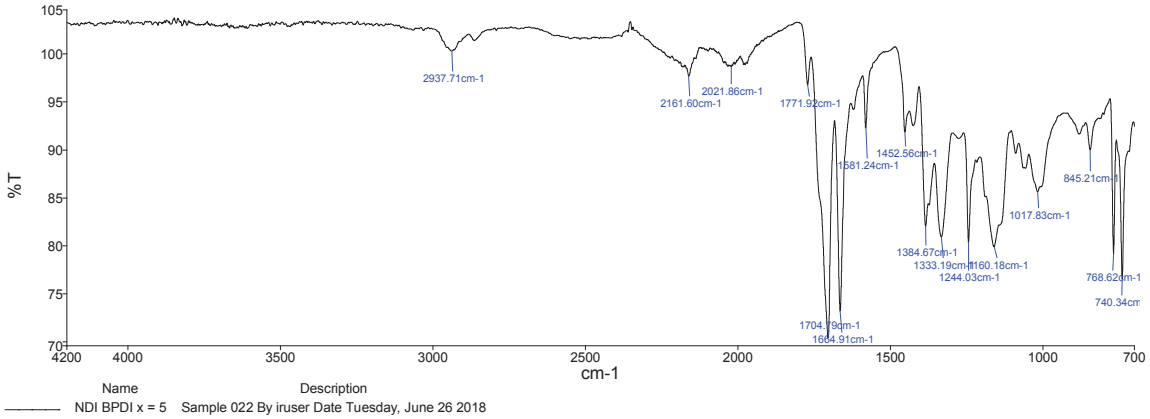

9.6. PMDI-based *co*-poly(ester-imide)s

9.6.1. PMDI/BPDI heptanedioyl-based *co*-poly(ester-imide)s

FTIR ν_{max} ATR (cm^{-1}): 2941 (aromatic νC-H), 1773 (imide -CO-N-CO-), 1708 (ester νC=O), 1385 (imide C-N stretch), 1191 (ester C-O-C), 1156 (imide ring deformation), 741 (imide ring deformation).

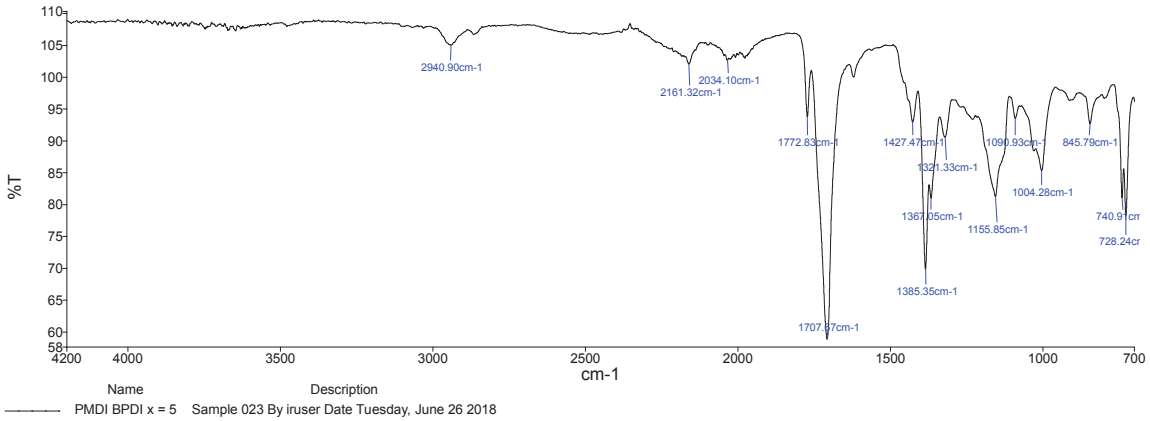

9.6.2. PMDI/HFDI heptanedioyl-based copolymer

9.7. All-aliphatic *co*-poly(ester-imide)s

9.7.1. NDI *x* = 1/8 copolymer

FTIR ν_{max} ATR (cm^{-1}): 2929 (aromatic C-H), 1736 (imide -CO-N-CO-), 1704 (ester C=O), 1373 (imide C-N stretch), 1191 (ester C-O-C), 1164 (imide ring deformation), 768 (imide ring deformation).

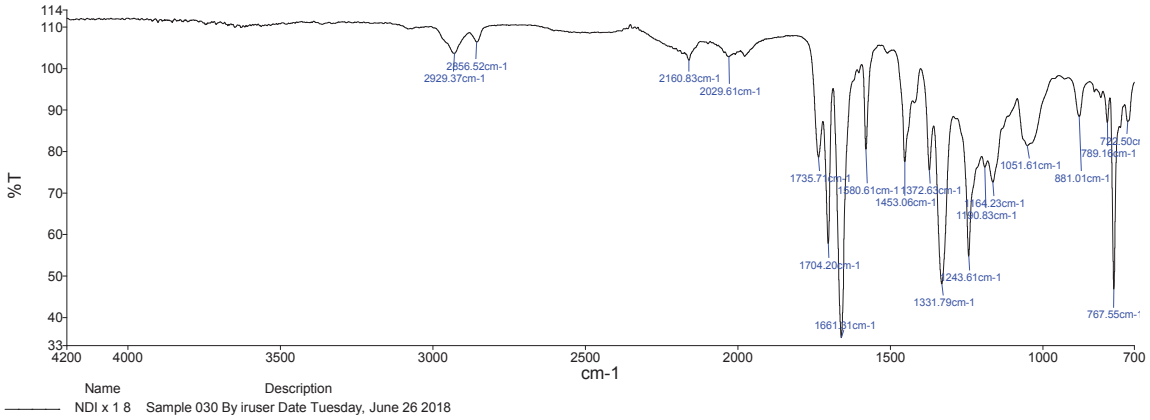

9.7.2. NDI *x* = 2/8 copolymer

FTIR ν_{max} ATR (cm^{-1}): 2930 (aromatic νC-H), 1735 (imide -CO-N-CO-), 1706 (ester νC=O), 1372 (imide C-N stretch), 1188 (ester C-O-C), 1156 (imide ring deformation), 767 (imide ring deformation).

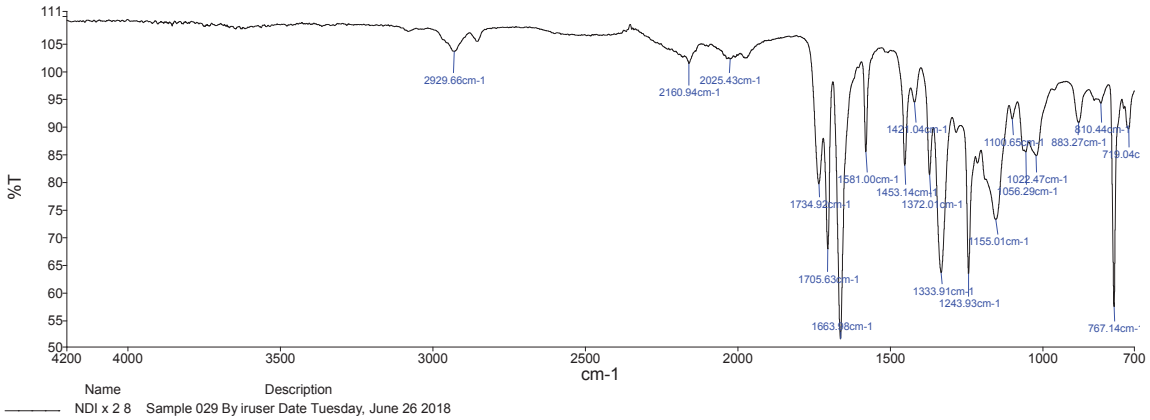

9.7.3. NDI *x* = 3/8 copolymer

FTIR ν_{max} ATR (cm^{-1}): 2929 (aromatic νC-H), 1736 (imide -CO-N-CO-), 1706 (ester νC=O), 1372 (imide C-N stretch), 1193 (ester C-O-C), 1164 (imide ring deformation), 768 (imide ring deformation).

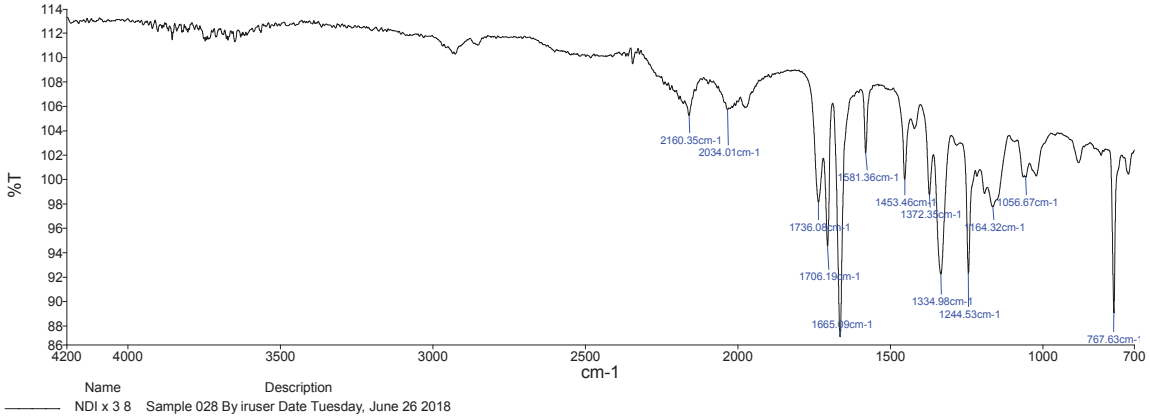

9.7.4. NDI *x* = 4/8 copolymer

FTIR ν_{max} ATR (cm^{-1}): 2930 (aromatic νC-H), 1731 (imide -CO-N-CO-), 1703 (ester νC=O), 1372 (imide C-N stretch), 1190 (ester C-O-C), 1145 (imide ring deformation), 768 (imide ring deformation).

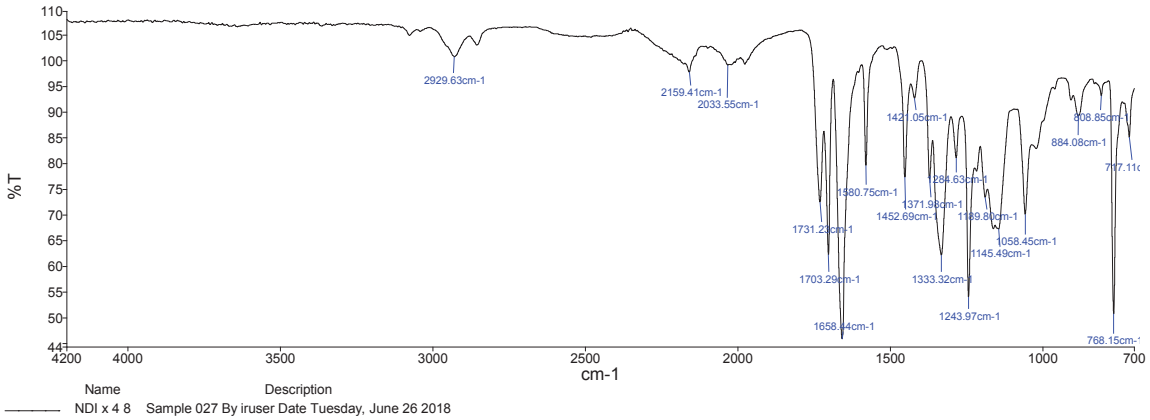

9.7.5. NDI *x* = 5/8 copolymer

FTIR ν_{max} ATR (cm^{-1}): 2929 (aromatic νC-H), 1732 (imide -CO-N-CO-), 1705 (ester νC=O), 1372 (imide C-N stretch), 1189 (ester C-O-C), 1159 (imide ring deformation), 766 (imide ring deformation).

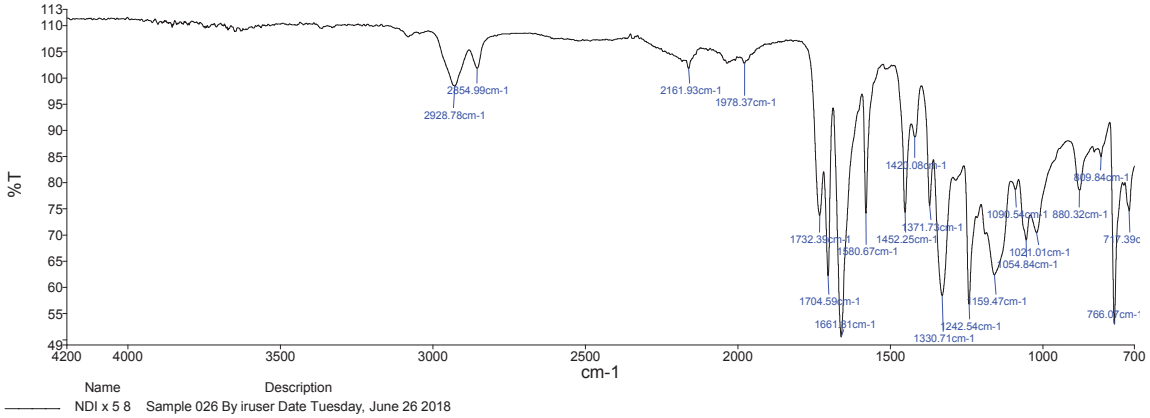

9.7.6. NDI *x* = 6/8 copolymer

FTIR ν_{max} ATR (cm^{-1}): 2935 (aromatic νC-H), 1734 (imide -CO-N-CO-), 1704 (ester νC=O), 1372 (imide C-N stretch), 1196 (ester C-O-C), 1146 (imide ring deformation), 771 (imide ring deformation).

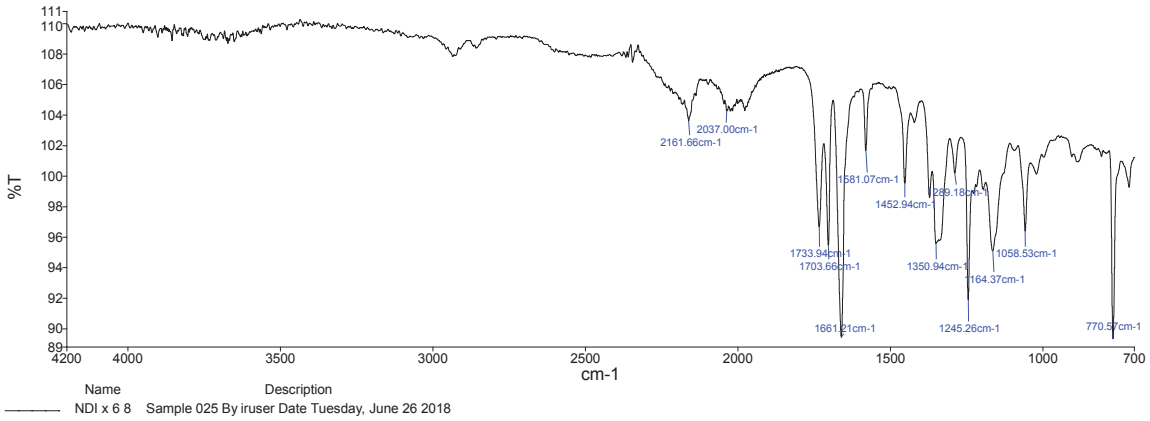

9.7.7. NDI *x* = 7/8 copolymer

FTIR ν_{max} ATR (cm^{-1}): 2927 (aromatic νC-H), 1733 (imide -CO-N-CO-), 1703 (ester νC=O), 1372 (imide C-N stretch), 1196 (ester C-O-C), 1059 (imide ring deformation), 768 (imide ring deformation).

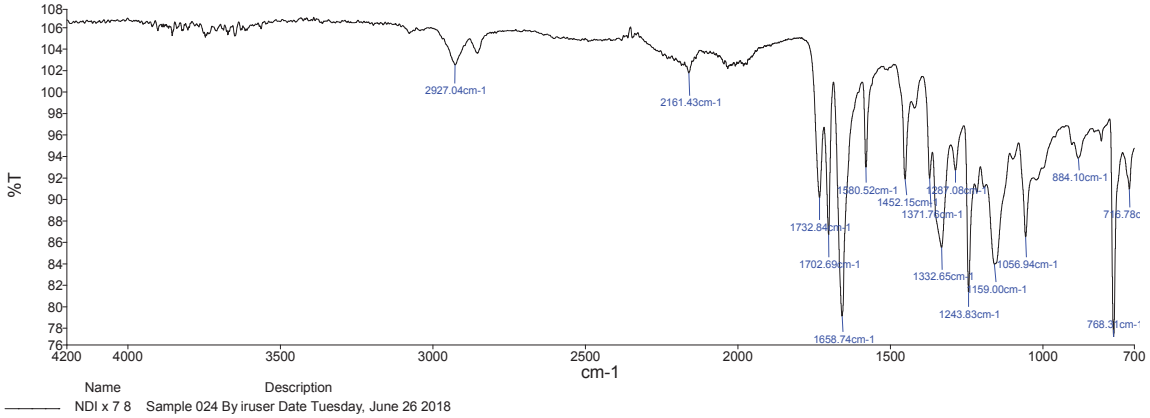

9.8. Poly(ether imide)s

9.8.1. NDI / HFDI / EDEA-based copolymer

FTIR ν_{max} ATR (cm^{-1}): 2867 (aromatic νC-H), 1704 (imide -CO-N-CO-), 1388 (aliphatic C-H rocking), 1331 (imide C-N stretch), 1242 (imide ring deformation), 1208 (C-O-C stretch), 766 (imide ring deformation).

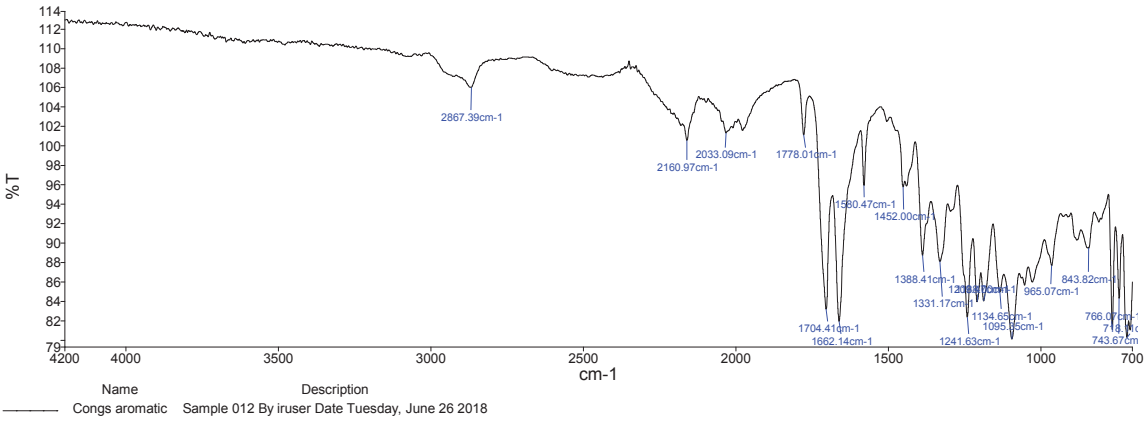

NDI / DADD / EDEA-based copolymer

FTIR ν_{max} ATR (cm^{-1}): 2923 (aromatic C-H), 1705 (imide -CO-N-CO-), 1374 (aliphatic C-H rocking), 1333 (imide C-N stretch), 1243 (imide ring deformation), 1191 (C-O-C stretch), 767 (imide ring deformation).